10-25-2013

The System I and System III Holocytochrome c Synthases in Cytochrome c Biogenesis

Brian San Francisco
Washington University in St. Louis

WASHINGTON UNIVERSITY IN ST. LOUIS

Division of Biology & Biomedical Sciences
Plant and Microbial Biosciences

Dissertation Examination Committee:
Robert G. Kranz, Chair
Robert E. Blankenship
Elizabeth S. Haswell
Joseph M. Jez
Toni M. Kutchan
Hani S. Zaher

The System I and System III Holocytochrome c Synthases in Cytochrome c Biogenesis

by

Brian San Francisco

A dissertation presented to the
Graduate School of Arts and Sciences
of Washington University in
partial fulfillment of the
requirements for the degree
of Doctor of Philosophy

October 2013

St. Louis, Missouri

Table of Contents

Acknowledgements

First, I would like to thank my family for their support (emotional, spiritual, and sometimes financial) throughout my graduate study. Without the appreciation for knowledge and inquiry that they instilled in me, a career in science could never become a reality. Thanks to my friends for the welcome distractions that they have provided. Spending ridiculous hours in the lab would have been a lot more difficult were it not for the ridiculous time spent out of it. Thanks to the members of my committee (especially Liz) for their insightful comments and a true desire to see me improve as a researcher and as a speaker. Thanks to all the past members of the Kranz lab, who provided the foundation for much of the work that we are doing today. I would like to thank Cindy, in particular, for teaching me virtually everything that I know about bench science, and for doing so with patience, grace, and only the occasional profane outburst. Thanks to the current members of the Kranz lab (and the honorary members, Sheri) for making it easy to get up and come in to work every morning (or afternoon). Finally, I would like to profoundly thank my advisor, Bob, for fostering my growth as a researcher, a critical thinker, and an adult during my graduate study. He has always considered my ideas thoughtfully, and has treated me more like a member of his family than a student. His dedication to his research and to the members of his lab is inspiring, and any future successes that I may enjoy as a scientist I owe to his mentoring.

Dedication

To Mom and Dad and Sam, my biggest supporters

To Buster and Horatio, for their constant, adorable misbehavior

And to RJT, for keeping me grounded

Abstract of the Dissertation

The System I and System III Holocytochrome c Synthases

in Cytochrome c Biogenesis

by

Brian San Francisco

Doctor of Philosophy in Plant and Microbial Biosciences

Washington University in St. Louis, 2013

Professor Robert G. Kranz, Chair

Cytochromes c are proteins that are involved in important redox reactions in organisms from every kingdom of life. C-type cytochromes, uniquely, possess a covalently bound heme. Since cytochromes c are assembled at their site(s) of function (outside of the cytoplasmic membrane in bacteria, in the chloroplast lumen, or in the mitochrondrial intermembrane space), their assembly poses unique challenges to heme trafficking and post translational modification. Three major systems exist in nature for cytochrome c assembly, termed systems I, II, and III. Using recombinant *Escherichia coli*, aspects of systems I and III were analyzed, with an emphasis on the synthase protein(s) and protein complexes that carry out the covalent attachment of heme to apocytochrome. Studies on system I focused on the integral membrane protein CcmF, the putative cytochrome c synthetase, which was shown to contain a stable and stoichiometric heme b. The ligands to the b-heme were identified (TM-His1 and TM-His2), and the midpoint potential of the heme b was determined and found to be consistent with its involvement in a critical redox reaction underlying the synthetase reaction. Additionally, a long-

suspected interaction between CcmF and the periplasmic heme chaperone, holoCcmE, was characterized, with the discovery that heme from holoCcmE is coordinated by two conserved periplasmic histidines in CcmF (P-His1 and P-His2) that flank the conserved WWD domain. It was also shown that CcmF, in complex with CcmH, is the holocytochrome c synthase for system I, able to synthesize cytochromes c in the absence of other Ccm components. Studies on system III, the human HCCS, constituted the first purification and biochemical characterization of an HCCS protein. It was discovered that HCCS purifies with a heme b and forms a stable complex with the human cytochrome c. Using a combination of mutagenesis (of both the apocytochrome and HCCS), functional analysis, and biochemical characterization (of HCCS, alone and in complex with cytochrome c), these studies facilitated an elaboration of the molecular mechanisms for holocytochrome c formation by HCCS.

Chapter 1: Introduction, Significance, Summary, and Scope of Thesis

Introduction

Heme type and structure, and cytochrome classifications

Cytochromes are an important class of heme proteins that facilitate electron transfer reactions in a wide range of biologically critical reactions. Cytochromes are broadly classified according to the type of heme they possess. Hemes (b, o, a, and c) are distinguished from one another by the type of covalent modification(s) to the heme. In heme biosynthesis, reduced iron (Fe^{2+}) is inserted into a porphyrin ring (known as protoporphyrin IX) by the ferrochelatase enzyme [1]. Within the heme macrocyle, each of the four pyrrole ring nitrogens supplies a planar ligand to the iron atom. Extending out from the heme macrocycle are vinyl groups at the 2- and 4-positions, and propionate groups at positions 6 and 7. Heme, thus synthesized, is known as heme b (or protoheme) and is incorporated (non-covalently) into many proteins, including cytochromes b (hence their nomenclature) and the globins (e.g., myoglobin). Typically, the side chains of certain amino acids (usually histidine, methionine, cysteine, or tyrosine) provide the 5^{th} and 6^{th} axial (i.e., non-planar) ligands to the heme iron. Alternatively, heme b may undergo subsequent covalent modification to form hemes a, o, or c (see Fig 1) [1,2,3]. The synthesis of heme a and heme o is carried out by single dedicated integral membrane proteins, respectively, and involves the addition of a 17-carbon hydroxyethylfarnesyl group to the heme 2-vinyl [3]. Heme a has an additional formyl group at the 8-position. Although both hemes a and o undergo covalent modifications to the porphyrin structure, these hemes are associated with their respective proteins non-covalently. Heme c (Fig 1) is unique in this regard; the vinyls of heme are covalently attached (via thioether linkages) to the target protein (usually, at the thiols of two cysteines in a conserved Cys-Xxx-Xxx-Cys-His motif)

[2,4,5]. Thus, synthesis of heme c is fundamentally the same as cytochrome c assembly, with protein folding occurring after covalent attachment.

The unique covalent attachment of heme in the c-type cytochromes is thought to confer additional stability to the holo-protein (i.e., to prevent heme loss) [6]. This theory is consistent with the fact that cytochromes c function outside of the cytoplasmic membrane. In fact, in some prokaryotes, cytochromes c operate at a great distance from the cytoplasmic membrane [7] (for example, in the reduction of insoluble metal oxides in the environment by the multiheme cytochromes c that comprise the *Shewanella* nanowire [8,9]). There are a few examples of other proteins that contain covalent heme. For example, the heme chaperone protein of system I, holoCcmE (discussed below), binds heme covalently through a histidine residue [10,11,12,13]. However, since this particular protein is not a cytochrome, per se (i.e., its primary function is not electron transfer), synthesis of holoCcmE is not formally considered cytochrome c biogenesis. A globin from cyanobacteria also has a covalent link to a histidine side chain [14,15,16].

The various heme types discussed above can be distinguished from one another by spectrophotometric techniques. Hemes, and heme proteins, exhibit three characteristic absorption maxima ("peaks") in the visible range, termed the α (550-560 nm), β (520-530 nm), and Soret (400-430 nm) [17]. Changes in the positions of these peaks are reflective of changes in the heme binding environment within a protein. A particularly sensitive method using UV-Vis absorption spectroscopy, known as the pyridine hemochrome, can further distinguish between hemes with zero, one, or two covalent modifications to the vinyls [18]. In this assay, the heme protein is denatured by sodium hydroxide and the native axial ligands are replaced by pyridine. Chemical reduction (typically, with the strong reducing agent sodium dithionite) of the pyridine hemochrome yields characteristic α maxima that can be used to discern the number of

covalent attachments to the heme vinyls: a 550 nm α absorption indicates covalent modification at both the 2- and 4-vinyls of heme, 553 nm is indicative of a single covalent modification, and 556 indicates no covalent attachments.

General requirements for formation of cytochrome c

Cytochromes c are assembled at their site of function. In prokaryotes, this is outside of the cytoplasmic membrane (i.e., in the periplasm of gram negative bacteria, and extra-cellularly in the gram positives). In eukaryotes, cytochromes c are matured in the intermembrane space of mitochondria or in the lumen of chloroplasts. In all cases, the site of cytochrome c assembly is separated from biosynthesis of heme and translation of the apoprotein by a lipid bilayer, thus posing unique challenges to heme trafficking, apocytochrome secretion, and the covalent attachment reaction. Cytochrome c synthesis, therefore, requires dedicated mechanisms to traffick heme and apocytochrome to the site of thioether formation [2,4,5]. Prokaryotic apocytochromes contain signal sequences that direct the unfolded polypeptide from the site of translation across a lipid bilayer (via the general Sec pathway) to the site of cytochrome c assembly [19,20]. In mitochondria, this is accomplished by components of the TOM complex [21].

Apocytochromes are defined by the conserved Cys-Xxx-Xxx-Cys-His motif. In holocytochrome formation, the thiol groups of the N- and C-terminal cysteines attack the 2- and 4- heme vinyls, respectively, to form thioether linkages, and the imidazole group of the histidine serves as an axial ligand to the iron of heme [22,23]. Thioether formation is a spontaneous (energy-independent) Markovnikov addition, where each of the reduced thiols attacks the more substituted α carbon of the heme vinyl, with addition of hydrogen to the less substituted β carbon (Fig 1). Rare, variant cytochrome c attachment motifs (including Cys-Xxx-Xxx-Cys-Lys, Cys-

Xxx15-Cys-His, and even Ala-Xxx-Xxx-Cys-His, with a single covalent link to heme) have been identified [24,25], but the requirements for cytochrome c assembly are the same. For covalent attachment to occur, the heme of iron must be in the reduced (Fe^{2+}) state, and the thiols of the cysteines must be reduced [22,26]. Unlike other cytochromes, the c-type cytochromes fold into their functional conformations only after covalent attachment of heme [27]; in the absence of heme, the unfolded polypeptide is often rapidly degraded.

Systems for cytochrome c formation in nature

Three major systems have evolved for cytochrome c biosynthesis, termed systems I, II and III (Fig 2) [2,4,5]. System III is found in the mitochondria of animals and some protozoa; system II is found in most gram positive bacteria, the cyanobacteria and the chloroplasts of plants and algae; system I is found in most gram negative bacteria, the archaea, and the mitochondria of plants and certain protozoa. Although the three systems differ in terms of complexity, mechanism, and phylogenetic distribution, each accomplishes covalent ligation of heme to the apocytochrome (usually, at Cys-Xxx-Xxx-Cys-His).

System I

Genetic analyses in *Rhodobacter capsulatus* [28,29,30,31] (and, subsequently, *Paracoccus denitrificans* [32,33,34], *Bradyrhizobium japonicum* [35,36], and *E. coli* [37]) in the late 1980s and early 1990s revealed a pathway for bacterial cytochrome c assembly. Called system I, this pathway consists of between 8 or 9 dedicated proteins (CcmABCDEFGH, in *E. coli*), most of which are integral membrane proteins (Fig 2). In some organisms, such as *R. capsulatus*, ccmH is split into two ORFs, encoded by ccmH and ccmI [28]. In bacteria, the *ccm* genes are usually found as an intact operon, but, sometimes, are split into several gene clusters [38]. In plants, some of the *ccm* genes are present in the mitochondrial genome and others are

nuclear-encoded [39,40]. The general Sec and Dsb pathways are required for apocytochrome secretion and (indirectly) reduction of the apocytochrome thiols, respectively [20,41]. The import of the nuclear-encoded apocytochrome into plant mitochondria is less well-understood. However, unlike apocytochrome secretion, heme translocation for cytochrome c maturation occurs exclusively as a function of the system I proteins [42].

Heme trafficking in system I proceeds in two steps (Fig 2): (i) formation and release of the heme chaperone protein, called holo (+ heme) CcmE, (from CcmABCD) and (ii) heme transfer from holoCcmE to the apocytochrome (putatively, via the CcmFH complex) to yield a holocytochrome c. Formation of holoCcmE occurs in the CcmCDE complex [43,44], where a unique covalent attachment is formed between the β carbon of the heme 2-vinyl and a conserved histidine residue (His130) in CcmE [10,11,12,13,45]. CcmC is a member of a heme-handling protein (HHP) superfamily [46] that also includes CcmF and the system II cytochrome c synthetase, CcsBA. The defining feature of these proteins is the conserved WWD domain [29], a hydrophobic, extra-cytoplasmic feature (for interaction with heme) that is flanked by two conserved histidines that serve as heme axial ligands. In the absence of CcmAB, CcmCDE form a stable holo (+ heme) complex, where heme, covalently attached to His130 of CcmE, is bound in the CcmC WWD domain with axial ligands from CcmC His60 and His184 [43].

Expression of CcmAB leads to formation of an ABC transporter complex (CcmABCD) that uses ATP hydrolysis to release covalent holoCcmE [47,48,49]. These studies were initially carried out in *R. capsulatus*, where the CcmABCD complex was first identified [49]. CcmA, CcmB, and CcmC each have homology to individual subunits of components of ABC-transporter complexes, with the classic Walker domain found in CcmA [50]. Hydrolysis of ATP by CcmABCD leads to the release of oxidized (Fe^{3+}) holoCcmE, which is proposed to chaperone its

heme to the site of cytochrome c formation, CcmFH, (see below) [44,51,52]. It has been established that formation of covalent holoCcmE occurs independent of ATP-hydrolysis (and in the absence of CcmAB altogether); thus, CcmABCD functions a holoCcmE release complex [48].

CcmG and CcmH are thioredox-active proteins that maintain the apocytochrome thiols (in the Cys-Xxx-Xxx-Cys-His motif) in the reduced state [28,39,53,54]. CcmG and CcmH each contain a conserved pair of cysteine residues (in the classical thioredoxin Cys-Xxx-Xxx-Cys motif) that are involved in reduction of the disulfide bond between the two cysteines in the apoctychrome (at Cys-Xxx-Xxx-Cys-His). The three-dimensional structures of the soluble domains of both CcmG [55,56] and CcmH [57,58] have been determined. There is significant evidence that CcmH interacts directly with the apocytochrome [39,57,59,60] and with CcmF [44,52,61,62]. CcmH is proposed to orient the thiols of the apocytochrome for thioether formation with the heme bound in the CcmF WWD domain. CcmG does not associate directly with the CcmFH complex (see below). Rather, the cysteines in CcmG are reduced by DsdD [63]; reduced CcmG, in turn, likely reduces the cysteines in CcmH, which is then thought to reduce the disulfide bond in the apocytochrome [54,64] (initially formed by the action of DsbA [65], or an environmental oxidant).

CcmF is a 13-transmembrane domain (TMD) integral membrane protein that contains four conserved histidines: two in transmembrane domains (TM-His1 and TM-His2) and two in periplasmic loops (P-His1 and P-His2) that flank the conserved WWD domain [44]. In the absence of other Ccm proteins, purified CcmF contains a stoichiometric and stable non-covalent heme b [44,66], which we have hypothesized plays a role in reducing the incoming heme from holoCcmE [42,66] (see Fig 2). Reduced heme (Fe^{2+}) is required for thioether formation [22,26],

and reduction would also favor the release of heme from CcmE His130 [42,43,66]. CcmF forms an integral membrane complex with CcmH, which has been purified [44] or co-immunoprecipitated [52,61,62]. CcmF (in complex with CcmH) is believed to be the site of thioether formation between the heme vinyls and the apocytochrome; thus, it has been termed the "cytochrome c heme lyase" or "cytochrome c synthetase" [42,67,68,69,70].

System II

Genetic analyses in *Chlamydomonas* [71,72,73,74] and some bacterial species (including *Bacillus* [75,76,77] and *Bordetella* [78,79,80]) in the mid-1990s revealed the presence of a pathway for cytochrome c assembly distinct from system I (Fig 2). These studies defined four proteins required for this pathway, termed system II: CcsA, CcsB, DsbD (or a related protein, CcdA, in some species), and CcsX (a thioredoxin involved in reduction of the apocytochrome Cys-Xxx-Xxx-Cys-His motif). The activities of DsbD and CcsX can be complemented by addition of thiol-reducing agents (e.g., dithiothreitol); therefore, DsbD and CcsX are thiol-reducing components of the system II pathway.

CcsA and CcsB consist of six and four TMDs, respectively. CcsA, a member of the heme handling protein (HHP) family, contains the conserved WWD domain flanked by two conserved histidines, and an additional conserved histidine in a transmembrane domain [50,81]. CcsB also contains a conserved transmembrane histidine and a large (up to 500 residues) poorly-conserved extra-cytoplasmic domain that is thought to be involved in apocytochrome handling [78]. Studies in *Bordetella* [79], and subsequent studies in heterologous *E. coli* [82], showed that CcsA and CcsB form a complex for cytochrome c assembly. The CcsBA protein complex, together, thus contains four conserved histidines (TM-His1 and 2, and P-His1 and 2) and the WWD domain, in a remarkably similar orientation to that of CcmF. In some species (such as

Helicobacter and *Wolinella*) system II is encoded as a single fused ORF, called *ccsBA*. Expression of CcsBA (from *Wolinella* [83] or *Helicobacter* [51]) heterologously in *E. coli* is sufficient to facilitate robust cytochrome c assembly; thus, CcsBA is the system II cytochrome c synthetase. The CcsBA complex is proposed to carry out the processes of heme translocation, apocytochrome binding, and thioether formation [42,82,84].

The CcsBA complex from *Helicobacter hepaticus* (expressed in *E. coli* as an N-terminal fusion to glutathione S-transferase) has been purified and characterized. Similar to CcmF, CcsBA purifies with a bound heme b. Mutation of either TM-His1 or TM-His2 abolishes or significantly impairs heme binding, while mutation of either P-His1 or P-His2 does not affect levels of the bound heme b. Each of the four histidines is required for cytochrome c assembly: substitution with alanine or glycine abolishes holocytochrome formation. Substitutions can be complemented chemically by adding imidazole directly to culture, thus confirming a heme ligand-type function for each His residue. Interestingly, imidazole complements only weakly under aerobic conditions, while anaerobically, imidazole restores function to near-WT levels. This suggests that the His residues in CcsBA may function to protect heme from oxidation as it is being channeled from its transmembrane binding site to the external WWD.

System III

The gene product responsible for cytochrome c formation in *Saccharomyces cerevisiae* was identified in 1987 by Dumont and colleagues [85]. Termed the holocytochrome c synthase (HCCS) or cytochrome c heme lyase (CCHL), this enzyme, when expressed in the *E. coli* cytoplasm (along with its cognate apocytochrome), is sufficient for holoctyochrome c formation (Fig 2) [86]. HCCS, which comprises system III, functions in the intermembrane space of the mitochondria of most eukaryotes (including humans). In some species, there is a dedicated heme

lyase (CC1HL) for covalent heme attachment to cytochrome c1 [85,87], while in others a single HCCS is active towards both cytochrome c and cytochrome c1 [67,88]. CC1HL is highly related to CCHL.

HCCS is required for the import of the nuclear-encoded apocytochrome into mitochondria [89,90]. Mitochondrial import of the unfolded apocytochrome is initially mediated by components of the TOM complex [21], and, subsequently, depends on recognition of the incoming N-terminus of the apocytochrome by HCCS. Covalent heme attachment by HCCS (and subsequent folding of the holocytochrome c) prevents the holocytochrome from re-exiting the intermembrane space [89,90,91,92]. Import of the membrane-bound cytochrome c1 occurs via a separate mechanism [93] that does not involve a cytochrome c heme lyase. A number of studies (all using the HCCS from *S. cerevisiae*) in yeast and *E. coli* have identified residues in the apocytochrome N-terminus (including the Cys-Xxx-Xxx-Cys-His motif) that are required for mitochondrial import and/or covalent heme attachment [86,94,95,96,97,98]. Cyc2p, a FAD-binding protein, is an accessory protein that is important, but not required, for maturation [99,100,101]. This protein is present only in *S. cerevisiae* and may play a role in reducing heme, but more work is needed to determine its precise function. An earlier report suggested that Cys-Pro-Xxx motifs in HCCS might be heme-binding sites [102] (Fig 2), but since these motifs are absent in some HCCSs [67], this is unlikely.

Other systems for cytochrome c assembly

Greater than 99 % of organisms rely on systems I, II, or III for cytochrome c biogenesis. However, some rare, alternative pathways exist for holocytochrome c formation. System IV, also called the ccb pathway, is a dedicated pathway for covalent heme attachment to a single cysteine in cytochrome b6 of the cytochrome b6f complex [103,104], present in the chloroplasts

of the oxygenic phototrophs [105]. Some archaea and a very few bacteria contain an abbreviated ccm pathway (which some have termed system I') that lacks a clear homolog of CcmH, and in which the covalent heme-binding histidine of CcmE has been replaced with a cysteine [106]. Finally, certain protozoa, which produce a unique cytochrome c with covalent attachment to a single Cys (i.e., Ala-Xxx-Xxx-Cys-His), do not appear to encode the genes for system I, II, or III [107,108,109]. The cytochrome c assembly pathway present in these organisms has been designated System V, although this nomenclature may be premature since the genes that comprise this apparent system have yet to be identified.

Evolutionary history of the three systems

Why are there three separate systems for cytochrome c assembly, and what, if any, are the advantages conferred? All mitochondria contain either system I or system III. Since the ancestor of the modern mitochondrion (an alpha-proteobacterium) contains system I, it is clear that system III evolved in mitochondria after the mitochondrial endosymbiosis [110,111,112]. We hypothesize that at some point after endosymbiosis, the complicated, ATP-dependent system I may have become "obsolete" and was replaced by the simpler system III. The protozoa are especially useful to consider in this regard, since some protozoal mitochondria contain system I and some contain system III. The protozoa that contain system I may be evolutionary "holdovers" stuck in the transition from system I to system III, and future studies may reveal some species that contain both systems. We speculate that the mitochondria of plants (all of which contain system I) and those protozoa that contain system I, may face more challenging environments for cytochrome c synthesis (possibly iron- or heme-poor, and certainly highly oxidizing) such that the advantages of the system I pathway are required (see below). Note that system I, as well as system II, has evolved to maintain heme in (or reduce heme to) the Fe^{2+}

state; thus, plants may have retained system I (in mitochondria) and system II (in chloroplasts) to protect heme from oxidation.

Dissecting the evolutionary history of systems I and II is complicated by the significant lateral gene transfer that has occurred with these two systems [38]. One would expect that system II (with its lower energetic requirement) should predominate unless system I confers some selection advantage. We showed previously that system I can synthesize cytochromes at 5-fold lower heme levels than can system II [113], and that holoCcmE of system I can function as a heme reservoir [51]. Thus, we speculate that the holoCcmE heme reservoir and high heme affinity of system I may have evolved (and was retained) to meet the challenges of synthesizing cytochromes in iron- or heme-poor environments. Attempts to correlate the occurrence of a given system (I or II) with a specific bacterial microhabitat (e.g., iron-poor or iron-rich) have been difficult, owing primarily to the lack of information about the microhabitats of microorganisms. Interestingly, some species (e.g., *Bordetella parapertussis*) encode the genes for both systems I and II. Whether both systems are actively expressed, or expressed differentially as a function of environmental conditions, has not been examined, but organisms such as these may offer clues as to the evolutionary advantages of a system I versus a system II cytochrome c assembly pathway.

Significance, Summary, and Scope of the Thesis

Early studies in the field of cytochrome c assembly were directed at identifying the gene products required for assembly. Reconstitution of each of the three major pathways heterologously in *E. coli* (Δ*ccm*, deleted for the endogeneous cytochrome c maturation genes) was a major advance in this regard. More recent approaches have been designed to elucidate the molecular mechanisms underlying cytochrome c assembly, including heme trafficking, control of redox state, and protein-protein interactions. Of particular interest to this thesis are the structural and mechanistic aspects of the synthase proteins and protein complexes of systems I (CcmFH) and III (HCCS), and the molecular details of their function (Fig 2).

At the beginning of this research, some limited biochemical progress had been made with several system I proteins: high-resolution three-dimensional structures had become available for the soluble domains of apoCcmE [114], CcmG [56] and CcmH [57]. Excitingly, the first biochemical and spectroscopic characterization of the putative system I synthetase, CcmF (from *E. coli*), had just been reported from the Kranz lab, with the discovery that CcmF (purified in the absence of other Ccm proteins) contained a stable and stoichiometric heme b [44]. A possible heme ligand (TM-His1) to the heme b had been identified, and, crucially, a revised topology for CcmF had been reported. The updated topology revealed that CcmF contained two additional TMDs, which repositioned the WWD domain adjacent to the outer leaflet of the cytoplasmic membrane, where it is flanked by two conserved His residues (P-His1 and P-His2). Importantly, the new topology illustrated the marked structural similarities between CcmF and the other WWD-domain containing proteins, CcsBA (the cytochrome c synthetase of system II) and CcmC.

Building off of these findings, the first aim of this research was to define and spectroscopically characterize the b-heme binding site within CcmF, with the ultimate goal of understanding the role of this heme in cytochrome c biogenesis. This research, discussed in chapter 2, identified the second axial ligand to the b-heme (TM-His2), and piloted the used of exogeneous imidazole to chemically complement the cytochrome c assembly defects of substitutions at either TM-His1 or TM-His2 in CcmF, thus solidifying the heme-binding function of these residues. The role of these histidines as axial ligands to the heme b was confirmed by resonance Raman spectroscopy, in collaboration with Dr. Kenton Rodgers (NDSU). A reliable and tractable assay for the determination of redox potentials was adapted (from the laboratory of Dr. Emma Raven, Leicester University) for use with membrane proteins, and was employed to determine the midpoint potential of the heme b in CcmF. This constituted the first functionally-relevant data pertaining to the heme b: since the midpoint potential was below (more negative than) that of the heme in holoCcmE, our hypothesis that the heme b may be involved in reduction of the incoming heme from holoCcmE (thus preparing it for attachment to the apocytochrome) is indeed feasible.

Another significant thrust of this research was devoted to understanding interactions between CcmF and other Ccm proteins. Formation of a complex between CcmF and CcmH had been well-documented [44,52,61,62], although the specific sites of interaction in each protein were (and are) still unknown. Less-well understood, however, was the interaction of CcmF with the periplasmic heme chaperone protein, holoCcmE. Although nearly every review on cytochrome c biosynthesis in the last decade had proposed formation of a holoCcmE-CcmF complex as an intermediate required for holocytochrome formation [42,67,68,69,70], data directly demonstrating this interaction had not been reported. Another similarly conspicuous gap

in our understanding of system I was the absence of direct experimental evidence that CcmF (in complex with CcmH) is the synthetase for system I. Unlike systems II and system III (which are single proteins or protein complexes whose expression in *E. coli* Δ*ccm* is sufficient for robust holocytochrome c formation), CcmF had never been shown to be capable of synthesizing cytochrome c in the absence of other Ccm proteins. The assignment of the synthetase activity was largely circumstantial in that it was based primarily on interactions with other Ccm proteins, some of which were experimentally-supported (e.g., with CcmH, which has a demonstrated apocytochrome binding function) and others that were more hypothetical (i.e., with holoCcmE).

Research in this thesis showed, directly, that CcmFH (along with CcmG) is the cytochrome c synthetase of system I: expression of CcmFGH (in the absence of other Ccm components) in *E. coli* Δ*ccm* is sufficient for robust covalent heme attachment to bacterial cytochromes c2 and c4. The synthetase activity required three conserved histidines in CcmF (TM-His1 and 2, and P-His1) as well as the conserved cysteine pairs in the thioredoxins CcmG and CcmH, and led to production of holocytochrome c with biochemical and spectroscopic properties indistinguishable from that produced by the full system I. These studies are discussed in chapter 4. Chapter 3 of this thesis discusses characterization of the CcmF-holoCcmE complex, trapped only in the absence of CcmH, with the discovery that complex formation depends on all four conserved His residues in CcmF. HoloCcmE must be released from complex with CcmABCD in order to interact with CcmF, and heme in holoCcmE was required for complex formation with CcmF: apoCcmE interacted at 20-fold lower levels than holoCcmE. Together, these results address two important remaining questions in cytochrome c biogenesis, and fill some of the larger gaps in the field.

For system III, progress in understanding the mechanisms underlying HCCS function had been severely impeded by difficulties in expression and purification [24]. In fact, despite the identification of HCCS as the gene product responsible for heme attachment to cytochrome *c* in *Saccharomyces cerevisiae* over twenty-five years ago [85], the enzyme had never been purified or characterized, and the mechanism by which HCCS mediates covalent heme attachment to the apocytochrome was poorly understood. Every review on mitochondrial cytochrome c assembly states this deficiency (e.g., [24,42,67,68]). Chapter 5 of this work discusses successful purification and characterization of the human HCCS from recombinant *E. coli*. The human HCCS was found to be membrane-associated (despite the absence of predicted TMDs) and was purified with endogenous heme coordinated by a conserved histidine (His154). The amino acids in the human apocytochrome required for covalent attachment were identified, and the non-substrate cytochrome c_2 from the alpha-proteobacterium *Rhodobacter capsulatus* was converted into a robust substrate for the human HCCS by engineering three sequence alterations. Trapped, intermediate complexes between HCCS, heme, and cytochrome c, with a conserved histidine in each protein serving as a heme axial ligand, were purified and characterized. These findings suggest mechanisms for heme binding, interaction with apocytochrome *c*, thioether formation, and release of mature holocytochrome *c* from HCCS.

References

1. O'Brian MR, Thony-Meyer L (2002) Biochemistry, regulation and genomics of haem biosynthesis in prokaryotes. Adv Microb Physiol 46: 257-318.
2. Kranz R, Lill R, Goldman B, Bonnard G, Merchant S (1998) Molecular mechanisms of cytochrome c biogenesis: three distinct systems. Mol Microbiol 29: 383-396.
3. Mogi T, Saiki K, Anraku Y (1994) Biosynthesis and functional role of haem O and haem A. Mol Microbiol 14: 391-398.
4. Page MD, Sambongi Y, Ferguson SJ (1998) Contrasting routes of c-type cytochrome assembly in mitochondria, chloroplasts and bacteria. Trends Biochem Sci 23: 103-108.
5. Thony-Meyer L (1997) Biogenesis of respiratory cytochromes in bacteria. Microbiol Mol Biol Rev 61: 337-376.
6. Allen JW, Ginger ML, Ferguson SJ (2005) Complexity and diversity in c-type cytochrome biogenesis systems. Biochem Soc Trans 33: 145-146.
7. Richardson DJ (2000) Bacterial respiration: a flexible process for a changing environment. Microbiology 146 (Pt 3): 551-571.
8. Gralnick JA, Newman DK (2007) Extracellular respiration. Mol Microbiol 65: 1-11.
9. Shi L, Squier TC, Zachara JM, Fredrickson JK (2007) Respiration of metal (hydr)oxides by Shewanella and Geobacter: a key role for multihaem c-type cytochromes. Mol Microbiol 65: 12-20.
10. Lee D, Pervushin K, Bischof D, Braun M, Thony-Meyer L (2005) Unusual heme-histidine bond in the active site of a chaperone. J Am Chem Soc 127: 3716-3717.
11. Reid E, Eaves DJ, Cole JA (1998) The CcmE protein from Escherichia coli is a haem-binding protein. FEMS Microbiol Lett 166: 369-375.
12. Schulz H, Hennecke H, Thony-Meyer L (1998) Prototype of a heme chaperone essential for cytochrome c maturation. Science 281: 1197-1200.
13. Uchida T, Stevens JM, Daltrop O, Harvat EM, Hong L, et al. (2004) The interaction of covalently bound heme with the cytochrome c maturation protein CcmE. J Biol Chem 279: 51981-51988.
14. Lecomte JT, Vuletich DA, Vu BC, Kuriakose SA, Scott NL, et al. (2004) Structural properties of cyanobacterial hemoglobins: the unusual heme-protein cross-link of Synechocystis sp. PCC 6803 Hb and Synechococcus sp. PCC 7002 Hb. Micron 35: 71-72.
15. Vu BC, Jones AD, Lecomte JT (2002) Novel histidine-heme covalent linkage in a hemoglobin. J Am Chem Soc 124: 8544-8545.
16. Vu BC, Vuletich DA, Kuriakose SA, Falzone CJ, Lecomte JT (2004) Characterization of the heme-histidine cross-link in cyanobacterial hemoglobins from Synechocystis sp. PCC 6803 and Synechococcus sp. PCC 7002. J Biol Inorg Chem 9: 183-194.
17. Palmer G, Reedijk J (1991) Nomenclature Committee of the International Union of Biochemistry (NC-IUB). Nomenclature of electron-transfer proteins. Recommendations 1989. Biochim Biophys Acta 1060: 599-611.
18. Berry EA, Trumpower BL (1987) Simultaneous determination of hemes a, b, and c from pyridine hemochrome spectra. Anal Biochem 161: 1-15.
19. Page MD, Ferguson SJ (1990) Apo forms of cytochrome c550 and cytochrome cd1 are translocated to the periplasm of Paracoccus denitrificans in the absence of haem

incorporation caused either mutation or inhibition of haem synthesis. Mol Microbiol 4: 1181-1192.
20. Page MD, Ferguson SJ (1989) A bacterial c-type cytochrome can be translocated to the periplasm as an apo form; the biosynthesis of cytochrome cd1 (nitrite reductase) from Paracoccus denitrificans. Mol Microbiol 3: 653-661.
21. Diekert K, de Kroon AI, Ahting U, Niggemeyer B, Neupert W, et al. (2001) Apocytochrome c requires the TOM complex for translocation across the mitochondrial outer membrane. Embo J 20: 5626-5635.
22. Barker PD, Ferrer JC, Mylrajan M, Loehr TM, Feng R, et al. (1993) Transmutation of a heme protein. Proc Natl Acad Sci U S A 90: 6542-6546.
23. Barker PD, Nerou EP, Freund SM, Fearnley IM (1995) Conversion of cytochrome b562 to c-type cytochromes. Biochemistry 34: 15191-15203.
24. Allen JW (2011) Cytochrome c biogenesis in mitochondria--Systems III and V. Febs J 278: 4198-4216.
25. Hartshorne S, Richardson DJ, Simon J (2006) Multiple haem lyase genes indicate substrate specificity in cytochrome c biogenesis. Biochem Soc Trans 34: 146-149.
26. Nicholson DW, Neupert W (1989) Import of cytochrome c into mitochondria: reduction of heme, mediated by NADH and flavin nucleotides, is obligatory for its covalent linkage to apocytochrome c. Proc Natl Acad Sci U S A 86: 4340-4344.
27. Barker PD, Ferguson SJ (1999) Still a puzzle: why is haem covalently attached in c-type cytochromes? Structure 7: R281-290.
28. Beckman DL, Kranz RG (1993) Cytochromes c biogenesis in a photosynthetic bacterium requires a periplasmic thioredoxin-like protein. Proc Natl Acad Sci U S A 90: 2179-2183.
29. Beckman DL, Trawick DR, Kranz RG (1992) Bacterial cytochromes c biogenesis. Genes Dev 6: 268-283.
30. Kranz RG (1989) Isolation of mutants and genes involved in cytochromes c biosynthesis in Rhodobacter capsulatus. J Bacteriol 171: 456-464.
31. Lang SE, Jenney FE, Jr., Daldal F (1996) Rhodobacter capsulatus CycH: a bipartite gene product with pleiotropic effects on the biogenesis of structurally different c-type cytochromes. J Bacteriol 178: 5279-5290.
32. Page MD, Ferguson SJ (1995) Cloning and sequence analysis of cycH gene from Paracoccus denitrificans: the cycH gene product is required for assembly of all c-type cytochromes, including cytochrome c1. Mol Microbiol 15: 307-318.
33. Page MD, Ferguson SJ (1997) Paracoccus denitrificans CcmG is a periplasmic protein-disulphide oxidoreductase required for c- and aa3-type cytochrome biogenesis; evidence for a reductase role in vivo. Mol Microbiol 24: 977-990.
34. Page MD, Pearce DA, Norris HA, Ferguson SJ (1997) The Paracoccus denitrificans ccmA, B and C genes: cloning and sequencing, and analysis of the potential of their products to form a haem or apo- c-type cytochrome transporter. Microbiology 143 (Pt 2): 563-576.
35. Ramseier TM, Winteler HV, Hennecke H (1991) Discovery and sequence analysis of bacterial genes involved in the biogenesis of c-type cytochromes. J Biol Chem 266: 7793-7803.
36. Ritz D, Thony-Meyer L, Hennecke H (1995) The cycHJKL gene cluster plays an essential role in the biogenesis of c-type cytochromes in Bradyrhizobium japonicum. Mol Gen Genet 247: 27-38.

37. Thony-Meyer L, Fischer F, Kunzler P, Ritz D, Hennecke H (1995) Escherichia coli genes required for cytochrome c maturation. J Bacteriol 177: 4321-4326.
38. Goldman BS, Kranz RG (1998) Evolution and horizontal transfer of an entire biosynthetic pathway for cytochrome c biogenesis: Helicobacter, Deinococcus, Archae and more. Mol Microbiol 27: 871-873.
39. Meyer EH, Giege P, Gelhaye E, Rayapuram N, Ahuja U, et al. (2005) AtCCMH, an essential component of the c-type cytochrome maturation pathway in Arabidopsis mitochondria, interacts with apocytochrome c. Proc Natl Acad Sci U S A 102: 16113-16118.
40. Spielewoy N, Schulz H, Grienenberger JM, Thony-Meyer L, Bonnard G (2001) CCME, a nuclear-encoded heme-binding protein involved in cytochrome c maturation in plant mitochondria. J Biol Chem 276: 5491-5497.
41. Thony-Meyer L, Kunzler P (1997) Translocation to the periplasm and signal sequence cleavage of preapocytochrome c depend on sec and lep, but not on the ccm gene products. Eur J Biochem 246: 794-799.
42. Kranz RG, Richard-Fogal C, Taylor JS, Frawley ER (2009) Cytochrome c biogenesis: mechanisms for covalent modifications and trafficking of heme and for heme-iron redox control. Microbiol Mol Biol Rev 73: 510-528, Table of Contents.
43. Richard-Fogal C, Kranz RG (2010) The CcmC:heme:CcmE complex in heme trafficking and cytochrome c biosynthesis. J Mol Biol 401: 350-362.
44. Richard-Fogal CL, Frawley ER, Bonner ER, Zhu H, San Francisco B, et al. (2009) A conserved haem redox and trafficking pathway for cofactor attachment. Embo J 28: 2349-2359.
45. Stevens JM, Daltrop O, Higham CW, Ferguson SJ (2003) Interaction of heme with variants of the heme chaperone CcmE carrying active site mutations and a cleavable N-terminal His tag. J Biol Chem 278: 20500-20506.
46. Lee JH, Harvat EM, Stevens JM, Ferguson SJ, Saier MH, Jr. (2007) Evolutionary origins of members of a superfamily of integral membrane cytochrome c biogenesis proteins. Biochim Biophys Acta 1768: 2164-2181.
47. Christensen O, Harvat EM, Thony-Meyer L, Ferguson SJ, Stevens JM (2007) Loss of ATP hydrolysis activity by CcmAB results in loss of c-type cytochrome synthesis and incomplete processing of CcmE. Febs J 274: 2322-2332.
48. Feissner RE, Richard-Fogal CL, Frawley ER, Kranz RG (2006) ABC transporter-mediated release of a haem chaperone allows cytochrome c biogenesis. Mol Microbiol 61: 219-231.
49. Goldman BS, Beckman DL, Bali A, Monika EM, Gabbert KK, et al. (1997) Molecular and immunological analysis of an ABC transporter complex required for cytochrome c biogenesis. J Mol Biol 268: 724-738.
50. Goldman BS, Beck DL, Monika EM, Kranz RG (1998) Transmembrane heme delivery systems. Proc Natl Acad Sci U S A 95: 5003-5008.
51. Feissner RE, Richard-Fogal CL, Frawley ER, Loughman JA, Earley KW, et al. (2006) Recombinant cytochromes c biogenesis systems I and II and analysis of haem delivery pathways in Escherichia coli. Mol Microbiol 60: 563-577.
52. Ren Q, Ahuja U, Thony-Meyer L (2002) A bacterial cytochrome c heme lyase. CcmF forms a complex with the heme chaperone CcmE and CcmH but not with apocytochrome c. J Biol Chem 277: 7657-7663.

53. Turkarslan S, Sanders C, Ekici S, Daldal F (2008) Compensatory thio-redox interactions between DsbA, CcdA and CcmG unveil the apocytochrome c holdase role of CcmG during cytochrome c maturation. Mol Microbiol 70: 652-666.
54. Monika EM, Goldman BS, Beckman DL, Kranz RG (1997) A thioreduction pathway tethered to the membrane for periplasmic cytochromes c biogenesis; in vitro and in vivo studies. J Mol Biol 271: 679-692.
55. Di Matteo A, Calosci N, Gianni S, Jemth P, Brunori M, et al. (2010) Structural and functional characterization of CcmG from Pseudomonas aeruginosa, a key component of the bacterial cytochrome c maturation apparatus. Proteins 78: 2213-2221.
56. Ouyang N, Gao YG, Hu HY, Xia ZX (2006) Crystal structures of E. coli CcmG and its mutants reveal key roles of the N-terminal beta-sheet and the fingerprint region. Proteins 65: 1021-1031.
57. Di Matteo A, Gianni S, Schinina ME, Giorgi A, Altieri F, et al. (2007) A strategic protein in cytochrome c maturation: three-dimensional structure of CcmH and binding to apocytochrome c. J Biol Chem 282: 27012-27019.
58. Zheng XM, Hong J, Li HY, Lin DH, Hu HY (2012) Biochemical properties and catalytic domain structure of the CcmH protein from Escherichia coli. Biochim Biophys Acta 1824: 1394-1400.
59. Verissimo AF, Yang H, Wu X, Sanders C, Daldal F (2011) CcmI subunit of CcmFHI heme ligation complex functions as an apocytochrome c chaperone during c-type cytochrome maturation. J Biol Chem 286: 40452-40463.
60. Di Silvio E, Di Matteo A, Malatesta F, Travaglini-Allocatelli C (2013) Recognition and binding of apocytochrome c to P. aeruginosa CcmI, a component of cytochrome c maturation machinery. Biochim Biophys Acta 1834: 1554-1561.
61. Rayapuram N, Hagenmuller J, Grienenberger JM, Bonnard G, Giege P (2008) The three mitochondrial encoded CcmF proteins form a complex that interacts with CCMH and c-type apocytochromes in Arabidopsis. J Biol Chem 283: 25200-25208.
62. Sanders C, Turkarslan S, Lee DW, Onder O, Kranz RG, et al. (2008) The cytochrome c maturation components CcmF, CcmH, and CcmI form a membrane-integral multisubunit heme ligation complex. J Biol Chem 283: 29715-29722.
63. Stirnimann CU, Rozhkova A, Grauschopf U, Grutter MG, Glockshuber R, et al. (2005) Structural basis and kinetics of DsbD-dependent cytochrome c maturation. Structure 13: 985-993.
64. Setterdahl AT, Goldman BS, Hirasawa M, Jacquot P, Smith AJ, et al. (2000) Oxidation-reduction properties of disulfide-containing proteins of the Rhodobacter capsulatus cytochrome c biogenesis system. Biochemistry 39: 10172-10176.
65. Metheringham R, Griffiths L, Crooke H, Forsythe S, Cole J (1995) An essential role for DsbA in cytochrome c synthesis and formate-dependent nitrite reduction by Escherichia coli K-12. Arch Microbiol 164: 301-307.
66. San Francisco B, Bretsnyder EC, Rodgers KR, Kranz RG (2011) Heme ligand identification and redox properties of the cytochrome c synthetase, CcmF. Biochemistry 50: 10974-10985.
67. Hamel P, Corvest V, Giege P, Bonnard G (2009) Biochemical requirements for the maturation of mitochondrial c-type cytochromes. Biochim Biophys Acta 1793: 125-138.

68. Mavridou DA, Ferguson SJ, Stevens JM (2013) Cytochrome c assembly. IUBMB Life 65: 209-216.
69. Sanders C, Turkarslan S, Lee DW, Daldal F (2010) Cytochrome c biogenesis: the Ccm system. Trends Microbiol 18: 266-274.
70. Sawyer EB, Barker PD (2012) Continued surprises in the cytochrome c biogenesis story. Protein Cell 3: 405-409.
71. Dreyfuss BW, Hamel PP, Nakamoto SS, Merchant S (2003) Functional analysis of a divergent system II protein, Ccs1, involved in c-type cytochrome biogenesis. J Biol Chem 278: 2604-2613.
72. Inoue K, Dreyfuss BW, Kindle KL, Stern DB, Merchant S, et al. (1997) Ccs1, a nuclear gene required for the post-translational assembly of chloroplast c-type cytochromes. J Biol Chem 272: 31747-31754.
73. Xie Z, Merchant S (1996) The plastid-encoded ccsA gene is required for heme attachment to chloroplast c-type cytochromes. J Biol Chem 271: 4632-4639.
74. Xie Z, Merchant S (1998) A novel pathway for cytochromes c biogenesis in chloroplasts. Biochim Biophys Acta 1365: 309-318.
75. Le Brun NE, Bengtsson J, Hederstedt L (2000) Genes required for cytochrome c synthesis in Bacillus subtilis. Mol Microbiol 36: 638-650.
76. Schiott T, Throne-Holst M, Hederstedt L (1997) Bacillus subtilis CcdA-defective mutants are blocked in a late step of cytochrome c biogenesis. J Bacteriol 179: 4523-4529.
77. Schiott T, von Wachenfeldt C, Hederstedt L (1997) Identification and characterization of the ccdA gene, required for cytochrome c synthesis in Bacillus subtilis. J Bacteriol 179: 1962-1973.
78. Beckett CS, Loughman JA, Karberg KA, Donato GM, Goldman WE, et al. (2000) Four genes are required for the system II cytochrome c biogenesis pathway in Bordetella pertussis, a unique bacterial model. Mol Microbiol 38: 465-481.
79. Feissner RE, Beckett CS, Loughman JA, Kranz RG (2005) Mutations in cytochrome assembly and periplasmic redox pathways in Bordetella pertussis. J Bacteriol 187: 3941-3949.
80. Kranz RG, Beckett CS, Goldman BS (2002) Genomic analyses of bacterial respiratory and cytochrome c assembly systems: Bordetella as a model for the system II cytochrome c biogenesis pathway. Res Microbiol 153: 1-6.
81. Hamel PP, Dreyfuss BW, Xie Z, Gabilly ST, Merchant S (2003) Essential histidine and tryptophan residues in CcsA, a system II polytopic cytochrome c biogenesis protein. J Biol Chem 278: 2593-2603.
82. Frawley ER, Kranz RG (2009) CcsBA is a cytochrome c synthetase that also functions in heme transport. Proc Natl Acad Sci U S A 106: 10201-10206.
83. Kern M, Scheithauer J, Kranz RG, Simon J (2010) Essential histidine pairs indicate conserved haem binding in epsilonproteobacterial cytochrome c haem lyases. Microbiology 156: 3773-3781.
84. Merchant SS (2009) His protects heme as it crosses the membrane. Proc Natl Acad Sci U S A 106: 10069-10070.
85. Dumont ME, Ernst JF, Hampsey DM, Sherman F (1987) Identification and sequence of the gene encoding cytochrome c heme lyase in the yeast Saccharomyces cerevisiae. Embo J 6: 235-241.

86. Pollock WB, Rosell FI, Twitchett MB, Dumont ME, Mauk AG (1998) Bacterial expression of a mitochondrial cytochrome c. Trimethylation of lys72 in yeast iso-1-cytochrome c and the alkaline conformational transition. Biochemistry 37: 6124-6131.
87. Zollner A, Rodel G, Haid A (1992) Molecular cloning and characterization of the Saccharomyces cerevisiae CYT2 gene encoding cytochrome-c1-heme lyase. Eur J Biochem 207: 1093-1100.
88. Bernard DG, Gabilly ST, Dujardin G, Merchant S, Hamel PP (2003) Overlapping specificities of the mitochondrial cytochrome c and c1 heme lyases. J Biol Chem 278: 49732-49742.
89. Dumont ME, Cardillo TS, Hayes MK, Sherman F (1991) Role of cytochrome c heme lyase in mitochondrial import and accumulation of cytochrome c in Saccharomyces cerevisiae. Mol Cell Biol 11: 5487-5496.
90. Nargang FE, Drygas ME, Kwong PL, Nicholson DW, Neupert W (1988) A mutant of Neurospora crassa deficient in cytochrome c heme lyase activity cannot import cytochrome c into mitochondria. J Biol Chem 263: 9388-9394.
91. Dumont ME, Ernst JF, Sherman F (1988) Coupling of heme attachment to import of cytochrome c into yeast mitochondria. Studies with heme lyase-deficient mitochondria and altered apocytochromes c. J Biol Chem 263: 15928-15937.
92. Nicholson DW, Hergersberg C, Neupert W (1988) Role of cytochrome c heme lyase in the import of cytochrome c into mitochondria. J Biol Chem 263: 19034-19042.
93. Arnold I, Folsch H, Neupert W, Stuart RA (1998) Two distinct and independent mitochondrial targeting signals function in the sorting of an inner membrane protein, cytochrome c1. J Biol Chem 273: 1469-1476.
94. Jeng WY, Chen CY, Chang HC, Chuang WJ (2002) Expression and characterization of recombinant human cytochrome c in E. coli. J Bioenerg Biomembr 34: 423-431.
95. Kleingardner JG, Bren KL (2011) Comparing substrate specificity between cytochrome c maturation and cytochrome c heme lyase systems for cytochrome c biogenesis. Metallomics 3: 396-403.
96. Patel CN, Lind MC, Pielak GJ (2001) Characterization of horse cytochrome c expressed in Escherichia coli. Protein Expr Purif 22: 220-224.
97. Rumbley JN, Hoang L, Englander SW (2002) Recombinant equine cytochrome c in Escherichia coli: high-level expression, characterization, and folding and assembly mutants. Biochemistry 41: 13894-13901.
98. Stevens JM, Zhang Y, Muthuvel G, Sam KA, Allen JW, et al. (2011) The mitochondrial cytochrome c N-terminal region is critical for maturation by holocytochrome c synthase. FEBS Lett 585: 1891-1896.
99. Bernard DG, Quevillon-Cheruel S, Merchant S, Guiard B, Hamel PP (2005) Cyc2p, a membrane-bound flavoprotein involved in the maturation of mitochondrial c-type cytochromes. J Biol Chem 280: 39852-39859.
100. Corvest V, Murrey DA, Hirasawa M, Knaff DB, Guiard B, et al. (2012) The flavoprotein Cyc2p, a mitochondrial cytochrome c assembly factor, is a NAD(P)H-dependent haem reductase. Mol Microbiol 83: 968-980.
101. Dumont ME, Schlichter JB, Cardillo TS, Hayes MK, Bethlendy G, et al. (1993) CYC2 encodes a factor involved in mitochondrial import of yeast cytochrome c. Mol Cell Biol 13: 6442-6451.

102. Steiner H, Kispal G, Zollner A, Haid A, Neupert W, et al. (1996) Heme binding to a conserved Cys-Pro-Val motif is crucial for the catalytic function of mitochondrial heme lyases. J Biol Chem 271: 32605-32611.
103. Kuras R, de Vitry C, Choquet Y, Girard-Bascou J, Culler D, et al. (1997) Molecular genetic identification of a pathway for heme binding to cytochrome b6. J Biol Chem 272: 32427-32435.
104. Kuras R, Saint-Marcoux D, Wollman FA, de Vitry C (2007) A specific c-type cytochrome maturation system is required for oxygenic photosynthesis. Proc Natl Acad Sci U S A 104: 9906-9910.
105. Lezhneva L, Kuras R, Ephritikhine G, de Vitry C (2008) A novel pathway of cytochrome c biogenesis is involved in the assembly of the cytochrome b6f complex in arabidopsis chloroplasts. J Biol Chem 283: 24608-24616.
106. Allen JW, Harvat EM, Stevens JM, Ferguson SJ (2006) A variant System I for cytochrome c biogenesis in archaea and some bacteria has a novel CcmE and no CcmH. FEBS Lett 580: 4827-4834.
107. Allen JW, Ginger ML, Ferguson SJ (2004) Maturation of the unusual single-cysteine (XXXCH) mitochondrial c-type cytochromes found in trypanosomatids must occur through a novel biogenesis pathway. Biochem J 383: 537-542.
108. Allen JW, Jackson AP, Rigden DJ, Willis AC, Ferguson SJ, et al. (2008) Order within a mosaic distribution of mitochondrial c-type cytochrome biogenesis systems? Febs J 275: 2385-2402.
109. Fulop V, Sam KA, Ferguson SJ, Ginger ML, Allen JW (2009) Structure of a trypanosomatid mitochondrial cytochrome c with heme attached via only one thioether bond and implications for the substrate recognition requirements of heme lyase. Febs J 276: 2822-2832.
110. Gray MW (1993) Origin and evolution of organelle genomes. Curr Opin Genet Dev 3: 884-890.
111. Kurland CG, Andersson SG (2000) Origin and evolution of the mitochondrial proteome. Microbiol Mol Biol Rev 64: 786-820.
112. Lang BF, Seif E, Gray MW, O'Kelly CJ, Burger G (1999) A comparative genomics approach to the evolution of eukaryotes and their mitochondria. J Eukaryot Microbiol 46: 320-326.
113. Richard-Fogal CL, Frawley ER, Feissner RE, Kranz RG (2007) Heme concentration dependence and metalloporphyrin inhibition of the system I and II cytochrome c assembly pathways. J Bacteriol 189: 455-463.
114. Arnesano F, Banci L, Barker PD, Bertini I, Rosato A, et al. (2002) Solution structure and characterization of the heme chaperone CcmE. Biochemistry 41: 13587-13594.

Figures

Figure 1. Structure of heme c and genes required for heme c formation.

Porphyrin ring carbon atoms are numbered according to the Fischer system. Diagram is modified from [42].

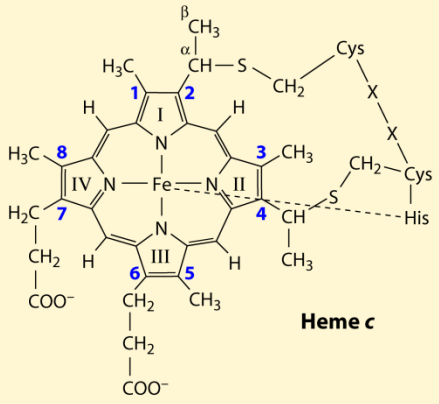

Heme *c*

System I = *ccmABCDEFGH*

System II = *ccsB ccsA*

System III = *CYC3* (CCHL)

Figure 2. Systems I, II, and III for cytochrome c biogenesis.

Models depict subpathways for trafficking of heme and apocytochrome during holocytochrome c formation. Representative organisms possessing each system are listed. Diagram is modified from [42].

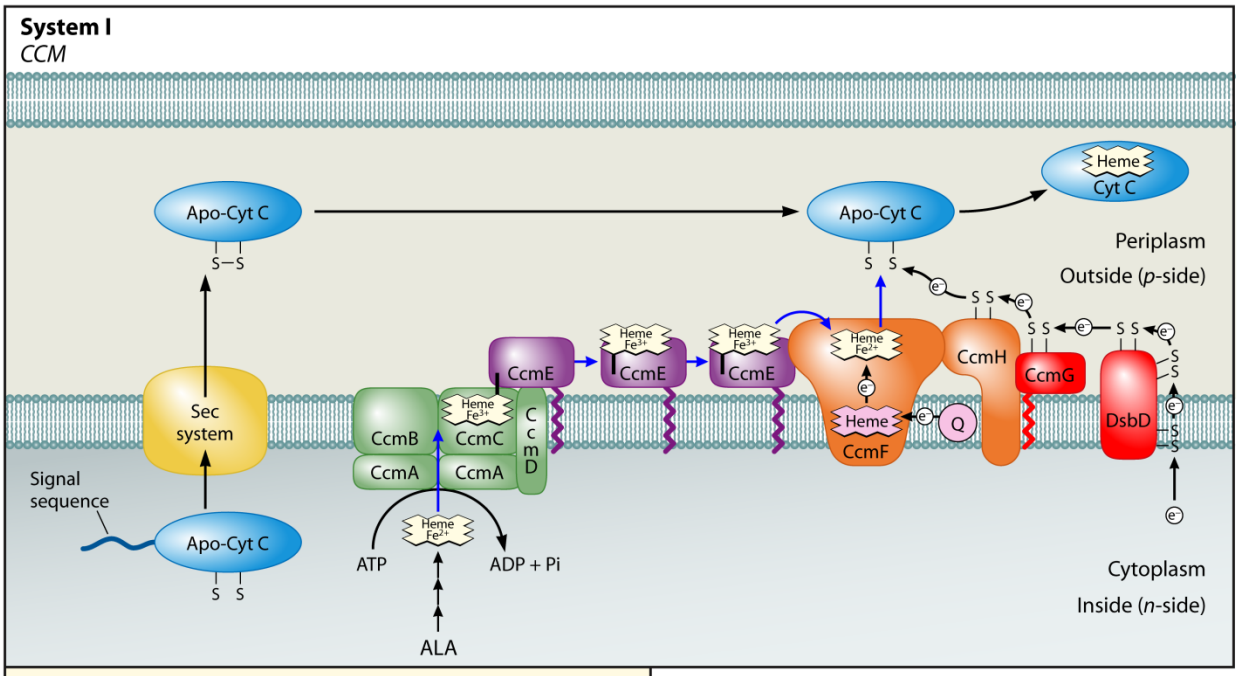

α Proteobacteria (e.g. Rhodobacter, Agrobacterium, Caulobacter)
γ Proteobacteria (e.g. Escherichia, Pseudomonas, Shewanella, Vibrio)
Some β proteobacteria (e.g. Nitrosomonas, Nitrospira)
Some δ proteobacateria (e.g. Myxococcus, Deslfovibrio)
Plant mitochondria (e.g. Oryza, Triticum, Arabidopsis)
Some protozoal mitochondria (e.g. Reclinomonas, Paramecium, Tetrahymena)
Deinococci (e.g. Deinococcus, Thermus)
Archaea (e.g. Archaeolglobus)

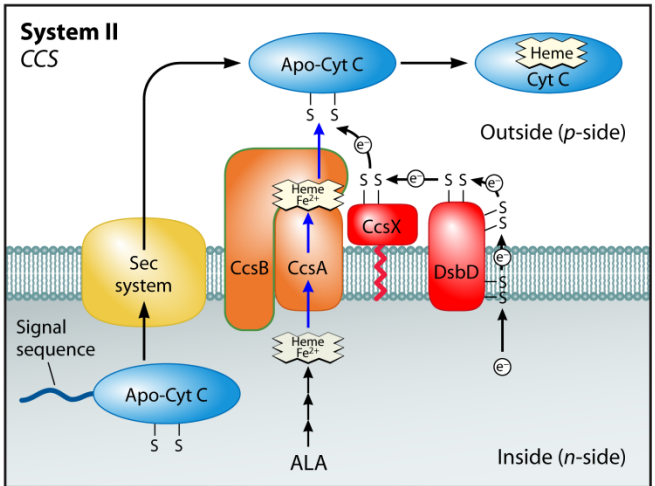

Chloroplasts (e.g. Chlamydomonas, Arabidopsis)
Gram positive bacteria (e.g. Mycobacterium, Bacillus)
Cyanobacteria (e.g. Synechocystis)
ε proteobacateria (e.g. Heliobacter, Wolinella)
Most β proteobacteria (e.g. Bordetella, Neisseria, Burkholderia)
Some δ proteobacateria (e.g. Geobacter, Bdellovibrio)

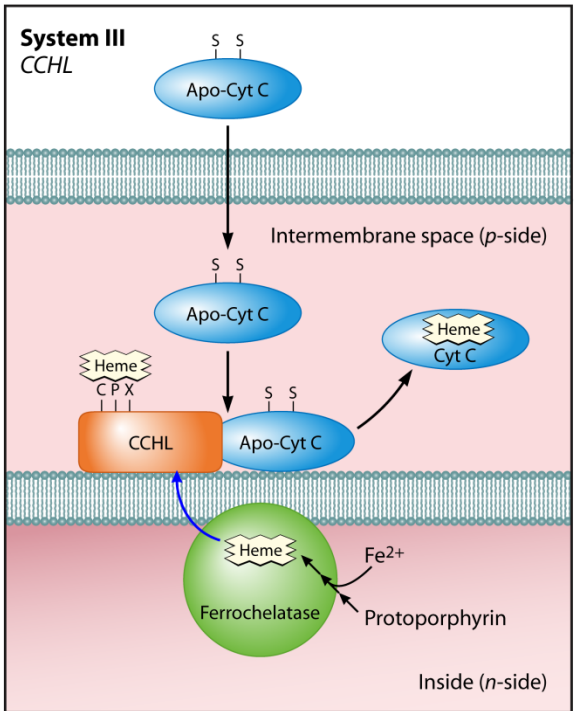

Fungal mitochondria (e.g. Saccharomyces)
Vertebrate mitochondria (e.g. Mouse, Human)
Invertebrate mitochondria (e.g. Caenorhabditis, Drosophila)
Some protozoal mitochondria (e.g. Plasmodium, Dictyostelium, Volvox, Chlamydomonus)

Chapter 2: Heme ligand identification and redox properties of the cytochrome c synthetase, CcmF

Brian San Francisco,[‡] Eric C. Bretsnyder,[‡] Kenton R. Rodgers,[§] and Robert G. Kranz [‡,*]

[‡]*Department of Biology, Washington University in St. Louis, St. Louis, Missouri 63130*

[§]*Department of Chemistry, Biochemistry, and Molecular Biology, North Dakota State University, Fargo, North Dakota 58102*

Published in *Biochemistry* (2011) 50: 10974-10985.

This work was supported by National Institutes of Health grants GM47909 to R. G. K. and AI072719 to K. R. R.

[*]To whom correspondence should be addressed. Telephone: 314-935-4278. Fax: 314-935-4432. E-mail: kranz@biology.wustl.edu

Abbreviations: Ccm, cytochrome *c* maturation; Cyt, cytochrome; TMD, transmembrane domain; BPER; bacterial protein extraction reagent; WT, wild-type; rR, resonance Raman; DDM, n-Dodecyl-β-D-Maltopyranoside.

Abstract

Cytochrome *c* maturation in many bacteria, archaea, and plant mitochondria involves the integral membrane protein CcmF, which is thought to function as a cytochrome *c* synthetase by facilitating the final covalent attachment of heme to the apocytochrome *c*. We previously reported that the *E. coli* CcmF protein contains a *b*-type heme that is stably and stoichiometrically associated with the protein and is not the heme attached to apocytochrome *c*. Here, we show that mutation of either of two conserved transmembrane histidines (His261 or His491) impairs stoichiometric *b*-heme binding in CcmF and results in spectral perturbations in the remaining heme. Exogeneous imidazole is able to correct cytochrome *c* maturation for His261 and His491 substitutions with small side chains (Ala or Gly), suggesting that a "cavity" is formed in these CcmF mutants in which imidazole binds and acts as a functional ligand to the *b*-heme. The results of resonance Raman spectroscopy on wild-type CcmF are consistent with a hexacoordinate low spin *b*-heme with at least one endogeneous axial His ligand. Analysis of purified recombinant CcmF proteins from diverse prokaryotes reveals that the *b*-heme in CcmF is widely conserved. We have also determined the reduction potential of the CcmF *b*-heme ($E_{m,7}$ = -147 mV). We discuss these results in the context of CcmF structure and functions as a heme reductase and cytochrome *c* synthetase.

Introduction

The *c*-type cytochromes are heme proteins present in nearly all organisms that participate in electron transfer, typically for the generation of an electrochemical proton gradient. *C*-type cytochromes function outside of the cytoplasmic membrane in prokaryotes, in the intermembrane space of the mitochondrion, and in the lumen of the chloroplast. Cytochromes *c* are commonly distinguished by covalent attachment of the two vinyl groups (α-carbons) of heme to the thiols of a conserved Cys-Xxx-Xxx-Cys-His motif in the apocytochrome. For thioether formation between heme and apocytochrome, the heme iron and the cysteine thiols must be in the reduced state (*1, 2*). In many prokaryotes, nearly all plant mitochondria and some protozoan mitochondria, cytochromes *c* are assembled by the cytochrome *c* maturation (*ccm*) pathway called system I (Figure 1A), which typically comprises eight or nine integral membrane proteins (In *E. coli*, CcmABCDEFGH) (*3-6*).

In system I, heme is initially bound at a site in CcmC (Figure 1A) (*7-9*). Here, a unique covalent attachment is formed between His130 of CcmE and the β-carbon of the 2-vinyl of heme (*10-12*). CcmE with covalent heme is released from CcmC by the action of CcmAB (an ABC transporter) (*13-15*). CcmE is believed to traffic heme to the site of cytochrome *c* assembly, putatively the CcmF/H synthetase complex, where the heme from holoCcmE is attached to apocytochrome *c* (*8, 16, 17*). Although studies have shown that CcmF and CcmH form an integral membrane complex (*8, 16, 18*), the function of this complex, including its role as a synthetase, is poorly understood.

We have proposed that formation of the covalent bond between CcmE and heme (within the holoCcmCDE complex) is favored by heme oxidation (to Fe^{3+}) (*5, 7, 8*). Consistent with this, the purified holoCcmCDE complex (*7, 8*) and purified holoCcmE (*8, 11, 12*) contain

covalent heme in the oxidized (Fe^{3+}) state. However, heme attachment to the apocytochrome requires that the heme from holoCcmE is reduced (Fe^{2+}) prior to ligation (*1, 2, 5*). A possible mechanism for reducing heme in holoCcmE before heme attachment to apocytochrome *c* has recently emerged: we discovered that CcmF contains a *b*-type heme, independent of all other Ccm proteins, that exists in 1:1 stoichiometry with the protein (*8*). We proposed that reduction of the heme in holoCcmE by the CcmF *b*-heme would facilitate release of the CcmE His130 covalent bond and prepare the heme for attachment to the apocytochrome (*5, 7*).

It is important to establish the spectral and redox properties of the *b*-heme in CcmF to understand the function(s) of CcmF in the maturation of cytochromes *c*. Topological studies have revealed that CcmF contains 13 transmembrane domains (TMDs; Figure 1B) (*8, 19*). There are four completely conserved histidines that might serve as axial ligands to the *b*-heme: two are predicted to be in periplasmic loops (His173 and His303 in CcmF from *E. coli*) and two are predicted to reside in TMDs (His261 and His491) (see stars in Figure 1B). Alanine substitutions at each of these histidines show severe defects in cytochrome *c* assembly (*16*). To identify the axial ligands to the *b*-heme in CcmF, we use spectroscopic and site-directed mutagenesis approaches as well as chemical complementation with exogeneous imidazole. We show that the *b*-heme is present in recombinant CcmF proteins from diverse organisms and determine the reduction potential of the CcmF *b*-heme. Our findings address the location of the *b*-heme in CcmF and allow us to propose redox control mechanisms in the CcmF synthetase reactions.

Experimental Procedures

Bacterial Growth Conditions. *Escherichia coli* strains (Table S1) were grown at 37^{o}C by shaking at 240 rpm in Luria-Bertani broth (LB; Difco) supplemented with the appropriate antibiotics (Sigma-Aldrich) and other media additives at the following concentrations, unless otherwise noted: carbenicillin, 50 μg ml^{-1}; chloramphenicol, 20 μg ml^{-1}; gentamicin, 10 μg ml^{-1}; kanamycin, 100 μg ml^{-1}; isopropyl-β-D-thiogalactopyranoside (IPTG, Gold Biotechnology), 1 mM; arabinose (Gold Biotechnology), 0.1 % (wt/vol).

Protein Expression and Purification. For expression, *E. coli* strains RK103 (*17*) or RK113 (this work, see Table S1) were used. Starter cultures were initiated from a single colony and grown overnight at 37^{o}C in 10 mL of LB with the appropriate antibiotics. 1 L of LB was inoculated to 1 % and was grown to an OD_{600} of 1.8, at which point the culture was induced with 1 mM IPTG for pGEX-based expression or 0.1 % arabinose (wt/vol) for pBAD-based expression for 14-16 hr. Cells were harvested at 5,000 x g for 12 min and frozen at -80^{o}C. Cell pellets were thawed and resuspended in 10 mL/gram wet wt of a modified 1 x TALON (Clontech) buffer (20 mM Tris-HCl, pH 8; 100 mM NaCl) and treated with 4-(2-aminoethyl) bezenesulfonyl fluoride hydrochloride (AEBSF, Gold Biotechnology; 1 mM) and egg white lysozyme (Sigma-Aldrich; 100 μg ml^{-1}) for 30 min while shaking on ice. Cells were disrupted by repeated sonication for 30 sec bursts on a Branson 250 sonicator (50 % duty, 60 % output) until clearing of the suspension was observed. Crude sonicate was centrifuged at 24,000 x g for 12 min to remove unbroken cells and cell debris, and membranes were isolated by centrifugation at 100,000 x g for 45 min. Membrane pellets were solubilized in 1 x modified TALON buffer with 1 % (wt/vol) Anatrace n-Dodecyl-β-D-Maltopyranoside (DDM, Affymetrix). Solubilized membranes (called “L” or load in Figures) were passed over TALON resin per the manufacturer’s recommendations and

bound protein was washed in 1 x modified TALON buffer with 0.1 % DDM with increasing concentrations of imidazole (in Figures, denoted as wash 1 "W1", 0 mM imidazole; wash 2 "W2", 2 mM imidazole; or wash 3 "W3", 5 mM imidazole). Bound hexahistidine-tagged protein was eluted in 1 x modified TALON buffer containing 0.1 % DDM and 75 mM imidazole (called "E" or elution in Figures). The purified protein was concentrated and subjected to buffer exchange in an Amicon Ultra Centrifugal Filter 30,000 MWCO (Millipore) after purification (called "EC" or concentrated elution in Figures) to reduce imidazole to less than 100 μM, unless otherwise noted. To address the accumulation of DDM, purification of CcmF was alternately carried out using 0.02 % DDM instead of 0.1 %. For these purifications, imidazole was removed by successive dialysis using Pierce SnakeSkin Pleated Dialysis Tubing 7,000 MWCO (Thermo Scientific) against 20 mM Tris, pH 8, 100 mM NaCl, 0.02 % DDM, and the protein was concentrated in an Amicon Ultra Centrifugal Filter 100,000 MWCO (Millipore). Using this method, the concentration of DDM was maintained at 0.02 % throughout purification and concentration.

Resonance Raman spectroscopy. Resonance Raman (rR) spectra were obtained using 30 to 40 μM CcmF protein from *E. coli*, purified with the endogeneous *b*-heme. Sample solutions contained 20 mM Tris, pH 8.0, 100 mM NaCl, and dodecyl maltoside at 0.02 %, 0.48 %, or 3.2 %. Heme carbonyl complexes of CcmF were prepared in 5 mm NMR tubes by exhaustive equilibration of the CcmF solution with water-saturated N_2 followed by titration of the sample with sodium dithionite to reduce the heme. The inert atmosphere in the tube was then displaced with either natural isotopic abundance CO or ^{13}CO (95 atom % ^{13}C). Raman scattering was excited using 413.1 nm emission from a Kr^+ laser. Sample tubes were spun at ~20 Hz and spectra were recorded at ambient temperature. Scattered light was collected in the 135^o

backscattering geometry, passed through a holographic notch filter to remove Rayleigh scattered light and depolarized. The Raman spectrum was recorded using a 0.6 m spectrograph equipped with a 2400 g/mm holographic grating and a LN_2 cooled CCD detector. Spectra were calibrated versus toluene, DMSO d^6, and dibromomethane. Vibrational frequencies reported here are reproducible to ±1 cm^{-1}.

Heme stains and other methods. Heme stains and immunoblots were performed as described in (*17, 20*). Proteins were separated by 12.5 % SDS-PAGE and transferred to Hybond C nitrocellulose membranes (GE Healthcare). Anti-His antibodies (Santa Cruz technologies) were used at a dilution of 1:5000. Protein A peroxidase (Sigma-Aldrich) was used as the secondary label. The chemiluminescent signal for heme stains and anti-His westerns was developed using the Pierce SuperSignal Femto kit (Thermo Scientific), and detected with an LAS-1000 Plus detection system (Fujifilm-GE Healthcare). Protein concentrations were determined using the Pierce BCA Protein Assay Kit (Thermo Scientific) using BSA as a standard. The concentration of heme in the CcmF protein preparations was determined by UV-visible absorption spectroscopy, pyridine extraction as described in (*21*) or heme stain as described in (*22*). Protein purity was assessed by Coomassie Blue staining of SDS-PAGE.

UV/Vis absorption spectroscopy. UV-visible absorption spectra were recorded with a Shimadzu UV-2101 PC UV-Vis scanning spectrophotometer at room temperature as described in (*23*). Chemically reduced spectra were generated by addition of sodium dithionite (sodium hydrosulfite) to the purified sample. Unless otherwise indicated, all spectra were recorded in 20 mM Tris-HCl (pH 8), 100 mM NaCl, 0.1 % DDM. To analyze the effect of imidazole on the electronic spectrum, small quantities of a concentrated imidazole solution (1 M, pH 7) were added to purified protein and spectra were recorded.

Cytochrome Reporter and Imidazole Complementation Assays. Cytochrome c_4:His6 production was assayed by the following methods using two different strains. (Method 1) Strain RK111 (Δ*ccm* carrying the arabinose-inducible chromosomal integrate of the *cyt* c_4:His6 gene) harboring pRGK406 (pGEX Δ*ccmF*) and one of the following pBAD *ccmF* plasmids (pRGK408, 409, 410, 411, 412, 413, 414, 415, 416, 417, or 418; see Table S1 in Supporting Information) was grown aerobically in 5 mLs of LB with appropriate antibiotics for 3 hr and induced for an additional 3 hr with 0.8 % arabinose (wt/vol). (Method 2) Strain RK103 ((*17*); Δ*ccm*) harboring pRGK332 ((*17*); carrying the arabinose-inducible *cyt* c_4:His6 gene) and one of the following pGEX system I-based plasmids (pRGK386 (*17*), pRGK403, pRGK404, pRGK405, or pRGK407; see Table S1 in Supporting Information) was grown aerobically in 5 mL LB with appropriate antibiotics for 3 hr and induced for an additional 3 hr with 0.2 % arabinose (wt/vol) and 1 mM IPTG. For both methods, cells were harvested by centrifugation at 10,000 x g for 5 min and the cell pellet was resuspended in 200 µL of Bacterial Protein Extraction Reagent (BPER, Thermo Scientific) to lyse cells and extract protein. Total protein concentration was determined using the Nanodrop 1000 spectrophotometer (Thermo Scientific) and 100 µg was analyzed by SDS-PAGE followed by heme stain. Imidazole complementation assays were performed in the same way with 10 mM imidazole (pH 7) added to the media prior to inoculation.

Determination of the Reduction Potential of CcmF. The reduction potential for the *b*-heme in CcmF was determined by reduction of a dye of known potential (*24*), using a modification of the Massey method (*25*). The assay contained 20 mM Tris-HCl, pH 7, 100 mM NaCl, DDM at 0.02 % or 1.2 %, 500 µM xanthine (Sigma-Aldrich), 20 µM CcmF and one of the following redox dyes: nile blue chloride (E_m = -116 mV) (*26*), resorufin (E_m = -50 mV) (*26*), or safranin O (E_m = -280 mV) (*26*). 50 to 100 nM of xanthine oxidase enzyme (Sigma-Aldrich)

was added to initiate the reaction. The reaction was performed at 25°C in a Coy Anaerobic Airlock Chamber after all solutions were allowed to equilibrate with N_2 overnight. Visible spectra were recorded every 2 min using a Shimadzu UV-1800 spectrophotometer until reduction was complete (typically between 1 and 2 hrs). The absorbance change for the *b*-heme peak was measured at 426 nm, where the change in absorbance of the dye is negligible, and the absorbance change for the dye was measured at 632 nm, where there is little contribution from heme absorbance. The changes in absorbance were analyzed by the Nernst equation terms: [25 mV ln (b-heme$_{red}$/b-heme$_{ox}$)] for the one-electron reduction of heme and [12.5 mV ln (dye$_{red}$/dye$_{ox}$)] for the two-electron reduction of dye, where b-heme$_{red}$/b-heme$_{ox}$ and dye$_{red}$/dye$_{ox}$ represent ratios of the molar concentrations of the reduced and oxidized forms of the *b*-heme and the dye, respectively. Values corresponding to the Nernst equation terms for the *b*-heme and the dye at each time point during the titration were plotted against each other on the *x*- and *y*-axes, respectively, yielding a straight line with a slope of 1. The *y*-intercept of this line represents the difference in potential between the *b*-heme and the known potential of the reference dye. Using this method, the reduction potential for the *b*-heme was calculated to within ± 2 mV based on four independent titrations. To establish the accuracy of this method, two heme proteins of known potential (cytochrome *c* and myoglobin) were titrated using the above method and their respective reduction potentials were found to be within 2 mV of published values. Potentials are given versus the standard hydrogen electrode.

Results

Resonance Raman Spectroscopy

Resonance Raman (rR) spectroscopy of heme proteins can yield considerable insight into structural, conformational and electronic properties of the heme cofactor. Specifically, it is possible to determine coordination number, oxidation number, and spin state of the iron, as well as heme conformation, axial ligand identity, the nature of axial ligand bonding, and nonbonded interactions with the protein (*27-30*). To gain some of this insight into the heme *b* that purifies with CcmF, we recorded Soret-excited rR spectra of ferric and ferrous WT CcmF. We also recorded spectra of the CcmF-CO complex to further probe the heme pocket.

Figure 2 shows the high- and low-frequency Soret excited rR spectra of ferric (top, red) and ferrous (bottom, violet) CcmF in 0.02 % DDM. The bands in the high frequency regions of these spectra report oxidation and spin states of the heme iron as well as the coordination number (*29, 30*). The ν_3 regions of the these spectra exhibit two bands (1491 and 1504 cm^{-1} for ferric CcmF; 1469 and 1491 cm^{-1} for ferrous CcmF) typical of pentacoordinate high-spin (5cHS) and hexacoordinate low-spin (6cLS) heme complexes in both oxidation states. Thus, the heme *b* in ferric and ferrous CcmF exists as an equilibrium mixture of 5cHS and 6cLS states. Note that for ferrous CcmF, the 1469 cm^{-1} ν_3 band corresponding to the 5cHS fraction (Figure 2, bottom) is considerably more intense than its 6cLS counterpart. However, this intensity ratio does not reflect the relative populations of the two states of the ferrous heme because the relative rR scattering cross sections are not the same. In an effort to estimate the population ratio, the UV-visible spectrum was fit so that the Soret band intensities from the HS and LS populations could be compared (Figure S1). Based on this analysis, ferrous CcmF contains approximately 20 % 5cHS heme.

To assess whether the heme heterogeneity is intrinsic to CcmF or induced by solubilizing the protein in detergent, Soret-excited rR spectra of ferric and ferrous CcmF were recorded from solutions containing 0.02 % (Figure 2), 0.48 %, and 3.2 % DDM. The high-frequency spectra of ferric CcmF are compared in Figure 2 (partial traces, red). The rR spectra clearly show that higher DDM concentrations correspond to greater HS heme populations. Thus, although heterogeneity was apparent in all of the preparations, low DDM concentrations clearly favor the 6cLS heme population of ferric CcmF. Two possible explanations for this detergent dependence are envisioned at this time. First, the two states of the heme could be reporting conformational states of the protein that are accessed as part of its native function. For example, these could be states whose populations are modulated by *in vivo* interaction with CcmH, holoCcmE, or apocytochrome *c*. Alternatively, the population of two ferric heme states may arise from a non-physiological CcmF conformer whose formation is induced by solubilizing the protein in DDM detergent. It is important to note that the relative populations of 5cHS and 6cLS ferrous CcmF were only slightly sensitive to detergent concentration (data not shown).

Raman scattering by $\nu_{Fe\text{-}His}$ modes of 5cHS ferrous hemes is typically well enhanced with blue excitation and usually occurs within the range of 200 to 245 cm^{-1} (*32*). Thus, if the axial ligand is an imidazole side chain of a histidine residue, we would expect to see a strong band in that frequency range. The second spectrum from the bottom (blue) in the low frequency range of Figure 2 shows the 441.6-nm excited rR spectrum of ferrous CcmF(WT). This spectrum exhibits an intense band at 210 cm^{-1}, within the frequency range of Fe-His stretching modes. Such bands are typical for a Fe−His unit wherein the proximal histidine ligand is the donor to a weak H-bond within the proximal heme pocket (*28, 31, 32*). Such H-bonds can involve water in a H-bond

network or O atoms from backbone carbonyl groups. Thus, in the 5cHS ferrous form, the proximal ligand is almost certainly the imidazole side chain of a histidine residue.

Vibrational frequencies of the FeCO group in heme—CO complexes are useful probes of the distal heme pocket. To further investigate the proximal ligand properties of CcmF with respect to the heme *b*, we recorded spectra of the CcmF—CO complex. By virtue of the π backbonding that typifies FeCO moieties, there is an inverse relationship between the sensitivity of the Fe—C and C—O bond strengths to the bonded and nonbonded interactions of the FeCO unit (*34-36*). This inverse relationship is clearly revealed on a heme FeCO backbonding correlation plot by the negative slope of the Fe—C stretching frequency versus the C—O stretching frequency for a large number of iron porphyrinates, including carbonyl complexes of heme proteins. Because the donor strength of the proximal ligand modulates the vertical position of a heme carbonyl complex on the correlation plot, the nature of the proximal ligand can be discerned from the position of the heme carbonyl complex relative to the positions of other heme carbonyls with known proximal ligands.

In order to place a particular complex on the correlation plot, the frequencies must be identified in the rR spectrum by isotope editing of the vibrational frequencies with ^{13}CO. By this method, the frequencies of modes involving distortions of the FeCO unit can be unambiguously identified. Figure 3A shows the regions of the rR spectrum of the CcmF—CO (green) and CcmF—^{13}CO (blue) complexes where bands arising from FeCO vibrations occur (*33*). Bands were assigned based on their ^{13}C sensitivity, which is apparent from the difference spectra shown in red. The bands at 494 and 572 cm^{-1} are assigned to the $\nu_{Fe—C}$ and the δ_{FeCO} modes, respectively. The band at 1962 cm^{-1} was assigned to the $\nu_{C—O}$ mode. Interestingly, the low frequency region of the CcmF—CO spectrum recorded in 3.2 % DDM (bottom, violet) reveals

two Fe—C stretching bands: one at 495 cm^{-1} (the same Raman shift observed at low DDM concentrations) and the other at 525 cm^{-1}. Thus, high DDM concentrations induce formation of a second CcmF—CO complex.

Figure 3B shows the FeCO backbonding correlation plot described above, with three inverse correlations between ν_{Fe-C} and ν_{C-O} frequencies for a wide selection of heme carbonyl complexes. The bottom (green) line in Figure 3B correlates Fe—C and C—O bond strengths for proximal ligands having anionic character, such as the strongly H-bond donating proximal imidazoles of the heme peroxidases and the proximal thiolates of the cytochromes P450. The middle (black) line correlates the analogous bond strengths in proteins that have charge neutral proximal ligands that are bound to the heme iron through an N atom. Nearly all of these complexes have proximal imidazole ligands from histidine residues. The top (blue) line correlates heme—CO complexes that are either pentacoordinate or have proximal O-atom donor ligands. The position of CcmF—CO in 0.48 % DDM is indicated by the half-filled red diamond in Figure 3B. This point falls on the proximal histidine correlation line, consistent with at least one endogenous axial histidine ligand for the heme *b* of CcmF. Note that this analysis does not facilitate identification of the specific coordinating histidine residue. The heme carbonyl that was only observed in 3.2 % DDM falls on the top line in Figure 3B, as shown by the half-filled red triangle. This position constitutes compelling evidence that the heme—CO complex in high DDM is either pentacoordinate or has a sixth axial ligand coordinated to iron through an oxygen atom. This result shows that in high DDM solutions, the second protein-based axial ligand that gives rise to 6cLS heme is unavailable to the heme in a significant fraction of these ferrous heme—CO complexes. This behavior is consistent with the correlation between the HS ferric heme population and DDM concentration illustrated in Figure 2.

Heme content of Ala substitutions

To identify the ligands to *b*-heme iron in CcmF, we focused on the four conserved histidines (His173 and His303 in periplasmic loops, and His261 and His491 in TMDs). Previously, we showed that purified CcmF with a His173Ala substitution contained wild-type (WT) levels of *b*-heme, while CcmF with a His261Ala substitution had approximately four-fold less heme (*8*). Here, we analyze heme levels in purified CcmF with alanine substitutions at His303 or His491. Figure 4A shows that CcmF His303Ala and CcmF His491Ala were each purified as full-length proteins with minimal degradation. Comparison of the Soret maxima in the electronic spectra indicates that CcmF His303Ala purified with heme levels similar to WT CcmF while CcmF His491Ala purified with less than 20 % of WT levels (note the differences in absorbance in Figures 4B, 4C, and 4D). This was confirmed by semi-quantitative heme stain to detect the *b*-heme, which runs at the dye front during SDS-PAGE (Figures 4E, 4F, and 4G). The purified concentrated preparations (lane 8 of Figures 4E, 4F, and 4G) show much less heme for CcmF His491Ala. The same concentration of purified CcmF was analyzed for each of the proteins; thus, the fractional heme loading in each protein can be directly compared. These data and previous findings in ref. (*8*), suggest that periplasmic His173 and His303 are not *b*-heme ligands, while transmembrane His261 and His491 are good candidates for ligands to the *b*-heme. In agreement with this, CcmF with glycine substitutions at His261 and His491 also contained approximately 20 % heme content relative to WT CcmF (data not shown).

Spectral perturbations in His261Cys

In making substitutions to His261 and His491, we observed that a His261Cys substitution in CcmF retained a high level of function relative to WT (see below) and that purified CcmF His261Cys (Figure 5A) contained approximately 50 % of the *b*-heme as WT (Figure 5B).

Cysteine has been shown to function as a ligand in place of the natural histidine ligand in many heme proteins, including myoglobin (*37-39*), cytochrome b_5 (*40*), and flavocytochrome b_2 (*41*). The UV/Vis absorption spectrum of CcmF His261Cys has several distinct features in comparison to the spectrum of WT CcmF (compare Figures 5C and 5D). Oxidized ("as purified") WT CcmF exhibits a sharp Soret maximum at 412 nm, whereas the Soret band for CcmF His261Cys is broad with a maximum at 406 nm. Additionally, the α and β absorptions in the visible region are much less pronounced for CcmF His261Cys than for WT CcmF. The position of the Soret at 406 nm is indicative of high-spin heme (*40*), but the breadth of the Soret band and the α and β absorptions suggest that ferric CcmF His261Cys may also contain a population of 6cLS heme (*42, 43*). Thus, while the UV/Vis absorption spectrum of ferric WT CcmF is dominated by features characteristic of 6cLS heme (*40*), the spectrum of ferric CcmF His261Cys is consistent with a mixture of 5cHS and 6cLS heme. The dithionite-reduced spectrum for CcmF His261Cys shows a Soret of 423 nm and exhibits clear α and β absorptions, although the α:β peak ratio is different than for WT CcmF. Based on the position of the Soret band and the clearly resolvable α and β maxima, ferrous CcmF His261Cys appears to contain predominantly low-spin heme (*40*). The presence of 6cLS heme in CcmF His261Cys suggests possible coordination by His491 and Cys261. While low-spin hemes with cysteine ligands typically exhibit Soret bands near 450 nm (*44*), Soret absorptions near 425 nm have been observed when the sulfur-iron bond is weakened or displaced (*39, 42, 43, 45*). These spectral perturbations observed in ferric and ferrous CcmF His261Cys (relative to the spectrum of WT CcmF) suggest that in the WT protein, His261 is an axial ligand to the *b*-heme.

Imidazole, the side chain of histidine, has been used as a surrogate proximal ligand to probe heme binding sites in proteins *in vitro* (e.g., *40, 42, 46*). To investigate the effect of

imidazole on heme in the His261Cys CcmF protein, UV/Vis spectra of purified CcmF His261Cys were recorded in the presence of imidazole. At a concentration of 30 mM imidazole, the spectrum of the oxidized His261Cys mutant shifts to resemble that of WT CcmF (compare solid lines in Figures 5C and 5E). The Soret band occurs at 414 nm (compared to 406 nm in the absence of imidazole) and pronounced α and β absorptions similar to WT CcmF can be observed. Upon reduction with sodium dithionite, the His261Cys (+ 30 mM imidazole) exhibits a Soret band at 423 nm and an α to β peak ratio similar to that of reduced WT CcmF. Addition of 30 mM imidazole to WT CcmF preparations did not change the UV/Vis spectrum (not shown). These data suggest that in the presence of imidazole, heme in His261Cys is predominantly 6cLS in both the oxidized and reduced states. The similarities in the spectra of CcmF His261Cys in the presence of imidazole and WT CcmF suggest that, in the WT protein, the *b*-heme may be liganded by the imidazole side chains of two His residues.

Functional restoration of CcmF His261 and His491 mutants by imidazole

Alanine substitutions at each of the four conserved histidine residues (His173, His261, His303, and His491) abolished *in vivo* function (cytochrome *c* assembly) in *E. coli* under aerobic conditions (Figure S2). Initially, we analyzed whether these alanine substitutions could be corrected for *in vivo* function by adding imidazole to *E. coli* cultures (Figure S1). *In vivo* chemical complementation by exogeneous imidazole is conceptually similar to the correction of heme binding by imidazole in the recombinant myoglobin His93Gly "cavity" mutant, for which 10 mM imidazole was optimal (*47*). This approach has also been used to correct the function of histidine mutants in the hydrogenase cytochrome *b* of *Azotobacter vinelandii* (*48*) and the CcsBA system II cytochrome *c* synthetases from *Helicobacter hepaticus* (*23*) and *Wolinella succinogenes* (*49*). The His491Ala mutant of CcmF was corrected for cytochrome c_4 assembly

at 10 mM imidazole (Figure S2, lane 12). To determine if glycine substitutions in CcmF could be corrected for function, we replaced transmembrane His491 or His261 with glycine and assayed for cytochrome c_4 assembly in the absence and presence of imidazole. Substitution of either His261 or His491 with glycine abolished or severely impaired cytochrome c_4 assembly *in vivo* (quantified in Figure 6A and 6B; representative heme stains for cytochrome c_4 are in Figure S3). Addition of 10 mM imidazole restored function to CcmF His261Gly and to His491Gly (Figure 6A and 6B). We propose that the CcmF His261Gly and His491Ala/Gly proteins form "cavities" in which imidazole can bind and serve as a ligand to the *b*-heme in CcmF. Based on these results, we predicted that amino acids with bulkier side chains (that are unable to function as *b*-heme ligands) would not accommodate imidazole binding in the "cavity", and thus would not permit functional correction. We tested this by engineering additional substitutions at His261 and His491. As mentioned above, His261Cys was roughly 70 % functional relative to wild-type in the absence of imidazole (Figure 6A). However, neither His261Tyr nor His261Met were functional above background levels, nor were these substitutions corrected substantially by imidazole (Figure 6A). The same was true for Cys and Tyr substitutions at His491 (Figure 6B). His491Arg showed a low level of function relative to WT (approximately 18 %), but imidazole did not improve the function of this mutant (Figure 6B). These results are consistent with His261 and His491 acting as heme ligands, such that when these His residues are substituted with amino acids containing small side chains (Gly or Ala), a cavity is formed in which imidazole can bind and serve as a surrogate heme axial ligand. The inability of imidazole to correct the cytochrome *c* assembly defect of CcmF His261Ala could be the result of the methyl group of Ala occluding the "cavity" such that imidazole is unable to bind. We have not investigated this further.

Conservation of the b-heme in CcmF

To determine if the *b*-heme in CcmF is conserved, we engineered CcmF proteins from a phylogenetically diverse group of prokaryotes (Figure 7A; gamma proteobacteria- *Escherichia coli* and *Shewanella oneidensis;* delta proteobacteria-*Desulfovibrio vulgaris,* alpha proteobacteria-*Roseobacter denitrificans;* deinococci-*Thermus thermophilus*). CcmF proteins from *E. coli* (NrfE, here called CcmF2) and *Shewanella* (here called CcmF3) that recognize and mature cytochromes *c* with alternate heme binding sites (Cys-Xxx-Xxx-Cys-Lys in *E. coli*; and, putatively, Cys-Xxx_{15}-Cys-His in *Shewanella*) were also engineered with hexahistidine tags and purified (Figure S4). Each of these CcmF homologs possesses the four conserved histidine residues studied above in the *E. coli* CcmF. Heme analysis by UV/Vis absorption spectroscopy (Figure 7B) and heme stain (Figure S4) revealed that each purified CcmF protein contained *b*-heme in approximately equimolar stoichiometry.

Reduction potential of the b-heme in CcmF

We determined the reduction potential for the CcmF *b*-heme using the purified CcmF from *E. coli* (Figure 8). Using a modification of the method of Massey (with xanthine/xanthine oxidase to generate reductant) (*25*), values for the midpoint potential of the CcmF *b*-heme (Fe^{3+}/Fe^{2+}) were determined against nile blue chloride (E_m= -116 mV) at pH 7 (*26*). The spectral results obtained from a typical reduction run with CcmF and nile blue chloride are shown in Figure 8A. The decreases in absorbance at 412 nm and 480 nm and the increase in absorbance at 426 nm are indicative of reduction of the CcmF *b*-heme. The decrease in absorbance at 632 nm is due to reduction of nile blue chloride. The linear Nernst plot for reduction of the *b*-heme and nile blue chloride produced the expected slope of 1 (Figure 8B), indicating that the reduced and oxidized forms of the dye and the heme were at their equilibrium concentrations at the time each

spectrum was recorded. This behavior ensures that there is no overpotential contribution to the midpoint potentials determined from these measurements. The reduction potential of the *b*-heme in CcmF was found to be -147 ± 2 mV. This value was confirmed using resorufin (E_m = -50 mV) (*26*) or safranin O (E_m = -280 mV) (*26*) as alternate redox dyes (Figure S5). It has been observed previously that the type of detergent (*50, 51*) and detergent concentration (*50*) can alter reduction potentials of *b*-type hemes in membrane proteins. To assess the effects of DDM, we determined the reduction potential of the CcmF *b*-heme in solutions containing 0.02 % (Figure 8) or 1.2 % DDM. The reduction potential in 1.2 % DDM was found to be substantially more positive (E_m = -110 ± 4 mV) than in 0.02 % DDM (Figure S6). This is likely attributable to the same DDM-dependent speciation of the ferric heme-*b* between HS and LS states that was revealed by the rR spectra (vide supra).

Discusssion

Here, we present several lines of evidence that TMD His261 and His491 are the ligands to the CcmF *b*-heme: (i) Gly or Ala substitutions at either His result in approximately 80 % less heme as compared to WT CcmF (Figure 4), (ii) substitution of His261 with Cys, a known heme ligand, yields a functional CcmF that shows improved heme binding relative to substitutions with non-ligand residues (Ala or Gly) and shows a perturbed UV/Vis spectrum (Figure 5), and (iii) exogeneous imidazole chemically corrects the in vivo cytochrome *c* synthetase function of small residue substitutions at CcmF His261 and His491, but not substitutions with bulkier residues (Figure 6). The results of rR spectroscopy confirm the presence of hexacoordinate, low-spin *b*-heme (Figure 2), and rR analysis of the heme-carbonyl complex suggests axial His coordination of the *b*-heme (Figure 3). Additionally, we show that the CcmF *b*-heme is widely conserved by analyzing recombinant CcmF proteins from diverse bacteria (Figure 7).

Implications of His261 and His491 as the b-heme axial ligands in CcmF

His261 in CcmF is located in TMD5, and His491 is located near the C-terminus in TMD12 (see Figure 1B). In order for these residues to coordinate the iron of the *b*-heme, we propose that TMD5 and TMD12 are positioned close to each other in the three-dimensional structure of CcmF. These findings suggest that the most likely position for the *b*-heme is directly below the periplasmic WWD domain in CcmF (refer to Figure 1B). The WWD domain is a highly conserved tryptophan-rich motif that is located at the outer leaflet of the inner membrane and has been shown to interact directly with heme in the WWD family member CcmC (*7*). In CcmC, heme axial ligands are provided by two His residues located in periplasmic loops that flank the WWD domain (*7, 8*). Similar to CcmC, we predict that the WWD domain of CcmF forms a heme binding site for heme from holoCcmE, with periplasmic His173 and His303 of

CcmF serving as heme axial ligands (Figure 1B). Thus, the positioning of the *b*-heme directly below the CcmF WWD domain is consistent with our hypothesized role for CcmF in reducing heme from holoCcmE prior to attachment to the apocytochrome (see below).

The function of CcmF b-heme as a holoCcmE reductase

Reduction of the heme in holoCcmE is required for covalent attachment of this heme to the apocytochrome *c*. We have previously discussed that reduction of the holoCcmE heme could also favor ejection of the CcmE His130 covalent linkage (*5*). To address our hypothesis that the *b*-heme in CcmF may be involved in electron transfer to holoCcmE (*5, 8*), we determined the reduction potential of the CcmF *b*-heme. We report here that the CcmF *b*-heme has a midpoint potential of -147 mV at pH 7 (Figure 8). Harvat et al. have reported a redox potential of -121 mV at pH 7.3 for holoCcmE′, a soluble version of CcmE without the single TMD (*52*). Despite the differences in the buffer conditions used in determining the reduction potentials for holoCcmE′ and here for CcmF (e.g., the presence of DDM), it is certainly feasible that CcmF functions as a holoCcmE reductase. However, the reduction potential of isolated, purified holoCcmE′ may not reflect the physiological potential of this heme prior to attachment to the apocytochrome *c*. Recall that, *en route* to attachment to apocytochrome *c*, the holoCcmE heme likely enters the WWD domain of CcmF, where heme axial ligands are provided by His173 and His303 of CcmF (see Figure 1B). In purified holoCcmE, Tyr134 of CcmE has been shown to serve as an axial ligand to the heme (*12, 53*). It is well-established that heme reduction potential is sensitive to changes in axial ligation (*38, 41, 54*), and tyrosine axial ligation is typically associated with a lowering of the reduction potential (i.e., more negative) relative to ligation by histidine (*38, 55, 56*). Thus, the heme ligand "switch" from CcmE Tyr134 to CcmF His173/His303 upon binding of holoCcmE in the CcmF WWD domain could result in an

increase in the reduction potential (i.e., more positive) of the heme in holoCcmE. Although the identity of the physiological electron donor to the CcmF *b*-heme is unknown, we previously showed that CcmF could be reduced by select quinone species *in vitro* in the presence of dithiothreitol (*8*). Further studies are needed to investigate these features of cytochrome *c* assembly.

Interaction between CcmF and holoCcmE

Although it is widely believed that the heme from holoCcmE moves onto the apocytochrome *c* via CcmF, to our knowledge, an interaction between CcmF and holoCcmE has never been detected. Thony-Meyer and colleagues have suggested that apoCcmE and CcmF interact (*16*). However, in that study, because the genes encoding CcmABCD were absent, all of the CcmE was in the apo- form, so the physiological relevance of this finding is unclear. Furthermore, while Ren et al. (*16*) showed that antisera to CcmF co-immunoprecipitated apoCcmE, the reverse co-immunoprecipitation with anti-sera to CcmE yielded "non-specific signals" (*16*). In our hands, the only protein that co-purifies with CcmF is CcmH (for example, see Figure 4 in ref. (*8*)). We have been unable to detect apo- or holoCcmE above background levels in purifications of hexahistidine-tagged CcmF. We suggest that holoCcmE may not co-purify with CcmF (or the CcmF/H complex) unless the apocytochrome *c* acceptor (Cys-Xxx-Xxx-Cys-His) is bound. This proposal is in part based on our recent findings on the "acceptor-dependent" nature of the CcmC-heme-CcmE complex of system I (*7*). CcmC does not bind detectable levels of heme in its WWD domain in the absence of CcmE (Figure 1A), indicating that heme binding in CcmC requires the presence of the heme acceptor, CcmE. By analogy, heme in holoCcmE may not enter the WWD domain of CcmF unless the heme acceptor protein, apocytochrome *c*, is present. Future work will be dedicated to better understanding the

interaction of holoCcmE with CcmF; specifically, investigating if the docking of holoCcmE in the CcmF WWD domain requires the presence of the apocytochrome *c* acceptor, and, if the holoCcmE/CcmF/CcmH complex can be "trapped," determining the reduction potential of the heme in holoCcmE when (and if) it is bound in the CcmF WWD domain.

Acknowledgements

We thank Dr. Robert Blankenship, Dr. Emma Raven, and Dr. Igor Efimov for helpful discussions on reduction potentials. We thank Dr. Cynthia Richard-Fogal for helpful discussions and manuscript comments. We also thank Dr. Huifen Zhu for construction of the CcmF His303Ala mutant (pRGK405).

References

(1) Barker, P. D., Ferrer, J. C., Mylrajan, M., Loehr, T. M., Feng, R., Konishi, Y., Funk, W. D., MacGillivray, R. T., and Mauk, A. G. (1993) Transmutation of a heme protein. *Proc Natl Acad Sci U S A 90*, 6542-6546.

(2) Nicholson, D. W., and Neupert, W. (1989) Import of cytochrome c into mitochondria: reduction of heme, mediated by NADH and flavin nucleotides, is obligatory for its covalent linkage to apocytochrome c. *Proc Natl Acad Sci U S A 86*, 4340-4344.

(3) Ferguson, S. J., Stevens, J. M., Allen, J. W., and Robertson, I. B. (2008) Cytochrome c assembly: a tale of ever increasing variation and mystery? *Biochim Biophys Acta 1777*, 980-984.

(4) Hamel, P., Corvest, V., Giege, P., and Bonnard, G. (2009) Biochemical requirements for the maturation of mitochondrial c-type cytochromes. *Biochim Biophys Acta 1793*, 125-138.

(5) Kranz, R. G., Richard-Fogal, C., Taylor, J. S., and Frawley, E. R. (2009) Cytochrome c biogenesis: mechanisms for covalent modifications and trafficking of heme and for heme-iron redox control. *Microbiol Mol Biol Rev 73*, 510-528.

(6) Sanders, C., Turkarslan, S., Lee, D. W., and Daldal, F. (2010) Cytochrome c biogenesis: the Ccm system. *Trends Microbiol 18*, 266-274.

(7) Richard-Fogal, C., and Kranz, R. G. (2010) The CcmC:heme:CcmE complex in heme trafficking and cytochrome c biosynthesis. *J Mol Biol 401*, 350-362.

(8) Richard-Fogal, C. L., Frawley, E. R., Bonner, E. R., Zhu, H., San Francisco, B., and Kranz, R. G. (2009) A conserved haem redox and trafficking pathway for cofactor attachment. *Embo J 28*, 2349-2359.

(9) Schulz, H., Fabianek, R. A., Pellicioli, E. C., Hennecke, H., and Thony-Meyer, L. (1999) Heme transfer to the heme chaperone CcmE during cytochrome c maturation requires the CcmC protein, which may function independently of the ABC-transporter CcmAB. *Proc Natl Acad Sci U S A 96*, 6462-6467.

(10) Lee, D., Pervushin, K., Bischof, D., Braun, M., and Thony-Meyer, L. (2005) Unusual heme-histidine bond in the active site of a chaperone. *J Am Chem Soc 127*, 3716-3717.

(11) Stevens, J. M., Daltrop, O., Higham, C. W., and Ferguson, S. J. (2003) Interaction of heme with variants of the heme chaperone CcmE carrying active site mutations and a cleavable N-terminal His tag. *J Biol Chem 278*, 20500-20506.

(12) Uchida, T., Stevens, J. M., Daltrop, O., Harvat, E. M., Hong, L., Ferguson, S. J., and Kitagawa, T. (2004) The interaction of covalently bound heme with the cytochrome c maturation protein CcmE. *J Biol Chem 279*, 51981-51988.

(13) Christensen, O., Harvat, E. M., Thony-Meyer, L., Ferguson, S. J., and Stevens, J. M. (2007) Loss of ATP hydrolysis activity by CcmAB results in loss of c-type cytochrome synthesis and incomplete processing of CcmE. *Febs J 274*, 2322-2332.

(14) Feissner, R. E., Richard-Fogal, C. L., Frawley, E. R., and Kranz, R. G. (2006) ABC transporter-mediated release of a haem chaperone allows cytochrome c biogenesis. *Mol Microbiol 61*, 219-231.

(15) Goldman, B. S., Beckman, D. L., Bali, A., Monika, E. M., Gabbert, K. K., and Kranz, R. G. (1997) Molecular and immunological analysis of an ABC transporter complex required for cytochrome c biogenesis. *J Mol Biol 268*, 724-738.

(16) Ren, Q., Ahuja, U., and Thony-Meyer, L. (2002) A bacterial cytochrome c heme lyase. CcmF forms a complex with the heme chaperone CcmE and CcmH but not with apocytochrome c. *J Biol Chem 277*, 7657-7663.
(17) Feissner, R. E., Richard-Fogal, C. L., Frawley, E. R., Loughman, J. A., Earley, K. W., and Kranz, R. G. (2006) Recombinant cytochromes c biogenesis systems I and II and analysis of haem delivery pathways in Escherichia coli. *Mol Microbiol 60*, 563-577.
(18) Sanders, C., Turkarslan, S., Lee, D. W., Onder, O., Kranz, R. G., and Daldal, F. (2008) The cytochrome c maturation components CcmF, CcmH, and CcmI form a membrane-integral multisubunit heme ligation complex. *J Biol Chem 283*, 29715-29722.
(19) Goldman, B. S., Beck, D. L., Monika, E. M., and Kranz, R. G. (1998) Transmembrane heme delivery systems. *Proc Natl Acad Sci U S A 95*, 5003-5008.
(20) Feissner, R., Xiang, Y., and Kranz, R. G. (2003) Chemiluminescent-based methods to detect subpicomole levels of c-type cytochromes. *Anal Biochem 315*, 90-94.
(21) Berry, E. A., and Trumpower, B. L. (1987) Simultaneous determination of hemes a, b, and c from pyridine hemochrome spectra. *Anal Biochem 161*, 1-15.
(22) Richard-Fogal, C. L., Frawley, E. R., Feissner, R. E., and Kranz, R. G. (2007) Heme concentration dependence and metalloporphyrin inhibition of the system I and II cytochrome c assembly pathways. *J Bacteriol 189*, 455-463.
(23) Frawley, E. R., and Kranz, R. G. (2009) CcsBA is a cytochrome c synthetase that also functions in heme transport. *Proc Natl Acad Sci U S A 106*, 10201-10206.
(24) Massey, V. (1991) in *Flavins and Flavoproteins* (Curti, B., Ronchi, S., and Zanetti, G., Eds.) pp 59-66, Walter de Gruyter & Co., New York.
(25) Efimov, I., Papadopoulou, N. D., McLean, K. J., Badyal, S. K., Macdonald, I. K., Munro, A. W., Moody, P. C., and Raven, E. L. (2007) The redox properties of ascorbate peroxidase. *Biochemistry 46*, 8017-8023.
(26) Clark, W. M. (1960) *Oxidation-Reduction Potentials of Organic Systems*, Waverly Press, Baltimore, MD.
(27) Li, X. Y., Czernuszewicz, R. S., Kincaid, J. R., Stein, P., and Stein, T. G. (1990) Consistent porphyrin force field. 2. Nickel octaethylporphyrin skeletal and substituent mode assignments from nitrogen-15, meso-d4, and methylene-d16 Raman and infrared isotope shifts. *J Phys Chem 94*, 47-61.
(28) Smulevich, G., Hu, S., Rodgers, K. R., Goodin, D. B., Smith, K. M., and Spiro, T. G. (1996) Heme-protein interactions in cytochrome c peroxidase revealed by site-directed mutagenesis and resonance Raman spectra of isotopically labeled hemes. . *Biospectroscopy 2*, 365-376.
(29) Spiro, T. G., and Editor (1988) *Biological Applications of Raman Spectroscopy, Vol 3: Resonance Raman Spectra of Heme and Metalloproteins*, John Wiley and Sons.
(30) Spiro, T. G., Czernuszewicz, R. S., and Li, X. Y. (1990) Metalloporphyrin structure and dynamics from Resonance Raman spectroscopy. *Coord Chem Rev 100*, 541-571.
(31) Rodgers, K. R., Lukat-Rodgers, G. S., and Barron, J. A. (1996) Structural basis for ligand discrimination and response initiation in the heme-based oxygen sensor FixL. *Biochemistry 35*, 9539-9548.
(32) Bangcharoenpaurpong, O., Schomacker, K. T., and Champion, P. M. (1984) Resonance Raman investigation of myoglobin and hemoglobin. *J Am Chem Soc 106*, 5688-5698.

(33) Lukat-Rodgers, G. S., Rodgers, K. R., Caillet-Saguy, C., Izadi-Pruneyre, N., and Lecroisey, A. (2008) Novel heme ligand displacement by CO in the soluble hemophore HasA and its proximal ligand mutants: implications for heme uptake and release. *Biochemistry 47*, 2087-2098.
(34) Ray, G. B., Li, X. Y., Ibers, J. A., Sessler, J. L., and Spiro, T. G. (1994) How far can proteins bend the FeCO unit? Distal polar and steric effects in heme proteins and models. *J Am Chem Soc 116*, 162-176.
(35) Smulevich, G., Evangelista-Kirkup, R., English, A., and Spiro, T. G. (1986) Raman and infrared spectra of cytochrome c peroxidase-carbon monoxide adducts in alternative conformational states. *Biochemistry 25*, 4426-4430.
(36) Spiro, T. G., and Wasbotten, I. H. (2005) CO as a vibrational probe of heme protein active sites. *J Inorg Biochem 99*, 34-44.
(37) Adachi, S., Nagano, S., Ishimori, K., Watanabe, Y., Morishima, I., Egawa, T., Kitagawa, T., and Makino, R. (1993) Roles of proximal ligand in heme proteins: replacement of proximal histidine of human myoglobin with cysteine and tyrosine by site-directed mutagenesis as models for P-450, chloroperoxidase, and catalase. *Biochemistry 32*, 241-252.
(38) Adachi, S., Nagano, S., Watanabe, Y., Ishimori, K., and Morishima, I. (1991) Alteration of human myoglobin proximal histidine to cysteine or tyrosine by site-directed mutagenesis: characterization and their catalytic activities. *Biochem Biophys Res Commun 180*, 138-144.
(39) Hildebrand, D. P., Ferrer, J. C., Tang, H. L., Smith, M., and Mauk, A. G. (1995) Trans effects on cysteine ligation in the proximal His93Cys variant of horse heart myoglobin. *Biochemistry 34*, 11598-11605.
(40) Wang, W. H., Lu, J. X., Yao, P., Xie, Y., and Huang, Z. X. (2003) The distinct heme coordination environments and heme-binding stabilities of His39Ser and His39Cys mutants of cytochrome b5. *Protein Eng 16*, 1047-1054.
(41) Mowat, C. G., Miles, C. S., Munro, A. W., Cheesman, M. R., Quaroni, L. G., Reid, G. A., and Chapman, S. K. (2000) Changing the heme ligation in flavocytochrome b2: substitution of histidine-66 by cysteine. *J Biol Inorg Chem 5*, 584-592.
(42) Dawson, J. H., Andersson, L. A., and Sono, M. (1982) Spectroscopic investigations of ferric cytochrome P-450-CAM ligand complexes. Identification of the ligand trans to cysteinate in the native enzyme. *J Biol Chem 257*, 3606-3617.
(43) Shelver, D., Kerby, R. L., He, Y., and Roberts, G. P. (1997) CooA, a CO-sensing transcription factor from Rhodospirillum rubrum, is a CO-binding heme protein. *Proc Natl Acad Sci U S A 94*, 11216-11220.
(44) Dawson, J. H., Andersson, L. A., and Sono, M. (1983) The diverse spectroscopic properties of ferrous cytochrome P-450-CAM ligand complexes. *J Biol Chem 258*, 13637-13645.
(45) Reynolds, M. F., Shelver, D., Kerby, R. L., Parks, R. B., Roberts, G. P., and Burstyn, J. N. (1998) EPR and Electronic Absorption Spectroscopies of the CO-Sensing CooA Protein Reveal a Cysteine-Ligated Low-Spin Ferric Heme. *J Am Chem Soc 120*, 9080-9081.

(46) Vetter, S. W., Terentis, A. C., Osborne, R. L., Dawson, J. H., and Goodin, D. B. (2009) Replacement of the axial histidine heme ligand with cysteine in nitrophorin 1: spectroscopic and crystallographic characterization. *J Biol Inorg Chem 14*, 179-191.
(47) Barrick, D. (1994) Replacement of the proximal ligand of sperm whale myoglobin with free imidazole in the mutant His-93-->Gly. *Biochemistry 33*, 6546-6554.
(48) Meek, L., and Arp, D. J. (2000) The hydrogenase cytochrome b heme ligands of Azotobacter vinelandii are required for full H(2) oxidation capability. *J Bacteriol 182*, 3429-3436.
(49) Kern, M., Scheithauer, J., Kranz, R. G., and Simon, J. (2010) Essential histidine pairs indicate conserved haem binding in epsilonproteobacterial cytochrome c haem lyases. *Microbiology 156*, 3773-3781.
(50) Lorence, R. M., Miller, M. J., Borochov, A., Faiman-Weinberg, R., and Gennis, R. B. (1984) Effects of pH and detergent on the kinetic and electrochemical properties of the purified cytochrome d terminal oxidase complex of Escherichia coli. *Biochim Biophys Acta 790*, 148-153.
(51) Matsuda, H., and Butler, W. L. (1983) Restoration of high-potential cytochrome b-559 in liposomes. *Biochim Biophys Acta 724*, 123-127.
(52) Harvat, E. M., Redfield, C., Stevens, J. M., and Ferguson, S. J. (2009) Probing the heme-binding site of the cytochrome c maturation protein CcmE. *Biochemistry 48*, 1820-1828.
(53) Garcia-Rubio, I., Braun, M., Gromov, I., Thony-Meyer, L., and Schweiger, A. (2007) Axial coordination of heme in ferric CcmE chaperone characterized by EPR spectroscopy. *Biophys J 92*, 1361-1373.
(54) Sligar, S. G., Egeberg, K. D., Sage, J. T., Morikis, D., and Champion, P. M. (1987) Alteration of Heme Axial LIgands by Site-Directed Mutagenesis: A Cytochrome Becomes a Catalytic Demethylase. *J Am Chem Soc 109*, 7896-7897.
(55) de Lacroix de Lavalette, A., Barucq, L., Alric, J., Rappaport, F., and Zito, F. (2009) Is the redox state of the ci heme of the cytochrome b6f complex dependent on the occupation and structure of the Qi site and vice versa? *J Biol Chem 284*, 20822-20829.
(56) Hildebrand, D. P., Burk, D. L., Maurus, R., Ferrer, J. C., Brayer, G. D., and Mauk, A. G. (1995) The proximal ligand variant His93Tyr of horse heart myoglobin. *Biochemistry 34*, 1997-2005.

Figures

Figure 1. Model for stystem I and membrane topology of CcmF

Adapted from reference (*5*). (A) Current working model of the system I cytochrome *c* biogenesis pathway. Model includes trafficking and oxidation states of heme as well as the subpathways for apocytochrome translocation and reduction. (B) Topology of the CcmF integral membrane protein from *E. coli*. Possible histidine axial ligands to heme are starred. The highly conserved WWD domain is shaded as are the hydrophobic patches. Completely conserved amino acids (red) were identified by individual protein alignments using CcmF ORFs from the following organisms: the alpha proteobacteria, *Agrobacterium tumefaciens* C58, *R. capsulatus*, *Caulobacter crescentus* CB15, and *Bradyrhizobium japonicum*; the beta proteobacteria, *Nitrospira mutliformis* ATCC 25196 and *Nitrosomonas europaea* ATCC 19718; the gamma proteobacteria, *E. coli* K-12 MG1655, *Pseudomonas fluorescens* Pf01, *Shewanella oneidensis* MR-1 and *Vibrio parahaemolyticus* RIMD 2210633; the delta proteobacteria, *Myxococcus xanthus* and *Desulfovibrio desulfuricans*; and the deinococci, *Deinococcus geothermalis* and *Thermus thermophilus*.

A

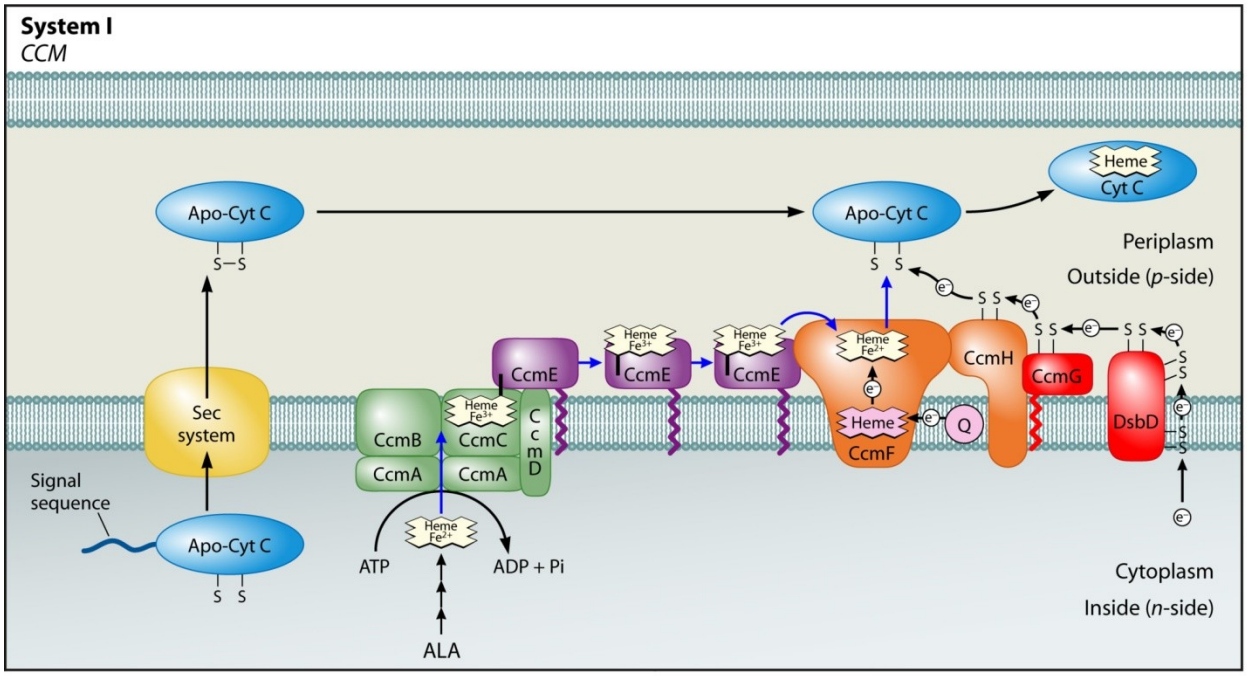
System I
CCM
Apo-Cyt C
Heme
Cyt C
Periplasm
Outside (p-side)
Sec
system
Signal
sequence
CcmE
CcmB
CcmC
CcmA
CcmA
CcmD
CcmH
CcmG
DsbD
CcmF
Heme
Q
ATP
ADP + Pi
ALA
Cytoplasm
Inside (n-side)

B

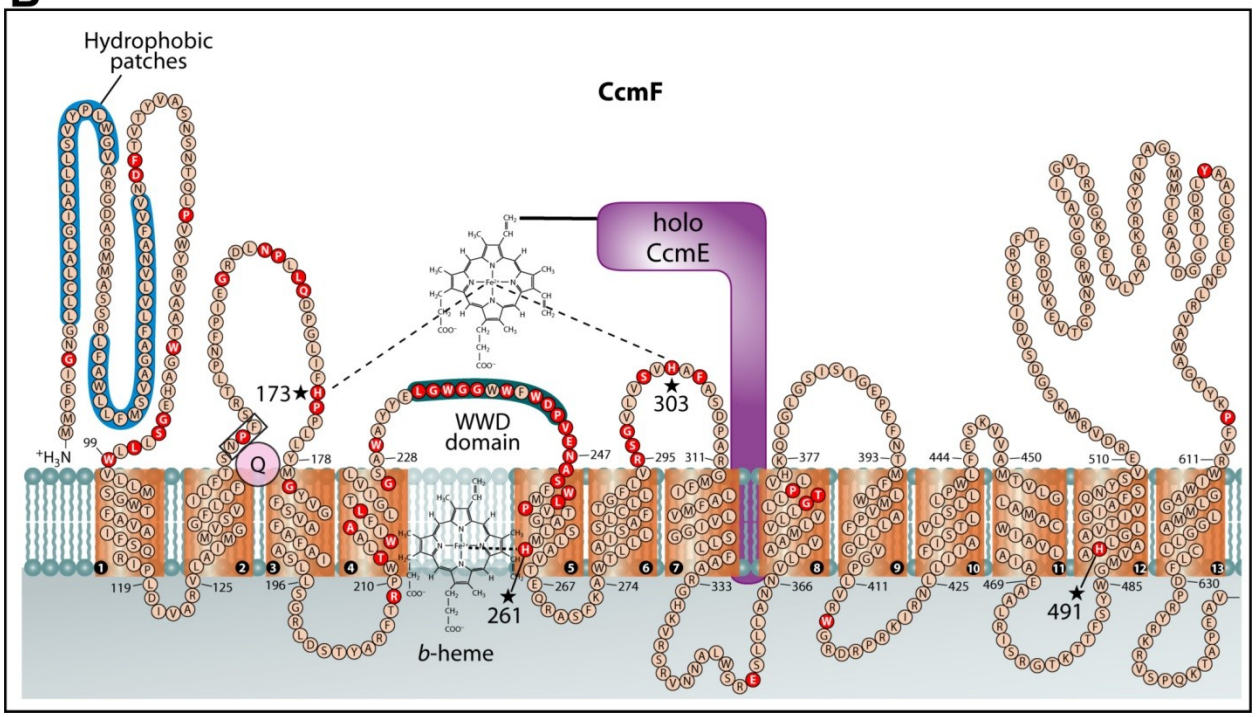
Hydrophobic
patches
CcmF
holo
CcmE
WWD
domain
173
303
261
491
Q
b-heme

Figure 2. Resonance Raman spectral analysis of the CcmF b-heme

Soret-excited resonance Raman spectra of the heme *b* in ferric (red) and ferrous (violet, blue) CcmF. Sample solutions were 88 μM in holoCcmF, 20 mM in Tris, pH 8, 100mM in NaCl, 0.02 % in dodecyl maltoside, ~2 nm in imidazole. HoloCcmF concentrations in the 3.2 % and 0.48 % DDM samples were 23 and 25 μM, respectively. The red and violet spectra were recorded using 10 mW of laser light at 413.1 nm (line focus of emission from Kr^+ laser). The low-frequency blue spectrum was recorded with 2 mW of 441.6-nm emission from a HeCd laser to identify the Fe−His stretching band.

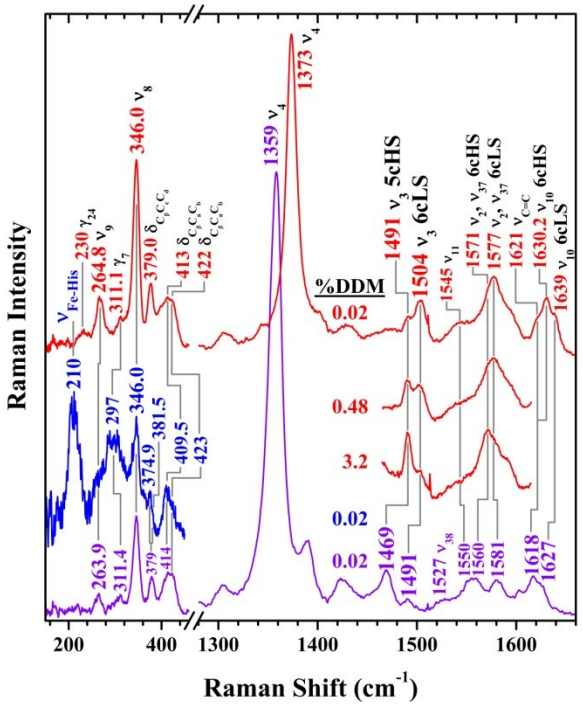
Raman Intensity
Raman Shift (cm-1)
%DDM
0.02
0.48
3.2
0.02
0.02
ν Fe-His
210
230 γ24
264.8 ν9
311.1 γ7
346.0 ν8
379.0 δCγCδCα
413 δCγCδCδ
422 δCγCγCδ
1359 ν4
1373 ν4
1491 ν3 5cHS
1504 ν3 6cLS
1545 ν11
1571 ν2, ν37 6cHS
1577 ν2, ν37 6cLS
1621 νC=C
1630.2 ν10 6cHS
1639 ν10 6cLS
297
346.0
381.5
374.9
409.5
423
263.9
311.4
379
414
1469
1491
1527 ν38
1550
1560
1581
1618
1627
200
400
1300
1400
1500
1600

Figure 3. Resonance Raman spectral analysis of CcmF-CO complexes

(A) Soret(413.1 nm)-excited rR spectra of natural abundance CcmF−CO (green) and CcmF−^{13}CO (blue) in the $\nu_{Fe\text{-}C}$ and $\nu_{C\text{-}O}$ frequency regions. The red traces are the difference spectra, whose amplitudes have been multiplied by a factor of two for ease of viewing. The difference features reveal the bands whose frequencies are ^{13}C dependent, thereby facilitating their assignments to FeCO modes, which are indicated in the labels above the bands. The violet trace shows the spectrum of natural abundance CcmF−CO in 3.2 % DDM. Note that this spectrum exhibits two Fe−C stretching bands. This heterogeneity is attributed to protein conformational changes driven by the high detergent concentration. (B) Heme FeCO backbonding correlation plot showing the positions of the two CcmF−CO conformers. The CcmF−CO complex that falls on the middle line (0.48 % DDM) most likely contains a proximal imidazole ligand from a His residue. Its position low and to the right on the imidazole line shows that the CO ligand interacts only weakly with the heme pocket. The CcmF−CO complex that falls on the top line (3.2 % DDM) is either pentacoordinate or has a proximal ligand that is bound through an oxygen atom.

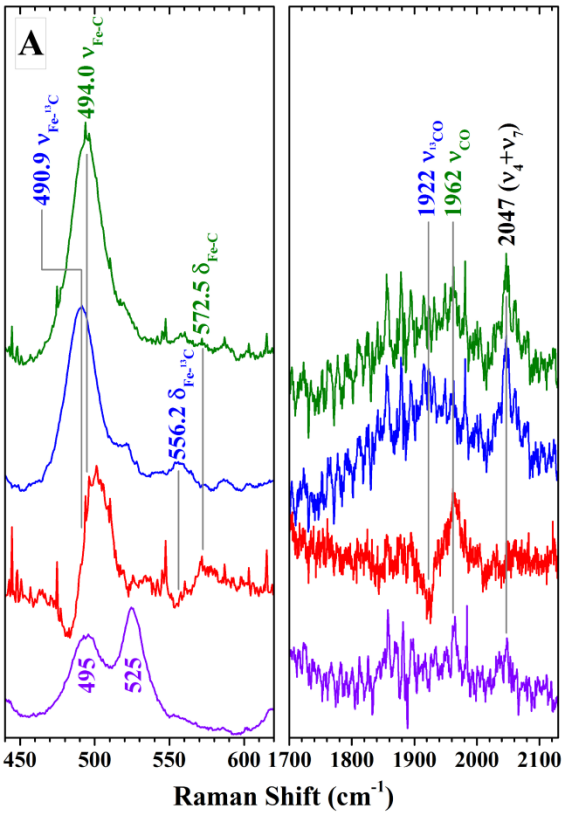
A
494.0 ν_{Fe-C}
490.9 $\nu_{Fe-^{13}C}$
572.5 δ_{Fe-C}
556.2 $\delta_{Fe-^{13}C}$
495
525
1922 $\nu_{^{13}CO}$
1962 ν_{CO}
2047 (ν_4+ν_7)
450 500 550 600 1700 1800 1900 2000 2100
Raman Shift (cm^{-1})

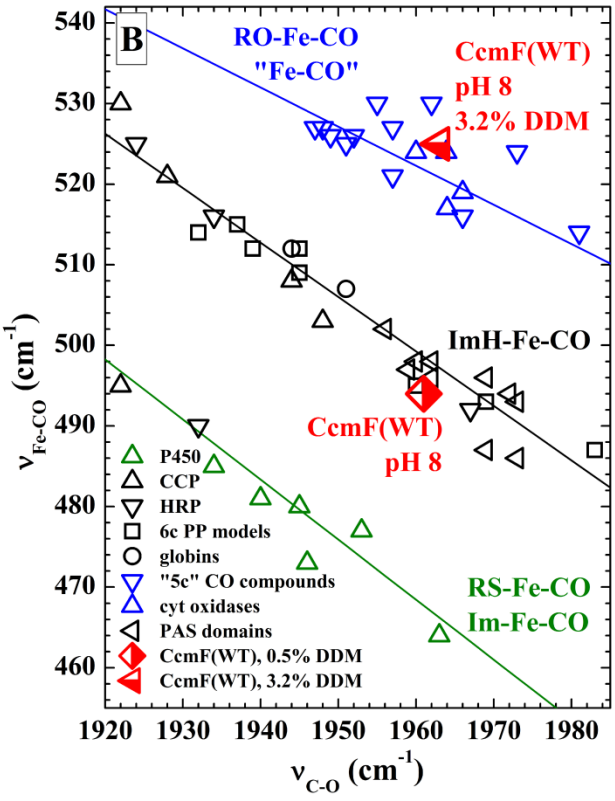
B
RO-Fe-CO
"Fe-CO"
CcmF(WT)
pH 8
3.2% DDM
ImH-Fe-CO
CcmF(WT)
pH 8
RS-Fe-CO
Im-Fe-CO
P450
CCP
HRP
6c PP models
globins
"5c" CO compounds
cyt oxidases
PAS domains
CcmF(WT), 0.5% DDM
CcmF(WT), 3.2% DDM
ν_{Fe-CO} (cm^{-1})
ν_{C-O} (cm^{-1})
540 530 520 510 500 490 480 470 460
1920 1930 1940 1950 1960 1970 1980

Figure 4. Heme levels in CcmF (WT), His303Ala, and His491Ala proteins.

Coomassie stain (A) of CcmF(WT), CcmF(H303A), and CcmF(H491A) showing purified full-length 54 kDa proteins (indicated by arrow). UV/Vis absorption spectra of CcmF(WT) (B), CcmF(H303A) (C), and CcmF(H491A) (D) as purified (oxidized; solid lines) and dithionite-reduced (dotted lines). Absorption maxima are indicated with arrows. Heme stains of CcmF(WT) (E), CcmF(H303A) (F), and CcmF(H491A) (G); free heme is indicated with arrows; M, molecular weight standards; L, load; FT, flow-through; W1-W3, washes 1-3; E, elution; EC, concentrated elution, as described in Experimental Procedures. 20 μM purified CcmF protein was analyzed by UV/Vis absorption spectroscopy (B, C, D) and 30 μg was analyzed by heme stain or Coomassie stain (A; E, F, G, lane 8).

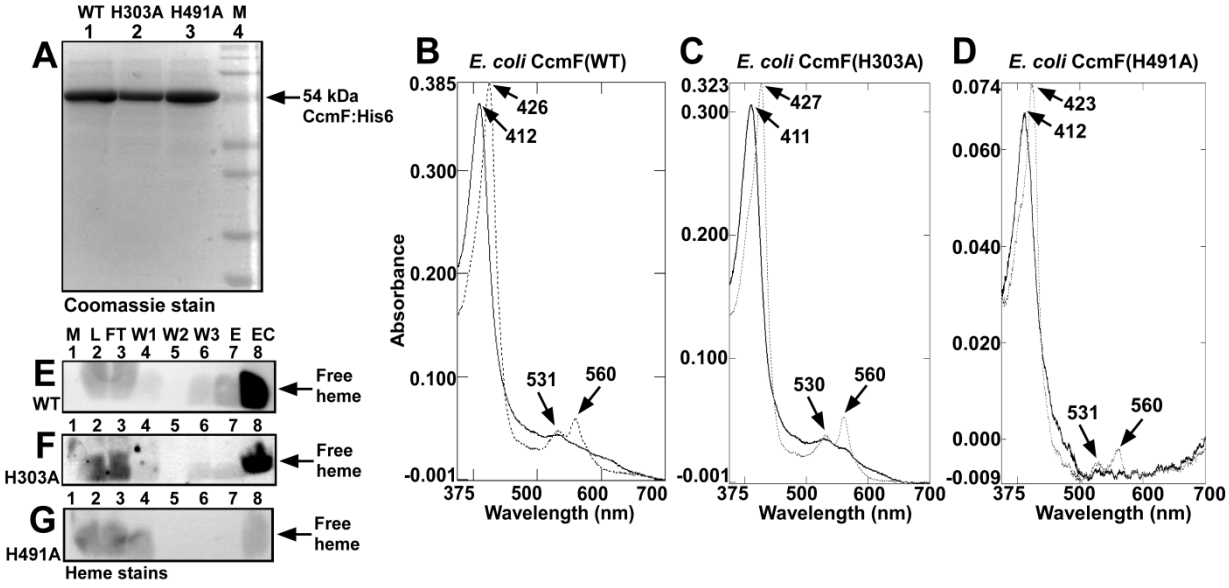
WT H303A H491A M
1 2 3 4
A
54 kDa
CcmF:His6
Coomassie stain
M L FT W1 W2 W3 E EC
1 2 3 4 5 6 7 8
E
WT
Free
heme
1 2 3 4 5 6 7 8
F
H303A
Free
heme
1 2 3 4 5 6 7 8
G
H491A
Free
heme
Heme stains
B
E. coli CcmF(WT)
C
E. coli CcmF(H303A)
D
E. coli CcmF(H491A)
Absorbance
Wavelength (nm)
426
412
531
560
427
411
530
560
423
412
531
560

Figure 5. Spectral analysis of CcmF His261Cys and wild-type CcmF (WT) proteins. Coomassie stain (A) and heme stain (B) of CcmF(WT) and CcmF(H261C) proteins. UV/Vis absorption spectra of CcmF(WT) (C), CcmF(H261C) (D), and CcmF(H261C) in the presence of 30 mM imidazole (E), oxidized (solid lines) and dithionite-reduced (dotted lines). Absorption maxima are indicated with arrows. Absorbance values between 500 nm and 700 nm have been multiplied by a factor of 3. 30 μg of purified protein was analyzed by Coomassie and heme stain (A, B). For UV/Vis absorption spectra approximately 20 μM purified protein was analyzed for wild-type, and approximately 40 μM purified protein was analyzed for His261Cys in the presence and absence of 30 mM imidazole.

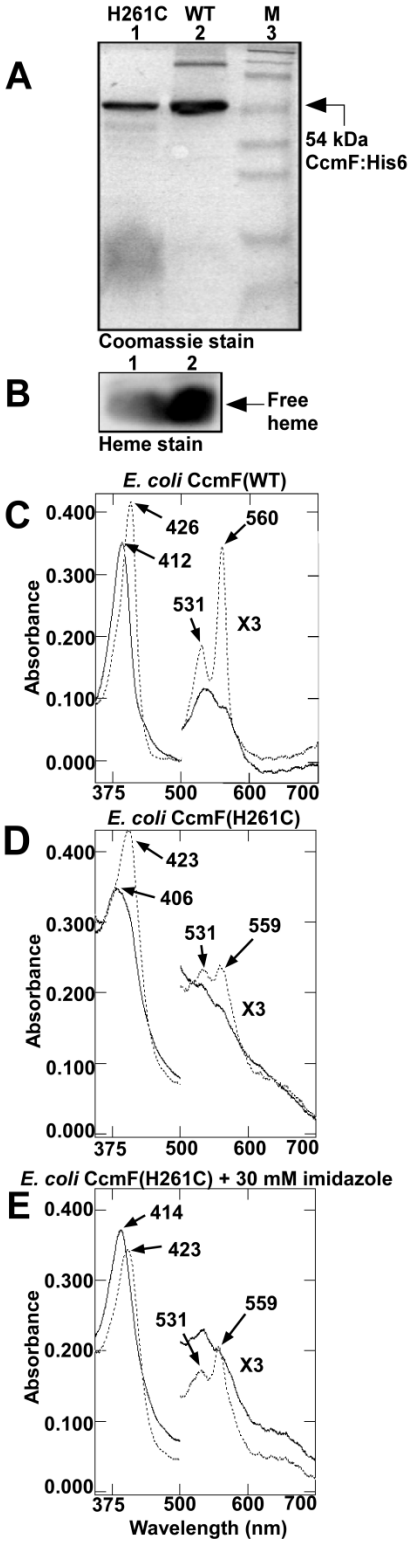
H261C
1
WT
2
M
3
A
54 kDa
CcmF:His6
Coomassie stain
1
2
B
Free
heme
Heme stain
E. coli CcmF(WT)
C
0.400
0.300
0.200
0.100
0.000
Absorbance
426
412
560
531
X3
375
500
600
700
E. coli CcmF(H261C)
D
423
406
531
559
X3
E. coli CcmF(H261C) + 30 mM imidazole
E
414
423
531
559
X3
Wavelength (nm)

Figure 6. Imidazole correction of CcmF His261 and His491 mutants.

The function of each of the indicated substitutions at CcmF His261 (A) or His491 (B) is reported as a percentage of wild-type CcmF (WT) function. Holocytochrome c_4 was quantified by measuring the chemiluminescent heme stain signal of 100 μg of BPER-isolated proteins from three independent experiments. Representative heme stains are provided in Supporting Information (Figure S3). Error bars denote standard deviation. "C" denotes control, which represents chemiluminescent signal in the absence of CcmF (any signal lower than the control is considered background).

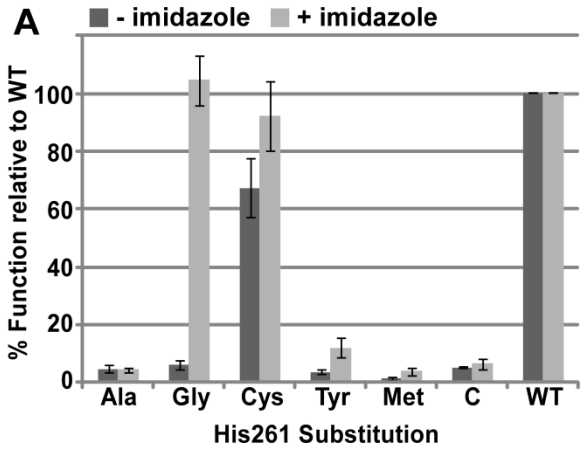
A
- imidazole
+ imidazole
% Function relative to WT
0
20
40
60
80
100
Ala
Gly
Cys
Tyr
Met
C
WT
His261 Substitution

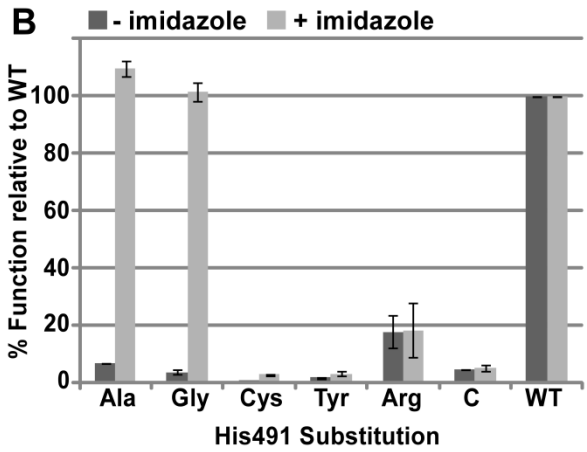
B
- imidazole
+ imidazole
% Function relative to WT
0
20
40
60
80
100
Ala
Gly
Cys
Tyr
Arg
C
WT
His491 Substitution

Figure 7. Phylogenetic distribution and spectral analysis of diverse CcmF proteins.

(A) Adapted from reference (*23*). Representative distribution of systems I, II and III among the bacteria and archaea. The system number is noted in parentheses after each group name, and stars indicate groups containing organisms from which recombinant hexahistidine-tagged CcmF was analyzed in the present study. (B) Reduced UV/Vis absorption spectra of CcmF from *E. coli* (*Ec*), *Thermus thermophilus* (*Tt*; Deinococcus group), *Desulfovibrio vulgaris* (*Dv*), *Roseobacter denitrificans* (*Rd*), and *Shewanella oneidensis* (*So*); *Shewanella oneidensis* CcmF-3 (*So*-F3), and *E. coli* CcmF-2 (*Ec*-F2). Absorption maxima are indicated with arrows. Spectra have been offset for clarity. Approximately 20 μM of each purified CcmF protein was analyzed for which Coomassie and heme stains are provided in Supporting Information (Figure S4).

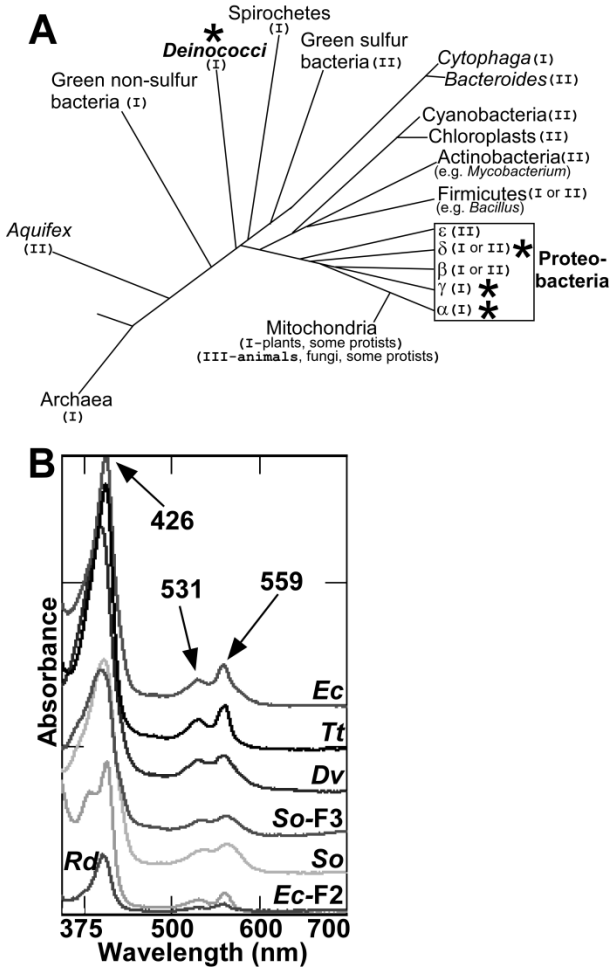
A
Spirochetes
(I)
Deinococci
(I)
Green sulfur
bacteria (II)
Cytophaga (I)
Bacteroides (II)
Green non-sulfur
bacteria (I)
Cyanobacteria (II)
Chloroplasts (II)
Actinobacteria (II)
(e.g. Mycobacterium)
Firmicutes (I or II)
(e.g. Bacillus)
Aquifex
(II)
ε (II)
δ (I or II)
β (I or II)
γ (I)
α (I)
Proteo-
bacteria
Mitochondria
(I-plants, some protists)
(III-animals, fungi, some protists)
Archaea
(I)
B
426
531
559
Absorbance
Ec
Tt
Dv
So-F3
So
Rd
Ec-F2
375
500
600
700
Wavelength (nm)

Figure 8. Redox titration of the CcmF *b*-heme.

Spectra collected during a typical reductive titration of CcmF *b*-heme with nile blue chloride (A) and the corresponding linear Nernst plot (B). Arrows in (A) indicate the direction of changes in absorption during the course of the titration. In (B), [25 mV ln (b-heme$_{red}$/b-heme$_{ox}$)] was used for the one-electron reduction of heme and [12.5 mV ln (dye$_{red}$/dye$_{ox}$)] was used for the two-electron reduction of dye, where b-heme$_{red}$/b-heme$_{ox}$ and dye$_{red}$/dye$_{ox}$ represent ratios of the molar concentrations of the reduced and oxidized forms of the *b*-heme and the dye, respectively. Conditions: 20 mM Tris-HCl, pH 7, 100 mM NaCl, 0.02 % DDM.

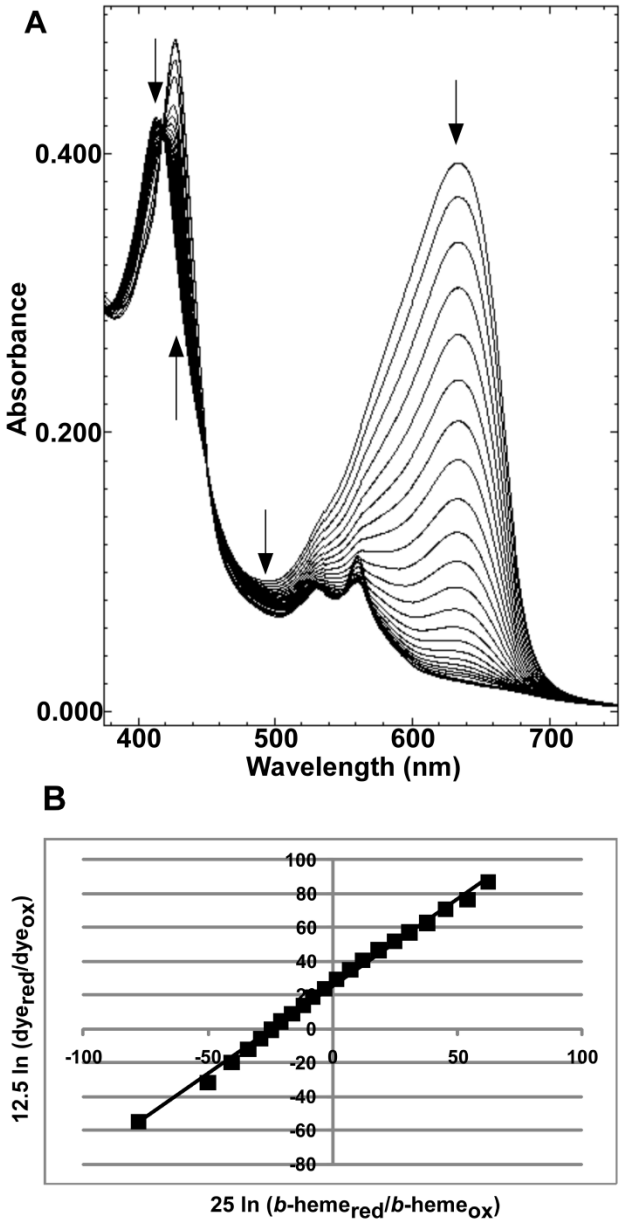
A
0.400
0.200
0.000
Absorbance
400
500
600
700
Wavelength (nm)
B
100
80
60
40
20
0
-20
-40
-60
-80
-100
-50
0
50
100
12.5 ln (dye$_{red}$/dye$_{ox}$)
25 ln (*b*-heme$_{red}$/*b*-heme$_{ox}$)

Supporting Information

Construction of strains and plasmids. All oligonucleotide primer sequences, plasmids, and strains are given in Table S1. To create RK113, we deleted the endogeneous *ccm* operon in *E. coli* BW25113 by P1 transduction. Briefly, P1 phage were grown first in LB media containing 5 mM $CaCl_2$ and 0.2 % glucose (wt/vol) with the donor strain (RK103 (*1*)). Donor cells were killed by addition of chloroform and phage were isolated. Dilutions of isolated phage (100 µL) were incubated with 100 µL of the recipient strain (BW25113) in LB containing 5 mM $CaCl_2$ and 100 mM $MgSO_4$ at 37^{o}C for 30 min. Physical interaction between the phage and cells was disrupted by addition of 66.7 mM sodium citrate (Fisher), pH 5.5, and the culture was added to 1 mL LB broth and incubated for one hour at 37^{o}C while shaking at 300 rpm. Transductants were selected by growth on LB + Kan, and cells were purified from P1 phage by repeated streaking on LB + Kan plates containing sodium citrate. Deletion of the *ccm* operon in RK113 was confirmed by genomic PCR. To create RK111, we used the pKNOCK system (*2*). Briefly, the *cyt* c_4:His6 gene along with the *araC* gene were cloned from pRGK332 (*1*) into pKNOCK-Gm (*2*). The *araC* gene was included to serve as the site for homologous recombination with the chromosome. Cloning was done in *E. coli* S17-1/λ*pir*, and the plasmid was conjugally transferred to *E. coli* RK103 (*1*). Putative exconjugants were selected for resistance to 10 ug ml^{-1} gentamicin, and correct integration of *cyt* c_4:His was verified by genomic PCR.

E. coli strains TB1 and HB101 were used as host strains for cloning. pRGK333 (*1*) containing the full system I operon (*ccmABCDEFGH*) was the template for all PCR amplifications unless otherwise indicated. A plasmid containing *ccmABCDE* (Δ*ccmFGH*) was constructed by PCR amplification of *ccmABCDE* with Ccm_N-term and Del_CcmF_Left, the product of which was digested, and ligated into BamHI and EcoRI digested pGEX-4T-1 (GE

Healthcare) to make pRGK402. To generate the His173Ala, His261Ala, and His303Ala mutants, short PCR products were amplified using Del_CcmE_Right and CcmF_His173Ala_Rev, CcmF_His261Ala_Rev, or CcmF_His303Ala_Rev. These products were gel purified and used in a second amplification with CcmH_XhoI_Rev using pRGK386 (*3*) as template to generate *ccmF*(His173Ala):His6*GH*, *ccmF*(His261Ala):His6*GH*, and *ccmF*(His303Ala):His6*GH* (His6 refers to a hexahistidine tag at the carboxy terminus of CcmF). The final, full-length products were ligated into NdeI and XhoI digested pRGK402 to generate pRGK403, pRGK404, and pRGK405, respectively. A plasmid containing *ccmABCDEGH* (Δ*ccmF*) was constructed by PCR amplification of *ccmGH* with Del_CcmF_Right and Ccm_C-term primers, the product of which was digested and ligated into EcoRI and NdeI digested pRGK402 to make pRGK406. For the His491Ala mutant, a short PCR product was generated by amplifying with CcmF_His491Ala_Fwd and CcmF_ 6xHis_NdeI_Rev. This product was gel purified and then used in a second amplification with Del_CcmE_Right to generate *ccmF* (His491Ala):His6. The final, full-length product was ligated into the single NdeI site of pRGK406 to generate pRGK407.

To insert *ccmF*:His6, *ccmF*(His261Ala):His6, or *ccmF*(His491Ala):His6 into pRGK330 (*1*) for arabinose-inducible expression in the absence of other *ccm* genes, the corresponding *ccmF* gene was amplified from pRGK386, pRGK404, or pRGK407, respectively, with CcmF_NcoI_Fwd and CcmF_6xHis_PstI_Rev, digested, and ligated into NcoI and PstI digested pRGK330 to make pRGK408, pRGK409, and pRGK410. His261Gly, Cys, Tyr, and Met were generated by amplifying with the appropriate reverse mismatch primer and CcmF_NcoI_Fwd to generate short PCR products. These products were gel purified and used in a second amplification with CcmF_6xHis_PstI_Rev. His491Gly, Cys, Tyr and Arg were generated by

amplifying with the appropriate forward mismatch primer and CcmF_6xHis_PstI_Rev to generate short PCR products. These products were gel purified and used in a second amplification with CcmF_NcoI_Fwd. The final, full-length products for all site-directed mutants at His261 and His491 described above were digested with NcoI and PstI and inserted into pRGK330 to generate pRGK411-418. Each of the final constructs was sequenced to confirm the mutation.

The *ccmF-3* gene from *Shewanella oneidensis* (SO_0478) was PCR amplified from genomic DNA, digested, and ligated into the NcoI and PstI sites in pRGK330 to generate pRGK420. The *ccmF* gene from *Roseobacter denitrificans* (RD1_3223) was amplified from genomic DNA, digested, and ligated into the EcoRI and KpnI sites of pRGK330 to make pRGK424. *Roseobacter denitrificans* genomic DNA was provided generously by the Blankenship lab. The *ccmF-2* gene from *E. coli* (b4074) was amplified from genomic DNA, digested, and ligated into the NcoI and XbaI sites of pRGK330 to make pRGK421. The *ccmF* genes from *Shewanella oneidensis* (SO-0266), *Desulfovibrio vulgaris* (DVU_1050), and *Thermus thermophilus* (TTHA1404) were each amplified from genomic DNA with the appropriate primers and cloned into pCR-Blunt II-TOPO (Invitrogen). From pCR-Blunt II-TOPO, the *ccmF* gene from *Shewanella oneidensis* was ligated into the NheI and XhoI sites of pRGK330 to make pRGK419, the *ccmF* gene from *Desulfovibrio vulgaris* was ligated into the NcoI and XbaI sites to make pRGK423, and the *ccmF* gene from *Thermus thermophilus* was ligated into the KpnI and NheI sites to make pRGK422. *Desulfovibrio vulgaris* subsp. *vulgaris* ATCC 29579 and *Thermus thermophilus* ATCC 27634 strains were obtained from ATCC and cultured according to ATCC recommendations, and genomic DNA was prepared using the Puregene System Cell and Tissue DNA Isolation Kit (Gentra Systems).

Table S1. Oligonucleotides, plasmids, and strains used in this study

Primer	Sequence (5'-3')	Plasmid Constructed
Del_CcmF_Left	CCGAATTCTGGCATCATATGGCTGGGTCCTTAT	pRGK402
Ccm_N-term	TTGCAGATCTATGCTTGAAGCCAGAG	pRGK402
Del_CcmE_Right	GACCCAGCCATATGATGCCAGAAATTGGTAACG	pRGK403-405, 407
CcmF_His173Ala_Rev	GCAGAGGCGGAGCGAAGATGAGCCCCGG	pRGK403
CcmF_His261Ala_Rev	CCGCCAGTGACGCCATCAGCGCAGTCC	pRGK404
CcmF_His303Ala_Rev	CAGACGCAAACGCGGCTACAGATACCAGCACGCC	pRGK405
CcmH_XhoI_Rev	GCGCTCGAGTTTTTATTCACTCTCCTGCGG	pRGK403-405
Del_CcmF_Right	GGCCATATGAAGCGCAAAGTATTGTTAATTCCG	pRGK406
Ccm_C-term	CGGAATTCTTTTTATTTACTCTCCTGC	pRGK406
CcmF_His491Ala_Fwd	GTGGCGGCTGCCCTTGGGCTG	pRGK407
CcmF_6xHis_NdeI_Rev	GATCATATGTCAGTGGTGGTGGTGGTGGTGTACGGCCTCCGGCGCAG	pRGK407
CcmF_6xHis_PstI_Rev	GATCTGCAGTCAGTGGTGGTGGTGGTGGTGTACGGCCTCCGGCGCAG	pRGK408-418
CcmF_NcoI_Fwd	CGCCATGGTGCCAGAAATTGGTAACGGAC	pRGK408-418
CcmF_His261Gly	CGCCAGTGAGCCCATCAGCGC	pRGK411
CcmF_His261Cys	CGCCAGTGAGCACATCAGCGC	pRGK412
CcmF_His261Tyr	CGCCAGTGAATACATCAGCGC	pRGK413
CcmF_His261Met	CGCCAGTGACATCATCAGCGC	pRGK414
CcmF_His491Gly	GTGGCGGCTGGCCTTGGGCTG	pRGK415
CcmF_His491Cys	GTGGCGGCTTGCCTTGGGCTG	pRGK416
CcmF_His491Tyr	GTGGCGGCTTACCTTGGGCTG	pRGK417
CcmF_His491Arg	GTGGCGGCTCGCCTTGGGCTG	pRGK418
Shew_CcmF_Fwd	GGCCATGGCCCCAGAACTGGGACACTTTTCGCTG	pRGK419
Shew_CcmF_Rev	GGGGTCGACTTAGTGGTGGTGGTGGTGGTTGAGCGGTAGCTAATTTCGC	pRGK419
Shew_CcmF3_Fwd	CGCCATGGTTCCAGAAATCGGGCA	pRGK420
Shew_CcmF3_Rev	ATCTGCAGTCAGTGGTGGTGGTGGTGGTGTTGGGTTACCGTCTC	pRGK420
Ecoli_CcmF2_Fwd	GCACCATGGTGACCCCGTTGACGGCCTTC	pRGK421
Ecoli_CcmF2_Rev	GCTCTAGATTAGTGGTGGTGGTGGTGGTGTTCATCGCGCTTCTTCCCCC	pRGK421
Thermus_CcmF_Fwd	ATGCTAGCAGGAGGAATTCACCATGACCCCGGCCCTTCTCGGCAAC	pRGK422
Thermus_CcmF_Rev	ACAAGCTTTCAGTGGTGGTGGTGGTGGTGCGCCGGGCTCACCCCCCTAG	pRGK422
Desulfo_CcmF_Fwd	AACCATGGCCCTTTCCGCCTACCTGCTTCTCGTAGCCTCGCTGCTGTTC	pRGK423
Desulfo_CcmF_Rev	AGGATCCTTAGTGGTGGTGGTGGTGGTGCGCCTCCGCTGTCTTCCGGC	pRGK423
Roseo_CcmF_Fwd	GCGAATTCACCATGATTACAGAACTCGGACA	pRGK424
Roseo_CcmF_Rev	ATGGTACCTCAGTGGTGGTGGTGGTGGTGTTCCGCAGGCACCGGTGCGGC	pRGK424

Plasmid	Description	Reference
pRGK330	pBAD CmR	(1)
pRGK332	pBAD cytochrome *c*4:His6	(1)
pRGK333	pGEX *ccmABCDEFGH*	(1)
pRGK386	pGEX *ccmABCDEF*:His6*GH*	(3)
pRGK402	pGEX *ccmABCDE*	This work
pRGK403	pGEX *ccmABCDEF*(His173Ala):His6*GH*	This work
pRGK404	pGEX *ccmABCDEF*(His261Ala):His6*GH*	This work
pRGK405	pGEX *ccmABCDEF*(His303Ala):His6*GH*	This work
pRGK406	pGEX *ccmABCDEGH*	This work
pRGK407	pGEX *ccmABCDEF*(His491Ala):His6*GH*	This work
pRGK408	pBAD *ccmF*:His6	This work
pRGK409	pBAD *ccmF*(His261Ala):His6	This work
pRGK410	pBAD *ccmF*(His491Ala):His6	This work
pRGK411	pBAD *ccmF*(His261Gly):His6	This work
pRGK412	pBAD *ccmF*(His261Cys):His6	This work
pRGK413	pBAD *ccmF*(His261Tyr):His6	This work
pRGK414	pBAD *ccmF*(His261Met):His6	This work
pRGK415	pBAD *ccmF(*His491Gly):His6	This work
pRGK416	pBAD *ccmF*(His491Cys):His6	This work
pRGK417	pBAD *ccmF*(His491Tyr):His6	This work
pRGK418	pBAD *ccmF*(His491Arg):His6	This work
pRGK419	pBAD *ccmF*:His6 (*S. oneidensis*)	This work
pRGK420	pBAD *ccmF-3*:His6 (*S. oneidensis*)	This work
pRGK421	pBAD *ccmF-2*:His6 (*E. coli*)	This work
pRGK422	pBAD *ccmF*:His6 (*T. thermophilus*)	This work
pRGK423	pBAD *ccmF*:His6 (*D. vulgaris*)	This work
pRGK424	pBAD *ccmF*:His6 (*R. denitrificans*)	This work

Strain	Description	Reference
RK103	MG1655 Δ*ccm*	(1)
RK111	MG1655 Δ*ccm cyt c*4:His6 chromosomal integrate	This work
RK113	BW25113 Δ*ccm* Δ*araBAD*	This work
ATCC 27634	*Thermus thermophilus*	This work
ATCC 29579	*Desulfovibrio vulgaris* subsp. *vulgaris*	This work

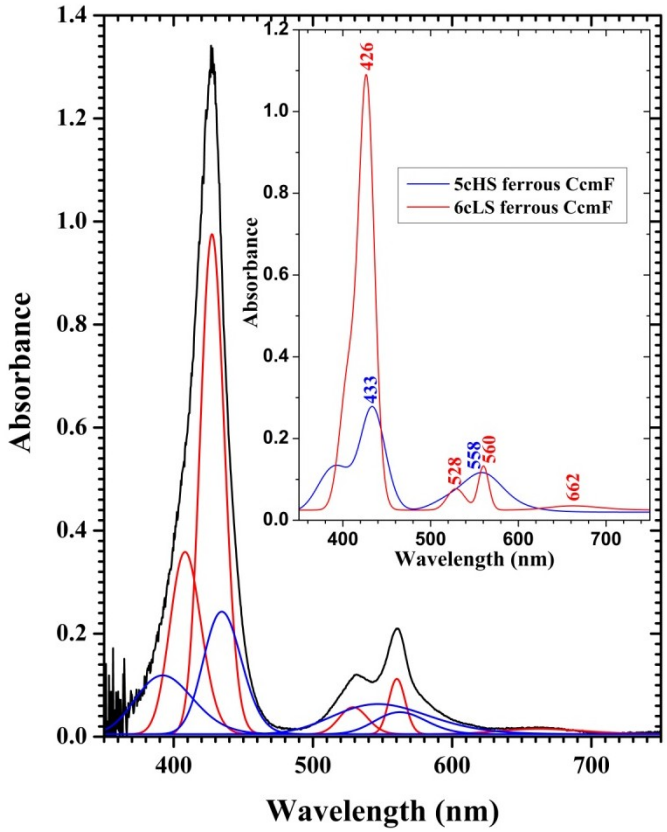

Figure S1. Peak fitting of the ferrous CcmF UV-visible absorbance spectrum.

The fit peaks reveal speciation between 6cLS (red) and 5cHS (blue) hemes with a significant fraction being 5cHS. Assuming that the extinction coefficients at the HS and LS Soret maxima are roughly equal, the samples of ferrous CcmF(WT) used in this study comprise approximately 20 % 5cHS heme. Based on similarities among the UV-visible spectra and insensitivity of the ν_3 ratios to [DDM] between 0.48 % and 0.02 %, this speciation is essentially independent of DDM concentration.

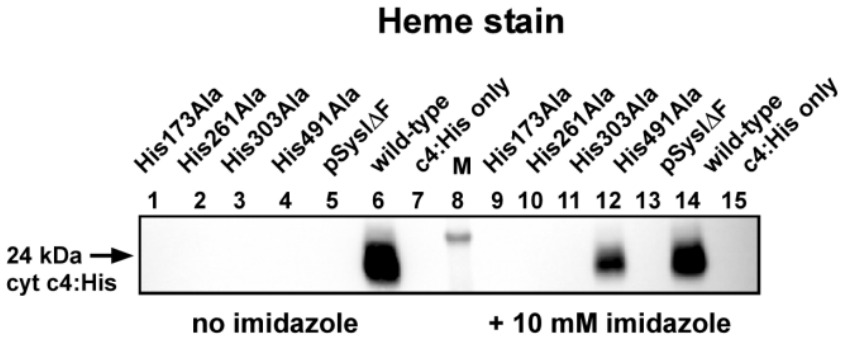

Figure S2. Cytochrome c_4:His6 assembly in the presence or absence of 10 mM imidazole. Arrow indicates 24 kDa holocytochrome c_4:His6 matured by a functional system I. "pSysIΔF" denotes a system I deleted for *ccmF*; "c4:His only" denotes an absence of all *ccm* genes; "M" denotes molecular weight standards (shown is the 28 kDa standard). 100 μg of BPER-isolated proteins was loaded into each lane for SDS-PAGE prior to heme staining.

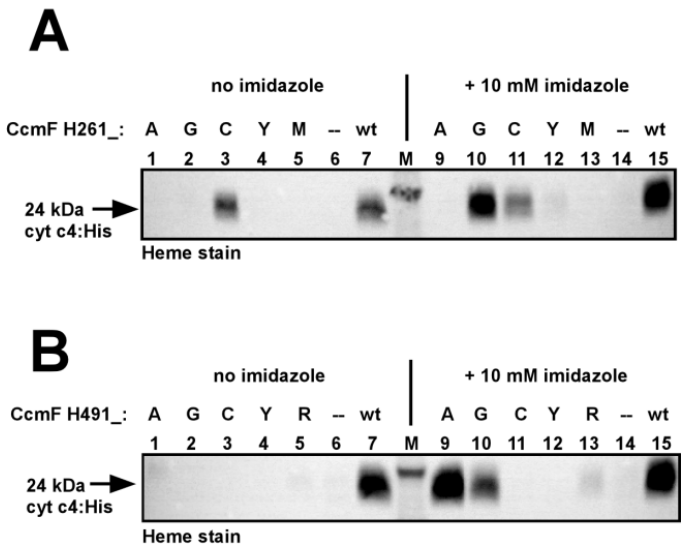

Figure S3. Cytochrome c assembly in the presence or absence of imidazole.

Representative heme stains showing cytochrome c_4:His6 assembly of mutants at His261 (A) and His491 (B) in the presence or absence of 10 mM imidazole (as described in Figure S1). Arrow indicates 24 kDa holocytochrome c_4:His6 matured by a functional system I. Substitutions: A, Ala; G, Gly; C, Cys; Y, Tyr; M, Met; R, Arg. The dash denotes the negative control condition (absence of CcmF) and "wt" denotes wild-type CcmF. "M" denotes molecular weight standards (shown is the 28 kDa standard). 100 μg of BPER-isolated proteins was loaded into each lane for SDS-PAGE prior to heme staining.

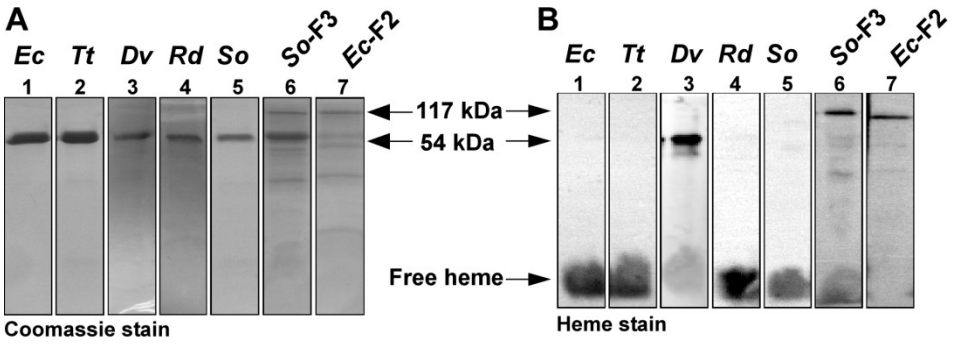

Figure S4. Purification of CcmF proteins from diverse bacteria.

Coomassie stain (A) and corresponding heme stain (B) after SDS-PAGE of CcmF:His6 from *E. coli* (*Ec*), *Thermus thermophilus* (*Tt*; Deinococcus group), *Desulfovibrio vulgaris* (*Dv*), *Roseobacter denitrificans* (*Rd*), *Shewanella oneidensis* (*So*), *Shewanella oneidensis* CcmF-3 (*So*-F3), and *E. coli* CcmF-2 (*Ec*-F2). Arrows indicate full-length 54 kDa CcmF:His6 and free heme at the SDS-PAGE dye front. Note that some of the *So*-CcmF3 and *Ec*-CcmF2 aggregate at approximately 117 kDa, possibly a dimeric form, under the conditions of SDS-PAGE used. Additionally, note that for *Dv*, *So*-CcmF3 and *Ec*-F2, some heme is retained in the full length protein and/or in the higher molecular weight forms. For each of the proteins analyzed, heme was found to be non-covalent as determined by pyridine hemachromagen (data not shown). Thus, *Dv*, *So*-CcmF3 and *Ec*-F2 may bind heme in a partially SDS-resistant, although non-covalent, manner. 30 μg of purified hexahistidine-tagged protein was analyzed for each.

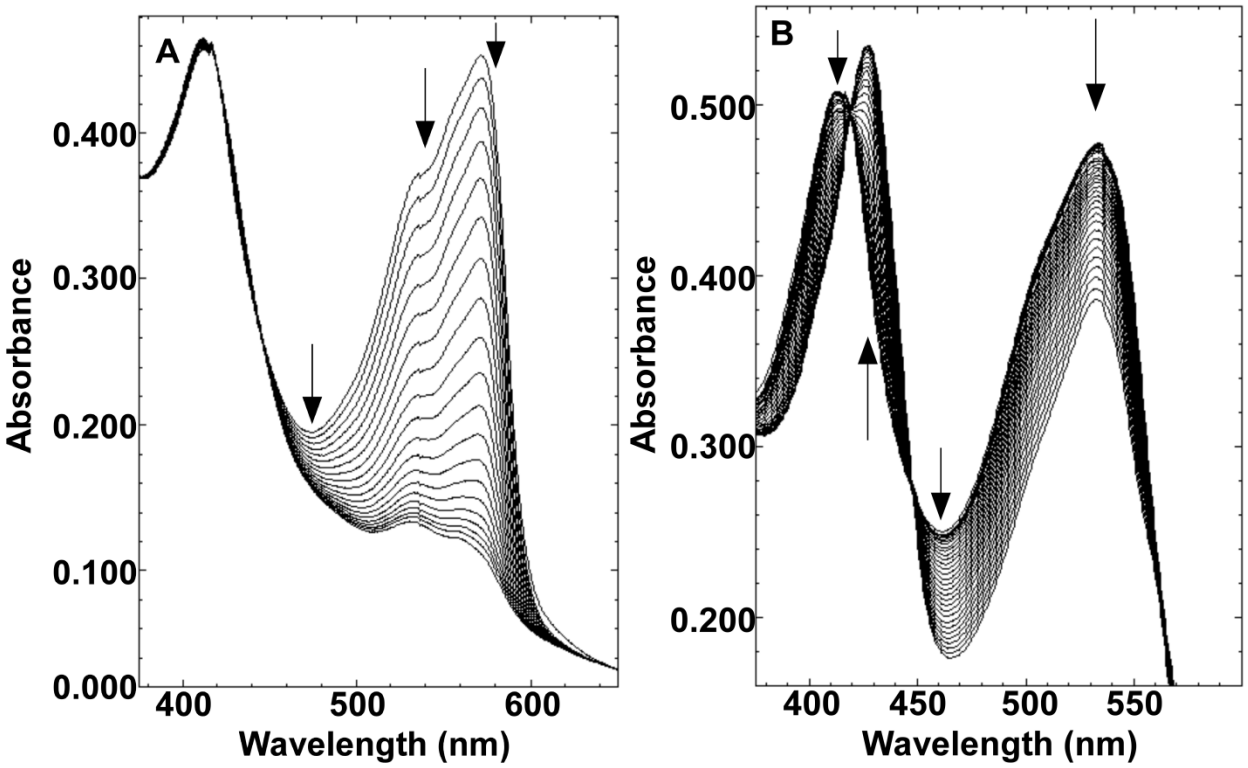

Figure S5. Redox titration of the CcmF *b*-heme with alternate redox dyes.

Spectra collected during reduction of CcmF *b*-heme with resorufin (A) or safranin O (B). Arrows indicate the direction of changes in absorption during the course of the titration. The decreases in absorbance at 534 nm and 572 nm in (A) are due to reduction of resorufin. In (B), the decrease in absorbance at 412 nm and the increase in absorbance at 426 nm are indicative of reduction of the CcmF *b*-heme, and the decrease in absorbance at 532 nm is due to reduction of safranin O. Note that the dye resorufin (E_m = -50 mV) (*4*) is completely reduced before reduction of the CcmF *b*-heme, while the CcmF *b*-heme is completely reduced before reduction of safranin O (E_m = -280 mV) (*4*). This indicates that the relative midpoint potential of the CcmF *b*-heme is in between that of resorufin and safranin O. Conditions: 20 mM Tris-HCl, pH 7, 100 mM NaCl, 0.02 % DDM.

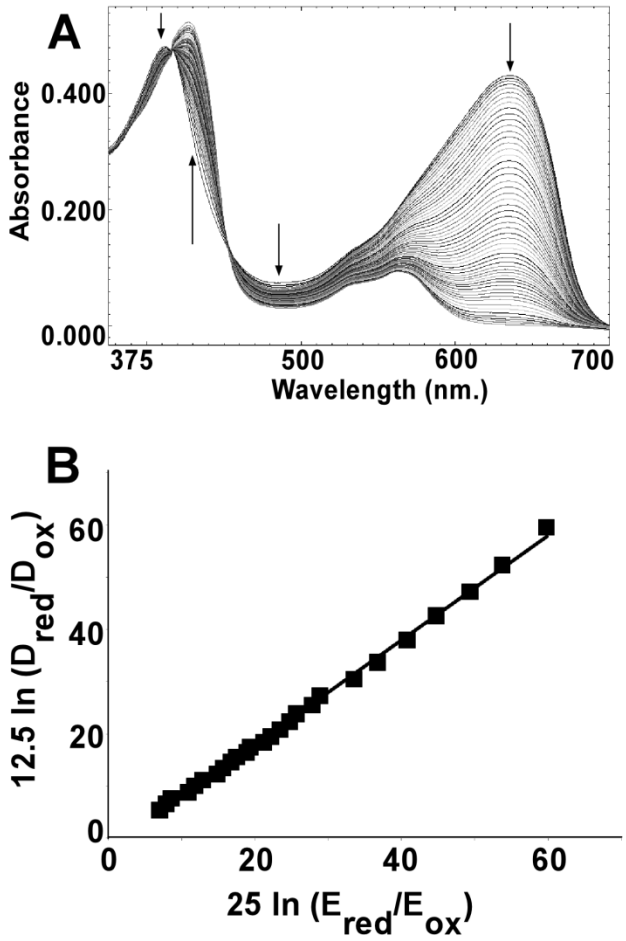

Figure S6. Redox titration of the CcmF *b*-heme in high DDM (1.2 %).

Spectra collected during a reductive titration of CcmF *b*-heme with nile blue chloride (E_m = -116 mV) (*4*) (A) and the corresponding linear Nernst plot (B). Arrows in (A) indicate the direction of changes in absorption during the course of the titration. In (B), [25 mV ln (*b*-heme$_{red}$/*b*-heme$_{ox}$)] was used for the one-electron reduction of heme and [12.5 mV ln (dye$_{red}$/dye$_{ox}$)] was used for the two-electron reduction of dye, where *b*-heme$_{red}$/*b*-heme$_{ox}$ and dye$_{red}$/dye$_{ox}$ represent ratios of the molar concentrations of the reduced and oxidized forms of the *b*-heme and the dye, respectively. The reduction potential in 1.2 % DDM was substantially more positive (E_m = -110 ± 4 mV) than in 0.02 % DDM. Conditions: 20 mM Tris-HCl, pH 7, 100 mM NaCl, 1.2 % DDM.

Supporting Information References

(1) Feissner, R. E., Richard-Fogal, C. L., Frawley, E. R., Loughman, J. A., Earley, K. W., and Kranz, R. G. (2006) Recombinant cytochromes c biogenesis systems I and II and analysis of haem delivery pathways in Escherichia coli. *Mol Microbiol 60*, 563-577.

(2) Alexeyev, M. F. (1999) The pKNOCK series of broad-host-range mobilizable suicide vectors for gene knockout and targeted DNA insertion into the chromosome of gram-negative bacteria. *Biotechniques 26*, 824-826.

(3) Richard-Fogal, C. L., Frawley, E. R., Bonner, E. R., Zhu, H., San Francisco, B., and Kranz, R. G. (2009) A conserved haem redox and trafficking pathway for cofactor attachment. *Embo J 28*, 2349-2359.

(4) Clark, W. M. (1960) *Oxidation-Reduction Potentials of Organic Systems*, Waverly Press, Baltimore, MD.

Chapter 3: Interaction of HoloCcmE with CcmF in Heme Trafficking and Cytochrome c Biosynthesis

Brian San Francisco and Robert G. Kranz

Department of Biology, Washington University in St. Louis, St. Louis, MO 63130

Submitted for publication to *J Mol Biol* (2013)

For correspondence: E-mail: kranz@biology.wustl.edu; Tel. (+1) 314 935 4278; Fax (+1) 314 935 4432.

Abstract

The periplasmic heme chaperone holoCcmE is essential for heme trafficking in the cytochrome c biosynthetic pathway in many bacteria, archaea, and plant mitochondria. This pathway, called system I, involves two steps: i) formation and release of holoCcmE (by CcmABCD), and ii) delivery of the heme in holoCcmE to the putative cytochrome c heme lyase complex, CcmFH. CcmFH is believed to facilitate the final covalent attachment of heme (from holoCcmE) to the apocytochrome c. Although all models for system I propose that holoCcmE delivers heme directly to CcmF, no interaction between holoCcmE and CcmF has been demonstrated. Here, a complex between holoCcmE and CcmF is "trapped", purified, and characterized. HoloCcmE must be released from the ABC-transporter complex CcmABCD to interact with CcmF, and the holo-form of CcmE interacts with CcmF at levels at least 20-fold higher than apoCcmE. Two conserved histidines (here termed P-His1 and P-His2) in separate periplasmic loops in CcmF are required for interaction with holoCcmE, and evidence is presented that P-His1 and P-His2 function as heme-binding ligands. These results show that heme in holoCcmE is essential for complex formation with CcmF, and that the heme of holoCcmE is coordinated by P-His1 and P-His2 within the WWD domain of CcmF. These features are strikingly similar to formation of the CcmC:heme:CcmE ternary complex (Richard-Fogal and Kranz, JMB 2010), and suggest common mechanistic and structural aspects.

Highlights

CcmF forms a complex with holoCcmE

HoloCcmE must be released from CcmABCD to interact with CcmF

Heme binding by holoCcmE is essential for complex formation with CcmF

CcmF P-His1 and P-His2 are required for binding holoCcmE

CcmH controls formation of the CcmF—holoCcmE complex

Keywords

Pathway

Biogenesis

Oxidation-Reduction

Heme trafficking

Cytochrome c Maturation

Abbreviations

TM, transmembrane

P, p-side (of cytoplasmic membrane)

ABC, ATP-binding cassette

GST, glutathione S-transferase

DDM, dodecyl maltoside

CCM, cytochrome c maturation

PMSF, phenylmethylsulfonylfluoride

Introduction

C-type cytochromes are heme proteins involved in vital electron transfer reactions in the cell. These cytochromes function outside of the cytoplasmic membrane in prokaryotes, in the lumen of chloroplasts, and in the intermembrane space of mitochondria. Cytochromes c are unique among heme proteins in that the heme is covalently attached to the protein (via thioether linkages between the 2- and 4-vinyls of heme and two thiols of a conserved Cys-Xxx-Xxx-Cys-His motif in the apoprotein). For covalent attachment to occur, both the apocytochrome thiols and the iron of heme must be reduced [1; 2]. In many bacteria, plant and protozoal mitochondria, and archaea, holocytochrome c formation requires the cytochrome c maturation (ccm) pathway, called system I (see Fig 1), which comprises eight dedicated membrane proteins (in *E. coli*, CcmABCDEFGH) [3; 4; 5; 6; 7].

System I can be conceptually described as two steps (see Fig 1): (i) formation and release of the heme chaperone protein, called holo (+ heme) CcmE, (from CcmABCD) and (ii) heme transfer from holoCcmE to the apocytochrome (putatively, via CcmFH) to yield a holocytochrome c. Formation of holoCcmE occurs in the CcmCDE complex [8; 9], where a unique covalent attachment is formed between the β carbon of the heme 2-vinyl and a conserved histidine residue (His130) in CcmE [10; 11; 12]. Expression of CcmAB leads to formation of an ABC transporter complex (CcmABCD) that uses ATP hydrolysis to release covalent holoCcmE [13; 14; 15]. Released, oxidized (Fe^{3+}) holoCcmE is proposed to chaperone its heme to the site of cytochrome c formation, CcmFH, but this has not been proven (see below) [9; 16; 17]. CcmF, which forms an integral membrane complex with CcmH, is believed to be the site of thioether formation between the heme vinyls and the apocytochrome; thus, it has been termed the "cytochrome c heme lyase". The CcmFH integral membrane complex has been purified [9] or co-

immunoprecipitated [17; 18; 19]. CcmF contains a separate and stable non-covalent heme b [9; 20], which we have hypothesized plays a role in reducing the incoming heme from holoCcmE [4; 20]. Reduction of heme (to Fe^{2+}) is a requirement for thioether formation [1; 2; 4], and would also favor the release of heme from CcmE His130 [4; 8; 20]. CcmG [21; 22; 23] and CcmH [24; 25] are thioredox proteins that maintain the apocytochrome thiols (in the Cys-Xxx-Xxx-Cys-His motif) in the reduced state [26; 27; 28]. In some species, such as *Rhodobacter capsulatus*, ccmH is split into two open reading frames (called ccmH and ccmI). While there is significant evidence that the apocytochrome interacts with the CcmFH cytochrome c heme lyase complex (via CcmH) [24; 26; 29; 30], there has been no data demonstrating that holoCcmE interacts with CcmF (see Discussion for details). Nonetheless, formation of a complex between holoCcmE and CcmF has been proposed in nearly every review on cytochrome c biogenesis during the last decade (e.g., [3; 4; 5; 6; 7]). Thus, the proposal that holoCcmE trafficks heme directly to CcmF (see Fig 1) for holocytochrome c formation remains unproven.

Here, we describe purification and characterization of an intermediate complex between holoCcmE and CcmF, achieved by purifying CcmF from detergent-solubilized membranes lacking CcmG and CcmH. We show that holoCcmE must be released from CcmCD in order to interact with CcmF, and that holoCcmE forms a complex with CcmF at levels at least 20-fold higher than apoCcmE. We demonstrate that two periplasmic histidines (His173 and His303, here called P-His1 and P-His2, respectively) in separate periplasmic loops in CcmF are required for interaction with holoCcmE, with evidence that these residues function as heme-binding ligands. We propose that heme in holoCcmE is a critical component for interaction with CcmF and we discuss how these results mirror formation of the CcmC:heme:CcmE ternary complex [8] (see Fig 1).

Results

The holoCcmE-CcmF complex

Although all current *in vivo* models for the system I pathway presume a holoCcmE—CcmF intermediate during holocytochrome c biosynthesis, we have been unable to co-purify holoCcmE at detectable levels in our preparations of CcmFH [9]. Our purifications of CcmF (and CcmFH complex) are typically from DDM-solubilized membranes that contain all Ccm proteins (CcmABCDEFGH). The inability to identify a complex between holoCcmE and CcmF could be due to a transient, short-lived interaction or current models for system I may be incorrect. In an attempt to detect an interaction between holoCcmE and CcmF, we expressed CcmF along with the minimal set of CCM components required for formation and release of holoCcmE from the CcmABCD complex (i.e., CcmABCDEF, or pGEX ΔCcmGH; Fig 2 A-D). Note that the proteins CcmG and CcmH are absent in these cells. Full-length hexahistidine-tagged CcmF (54-kDa) was TALON-purified as a single polypeptide to greater than 90% purity (Fig 2A, lane 8) that reacted with CcmF antisera (Fig 2B, lane 8). Heme staining revealed that, in addition to the CcmF b-type heme (which dissociates from the protein and migrates as free heme during denaturing SDS-PAGE) preparations of CcmF from membranes lacking CcmG and CcmH contained 20-kDa holoCcmE (Fig 2C, lane 8). Immunodetection with CcmE antisera confirmed that the 20-kDa covalent heme species was holoCcmE (Fig 2D, lane 8).

UV-Vis absorption spectra of the oxidized (as purified) CcmF-holoCcmE preparation showed a Soret maximum at 412 nm and broad α and β absorptions between 500 and 600 nm (Fig 2E). Chemical reduction with sodium dithionite yielded a Soret maximum at 426 nm and sharp α and β absorptions at 559 and 530, respectively. These spectral features, in addition to the 556 nm absorption in the reduced pyridine hemochrome (Fig 2E, inset) are characteristic of non-

covalent, b-type hemes [32], and are indistinguishable from those of the CcmF b-heme [9; 20]. Because the holoCcmE polypeptide is not readily detectable by Coomassie staining (Fig 2A, lane 8), it is likely that holoCcmE is less than stoichiometric with CcmF in the CcmF-holoCcmE complex. This result, together with only slight differences in the electronic absorptions of holoCcmE and CcmF, make it difficult to discern the spectral contributions of the heme from holoCcmE. We next wanted to analyze the role of other Ccm proteins as well as specific residues in CcmF in formation of the holoCcmE-CcmF complex.

HoloCcmE co-purifies with CcmF in the absence of CcmG and CcmH

As mentioned above, purifications of CcmF from membranes containing all Ccm proteins (CcmABCDEFGH) typically do not yield detectable holoCcmE. Therefore, we directly compared levels of holoCcmE that co-purified with CcmF in the presence of all Ccm proteins (expressed from pSysI) to those that co-purified with CcmF in the absence of CcmG and CcmH (expressed from pSysI ΔGH). As controls, we included in this analysis constructs lacking *ccmF* (pSysI ΔFGH, or pGEX *ccmABCDE*) and *ccmE* (pSysI ΔEGH, pGEX *ccmABCDF*:His6). With the exception of ΔFGH, CcmF was purified as a single full-length polypeptide (54-kDa; Fig 3A, lanes 2-4) that reacted with CcmF antisera (Fig 3B, lanes 2-4). Immunoblotting with CcmH antisera showed that co-purified 34-kDa CcmH was present only in CcmF purifications from the pSysI background, as expected (Fig 3C, lane 4). Heme staining and anti-CcmE immunoblotting of TALON-purified fractions revealed that, in the absence of CcmG and CcmH, CcmF co-purified with approximately 10-fold more holoCcmE than when CcmG and CcmH were present (Fig 3D and E, compare lanes 3 and 4; quantified in Fig 3H). In the absence of CcmF (pSysI ΔFGH), no holoCcmE was detected by heme stain or anti-CcmE immunoblot (Fig 3D and E, lane 1), showing that there was no detectable retention of holoCcmE on the TALON resin.

Similarly, in the absence of CcmE (pSysI ΔEGH), no 20-kDa covalent heme species or reactivity with CcmE antisera were observed (Fig 3D and E, lane 2). Analysis of DDM-solubilized membrane fractions by heme staining and immunoblotting with CcmE antisera showed that all membranes (with the exception of those from pSysI ΔEGH) contained holoCcmE at levels at least as high as that of pSysI ΔGH (Fig 3F and G; quantified in Fig 3I). Therefore, the 10-fold higher levels of holoCcmE that co-purified with CcmF from pSysI ΔGH are not due to increased expression of holoCcmE from this construct. We conclude that CcmH prevents (controls) trapping of the holoCcmE/CcmF complex (see Discussion).

HoloCcmE must be released from CcmCD to interact with CcmF

The first step in heme translocation in the system I (CCM) pathway involves formation of covalent (holo) CcmE, which occurs via complex formation with CcmC and CcmD [8; 9; 35]. Subsequently, CcmA and CcmB form an ABC transporter "release complex" with CcmC and CcmD, which uses ATP hydrolysis to release holoCcmE for heme trafficking to (putatively) CcmFH [13; 14; 15]. In the absence of CcmAB, holoCcmE becomes "trapped" with CcmCD in a very stable intermediate complex [8], and holocytochrome c formation is blocked at this step. We examined whether interaction between CcmF and holoCcmE is dependent on release of holoCcmE from CcmABCD. We engineered an in-frame deletion of *ccmAB* in pSysI ΔGH to yield pSysI ΔGH delAB (pGEX *ccmCDEF*:His6), with a GST translational fusion to CcmC rather than CcmA.

CcmF was expressed from pSysI ΔGH delAB and purified as a single full-length polypeptide (54-kDa; Fig 4A, lane 3) that reacted with CcmF antisera (Fig 4B, lane 3). Heme staining and anti-CcmE immunoblotting revealed that the absence of CcmAB resulted in at least a 10-fold decrease in the amount of holoCcmE that co-purified with CcmF (Fig 4C and D,

compare lanes 2 and 3; quantified in Fig 4G). Analysis of DDM-solubilized membrane fractions by heme staining and immunoblotting with CcmE antisera showed that membranes from pSysI ΔGH delAB contained holoCcmE at levels at least as high as that of pSysI ΔGH (Fig 4E and F; quantified in Fig 4H). To confirm that release of holoCcmE from CcmCD was blocked by deletion of ccmAB, we purified GST:CcmC from the flow-through fraction of the TALON column (Fig 4 I-L). Purified full-length GST:CcmC (48-kDa) and free GST each reacted with GST antisera (Fig 4K, lane 1). Heme staining (Fig 4J, lane 6) and immunodetection with CcmE antisera (Fig 4L, lane 1) revealed that purified GST:CcmC contained high levels of trapped (unreleased) holoCcmE. Thus, in the absence of CcmAB, holoCcmE is trapped on CcmC, which effectively abolishes formation of the CcmF-holoCcmE complex. Only released holoCcmE interacts with CcmF, as previous models have hypothesized. This strongly suggests that the interaction we detect between holoCcmE and CcmF is a true intermediate during holocytochrome c formation.

ApoCcmE does not interact with CcmF

CcmE binds heme through a unique covalent bond between conserved His130 and the 2-vinyl of the heme [10; 11; 12]. Previous work has shown that mutation of His130 to alanine abolishes covalent bond formation between heme and CcmE [36], although CcmE(His130Ala) still forms a complex with CcmCD and is likely released upon ATP hydrolysis by CcmAB [8]. Since released CcmE(His130Ala) is completely apo- (lacking heme), holocytochrome c formation is blocked at this step (i.e., the covalent bond to heme in holoCcmE is necessary for CcmE to chaperone heme to, putatively, CcmFH). To test whether apo-CcmE could interact with CcmF, we engineered the His130Ala substitution in *ccmE* in pSysI ΔGH to yield pSysI ΔGH mutE (pGEX *ccmABCDE*(His130Ala)*F*:His6). CcmF was expressed from pSysI ΔGH mutE and purified as a

single full-length polypeptide (54-kDa; Fig 5A, lane 3) that reacted with CcmF antisera (Fig 5B, lane 3). As expected, heme staining showed no evidence of holoCcmE in purified CcmF fractions (Fig 5C, lane 3; quantified in Fig 5G), since mutation of His130 results in only the apo-form of CcmE (Fig 5E, lane 3; quantified in Fig 5H). Immunoblotting with CcmE antisera revealed approximately a 20-fold decrease in the amount of apoCcmE that co-purified with CcmF (Fig 5D, compare lanes 2 and 3; quantified in Fig 5G), even though DDM-solubilized membranes from pSysI ΔGH mutE contained apoCcmE at levels at least as high as those of pSysI ΔGH (Fig 5F, compare lanes 2 and 3; quantified in Fig 5H). Thus, apoCcmE is not capable of interaction with CcmF, which suggests that holoCcmE—CcmF complex formation is heme-dependent (see Discussion).

CcmF P-His1 and P-His2 exhibit heme ligand activity

CcmF contains four conserved His residues (see Fig 6): His261 in TMD5 and His491 in TMD12 (here called TM-His1 and TM-His2, respectively); and His173 and His303 in periplasmic loops flanking the conserved WWD domain (here called P-His1 and P-His2, respectively). Alanine substitutions at any of the His residues in CcmF abolishes holocytochrome c formation [9; 17; 20]. TM-His1 and TM-His2 are ligands to the b-heme in CcmF: mutation of either of these transmembrane His residues results in a loss of nearly all b-heme in the purified protein [9; 20]. However, the roles of P-His1 and P-His2 are unknown. Based on their position flanking the WWD domain (which, in CcmC, has been shown to be the site of interaction with the holoCcmE heme [8]), we hypothesize that P-His1 and P-His2 in CcmF may be ligands to the incoming heme from holoCcmE (see Fig 6 and Discussion).

Previously, we showed that the cytochrome c assembly defects of glycine substitutions at TM-His1 and TM-His2 could be corrected in vivo by addition of 10 mM imidazole directly to

culture [20]. Conceptually, this is similar to the correction of heme binding in the myoglobin His93Gly "cavity" mutant by imidazole [37]. Thus, functional correction of a histidine mutant by imidazole can be suggestive of a heme ligand function. To test whether P-His1 or P-His2 might exhibit a ligand function, we engineered alanine, glycine, cysteine, tyrosine, or methionine substitutions at each His residue and assayed for holocytochrome c4 formation in the absence and presence of imidazole. Heme staining of BPER fractions revealed that in the absence of imidazole, none of the engineered substitutions at P-His1 or P-His2 supported holocytochrome c formation (Fig 7A and B, lanes 1-7; quantified in Fig 7C and D). However, 10 mM imidazole corrected the holocytochrome c assembly defects of glycine substitutions at P-His1 and P-His2 to approximately 50% levels of WT (Fig 7A and B, lane 10; quantified in Fig 7C and D). Substitution of P-His1 with bulkier amino acids did not result in detectable holocytochrome c4 formation in the presence of imidazole (Fig 7A, lanes 9-15; quantified in Fig 7C). The tyrosine and methionine substitutions at P-His2 were corrected to approximately 10% and 5% levels of WT, respectively, suggesting that the P-His2 position may be more flexible than the P-His1 (i.e., for imidazole). We conclude that the glycine substitutions at P-His1 and P-His2 result in the formation of a cavity in which imidazole can bind and serve as a ligand to support holocytochrome c formation. However, bulkier amino acids (including perhaps the methyl side group of alanine) may present a steric hindrance to imidazole correction. Since we have previously shown that neither P-His1 nor P-His2 were ligands to the CcmF b-heme, we theorize that the apparent ligand function of these residues is related to the incoming heme from holoCcmE.

CcmF P-His1 and P-His2 are required for interaction with holoCcmE

To directly test if P-His1 and P-His2 are required for interaction with holoCcmE, we engineered alanine substitutions at each residue, as well as a double alanine substitution, in the pSysI ΔGH background and assayed for holoCcmE in preparations of CcmF. CcmF was expressed from pSysI ΔGH(P-His1Ala), pSysI ΔGH(P-His2Ala), or pSysI ΔGH(P-His1Ala/P-His2Ala) and purified as a single full-length polypeptide (54-kDa; Fig 8A, lanes 3-5) that reacted with CcmF antisera (Fig 8B, lanes 3-5). Heme staining and immunoblotting with CcmE antisera showed approximately a 5-fold decrease in the amount of holoCcmE that co-purified with CcmF for each of the single substitutions (Fig 8C and D, compare lane 2 to 3 and 4; quantified in Fig 8G), and approximately a 10-fold decrease for the double mutant (Fig 8C and D, compare lanes 2 and 5; quantified in Fig 8G). DDM-solubilized membranes from all backgrounds contained similar levels of holoCcmE (Fig 8E and F; quantified in Fig 8H). Thus, P-His1 and P-His2 in CcmF are essential for interaction with holoCcmE, and are likely the ligands to the heme from holoCcmE.

The CcmF b-heme is required for interaction with holoCcmE

CcmF contains two conserved histidines in transmembrane domains (TM-His1 and TM-His2) that are ligands to the CcmF b-heme. Substitution of either histidine residue with alanine abolishes b-heme binding in CcmF to undetectable levels [20]. To test if the CcmF b-heme is required for interaction with holoCcmE, we engineered alanine substitutions at TM-His1 and TM-His2 in the pSysI ΔGH background and assayed for holoCcmE in preparations of CcmF. CcmF was expressed from pSysI ΔGH(TM-His1Ala) or pSysI ΔGH(TM-His2Ala) and purified as a full-length polypeptide (54-kDa; Fig 9A, lanes 3-4) that reacted with CcmF antisera (Fig 9B, lanes 3-4). Heme staining and immunoblotting with CcmE antisera showed approximately an 8-fold decrease in the amount of holoCcmE that co-purified with CcmF for each substitution (Fig

9C and D, compare lane 2 to 3 and 4; quantified in Fig 9G). DDM-solubilized membranes from all backgrounds contained similar levels of holoCcmE (Fig 9E and F; quantified in Fig 9H). Note that purified CcmF (TM-His1Ala) and CcmF (TM-His2Ala) do not contain the b-heme (see "free heme" in Fig 9C, compare lane 2 to 3 and 4). This is in stark contrast to the P-His1 and P-His2 substitutions, which showed b-heme levels identical to WT CcmF (see "free heme" in Fig 8C). Thus, the b-heme in CcmF (with ligands from TM-His1 and TM-His2) is essential for interaction with holoCcmE.

Discussion

Requirements for formation of the holoCcmE—CcmF complex

Here, we report isolation of an integral membrane protein complex between the system I heme chaperone, holoCcmE, and the putative cytochrome c synthetase, CcmF. Interaction between these two essential CCM proteins has long been suspected, but never shown directly. Ren and colleagues (2002) previously reported that CcmE could be immunoprecipitated from cell extracts using CcmF antisera (see Fig 4 of [17]). However, since only the apo-form of CcmE was analyzed in that study (the strain utilized lacked the genes for ccmABCD altogether), the relevance of that finding to holocytochrome c formation is unclear. Despite the fact that only apoCcmE was analyzed, many CCM models have cited the findings of Ren and colleagues as evidence of interaction between holoCcmE and CcmF. In our study, using a strain expressing CcmABCDE and CcmF, we showed that covalent, released holoCcmE interacts with CcmF at levels at least 20-fold higher than the apo-form of CcmE (see Fig 5). Given that the predicted function of CcmF is to facilitate heme transfer from holoCcmE to the apocytochrome, it is not surprising that the holo-form of CcmE preferentially binds. Ren and colleagues also reported that point mutants in CcmF (including alanine substitutions at P-His1 and P-His2) showed unaltered interactions with (apo) CcmE, relative to WT CcmF. In contrast, we found that substitution of either P-His1 or P-His2 caused a 5-fold decrease in the levels of holoCcmE that co-purified with CcmF (relative to WT CcmF), and that the double mutant showed a 10-fold decrease (see Fig 8). The critical roles of P-His1 and P-His2 (which are in periplasmic loops adjacent to the CcmF WWD domain; see Fig 6) in binding holoCcmE had been proposed previously, and is further elaborated upon below. We suggest that the apoCcmE detected in

preparations of CcmF represents a low background level (likely non-physiological), and that the holoCcmE "trapped" in complex with CcmF is the true physiological intermediate in system I.

Implications of P-His1 and P-His2 binding heme from holoCcmE

CcmF is a member of the heme-handling superfamily of proteins [38], which also includes CcmC and the system II cytochrome c synthetase, CcsBA. The hallmark of the heme-handling proteins is the "WWD domain" [39; 40; 41; 42], a conserved tryptophan-rich periplasmic loop that is flanked by two conserved histidine residues in adjacent periplasmic loops. CcmC, which is sometimes referred to as the holoCcmE synthase (due to its well-described role in formation of holoCcmE) [14; 35] forms a stable intermediate complex with holoCcmE (in the absence of CcmAB) [8]. In the "trapped" holoCcmCDE complex, heme from holoCcmE is bound in the WWD domain of CcmC, and the two flanking histidines (CcmC His60 and His184) supply the 5th and 6th axial ligands to heme. Richard-Fogal and Kranz (2010) showed that substitution of either histidine, as well as certain tryptophans in the WWD domain of CcmC, caused perturbations in the absorption spectrum of the CcmCDE complex [8]. In the absence of heme, there was no detectable interaction between (apo) CcmE and CcmC, indicating that the WWD domain of CcmC is a platform for interaction with heme rather than for the CcmE polypeptide. Thus, we proposed that heme, CcmC, and CcmE are each essential to form the stable "ternary" complex [8].

By analogy to the CcmCDE complex, we have hypothesized that the WWD domain of CcmF is the site of interaction for heme from holoCcmE, after it is released from CcmCD. Several of our findings here are in agreement with this hypothesis: i) CcmF P-His1 and P-His2 (which flank the WWD domain) exhibited ligand-type activity (Gly substitutions at these residues were functionally restored by adding exogeneous imidazole), ii) P-His1 and P-His2

were required for interaction with holoCcmE, iii) only the holo-form of CcmE (i.e., with heme), and not apoCcmE, interacted with CcmF, and iv) only holoCcmE released from CcmCD interacted with CcmF. The requirement for both heme (i.e., "holo" CcmE) and the WWD domain-flanking histidines for formation of the holoCcmE—CcmF complex is remarkably similar to formation of the holoCcmCDE complex.

Identifying the CcmF WWD domain as the binding site for holoCcmE also has implications for understanding the cytochrome c heme lyase function of CcmF. Experimentally established models for the membrane topology of CcmF [9] suggest that the b-heme (with ligands from TM-His1 and TM-His2) is positioned spatially below the WWD domain (see Fig 6). Given this transmembrane "architecture," a mechanism for reduction of the incoming heme from holoCcmE (in the WWD domain) by electron transfer directly from the b-heme can be readily envisioned. Further studies will be needed to test this. In particular, since the holoCcmE that co-purifies with CcmF is sub-stoichiometric, it will be necessary to further enrich for holoCcmE in the complex to begin these and other spectroscopic studies.

Absence of CcmGH is critical to formation of the holoCcmE—CcmF complex

Surprisingly, we found that levels of the "trapped" holoCcmE—CcmF complex increased 10-fold when CcmGH were absent (see Fig 3). In fact, purification of CcmF from this particular background (pSysI ΔGH) initially enabled us to detect the holoCcmE—CcmF complex. CcmG is a periplasmic thioredoxin that has been shown to reduce the cysteines of CcmH (in vitro) (e.g., [28]), but it does not co-purify with the CcmFH complex [9; 19]. By contrast, interaction between CcmF and CcmH is well established [9; 17; 18; 19]. CcmH is a polytopic membrane protein with two transmembrane α helices and a large C-terminal periplasmic domain (see Fig 6). Apart from the two conserved cysteine residues in the N-terminal periplasmic domain, which have been shown

to reduce the apocytochrome thiols (in the Cys-Xxx-Xxx-Cys-His motif) [24; 28; 43], discrete functional domains within CcmH have not been well defined. Recently, Verissimo and colleagues (2011) and Di Silvio and colleagues (2013) have shown that CcmI, which is analogous to the C-terminus of *E. coli* CcmH, interacts with the C-terminus of apocytochrome c (not at Cys-Xxx-Xxx-Cys-His), but not holocytochrome c [29; 30]. Given our results here, it is likely that CcmH may also modulate the interaction between CcmF and holoCcmE. For example, in the absence of apocytochrome, CcmH may occlude the CcmF WWD domain from interaction with holoCcmE, thus only "permitting" holoCcmE reduction (to Fe^{2+}) when the apocytochrome c "acceptor" is present. Alternatively, but not mutually exclusively, CcmH may facilitate the rapid release of CcmE from the CcmF WWD domain. We have proposed that reduction of heme in holoCcmE accomplishes two reactions (see Fig 10). First, reduction of heme (to Fe^{2+}) would favor the ejection of His130 imidazole from the β carbon of the heme 2-vinyl (see Fig 10A, reverse blue arrow). Second, reduced heme is required for the 2- and 4-vinyls of heme to form thioether linkages with the apocytochrome c thiols (at Cys-Xxx-Xxx-Cys-His; see Fig 10B). It makes 'sense' to only allow the first reaction to occur (ejection of CcmE His130) when the acceptor is properly positioned (by CcmH) for the second reaction. Thus, the synthetase reactions are elegantly orchestrated by the holoCcmE:CcmF:CcmH complex.

Materials and Methods

Bacterial Growth Conditions. *Escherichia coli* strains (Supplemental Table 1) were grown at 37^{o}C by shaking at 230 rpm in Luria-Bertani broth (LB; Difco) supplemented with the appropriate antibiotics (Sigma-Aldrich) and other media additives at the following concentrations, unless otherwise noted: carbenicillin, 50 ug ml^{-1}; chloramphenicol, 20 ug ml^{-1}; gentamicin, 10 ug ml^{-1}; IPTG (Gold Biotechnology), 1 mM; arabinose (Gold Biotechnology), 0.2 % (wt/vol).

Protein Expression and Purification. *E. coli* Δ*ccm* strain RK103 (Table S1) [16] was used for expression. Starter cultures were initiated from a single colony and grown overnight in 10 mL of LB with the appropriate antibiotics. 1 L of LB and was inoculated with the 10 mL starter culture and grown to an OD_{600} of 1.8, then induced with 1 mM IPTG for 14-16 hr. Cells were harvested at 5,000 x g and frozen at -80^{o}C. Cell pellets were thawed and resuspended in PBS (100 mM NaCl, 7.5 mM Na_2HPO_4, 2 mM NaH_2PO_4) and treated with 1 mM PMSF (Sigma-Aldrich) and 100 μg ml^{-1} egg white lysozyme (Sigma-Aldrich) for 30 min while shaking on ice. Cells were disrupted by repeated sonication for 30 sec bursts on a Branson 250 sonicator (50% duty, 8 output) until clearing of the suspension was observed. Crude sonicate was centrifuged at 24,000 x g for 20 min to clear cell debris, and membranes were isolated by centrifugation at 100,000 x g for 45 min. Membrane pellets were solubilized in a modified 1x TALON (Clontech) buffer (50 mM Tris-HCL, pH 7; 300 mM NaCl) with 1 % (wt/vol) dodecyl maltoside (DDM, Anatrace) on ice for 1 hr. DDM-solubilized membranes were centrifuged at 24,000 x g for 20 min to remove unsolubilized material. Solubilized membranes (L; load) were passed over TALON resin per the manufacturer's recommendations and washed in 1 x modified TALON buffer with 0.02 % DDM with increasing concentrations of imidazole (wash 1 (W1), 0 mM imidazole; wash 2 (W2), 2 mM

imidazole; wash 3 (W3), 5 mM imidazole). Bound hexahistidine-tagged protein was eluted in 1 x modified TALON buffer containing 0.02 % dodecyl maltoside and 150 mM imidazole (E; elution). Total protein concentration was determined using the Nanodrop 1000 spectrophotometer (Thermo Scientific).

Cytochrome Reporter and Imidazole Complementation Assays. Cytochrome c_4:His6 production was assayed in RK111 (Δ*ccm* carrying the arabinose-inducible chromosomal integrate of the *cyt* c_4:His6 gene [20]) harboring pRGK402 (pGEX ABCDE [20]) and one of the following pBAD *ccmF*:His6*GH* plasmids (pRGK434, 435, 436, 437, 438, 439, 440, 441, 442, or 443; see Supplemental Table 1). Starter cultures were initiated from a single colony and grown overnight in LB with the appropriate antibiotics. 5 mL of LB was inoculated using 800 mL of starter culture and grown for 3 hr, then induced for 3 hr with 0.8 % (wt/vol) arabinose. Cells were harvested by centrifugation at 10,000 x g and the cell pellet was resuspended in 200 µL of BPER (Thermo Scientific) to lyse cells and extract protein. Total protein concentration was determined using the Nanodrop 1000 spectrophotometer (Thermo Scientific) and 100 µg was analyzed by SDS-PAGE followed by heme stain. Imidazole complementation assays were performed in the same way, with 10 mM imidazole (pH 7) added to the media prior to inoculation.

Production of antibodies to CcmF. *E. coli* CcmF was engineered with a hexahistidine tag as described in [9], and was expressed from pRGK386 in *E. coli* strain RK103 [16]. Cell growth, protein expression, and purification were carried out as described above. Eluted hexahistidine-tagged CcmF was analyzed by 12.5 % SDS-PAGE and electroeluted from gel fragments over 4-5 hr at 25 mV into 1x SDS-PAGE buffer (3.5 mM SDS, 50 mM Tris, 384 mM glycine). Purity of the preparations (assessed by Coomassie Blue staining) was greater than 95 %. Antiserum was generated in rabbits at a commercial facility (Cocalico Biologicals). Antibodies were purified

from serum by ammonium sulfate precipitation and adsorbed against crude *E. coli* extract containing all other Ccm proteins.

Heme stains and other methods. Heme stains and immunoblots were performed as described previously [16; 31]. Proteins were separated by 12.5 % SDS-PAGE and transferred to Hybond C nitrocellulose membranes (GE Healthcare). Anti-CcmF antibodies were used at a dilution of 1:10000, anti-CcmE antibodies at 1:10000, anti-GST antibodies at 1:10000, and anti-CcmH antibodies at 1:5000. Protein A peroxidase (Sigma-Aldrich) was used as the secondary label. The chemiluminescent signal for heme stains was developed using the SuperSignal Femto kit (Thermo Scientific) or, for immunoblots, the Immobilon Western kit (Millipore), and detected with an LAS-1000 Plus detection system (Fujifilm-GE Healthcare). The abundance of holoCcmE was determined by densitometry analysis of the chemiluminescent signal from heme stains and anti-CcmE immunoblots using the Science Lab 99-Image Gauge version 3.4 software (Fujifilm-GE Healthcare). Heme concentration in protein preparations was determined by pyridine extraction as described in [32] or heme staining as described in [33]. Protein purity was assessed by Coomassie Blue staining of SDS-PAGE.

UV/Vis absorption spectroscopy. UV-visible absorption spectra were recorded with a Shimadzu UV-2101 PC UV-Vis scanning spectrophotometer at room temperature as described previously [34]. All spectra were recorded in the same buffer (modified 1x TALON buffer) in which the proteins were purified. Chemically reduced spectra were generated by addition of sodium dithionite (sodium hydrosulfite).

Construction of plasmids. All oligonucleotide primer sequences, plasmids, and strains are given in Table S1. All oligonucleotides were synthesized by Sigma-Aldrich. To delete *ccmAB* from pRGK385 (pGEX ΔGH), primers “delABloop_BglII_Fwd” and “delABloop_BglII_Rev” were

used to PCR amplify around pRGK385, excluding *ccmAB*. The resulting PCR product was gel purified, digested and re-circularized by ligation at the resulting BglII sites to yield pRGK427 (pGEX ΔGH delAB). All nucleotide substitutions were generated using the QuikChange I Site-Directed Mutagenesis Kit (Agilent Technologies) per the manufacturer's recommendations. Substitutions were engineered into pBAD-based pRGK388 for cytochrome reporter assays, or into pGEX-based pRGK385 (pGEX ΔGH) for protein expression and purification. To engineer the double P-His1Ala/P-His2Ala mutation, primers "ccmF_H303A_Fwd" and "ccmF_H303A_Rev" were used to introduce the P-His2Ala substitution into pRGK429 (pGEX ΔGH P-His1Ala). Each of the final constructs was sequenced to verify the mutation(s).

Acknowledgements

We thank Joseph P. Argus and Eric C. Bretsnyder for generation of antibodies to CcmF, and Joel Rankin for technical contributions. This work was supported by National Institutes of Health Grant R01 GM47909 to R.G.K.

References

1. Barker, P. D., Ferrer, J. C., Mylrajan, M., Loehr, T. M., Feng, R., Konishi, Y., Funk, W. D., MacGillivray, R. T. & Mauk, A. G. (1993). Transmutation of a heme protein. *Proc Natl Acad Sci U S A* **90**, 6542-6.
2. Nicholson, D. W. & Neupert, W. (1989). Import of cytochrome c into mitochondria: reduction of heme, mediated by NADH and flavin nucleotides, is obligatory for its covalent linkage to apocytochrome c. *Proc Natl Acad Sci U S A* **86**, 4340-4.
3. Hamel, P., Corvest, V., Giege, P. & Bonnard, G. (2009). Biochemical requirements for the maturation of mitochondrial c-type cytochromes. *Biochim Biophys Acta* **1793**, 125-38.
4. Kranz, R. G., Richard-Fogal, C., Taylor, J. S. & Frawley, E. R. (2009). Cytochrome c biogenesis: mechanisms for covalent modifications and trafficking of heme and for heme-iron redox control. *Microbiol Mol Biol Rev* **73**, 510-28, Table of Contents.
5. Mavridou, D. A., Ferguson, S. J. & Stevens, J. M. (2013). Cytochrome c assembly. *IUBMB Life* **65**, 209-16.
6. Sanders, C., Turkarslan, S., Lee, D. W. & Daldal, F. (2010). Cytochrome c biogenesis: the Ccm system. *Trends Microbiol* **18**, 266-74.
7. Sawyer, E. B. & Barker, P. D. (2012). Continued surprises in the cytochrome c biogenesis story. *Protein Cell* **3**, 405-9.
8. Richard-Fogal, C. & Kranz, R. G. (2010). The CcmC:heme:CcmE complex in heme trafficking and cytochrome c biosynthesis. *J Mol Biol* **401**, 350-62.
9. Richard-Fogal, C. L., Frawley, E. R., Bonner, E. R., Zhu, H., San Francisco, B. & Kranz, R. G. (2009). A conserved haem redox and trafficking pathway for cofactor attachment. *Embo J* **28**, 2349-59.
10. Lee, D., Pervushin, K., Bischof, D., Braun, M. & Thony-Meyer, L. (2005). Unusual heme-histidine bond in the active site of a chaperone. *J Am Chem Soc* **127**, 3716-7.
11. Stevens, J. M., Daltrop, O., Higham, C. W. & Ferguson, S. J. (2003). Interaction of heme with variants of the heme chaperone CcmE carrying active site mutations and a cleavable N-terminal His tag. *J Biol Chem* **278**, 20500-6.
12. Uchida, T., Stevens, J. M., Daltrop, O., Harvat, E. M., Hong, L., Ferguson, S. J. & Kitagawa, T. (2004). The interaction of covalently bound heme with the cytochrome c maturation protein CcmE. *J Biol Chem* **279**, 51981-8.
13. Christensen, O., Harvat, E. M., Thony-Meyer, L., Ferguson, S. J. & Stevens, J. M. (2007). Loss of ATP hydrolysis activity by CcmAB results in loss of c-type cytochrome synthesis and incomplete processing of CcmE. *Febs J* **274**, 2322-32.
14. Feissner, R. E., Richard-Fogal, C. L., Frawley, E. R. & Kranz, R. G. (2006). ABC transporter-mediated release of a haem chaperone allows cytochrome c biogenesis. *Mol Microbiol* **61**, 219-31.
15. Goldman, B. S., Beckman, D. L., Bali, A., Monika, E. M., Gabbert, K. K. & Kranz, R. G. (1997). Molecular and immunological analysis of an ABC transporter complex required for cytochrome c biogenesis. *J Mol Biol* **268**, 724-38.
16. Feissner, R. E., Richard-Fogal, C. L., Frawley, E. R., Loughman, J. A., Earley, K. W. & Kranz, R. G. (2006). Recombinant cytochromes c biogenesis systems I and II and analysis of haem delivery pathways in Escherichia coli. *Mol Microbiol* **60**, 563-77.

17. Ren, Q., Ahuja, U. & Thony-Meyer, L. (2002). A bacterial cytochrome c heme lyase. CcmF forms a complex with the heme chaperone CcmE and CcmH but not with apocytochrome c. *J Biol Chem* **277**, 7657-63.
18. Rayapuram, N., Hagenmuller, J., Grienenberger, J. M., Bonnard, G. & Giege, P. (2008). The three mitochondrial encoded CcmF proteins form a complex that interacts with CCMH and c-type apocytochromes in Arabidopsis. *J Biol Chem* **283**, 25200-8.
19. Sanders, C., Turkarslan, S., Lee, D. W., Onder, O., Kranz, R. G. & Daldal, F. (2008). The cytochrome c maturation components CcmF, CcmH, and CcmI form a membrane-integral multisubunit heme ligation complex. *J Biol Chem* **283**, 29715-22.
20. San Francisco, B., Bretsnyder, E. C., Rodgers, K. R. & Kranz, R. G. (2011). Heme ligand identification and redox properties of the cytochrome c synthetase, CcmF. *Biochemistry* **50**, 10974-85.
21. Di Matteo, A., Calosci, N., Gianni, S., Jemth, P., Brunori, M. & Travaglini-Allocatelli, C. (2010). Structural and functional characterization of CcmG from Pseudomonas aeruginosa, a key component of the bacterial cytochrome c maturation apparatus. *Proteins* **78**, 2213-21.
22. Ouyang, N., Gao, Y. G., Hu, H. Y. & Xia, Z. X. (2006). Crystal structures of E. coli CcmG and its mutants reveal key roles of the N-terminal beta-sheet and the fingerprint region. *Proteins* **65**, 1021-31.
23. Beckman, D. L. & Kranz, R. G. (1993). Cytochromes c biogenesis in a photosynthetic bacterium requires a periplasmic thioredoxin-like protein. *Proc Natl Acad Sci U S A* **90**, 2179-83.
24. Di Matteo, A., Gianni, S., Schinina, M. E., Giorgi, A., Altieri, F., Calosci, N., Brunori, M. & Travaglini-Allocatelli, C. (2007). A strategic protein in cytochrome c maturation: three-dimensional structure of CcmH and binding to apocytochrome c. *J Biol Chem* **282**, 27012-9.
25. Zheng, X. M., Hong, J., Li, H. Y., Lin, D. H. & Hu, H. Y. (2012). Biochemical properties and catalytic domain structure of the CcmH protein from Escherichia coli. *Biochim Biophys Acta* **1824**, 1394-400.
26. Meyer, E. H., Giege, P., Gelhaye, E., Rayapuram, N., Ahuja, U., Thony-Meyer, L., Grienenberger, J. M. & Bonnard, G. (2005). AtCCMH, an essential component of the c-type cytochrome maturation pathway in Arabidopsis mitochondria, interacts with apocytochrome c. *Proc Natl Acad Sci U S A* **102**, 16113-8.
27. Turkarslan, S., Sanders, C., Ekici, S. & Daldal, F. (2008). Compensatory thio-redox interactions between DsbA, CcdA and CcmG unveil the apocytochrome c holdase role of CcmG during cytochrome c maturation. *Mol Microbiol* **70**, 652-66.
28. Monika, E. M., Goldman, B. S., Beckman, D. L. & Kranz, R. G. (1997). A thioreduction pathway tethered to the membrane for periplasmic cytochromes c biogenesis; in vitro and in vivo studies. *J Mol Biol* **271**, 679-92.
29. Verissimo, A. F., Yang, H., Wu, X., Sanders, C. & Daldal, F. (2011). CcmI subunit of CcmFHI heme ligation complex functions as an apocytochrome c chaperone during c-type cytochrome maturation. *J Biol Chem* **286**, 40452-63.
30. Di Silvio, E., Di Matteo, A., Malatesta, F. & Travaglini-Allocatelli, C. (2013). Recognition and binding of apocytochrome c to P. aeruginosa CcmI, a component of cytochrome c maturation machinery. *Biochim Biophys Acta* **1834**, 1554-61.

31. Feissner, R., Xiang, Y. & Kranz, R. G. (2003). Chemiluminescent-based methods to detect subpicomole levels of c-type cytochromes. *Anal Biochem* **315**, 90-4.
32. Berry, E. A. & Trumpower, B. L. (1987). Simultaneous determination of hemes a, b, and c from pyridine hemochrome spectra. *Anal Biochem* **161**, 1-15.
33. Richard-Fogal, C. L., Frawley, E. R., Feissner, R. E. & Kranz, R. G. (2007). Heme concentration dependence and metalloporphyrin inhibition of the system I and II cytochrome c assembly pathways. *J Bacteriol* **189**, 455-63.
34. Frawley, E. R. & Kranz, R. G. (2009). CcsBA is a cytochrome c synthetase that also functions in heme transport. *Proc Natl Acad Sci U S A* **106**, 10201-6.
35. Schulz, H., Fabianek, R. A., Pellicioli, E. C., Hennecke, H. & Thony-Meyer, L. (1999). Heme transfer to the heme chaperone CcmE during cytochrome c maturation requires the CcmC protein, which may function independently of the ABC-transporter CcmAB. *Proc Natl Acad Sci U S A* **96**, 6462-7.
36. Harvat, E. M., Redfield, C., Stevens, J. M. & Ferguson, S. J. (2009). Probing the heme-binding site of the cytochrome c maturation protein CcmE. *Biochemistry* **48**, 1820-8.
37. Barrick, D. (1994). Replacement of the proximal ligand of sperm whale myoglobin with free imidazole in the mutant His-93-->Gly. *Biochemistry* **33**, 6546-54.
38. Lee, J. H., Harvat, E. M., Stevens, J. M., Ferguson, S. J. & Saier, M. H., Jr. (2007). Evolutionary origins of members of a superfamily of integral membrane cytochrome c biogenesis proteins. *Biochim Biophys Acta* **1768**, 2164-81.
39. Beckman, D. L., Trawick, D. R. & Kranz, R. G. (1992). Bacterial cytochromes c biogenesis. *Genes Dev* **6**, 268-83.
40. Goldman, B. S., Beck, D. L., Monika, E. M. & Kranz, R. G. (1998). Transmembrane heme delivery systems. *Proc Natl Acad Sci U S A* **95**, 5003-8.
41. Hamel, P. P., Dreyfuss, B. W., Xie, Z., Gabilly, S. T. & Merchant, S. (2003). Essential histidine and tryptophan residues in CcsA, a system II polytopic cytochrome c biogenesis protein. *J Biol Chem* **278**, 2593-603.
42. Kranz, R., Lill, R., Goldman, B., Bonnard, G. & Merchant, S. (1998). Molecular mechanisms of cytochrome c biogenesis: three distinct systems. *Mol Microbiol* **29**, 383-96.
43. Setterdahl, A. T., Goldman, B. S., Hirasawa, M., Jacquot, P., Smith, A. J., Kranz, R. G. & Knaff, D. B. (2000). Oxidation-reduction properties of disulfide-containing proteins of the Rhodobacter capsulatus cytochrome c biogenesis system. *Biochemistry* **39**, 10172-6.

Figures

Fig 1. Current working model of the system I cytochrome c biogenesis pathway.

Model includes trafficking and oxidation states of heme as well as apocytochrome translocation and reduction. Adapted from (Kranz, Richard-Fogal et al. 2009).

System I

CCM

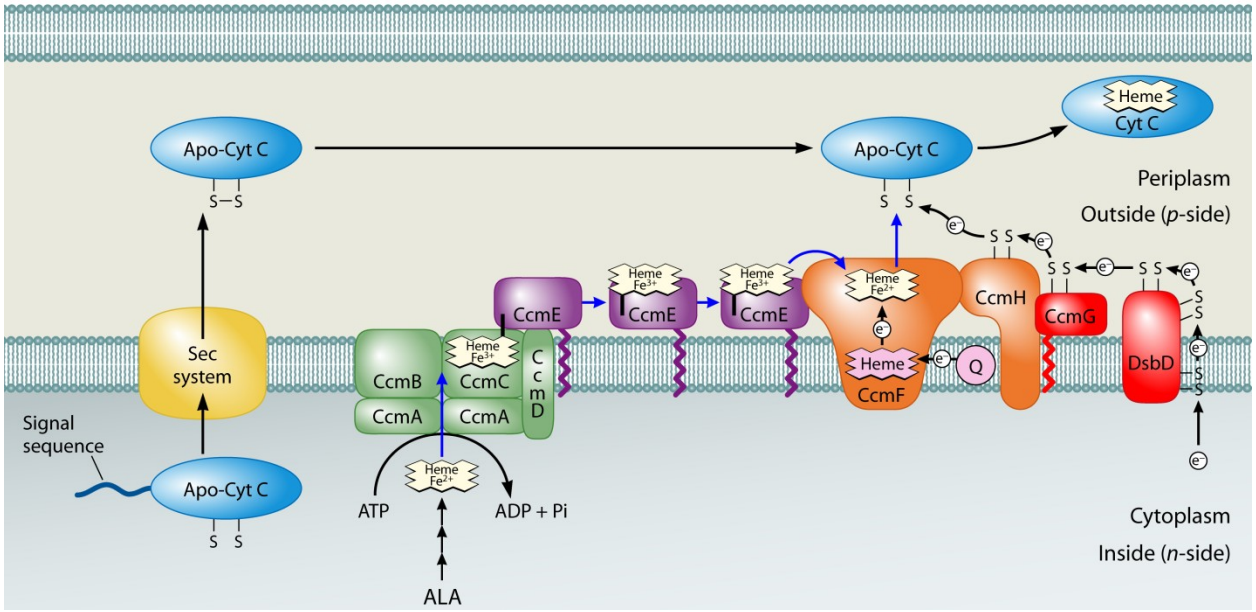
Apo-Cyt C
S—S
Sec system
Signal sequence
Apo-Cyt C
S S
CcmB
CcmC
CcmA
CcmA
Heme Fe3+
Heme Fe2+
CcmD
CcmE
CcmE
CcmE
Heme Fe3+
Heme Fe3+
ATP
ADP + Pi
ALA
Apo-Cyt C
S S
Heme Cyt C
Periplasm
Outside (p-side)
e-
Heme Fe2+
Heme
CcmF
Q
CcmH
CcmG
DsbD
S S
Cytoplasm
Inside (n-side)

Fig 2. The CcmF-holoCcmE complex.

(A) Coomassie blue staining of purified CcmF:His6 showing 54-kDa CcmF. (B) Anti-CcmF immunoblot of purified CcmF:His6 showing 54-kDa CcmF. (C) Heme staining of purified CcmF showing free heme (CcmF b-heme) and co-purified 20-kDa holoCcmE. (D) Anti-CcmE immunoblot showing co-purified 20-kDa CcmE. For (A)-(D), abbreviations are CS, crude sonicate; S, soluble fraction; L, load (DDM-solubilized membranes); W1, wash 1; W2, wash 2; W3, wash 3; E1, elution 1; E2, elution 2; E3, elution 3; E4, elution 4; M, molecular weight standards. (E) UV-Vis absorption spectra of CcmF-holoCcmE complex as purified (dotted line) or reduced with sodium dithionite (solid line). The region from 500-700 nm has been multiplied by a factor of 3. (Inset) Sodium dithionite-reduced pyridine hemochrome spectrum of purified CcmF-holoCcmE complex from 500-600 nm. Absorption maxima are indicated.

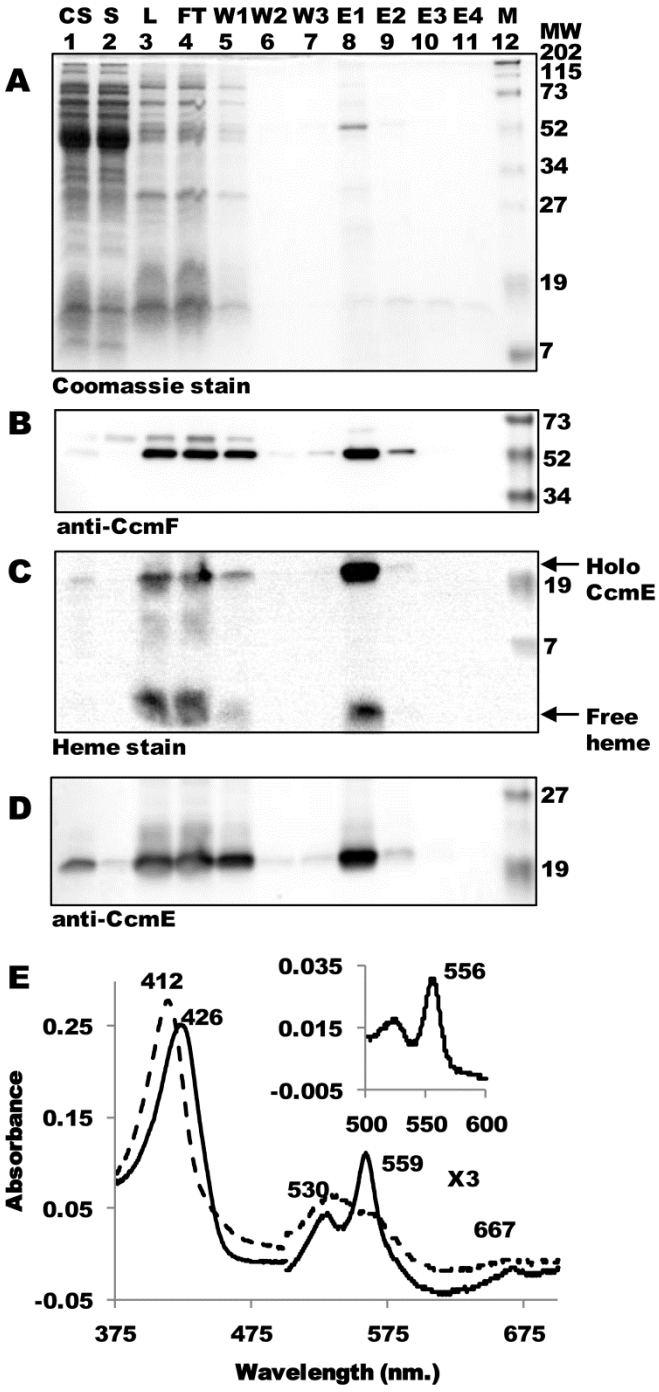
CS S L FT W1 W2 W3 E1 E2 E3 E4 M
1 2 3 4 5 6 7 8 9 10 11 12
MW
202
115
73
52
34
27
19
7
A
Coomassie stain
B
73
52
34
anti-CcmF
C
Holo CcmE
19
7
Free heme
Heme stain
D
27
19
anti-CcmE
E
412
426
556
0.035
0.015
-0.005
500 550 600
559
X3
530
667
0.25
0.15
0.05
-0.05
Absorbance
375 475 575 675
Wavelength (nm.)

Fig 3. HoloCcmE co-purifies with CcmF in the absence of CcmGH.

(A) Coomassie blue staining of TALON-purified proteins from ΔFGH, ΔEGH, ΔGH, and pSysI backgrounds showing purified 54-kDa CcmF. (B) Anti-CcmF immunoblot of TALON-purified proteins showing 54-kDa CcmF. (C) Anti-CcmH immunoblot of TALON-purified proteins showing 34 kDa CcmH. (D) Heme staining of TALON-purified proteins showing free heme (CcmF b-heme) and co-purified 20-kDa holoCcmE. (E) Anti-CcmE immunoblot of TALON-purified proteins showing co-purified 20-kDa CcmE. For (A)-(E), 6 ug purified protein was analyzed. (F) Heme staining of DDM-solubilized membrane fractions from ΔFGH, ΔEGH, ΔGH, and pSysI backgrounds showing 20 kDa holoCcmE. (G) Anti-CcmE immunoblot of DDM-solubilized membrane fractions showing 20 kDa CcmE. For (F) and (G), 70 ug total protein was analyzed. (H) Quantification of the results of heme staining (holoCcmE) and anti-CcmE immunoreactivity (total CcmE) from TALON-purified fractions from three independent experiments. (I) Quantification of the results of heme staining and anti-CcmE immunoreactivity from DDM-solubilized membrane fractions from three independent experiments. For (H) and (I), percent holoCcmE and total CcmE is relative to ΔGH, which has been set at 100%. Error bars denote SD.

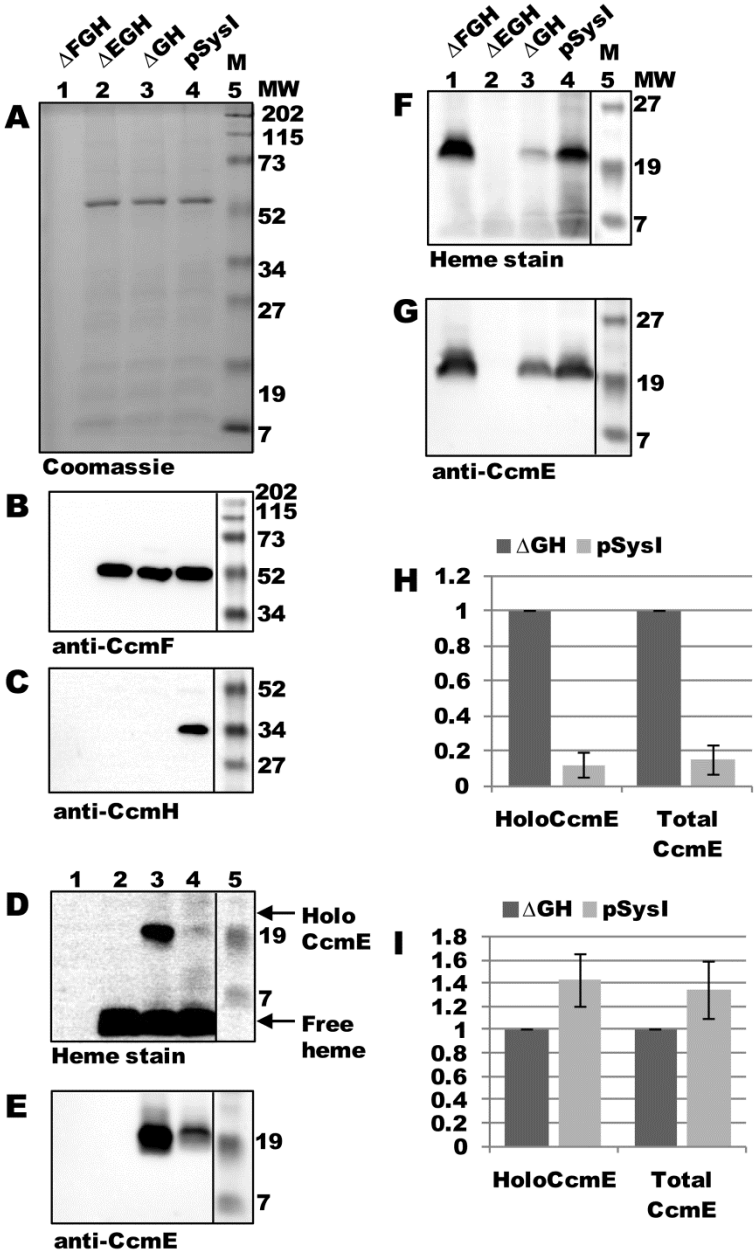
ΔFGH
ΔEGH
ΔGH
pSysI
M
1 2 3 4 5 MW
A
202
115
73
52
34
27
19
7
Coomassie
B
anti-CcmF
C
anti-CcmH
D
Holo CcmE
Free heme
Heme stain
E
anti-CcmE
F
Heme stain
G
anti-CcmE
H
ΔGH
pSysI
HoloCcmE
Total CcmE
I

Fig 4. HoloCcmE must be released from CcmABCD to interact with CcmF.

(A) Coomassie blue staining of TALON-purified proteins from ΔGH and ΔGH delAB backgrounds showing purified 54-kDa full-length CcmF. (B) Anti-CcmF immunoblot of purified CcmF proteins showing 54-kDa full-length CcmF. (C) Heme staining of purified CcmF proteins showing free heme (CcmF b-heme) and co-purified 20-kDa holoCcmE. (D) Anti-CcmE immunoblot of purified CcmF proteins showing co-purified 20-kDa CcmE. For (A)-(D), 5 ug purified protein was analyzed. (E) Heme staining of DDM-solubilized membrane fractions from ΔGH and ΔGH delAB backgrounds showing 20 kDa holoCcmE. (F) Anti-CcmE immunoblot of DDM-solubilized membrane fractions showing 20 kDa CcmE. For (E) and (F), 70 ug total protein was analyzed. (G) Quantification of the results of heme staining (holoCcmE) and anti-CcmE immunoreactivity (total CcmE) from purified fractions from three independent experiments. (H) Quantification of the results of heme staining and anti-CcmE immunoreactivity from DDM-solubilized membrane fractions from three independent experiments. For (G) and (H), percent holoCcmE and total CcmE is relative to ΔGH, which has been set at 100%. Error bars denote SD. (I) Coomassie blue staining of purified GST-tagged CcmC from ΔGH delAB showing 48-kDa full-length GST-CcmC, 26-kDa GST, and 20 kDa CcmE. (J) Heme staining of purified GST-tagged CcmC showing co-purified 20-kDa holoCcmE. (K) Anti-GST immunoblot of purified GST-tagged CcmC showing 48-kDa full-length GST-CcmC and 26-kDa GST. (L) Anti-CcmE immunoblot of purified GST-tagged CcmC showing co-purified 20-kDa CcmE.

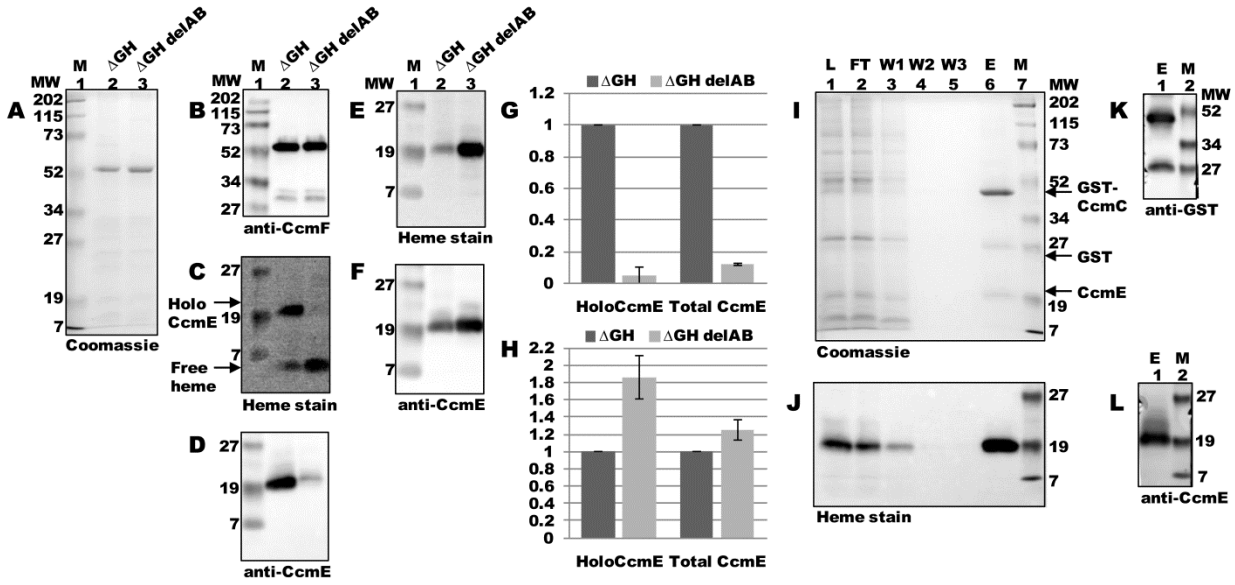
A
MW
M
1
ΔGH
2
ΔGH delAB
3
202
115
73
52
34
27
19
7
Coomassie
B
anti-CcmF
C
Holo CcmE
Free heme
Heme stain
D
anti-CcmE
E
Heme stain
F
anti-CcmE
G
ΔGH
ΔGH delAB
HoloCcmE
Total CcmE
H
I
L
FT
W1
W2
W3
E
6
GST-CcmC
GST
CcmE
J
K
anti-GST
L

Fig 5. ApoCcmE does not co-purify with CcmF.

(A) Coomassie blue staining of TALON-purified proteins from ΔGH and ΔGH mutE (CcmE His130Ala) backgrounds showing purified 54-kDa CcmF. (B) Anti-CcmF immunoblot of purified CcmF proteins showing 54-kDa CcmF. (C) Heme staining of purified CcmF proteins showing free heme (CcmF b-heme) and co-purified 20-kDa holoCcmE. (D) Anti-CcmE immunoblot of purified CcmF proteins showing co-purified 20-kDa CcmE. For (A)-(D), 5 ug purified protein was analyzed. (E) Heme staining of DDM-solubilized membrane fractions from ΔGH and ΔGH mutE backgrounds showing 20 kDa holoCcmE. (F) Anti-CcmE immunoblot of DDM-solubilized membrane fractions showing 20 kDa CcmE. For (E) and (F), 70 ug total protein was analyzed. (G) Quantification of the results of heme staining (holoCcmE) and anti-CcmE immunoreactivity (total CcmE) from purified fractions from three independent experiments. (H) Quantification of the results of heme staining and anti-CcmE immunoreactivity from DDM-solubilized membrane fractions from three independent experiments. For (G) and (H), percent holoCcmE and total CcmE is relative to ΔGH, which has been set at 100%. Error bars denote SD.

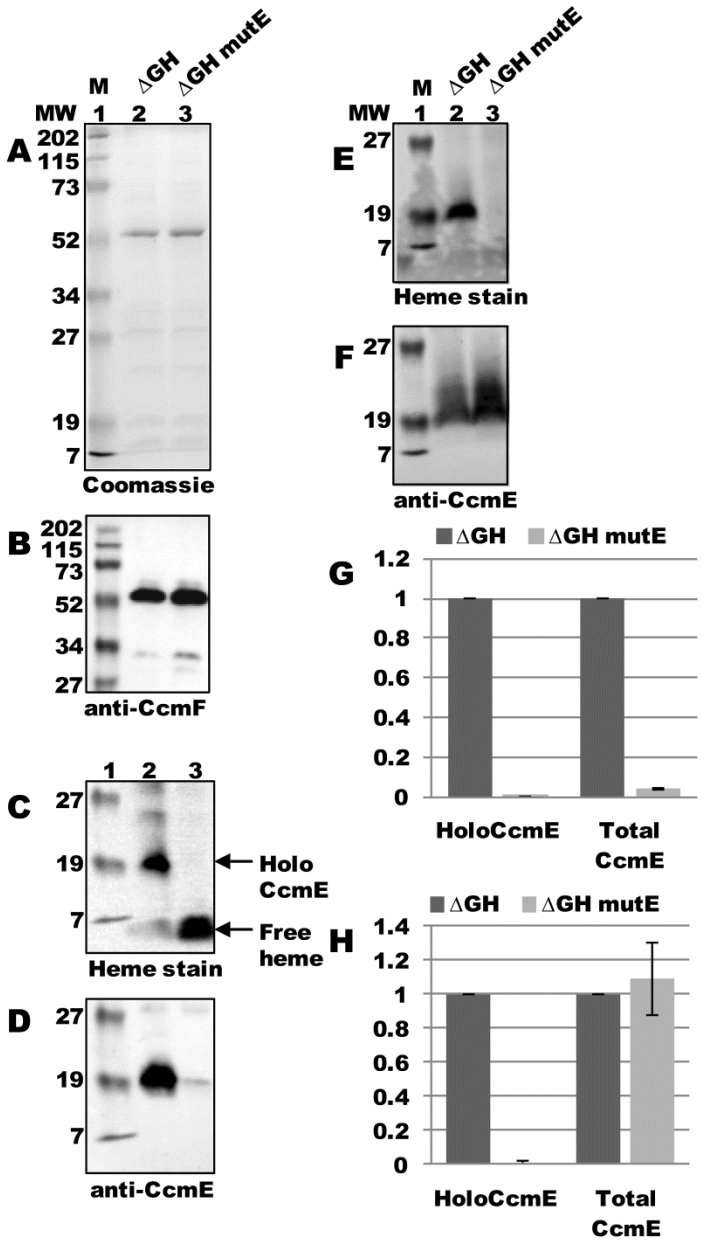
M
ΔGH
ΔGH mutE
MW
1
2
3
A
202
115
73
52
34
27
19
7
Coomassie
B
anti-CcmF
C
Holo CcmE
Free heme
Heme stain
D
anti-CcmE
E
Heme stain
F
anti-CcmE
G
ΔGH
ΔGH mutE
1.2
1
0.8
0.6
0.4
0.2
0
HoloCcmE
Total CcmE
H

Fig 6. Topology of the CcmF and CcmH integral membrane proteins from *E. coli*.

Possible histidine axial ligands to heme are starred (His173=P-His1; His303=P-His2; His261=TM-His1; His491=TM-His2). The highly conserved WWD domain is shaded as are the hydrophobic patches. Completely conserved amino acids (red) were identified by individual protein alignments using CcmF ORFs from selected organisms, as described in (Kranz, Richard-Fogal et al. 2009). Diagram is from (Kranz, Richard-Fogal et al. 2009).

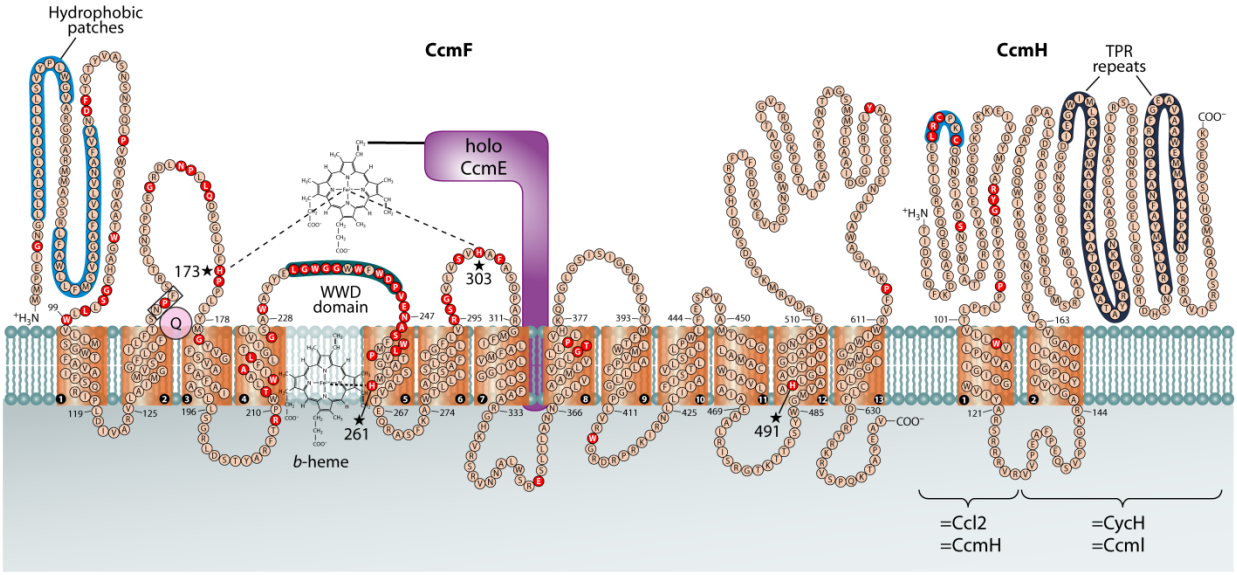
Hydrophobic patches
CcmF
CcmH
TPR repeats
holo CcmE
WWD domain
173★
303
261
491
Q
b-heme
COO⁻
+H3N
=Ccl2
=CcmH
=CycH
=CcmI

Fig 7. Maturation of cytochrome c4 in the presence or absence of imidazole.

Heme staining of B-PER cell extracts showing 24-kDa holocytochrome c4 matured by full system I with the indicated substitutions at CcmF P-His1 (A) or P-His2 (B) in the presence or absence of 10 mM imidazole added to culture. P-His1 and P-His2 were each changed to the indicated residues. M, molecular weight standards; C, vector control. 100 ug total protein was analyzed. Quantification of chemiluminescent signal from heme staining of B-PER isolated proteins from three independent experiments for P-His1 substitutions (C) or P-His2 substitutions (D). Holocytochrome c4 signal is relative to WT, which has been set at 100%. Error bars denote SD. ND, no signal detected.

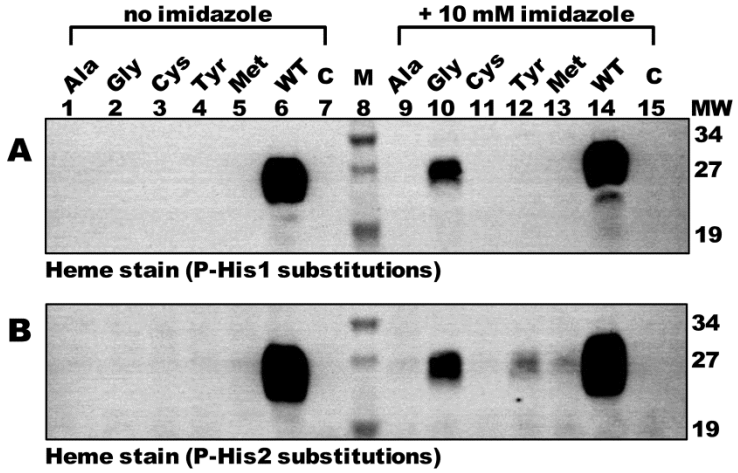
no imidazole
+ 10 mM imidazole
Ala Gly Cys Tyr Met WT C M Ala Gly Cys Tyr Met WT C
1 2 3 4 5 6 7 8 9 10 11 12 13 14 15
MW
A
34
27
19
Heme stain (P-His1 substitutions)
B
34
27
19
Heme stain (P-His2 substitutions)

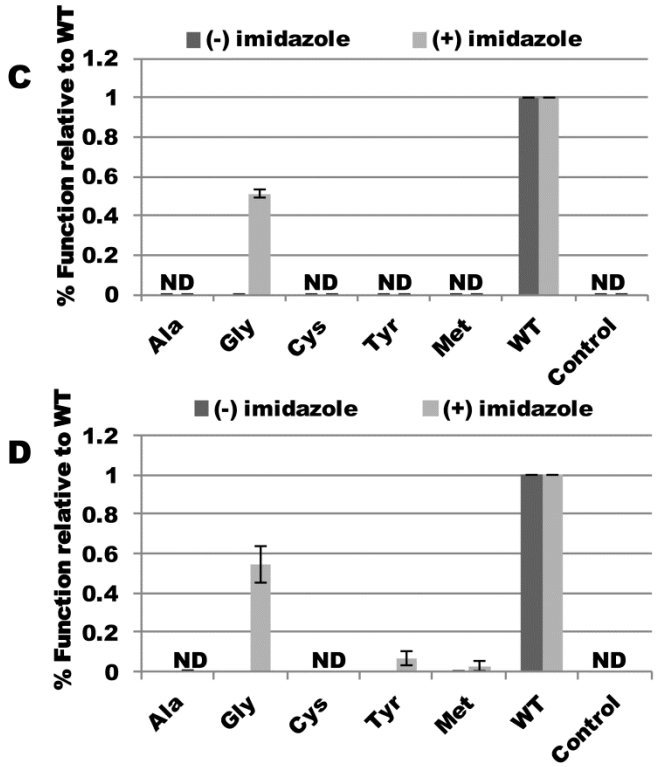
C
(-) imidazole
(+) imidazole
% Function relative to WT
1.2
1
0.8
0.6
0.4
0.2
0
ND ND ND ND ND
Ala Gly Cys Tyr Met WT Control
D
(-) imidazole
(+) imidazole
% Function relative to WT
1.2
1
0.8
0.6
0.4
0.2
0
ND ND ND
Ala Gly Cys Tyr Met WT Control

Fig 8. CcmF P-His1 and P-His2 are required for co-purification of holoCcmE.

(A) Coomassie blue staining of TALON-purified proteins from ΔGH, ΔGH (P-His1Ala), ΔGH (P-His2Ala), and ΔGH (P-His1Ala/P-His2Ala) backgrounds showing 54-kDa CcmF. (B) Anti-CcmF immunoblot of purified CcmF proteins showing 54-kDa CcmF. (C) Heme staining of purified CcmF proteins showing free heme (CcmF b-heme) and co-purified 20-kDa holoCcmE. (D) Anti-CcmE immunoblot of purified CcmF proteins showing co-purified 20-kDa CcmE. For (A)-(D), 6 ug purified protein was analyzed. (E) Heme staining of DDM-solubilized membrane fractions from ΔGH and each ΔGH mutant background showing 20 kDa holoCcmE. (F) Anti-CcmE immunoblot of DDM-solubilized membrane fractions showing 20 kDa CcmE. For (E) and (F), 70 ug total protein was analyzed. (G) Quantification of the results of heme staining (holoCcmE) and anti-CcmE immunoreactivity (total CcmE) from purified fractions from three independent experiments. (H) Quantification of the results of heme staining and anti-CcmE immunoreactivity from DDM-solubilized membrane fractions from three independent experiments. For (G) and (H), percent holoCcmE and total CcmE is relative to ΔGH, which has been set at 100%. Error bars denote SD.

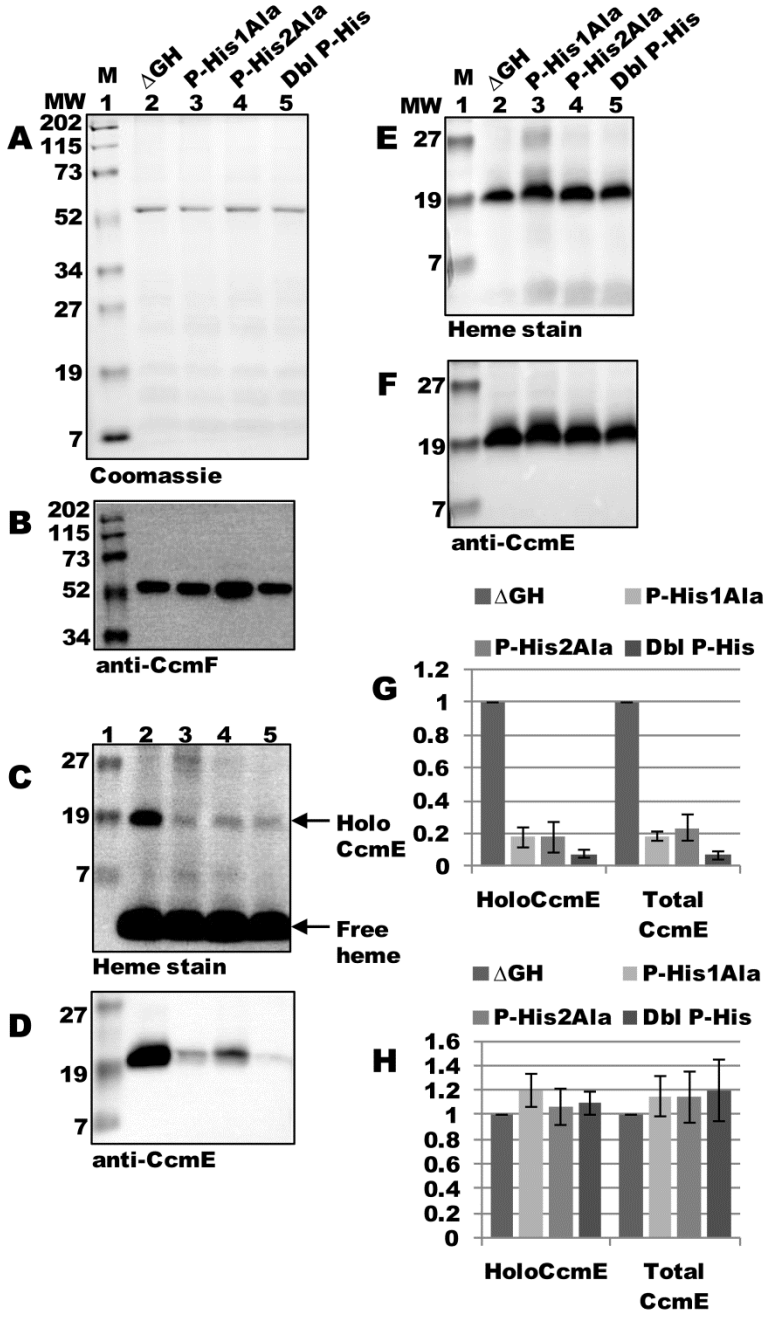
M
ΔGH
P-His1Ala
P-His2Ala
Dbl P-His
MW 1 2 3 4 5
A
202
115
73
52
34
27
19
7
Coomassie
B
anti-CcmF
C
Holo CcmE
Free heme
Heme stain
D
anti-CcmE
E
Heme stain
F
anti-CcmE
G
HoloCcmE
Total CcmE
H
HoloCcmE
Total CcmE

Fig 9. CcmF b-heme is required for co-purification of holoCcmE.

(A) Coomassie blue staining of TALON-purified proteins from ΔGH, ΔGH (TM-His1Ala), and ΔGH (TM-His2Ala) backgrounds showing 54-kDa CcmF. (B) Anti-CcmF immunoblot of purified CcmF proteins showing 54-kDa CcmF. (C) Heme staining of purified CcmF proteins showing free heme (CcmF b-heme) and co-purified 20-kDa holoCcmE. (D) Anti-CcmE immunoblot of purified CcmF proteins showing co-purified 20-kDa CcmE. For (A)-(D), 5 ug purified protein was analyzed. (E) Heme staining of DDM-solubilized membrane fractions from ΔGH and each ΔGH mutant background showing 20 kDa holoCcmE. (F) Anti-CcmE immunoblot of DDM-solubilized membrane fractions showing 20 kDa CcmE. For (E) and (F), 70 ug total protein was analyzed. (G) Quantification of the results of heme staining (holoCcmE) and anti-CcmE immunoreactivity (total CcmE) from purified fractions from three independent experiments. (H) Quantification of the results of heme staining and anti-CcmE immunoreactivity from DDM-solubilized membrane fractions from three independent experiments. For (G) and (H), percent holoCcmE and total CcmE is relative to ΔGH, which has been set at 100%. Error bars denote SD.

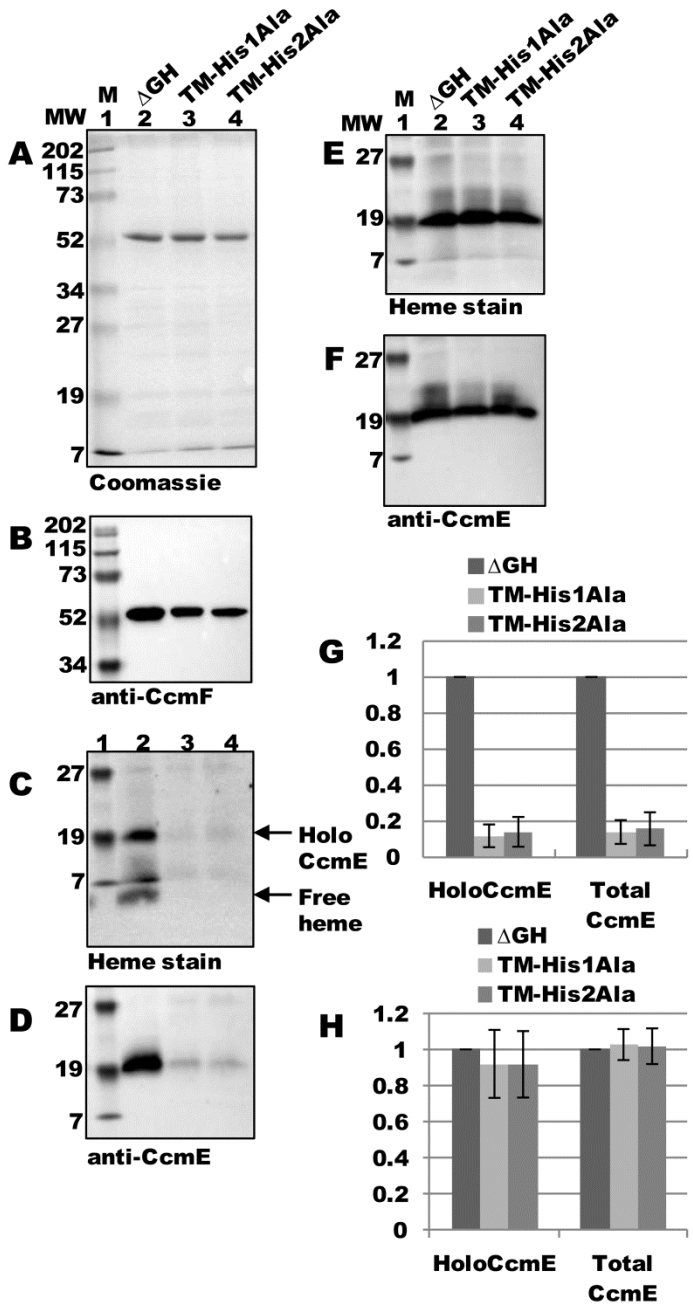
M
ΔGH
TM-His1Ala
TM-His2Ala
MW
1
2
3
4
A
202
115
73
52
34
27
19
7
Coomassie
B
anti-CcmF
C
Holo CcmE
Free heme
Heme stain
D
anti-CcmE
E
Heme stain
F
anti-CcmE
G
HoloCcmE
Total CcmE
H
HoloCcmE
Total CcmE

Fig 10. Mechanisms for formation of holoCcmE and cytochrome c.

Proposed reaction mechanisms for formation of holoCcmE (His130) (A) and holocytochrome c (B). Noted are the oxidation states of iron (Fe^{3+} or Fe^{2+}); red half arrows are one-electron transfers, and full red arrows are two-electron transfers. Transfer of the proton from the imidazolium to the alpha carbon in (A) is probably solvent- or protein-mediated (i.e., the proton may be abstracted at an early step, with a solvent- or protein-mediated protonation of the alpha carbon occurring at a later step). Reduction of heme (from Fe^{3+} to Fe^{2+}) could favor ejection of the CcmE His130 imidazole adduct (reverse blue arrow) and is required for holocytochrome c formation. For simplicity, only a single vinyl of heme is shown. Adapted from (Kranz, Richard-Fogal et al. 2009).

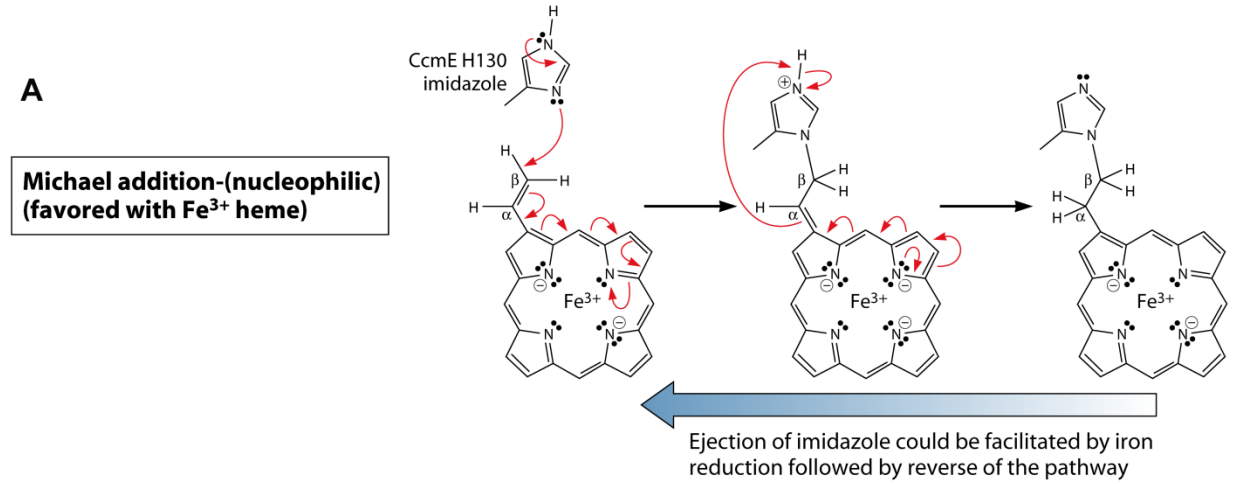
A
Michael addition-(nucleophilic) (favored with Fe3+ heme)
CcmE H130 imidazole
Fe3+
Fe3+
Fe3+
Ejection of imidazole could be facilitated by iron reduction followed by reverse of the pathway

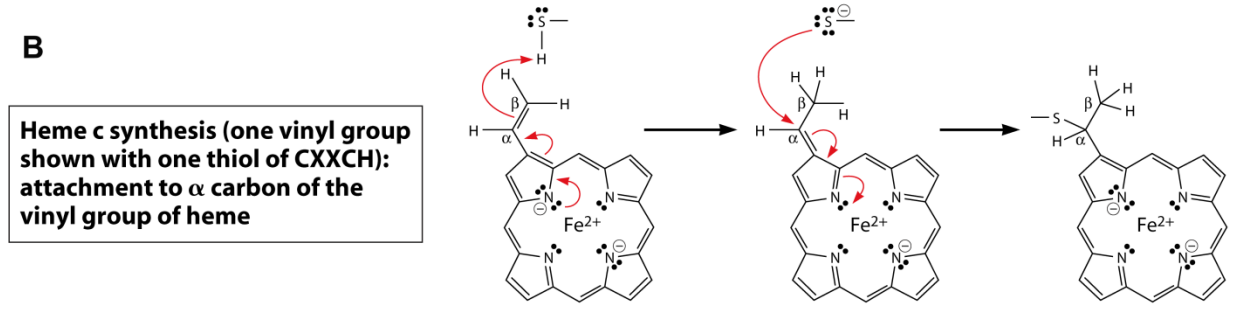
B
Heme c synthesis (one vinyl group shown with one thiol of CXXCH): attachment to α carbon of the vinyl group of heme
Fe2+
Fe2+
Fe2+

Chapter 4: The CcmFH complex is the system I holocytochrome c synthetase: engineering cytochrome c maturation independent of CcmABCDE

Brian San Francisco and Robert G. Kranz

Department of Biology, Washington University in St. Louis, St. Louis, MO 63130

Submitted for publication to *Mol Microbiol* (2013)

For correspondence: E-mail: kranz@biology.wustl.edu; Tel. (+1) 314 935 4278; Fax (+1) 314 935 4432.

Running title: CcmFH is the sytem I holocytochrome c synthetase

Keywords: cytochrome c maturation, synthetase, heme trafficking, biosynthesis, pathway

Summary

Cytochrome c maturation (ccm) in many bacteria, archaea, and plant mitochondria requires eight membrane proteins, CcmABCDEFGH, called system I. This pathway delivers and attaches heme covalently to two cysteines (of Cys-Xxx-Xxx-Cys-His) in the cytochrome c. All models propose that CcmFH facilitates covalent attachment of heme to the apocytochrome; namely, that it is the synthetase. However, holocytochrome c synthetase activity has not been directly demonstrated for CcmFH. We report formation of holocytochromes c by CcmFH and CcmG, a periplasmic thioredoxin, independent of CcmABCDE (we term this activity CcmFGH-ind). Cytochrome c produced in the absence of CcmABCDE is indistinguishable from cytochrome c produced by the full system I, with a cleaved signal sequence and two covalent bonds to heme. We engineer increased cytochrome c production by CcmFGH-ind, with yields approaching those from the full system I. Three conserved histidines in CcmF (TM-His1, TM-His2, and P-His1) are required for activity, as are the conserved cysteine pairs in CcmG and CcmH. These findings establish that CcmFH is the system I holocytochrome c synthetase, and provide unique mechanistic and evolutionary insights into cytochrome c biosynthesis.

Introduction

C-type cytochromes are heme proteins that carry out essential electron transfer reactions in organisms from every kingdom of life. These cytochromes function outside of the cytoplasmic membrane in prokaryotes, in the lumen of chloroplasts, and in the intermembrane space of mitochondria. Cytochromes c are characterized by covalent attachment between the heme and the apoprotein (via thioether linkages between the 2- and 4-vinyls of heme and two thiols of a conserved Cys-Xxx-Xxx-Cys-His motif in the apoprotein). Because c-type cytochromes are assembled at their site of action (separated from heme biosynthesis by a lipid bilayer), holocytochrome c formation poses unique challenges to heme trafficking and post-translational modification. Three major pathways (called systems I, II, and III) exist in nature to direct the covalent attachment of heme to cytochrome c. In many bacteria, plant and protozoal mitochondria, and archaea, holocytochrome c formation is carried out by the cytochrome c maturation (*ccm*) pathway, called system I, which comprises eight membrane proteins (in *E. coli*, CcmABCDEFGH) (Hamel *et al.*, 2009; Kranz *et al.*, 2009; Mavridou *et al.*, 2013; Sanders *et al.*, 2010; Sawyer and Barker, 2012).

At the center of heme trafficking in system I is the periplasmic heme chaperone protein, CcmE. CcmE forms a unique and well-studied covalent intermediate with heme, between a conserved histidine (His130, in *E. coli* CcmE) and the β carbon of the heme 2-vinyl (Lee *et al.*, 2005; Stevens *et al.*, 2003; Uchida *et al.*, 2004). Heme in "holo" (heme bound) CcmE is transferred to the apocytochrome (putatively, by the action of CcmFH), but details of this aspect of system I are just emerging. CcmABCD (an ABC transporter complex) are involved in formation and ATP-dependent release of holoCcmE, presumably now free to associate with CcmF (Christensen *et al.*, 2007; Feissner *et al.*, 2006a; Goldman *et al.*, 1997; Schulz *et al.*,

1999). CcmF forms an integral membrane complex with CcmH (Rayapuram *et al.*, 2008; Ren *et al.*, 2002; Richard-Fogal *et al.*, 2009; Sanders *et al.*, 2008), and is believed to be the site of thioether formation between the heme and the apocytochrome. CcmF contains a separate, stably bound non-covalent heme b (Richard-Fogal *et al.*, 2009; San Francisco *et al.*, 2011), which we have proposed is involved in reducing the incoming heme from holoCcmE (Kranz *et al.*, 2009; Richard-Fogal *et al.*, 2009; San Francisco *et al.*, 2011). Reduced heme (Fe^{2+}) is required for thioether formation with the apocytochrome (Barker *et al.*, 1993; Nicholson and Neupert, 1989), and reduction of the heme in holoCcmE would also favor discharge of heme from the covalent His130 intermediate (Kranz *et al.*, 2009; Richard-Fogal and Kranz, 2010; San Francisco *et al.*, 2011). CcmG (Beckman and Kranz, 1993; Di Matteo *et al.*, 2010; Ouyang *et al.*, 2006) and CcmH (Di Matteo *et al.*, 2007; Zheng *et al.*, 2012) are membrane-tethered thioredox-active proteins that likely maintain the thiol groups of the apocytochrome (in the conserved Cys-Xxx-Xxx-Cys-His motif) in the reduced state (Meyer *et al.*, 2005; Monika *et al.*, 1997; Setterdahl *et al.*, 2000; Turkarslan *et al.*, 2008).

CcmF (in complex with CcmH) has been referred to extensively as the "cytochrome c heme lyase" or "cytochrome c synthetase" of system I, although the assignment of this function to CcmF is largely circumstantial. It is well-established that CcmF forms a complex with CcmH (Rayapuram *et al.*, 2008; Ren *et al.*, 2002; Richard-Fogal *et al.*, 2009; Sanders *et al.*, 2008), and there is evidence that CcmH interacts directly with the apocytochrome (Di Matteo *et al.*, 2007; Di Silvio *et al.*, 2013; Meyer *et al.*, 2005; Verissimo *et al.*, 2011). However, interaction(s) between holoCcmE (the protein assumed to deliver heme to site of thioether formation with the apocytochrome) and CcmFH have not been demonstrated (an earlier report only studied interaction of apoCcmE with CcmF (Ren *et al.*, 2002), so the physiological significance of this

result is unclear). The absence of direct experimental evidence demonstrating that CcmFH is the cytochrome c synthetase thus constitutes a major gap in our understanding of the system I pathway.

Here, we report maturation of holocytochrome c by CcmFH and CcmG, in the absence of CcmABCDE. The cytochrome c produced by the CcmABCDE-independent pathway (here termed "CcmFGH-ind") is biochemically and spectroscopically indistinguishable from cytochrome c produced by the full system I, and we engineer production of cytochrome c by the CcmFGH-ind pathway at levels approaching those of the full system I. Three of the conserved histidines in CcmF (TM-His1, TM-His2, and P-His1), as well as the conserved cysteine pairs in the thioredox proteins CcmG and CcmH, are required for holocytochrome formation by CcmFGH-ind. These findings establish that CcmFH is the holocytochrome c synthetase for system I (with thioreduction mediated by CcmG). We discuss evolutionary and mechanistic implications, comparing CcmFGH-ind with the system II cytochrome c synthetase, CcsBA.

Results

CcmFH and CcmG mature cytochrome c in the absence of CcmABCDE

Conceptually, system I occurs in two steps: i) formation and release of holoCcmE (by CcmABCD), and ii) heme delivery to CcmFH (by holoCcmE), the putative site of holocytochrome c formation (hence, the "cytochrome c synthetase"). Studies in our lab (Feissner *et al.*, 2006a; Goldman *et al.*, 1997; Richard-Fogal and Kranz, 2010; Richard-Fogal *et al.*, 2009) and others (Christensen *et al.*, 2007; Ren and Thony-Meyer, 2001) have addressed step one, analyzing intermediates during formation of holoCcmE (such as the stable CcmCDE complex), and the ATP-dependent release of holoCcmE. However, less is known about the second step. To study the two steps independently, we engineered the IPTG-inducible pGEX with the genes encoding step one of the pathway, *ccmABCDE*, and an arabinose-inducible pBAD-based plasmid with the genes encoding step two, *ccmFGH*. Heme staining of BPER cell extracts revealed that expression of all Ccm proteins with the arabinose-inducible chromosmally-integrated cytochrome c4 (San Francisco *et al.*, 2011), led to robust production of holocytochrome c4 (Fig 1A, lane 5). Note that, typically, only heme that is covalently bound remains with the cytochrome c after denaturing SDS-PAGE, and this heme is readily detectable by heme stain (Feissner *et al.*, 2003). Surprisingly, we noticed that cells containing only CcmFGH (i.e., lacking *ccmABCDE*), also produced holocytochrome c4 (Fig 1A, lane 4). Thus, it appeared that holocytochrome formation could proceed in the absence of CcmABCDE, albeit at levels less than one-tenth those when CcmABCDE were present, under these conditions. We confirmed chromosomal deletion of the *ccmA-H* operon in our *E. coli* Δ*ccm* strains (Feissner *et al.*, 2006b; San Francisco *et al.*, 2011) by genomic PCR (Fig S1).

The holocytochrome c synthetase activity of CcmFGH-ind is not limited to the di-heme cytochrome c4, but also extends to the mono-heme cytochrome c2 (Fig 1B and C, lane 4). The cytochrome c2 plasmid used here has an in-frame C-terminal fusion to *E. coli* alkaline phosphatase (Pho), expressed from an IPTG-inducible promoter (Beckman *et al.*, 1992). We conclude that CcmFGH, in the absence of other Ccm components, can attach heme to two unrelated (other than the Cys-Xxx-Xxx-Cys-His motif) cytochrome c substrates. Furthermore, since alkaline phosphatase is secreted to the periplasm, covalent heme attachment to the cytochrome c2:Pho fusion protein must occur in the periplasm (i.e., where CcmFGH function).

Properties of cytochrome c produced by CcmFGH-ind

We wanted to further characterize the di-heme holocytochrome c4 produced by CcmFGH-ind. To confirm proper periplasmic secretion (and cleavage of the periplasmic signal sequence), and to analyze the spectral properties of the cytochrome c produced by CcmFGH-ind, we grew 1L cultures and purified hexahistidine-tagged holocytochrome c4 from the soluble fraction (Fig 2A-C). The full-length 24 kDa holocytochrome c4 and the proteolyzed 12 kDa holocytochrome c4' were detectable by Coomassie blue staining of SDS-PAGE (Fig 2A, lane 8 "E1"). Note that it is common for endogeneous proteolysis of the 24 kDa cytochrome to occur, yielding two 12 kDa mono-heme forms (Feissner *et al.*, 2006b); however, only the C-terminal of these products is purified (along with the full-length 24 kDa protein) since the hexahistidine tag is at the C-terminus of the protein. The purified 24 and 12 kDa forms contained covalent heme (Fig 2B, lane 8), and reacted with cytochrome c4 antisera (Fig 2C, lane 8). The UV-Vis absorption spectrum (Fig 2D, red line) and reduced pyridine hemochrome (Fig 2D, inset, red line) of the purified cytochrome c4 are consistent with two covalent attachments between the thiols of cytochrome c (in Cys-Xxx-Xxx-Cys-His) and the vinyls of heme. The spectral features

of cytochrome c4 produced by CcmFGH-ind (e.g., 552-nm absorption maximum in the spectrum of the reduced sample, and 550-nm absorption maximum in the reduced pyridine hemochrome spectrum) are indistinguishable from those of the cytochrome c4 produced when all system I proteins are present (CcmABCDEFGH; Fig 2D, blue line; Fig 2D, inset, blue line). Mass spectral analysis of cytochrome c4 purified from cells expressing CcmFGH-ind or the full system I identified species of the expected molecular weights in each preparation (i.e., within 2 Daltons of the published molecular weights for the full-length holocytochrome c4 and proteolyzed holocytochrome c4' (Feissner *et al.*, 2006b); Fig S2). This further confirmed covalent attachment of heme and proper cleavage of the periplasmic secretion signal (Fig S2B). In these large-scale cultures, yields of holocytochrome c via CcmFGH-ind were approximately one-sixth those of the full system I.

Engineering optimal holocytochrome c production by CcmFGH-ind

To engineer increased cytochrome c maturation in the absence of CcmABCDE, we piloted the following strategies: i) increasing the concentration of inducer (arabinose; "↑ arab" condition), ii) raising intracellular heme levels by addition of the heme biosynthetic precursor α-aminolevulinic acid (ALA; "ALA" condition), iii) decreasing oxygen tension by reduced shaking during growth ("↓ rpm" condition), and iv) engineering the cytochrome c4 gene for increased expression (by gene dosage) from a single pBAD-based vector, downstream of *ccmF*:His6*GH* ("p-c4" condition). Addition of ALA and increasing cytochrome c4 gene dosage led to the largest increases in yields of holocytochrome c (Fig 3A, lanes 4 and 6, respectively; Fig 3B, red and orange lines; quantified in Fig 3C). Additively, with each of the four modifications together, levels of holocytochrome c4 produced by CcmFGH-ind increased approximately 6-fold (up to 0.3 mg per L culture), similar to yields of holocytochrome c4 when CcmABCDE are present (Fig

3A, compare lanes 7 and 9; Fig 3B, compare light blue and brown lines; quantified in Fig 3C). In cells carrying CcmABCDE in the absence of CcmFGH, no holocytochrome c formation was detected (Fig 3A, lane 8). In the presence of CcmABCDE and CcmFGH (i.e., full system I) and each of the four modifications described above, yields of cytochrome c4 were approximately 1 mg per L culture (Fig 3A, lane 10; Fig 3B, top blue line; quantified in Fig 3C). Analysis of membrane fractions by immunoblot confirmed the presence of CcmF and CcmH, respectively (except in the strain carrying only pGEX CcmABCDE; Fig 3D and 3E, lane 8), and the absence of CcmE (except for those cells carrying pGEX CcmABCDE; Fig 3F). These results demonstrate that, under optimized conditions, CcmFGH-ind is a robust synthetase capable of producing substantial levels of periplasmic holocytochrome c.

The role of conserved histidines in CcmF in CcmFGH-ind

CcmF contains four conserved histidine residues: TM-His1 and TM-His2 in transmembrane domains 5 and 12, respectively, and P-His1 and P-His2, located in periplasmic loops flanking the WWD domain (see Fig 4A). P-His1 and P-His2 are proposed to ligate heme from holoCcmE when it is bound in the WWD domain, en route to covalent attachment to apocytochrome c; TM-His1 and TM-His2 are ligands to the stable heme b (San Francisco *et al.*, 2011), which may play a role in reducing the holoCcmE heme (bound in the WWD domain) prior to covalent attachment. In the context of the full system I, each of the four histidines is essential for holocytochrome c formation (Richard-Fogal *et al.*, 2009; San Francisco *et al.*, 2011). To test whether holocytochrome c formation via CcmFGH-ind required these four histidines, we engineered substitutions at each residue (in pRGK388) and assayed for heme attachment to cytochrome c4. Substitutions at TM-His1, TM-His2, and P-His1 abolished holocytochrome formation to undetectable levels, indicating that these residues are absolutely

required for heme attachment to cytochrome c via the CcmABCDE-independent pathway (Fig 5A, lanes 3, 4, and 6; quantified in Fig 5B). Substitution of P-His2 with glycine supported holocytochrome formation at approximately 20 % levels of WT (Fig 5A, lane 5; quantified in Fig 5B). This contrasts with the absolute requirement for P-His2 in the context of the full system I (i.e., in the presence of CcmABCDE), and may be suggestive of a holoCcmE-specific role for P-His2 in cytochrome c formation (see Discussion).

To test whether other substitutions could support holocytochrome formation at P-His1 or P-His2, we engineered alanine, cysteine, methionine, or tyrosine substitutions at P-His1 or P-His2. While no P-His1 substitution supported holocytochrome c formation (Fig 5C, upper panel), we discovered that P-His2Cys supported cytochrome c assembly at approximately 60 % WT levels (Fig 5C, lower panel, lane 4; quantified in Fig 5D). P-His2Ala was similar to substitution with glycine (20 % function relative to WT; Fig 5C, lower panel, lane 3; quantified in Fig 5D) while methione and tyrosine substitutions were 3 % and 10 % WT levels, respectively (Fig 5C, lower panel, lanes 5 and 6; quantified in Fig 5D). The inability for any engineered substitution at P-His1 to support holocytochrome formation indicates that this residue cannot vary from the natural histidine, similar to results with full system I.

Conserved cysteines in CcmG and CcmH are required for CcmFGH-ind

CcmG and CcmH each contain a conserved pair of thioredox-active cysteines that are required for cytochrome c synthesis in the context of the full system I (Fabianek *et al.*, 1998; Fabianek *et al.*, 1999; Robertson *et al.*, 2008). To test whether holocytochrome c formation by CcmFGH-ind required these thioredoxin functions, we engineered serine substitutions at the conserved cysteine pairs in CcmG or CcmH and assayed for cytochrome c formation. Similar to the full system I, in the absence of the conserved cysteine pair in either CcmG or CcmH, no

holocytochrome formation was observed (Fig 6A, lanes 3 and 4; quantified in Fig 6B). Thus, the redox-active cysteine pairs of CcmG and CcmH are required for holocytochrome c formation via CcmFGH-ind.

Discussion

CcmF has been referred to as the "cytochrome c heme lyase" or the "cytochrome c synthetase" in nearly every review on system I in the last decade (e.g., (Hamel *et al.*, 2009; Kranz *et al.*, 2009; Mavridou *et al.*, 2013; Sanders *et al.*, 2010; Sawyer and Barker, 2012)). However, direct experimental evidence demonstrating this activity for CcmF has been lacking. Here, we demonstrate that holocytochrome c formation can occur completely (and robustly) in the absence of the CcmABCDE components of the system I pathway, thus establishing that the cytochrome c synthetase activity of system I inheres in CcmFH (and CcmG). We suspect that the synthetase activity of CcmFH (with CcmG) has gone unnoticed thus far due to challenges in expressing these membrane proteins and engineering conditions for optimal biogenesis. Only of late have we been able to express and purify CcmF in sufficient quantities to begin biochemical characterization of this protein (Richard-Fogal *et al.*, 2009; San Francisco *et al.*, 2011). Indeed, the discovery that CcmF contained a stable heme b (coordinated by TM-His1 and TM-His2) was made only recently (Richard-Fogal *et al.*, 2009). Thus, we attribute our observation of this "new" CcmFGH-ind synthetase activity to our recent ability to successfully modulate expression of stable, functional CcmFH and CcmG in *E. coli*, and control the expression of substrate cytochromes c (e.g., the diheme cytochrome c4 and monoheme cytochrome c2 used here).

Requirements for CcmFGH-ind versus the full system I

Many of the requirements for cytochrome c assembly by the full system I extend to CcmFGH-ind. In system I, the thio-active proteins CcmG and CcmH each contain a conserved pair of cysteines that are required for holocytochrome formation (Fabianek *et al.*, 1998; Fabianek *et al.*, 1999; Robertson *et al.*, 2008). CcmG and CcmH are involved in maintaining the thiols of the apocytochrome (at Cys-Xxx-Xxx-Cys-His) in the reduced state, which is a requirement for

thioether formation with the heme vinyls. The conserved cysteines in CcmG (which are reduced by the membrane protein DsbD) likely function to reduce the thiols of CcmH (Meyer *et al.*, 2005; Monika *et al.*, 1997; Setterdahl *et al.*, 2000; Turkarslan *et al.*, 2008). CcmH also has a direct apocytochrome binding function (Di Matteo *et al.*, 2007; Di Silvio *et al.*, 2013; Meyer *et al.*, 2005; Verissimo *et al.*, 2011), and it is proposed that, via interaction with CcmF, CcmH physically positions the apocytochrome (with reduced cysteine thiols) for covalent heme attachment (Meyer *et al.*, 2005; Verissimo *et al.*, 2011). We discovered that mutation of either of the cysteine pairs in CcmG or CcmH abolished holocytochrome formation by CcmFGH-ind (Fig 6). The requirement for the conserved redox-active cysteine pairs in CcmG and CcmH demonstrates that the CcmFGH-ind pathway is "intact" with regard to handling of the apocytochrome. This suggests that the lower cytochrome c maturation activity of CcmFGH-ind (relative to full system I) is likely due to less efficient heme delivery (i.e., the absence of the holoCcmE "heme reservoir" (Feissner *et al.*, 2006b); see below). This finding also highlights the significant evolutionary advantage of the full system I.

Holocytochrome c formation by the full system I requires conserved histidines in CcmF: mutation of any of the four (Fig 4A) renders the system non-functional (Ren *et al.*, 2002; Richard-Fogal *et al.*, 2009; San Francisco *et al.*, 2011). We have shown experimentally that TM-His1 and TM-His2 are ligands to the b-heme (San Francisco *et al.*, 2011), while P-His1 and P-His2 are proposed to ligate the incoming heme from holoCcmE when it is bound in the WWD domain (Kranz *et al.*, 2009; Richard-Fogal *et al.*, 2009; San Francisco *et al.*, 2011). For CcmFGH-ind, we found that TM-His1, TM-His2, and P-His1 were each indispensable for holocytochrome formation. However, CcmFGH-ind was only partially dependent on P-His2 (Ala or Gly substitutions at this position retained approximately 20 % activity, and Cys, 60 %,

relative to WT). Since these same substitutions show no activity in the context of the full system I, we propose that P-His2 may have a function that is specific to the system I heme chaperone, holoCcmE. The lack of a requirement for P-His2 likely reflects the fundamentally different mechanism of heme trafficking to the WWD domain in CcmFGH-ind. Below, we suggest two possible trafficking routes for the endogeneous heme that is attached to cytochrome c by CcmFGH-ind.

Similarities between CcmFGH-ind and CcsBA: evolutionary insights

The assignment of the synthetase (heme lyase) activity of system I to CcmF has been based in part on its topological similarity to the cytochrome c synthetase of system II, CcsBA (see Fig 4). System II is present in many gram positive (and other) bacteria, cyanobacteria, and the chloroplasts of plants and algae (Ahuja *et al.*, 2009; Simon and Hederstedt, 2011; Xie and Merchant, 1998). CcsBA, when expressed heterologously in *E. coli* Δ*ccm* is sufficient for assembly of cytochrome c (Feissner *et al.*, 2006b; Frawley and Kranz, 2009; Kern *et al.*, 2010; Richard-Fogal *et al.*, 2012); thus, it is the system II holocytochrome c synthetase. CcsBA is proposed to traffick heme across the cytoplasmic membrane, in addition to facilitating thioether formation between the heme and apocytochrome (Frawley and Kranz, 2009; Hamel *et al.*, 2003; Kranz *et al.*, 2009; Merchant, 2009). Thus, it is a heme transporter and a holocytochrome c synthetase. The membrane topologies of CcmF and CcsBA are strikingly similar (see Fig 4): each contains four completely conserved His residues (two in transmembrane domains, here called TM-His1 and TM-His2; and two in extra-cytoplasmic loops, here called P-His1 and P-His2) and the conserved WWD domain, a hydrophobic, extra-cytoplasmic feature that has been shown (in the system I protein CcmC) to interact directly with heme (Richard-Fogal and Kranz, 2010). Additionally, both CcsBA (Frawley and Kranz, 2009) and CcmF (Richard-Fogal *et al.*,

2009) bind a non-covalent heme b (see Fig 4). However, in CcsBA, this heme b is ultimately attached to cytochrome c, whereas the stable heme b in CcmF (in the context of the full system I) may play a role in reducing heme bound in the WWD domain (from holoCcmE).

The marked similarities between CcmF and CcsBA, coupled with the finding here that CcmF (together with CcmH and CcmG) is a cytochrome c synthetase, raise several interesting questions. First, how is heme trafficked to the site of thioether formation with the apocytochrome (presumably, at the CcmF WWD domain with axial ligation by P-His1) in CcmFGH-ind synthesis? We envision two possible scenarios: i) heme enters the WWD domain of CcmF directly from the cytoplasmic membrane outer leaflet, possibly, (where it is subsequently reduced by the transmembrane heme b), or ii) similar to the proposed mechanism for CcsBA, the transmembrane heme b may be channeled to the external WWD domain for attachment to the apocytochrome. While experiments addressing these hypotheses will be challenging, the possibility that the CcmFGH-ind synthetase may be CcsBA-like (with respect to the channeling of heme from the transmembrane binding site to the WWD domain) is intriguing from an evolutionary perspective.

The complex phylogenetic distribution of systems I and II suggest significant lateral transfer (Goldman and Kranz, 1998), making it difficult to discern clear evolutionary patterns. We have shown previously that system I can mature cytochromes c at 5-fold lower heme concentrations than can system II (Richard-Fogal *et al.*, 2007), and that holoCcmE can function as a "heme reservoir" (i.e., when heme synthesis is completely inhibited) (Feissner *et al.*, 2006a). On the basis of these results, we have speculated that the holoCcmE reservoir aspect of system I may have evolved for cytochrome c synthesis under conditions of iron (or heme) scarcity. The ability to use heme at very low levels, and as a reservoir when no iron is present, represents a

possible selection advantage. Since the CcmFGH-ind synthetase lacks the holoCcmE reservoir, it might be considered a "prototype" of an intermediate, or a "transition," on the evolutionary path from system II to the full system I. CcmFGH-ind synthesis thus provides a unique opportunity to directly compare holocytochrome c formation (under low heme conditions) by system I with and without the holoCcmE reservoir.

CcmFGH-ind: a viable candidate for in vitro reconstitution

One of the remaining challenges in the field of cytochrome c biogenesis is in vitro reconstitution of each of the systems for holocytochrome formation. Reconstitution of the synthetase reactions would be especially informative, as they are common to all three major pathways. To date, system II has been a more attractive candidate for in vitro reconstitution than system I, since it consists of a single protein complex. Our findings here demonstrate that the system I synthetase (CcmFGH-ind) is now a viable candidate for in vitro reconstitution as well. The CcmFGH-ind synthetase activity reported here thus represents a significant advance for the field, in terms of the proof of its function, the unique evolutionary and mechanistic insights it provides, and the potential for in vitro reconstitution.

Experimental Procedures

Bacterial Growth Conditions. Unless otherwise noted, *Escherichia coli* strains (Table S1) were grown at 37^{o}C by shaking at 230 rpm in Luria-Bertani broth (LB; Difco) supplemented with the appropriate antibiotics (Sigma-Aldrich) and other media additives at the following concentrations: carbenicillin, 50 μg mL^{-1}; chloramphenicol, 20 μg mL^{-1}; gentamicin, 10 μg mL^{-1}; kanamycin, 20 μg mL^{-1}; IPTG (Gold Biotechnology), 1 mM; arabinose (Gold Biotechnology), 0.2 % (wt/vol); ALA (Sigma-Aldrich), 50 μg ml^{-1}.

Protein Expression and Purification. E. coli Δ*ccm* strains RK103 (Feissner *et al.*, 2006b) or RK111 (Δ*ccm* carrying the arabinose-inducible chromosomal integrate of the *cyt* c_4:His6 gene) (San Francisco *et al.*, 2011) (Table S1) were used for expression. Starter cultures were inoculated from a single colony and grown overnight in 10 mL of LB with the appropriate antibiotics. 1 L of LB was inoculated with the 10 mL starter culture and grown to an OD_{600} of 1.8, then induced with IPTG and/or arabinose for 14-16 hr. Cells were harvested at 5,000 x g and frozen at -80^{o}C. Cell pellets were thawed and resuspended in PBS (100 mM NaCl, 7.5 mM Na_2HPO_4, 2 mM NaH_2PO_4, pH 7) and treated with 1 mM PMSF (Sigma-Aldrich) and 100 μg ml^{-1} egg white lysozyme (Sigma-Aldrich) for 30 min while shaking on ice. Cells were disrupted by repeated sonication for 30 sec bursts on a Branson 250 sonicator (50% duty, 8 output) until clearing of the suspension was observed. Crude sonicate was centrifuged at 24,000 x g for 20 min to clear cell debris, and the soluble and membrane fractions were separated by centrifugation at 100,000 x g for 45 min. Soluble fractions (L; load) were passed over TALON resin per the manufacturer's recommendations and washed in 1 x modified TALON buffer with increasing concentrations of imidazole (wash 1 (W1), 0 mM imidazole; wash 2 (W2), 2 mM imidazole; wash 3 (W3), 5 mM imidazole). Bound hexahistidine-tagged protein was eluted in 1 x modified

TALON buffer containing 150 mM imidazole (E; elution). Total protein concentration was determined using the Nanodrop 1000 spectrophotometer (Thermo Scientific). For growth by shaking at 120 rpm ("↓ rpm" condition), starter cultures were initiated from a single colony and grown overnight in 100 mL of LB with the appropriate antibiotics. 1 L of LB was inoculated with the 100 mL starter culture and grown to an OD_{600} of 1.8, then induced with IPTG and/or arabinose for 14-16 hr. For the "↑ arabinose" condition, expression was induced with 0.4 % arabinose rather than 0.2 %. For the "ALA" condition, 50 μg mL^{-1} ALA was added to culture at the time of induction. For analysis of crude membrane fractions, membrane pellets (isolated by centrifugation at 100,000 x g) were solubilized in a modified 1x TALON (Clontech) buffer (50 mM Tris-HCL, pH 7; 300 mM NaCl) with 1 % (wt/vol) dodecyl maltoside (DDM, Anatrace) by agitation on ice for 1 hr, and then centrifuged at 24,000 x g for 20 min to remove unsolubilized material.

Heme stains and other methods. Heme stains and immunoblots were performed as described previously (Feissner *et al.*, 2003; Feissner *et al.*, 2006b). Proteins were separated by 12.5 % SDS-PAGE and transferred to Hybond C nitrocellulose membranes (GE Healthcare). For immunoblots, anti-CcmF antibodies were used at a dilution of 1:10000, anti-CcmE antibodies at 1:10000, anti-cytochrome c4 antibodies at 1:10000, and anti-CcmH antibodies at 1:5000. Protein A peroxidase (Sigma-Aldrich) was used as the secondary label. The chemiluminescent signal for heme stains was developed using the SuperSignal Femto kit (Thermo Scientific) or, for immunoblots, the Immobilon Western kit (Millipore), and detected with an LAS-1000 Plus detection system (Fujifilm-GE Healthcare). The abundance of holocytochrome c4 was determined by pyridine extraction as described in (Berry and Trumpower, 1987), or by densitometry analysis of the chemiluminescent signal from heme staining using the Science Lab

99-Image Gauge version 3.4 software (Fujifilm-GE Healthcare) as described in (Richard-Fogal *et al.*, 2007). Protein purity was assessed by Coomassie Blue staining of SDS-PAGE.

UV/Vis absorption spectroscopy. UV-visible absorption spectra were recorded with a Shimadzu UV-2101 PC UV-Vis scanning spectrophotometer at room temperature as described previously (Frawley and Kranz, 2009). All spectra were recorded in the same buffer (modified 1x TALON buffer) in which the proteins were purified. Chemically reduced spectra were generated by addition of sodium dithionite (sodium hydrosulfite).

Construction of plasmids. All oligonucleotide primer sequences, plasmids, and strains are given in Table S1. The single pBAD-based plasmid containing *ccmF*:His6*GH* and *cyt* c_4:His6 was constructed by PCR amplification of the *cyt* c_4:His6 gene (and the upstream RBS) from pRGK332 (Feissner *et al.*, 2006b) and insertion of the resulting fragment into the single PstI site downstream of *ccmF*:His6*GH* in pRGK388 (Richard-Fogal *et al.*, 2009) to create pRGK448. The resulting plasmids were screened by restriction digest to confirm correct orientation of the insert, and then sequenced. All substitutions in pRGK388 (i.e., CcmG (Cys80Ser/Cys83Ser), CcmH (Cys43Ser/Cys46Ser), CcmF(His261Gly), and CcmF(His491Ala)) were engineered using the QuikChange I Site-Directed Mutagenesis Kit (Agilent Technologies) per the manufacturer's recommendations. All oligonucleotides were synthesized by Sigma-Aldrich. Each of the final constructs was sequenced to verify the mutation(s).

Proteomics analysis. Proteomics analyses were carried out by the Washington University Resource for Biomedical and Bio-organic Mass Spectrometry Facility. Briefly, TALON-purified holocytochrome c4:His6 samples (produced by the full system I or by CcmFGH-ind) were loaded onto an Agilent 2.1 X 15 mm C8 Zorbax Cartridge-Column and eluted using a 9.5 min gradient with a flow rate of 200 μL/min. A positive ion mass spectrum was acquired using a

Bruker Maxis Q-ToF mass spectrometer equipped with an electrospray ionization source. Protein molecular ions were identified with multiple charge states and deconvoluted to identify the molecular weight(s) of the main species.

Genomic PCR. *E. coli* strains (WT *E. coli* K-12 MG1655; Δ*ccm* (RK103); Δ*ccm cyt* c_4:His6 chromosomal integrate (RK111); and RK111 carrying pBAD *ccmF*:His6*GH*) were streaked onto LB plates containing the appropriate antibiotics and incubated at 37 C overnight. Single colonies were resuspended in 100 µL H_2O by vortexing, placed at 90 C for 10 min to lyse cells, and centrifuged at 16 000 x g for 5 min to remove cell debris. 1 µL of the supernatant (containing cellular DNA) was used as the template in each of four PCRs with the following primer sets: A) delCcmF-right + delCcmH-left, B) delCcmC-right + delCcmF-left, C) delCcmB-right + delCcmE-left, D) menBflank-right + menBflank-left. Oligonucleotide primer sequences are given in Table S1. PCRs were performed using GoTaq Green Master Mix (Promega) for 25 cycles, per the manufacturer's recommendations. PCR products were visualized by ethidium bromide staining of agarose gels (0.8 %).

Acknowledgements

We thank Molly C. Sutherland for the genomic PCR protocol and for helpful discussions. This study was supported by National Institutes of Health Grant R01 GM47909 to R.G.K. The mass spectral analysis (shown in Fig S2) was supported in part by National Institute of General Medical Sciences Grant 8 P41 GM103422-35 from the National Institutes of Health, for equipment.

References

Ahuja, U., Kjelgaard, P., Schulz, B.L., Thony-Meyer, L., and Hederstedt, L. (2009) Haem-delivery proteins in cytochrome c maturation System II. *Mol Microbiol* 73: 1058-1071.

Barker, P.D., Ferrer, J.C., Mylrajan, M., Loehr, T.M., Feng, R., Konishi, Y., Funk, W.D., MacGillivray, R.T., and Mauk, A.G. (1993) Transmutation of a heme protein. *Proc Natl Acad Sci U S A* 90: 6542-6546.

Beckman, D.L., Trawick, D.R., and Kranz, R.G. (1992) Bacterial cytochromes c biogenesis. *Genes Dev* 6: 268-283.

Beckman, D.L., and Kranz, R.G. (1993) Cytochromes c biogenesis in a photosynthetic bacterium requires a periplasmic thioredoxin-like protein. *Proc Natl Acad Sci U S A* 90: 2179-2183.

Berry, E.A., and Trumpower, B.L. (1987) Simultaneous determination of hemes a, b, and c from pyridine hemochrome spectra. *Anal Biochem* 161: 1-15.

Christensen, O., Harvat, E.M., Thony-Meyer, L., Ferguson, S.J., and Stevens, J.M. (2007) Loss of ATP hydrolysis activity by CcmAB results in loss of c-type cytochrome synthesis and incomplete processing of CcmE. *Febs J* 274: 2322-2332.

Di Matteo, A., Gianni, S., Schinina, M.E., Giorgi, A., Altieri, F., Calosci, N., Brunori, M., and Travaglini-Allocatelli, C. (2007) A strategic protein in cytochrome c maturation: three-dimensional structure of CcmH and binding to apocytochrome c. *J Biol Chem* 282: 27012-27019.

Di Matteo, A., Calosci, N., Gianni, S., Jemth, P., Brunori, M., and Travaglini-Allocatelli, C. (2010) Structural and functional characterization of CcmG from Pseudomonas aeruginosa, a key component of the bacterial cytochrome c maturation apparatus. *Proteins* 78: 2213-2221.

Di Silvio, E., Di Matteo, A., Malatesta, F., and Travaglini-Allocatelli, C. (2013) Recognition and binding of apocytochrome c to P. aeruginosa CcmI, a component of cytochrome c maturation machinery. *Biochim Biophys Acta* 1834: 1554-1561.

Fabianek, R.A., Hennecke, H., and Thony-Meyer, L. (1998) The active-site cysteines of the periplasmic thioredoxin-like protein CcmG of Escherichia coli are important but not essential for cytochrome c maturation in vivo. *J Bacteriol* 180: 1947-1950.

Fabianek, R.A., Hofer, T., and Thony-Meyer, L. (1999) Characterization of the Escherichia coli CcmH protein reveals new insights into the redox pathway required for cytochrome c maturation. *Arch Microbiol* 171: 92-100.

Feissner, R., Xiang, Y., and Kranz, R.G. (2003) Chemiluminescent-based methods to detect subpicomole levels of c-type cytochromes. *Anal Biochem* 315: 90-94.

Feissner, R.E., Richard-Fogal, C.L., Frawley, E.R., and Kranz, R.G. (2006a) ABC transporter-mediated release of a haem chaperone allows cytochrome c biogenesis. *Mol Microbiol* 61: 219-231.

Feissner, R.E., Richard-Fogal, C.L., Frawley, E.R., Loughman, J.A., Earley, K.W., and Kranz, R.G. (2006b) Recombinant cytochromes c biogenesis systems I and II and analysis of haem delivery pathways in Escherichia coli. *Mol Microbiol* 60: 563-577.

Frawley, E.R., and Kranz, R.G. (2009) CcsBA is a cytochrome c synthetase that also functions in heme transport. *Proc Natl Acad Sci U S A* 106: 10201-10206.

Goldman, B.S., Beckman, D.L., Bali, A., Monika, E.M., Gabbert, K.K., and Kranz, R.G. (1997) Molecular and immunological analysis of an ABC transporter complex required for cytochrome c biogenesis. *J Mol Biol* 268: 724-738.

Goldman, B.S., and Kranz, R.G. (1998) Evolution and horizontal transfer of an entire biosynthetic pathway for cytochrome c biogenesis: Helicobacter, Deinococcus, Archae and more. *Mol Microbiol* 27: 871-873.

Hamel, P., Corvest, V., Giege, P., and Bonnard, G. (2009) Biochemical requirements for the maturation of mitochondrial c-type cytochromes. *Biochim Biophys Acta* 1793: 125-138.

Hamel, P.P., Dreyfuss, B.W., Xie, Z., Gabilly, S.T., and Merchant, S. (2003) Essential histidine and tryptophan residues in CcsA, a system II polytopic cytochrome c biogenesis protein. *J Biol Chem* 278: 2593-2603.

Kern, M., Scheithauer, J., Kranz, R.G., and Simon, J. (2010) Essential histidine pairs indicate conserved haem binding in epsilonproteobacterial cytochrome c haem lyases. *Microbiology* 156: 3773-3781.

Kranz, R.G., Richard-Fogal, C., Taylor, J.S., and Frawley, E.R. (2009) Cytochrome c biogenesis: mechanisms for covalent modifications and trafficking of heme and for heme-iron redox control. *Microbiol Mol Biol Rev* 73: 510-528, Table of Contents.

Lee, D., Pervushin, K., Bischof, D., Braun, M., and Thony-Meyer, L. (2005) Unusual heme-histidine bond in the active site of a chaperone. *J Am Chem Soc* 127: 3716-3717.

Mavridou, D.A., Ferguson, S.J., and Stevens, J.M. (2013) Cytochrome c assembly. *IUBMB Life* 65: 209-216.

Merchant, S.S. (2009) His protects heme as it crosses the membrane. *Proc Natl Acad Sci U S A* 106: 10069-10070.

Meyer, E.H., Giege, P., Gelhaye, E., Rayapuram, N., Ahuja, U., Thony-Meyer, L., Grienenberger, J.M., and Bonnard, G. (2005) AtCCMH, an essential component of the c-type cytochrome maturation pathway in Arabidopsis mitochondria, interacts with apocytochrome c. *Proc Natl Acad Sci U S A* 102: 16113-16118.

Monika, E.M., Goldman, B.S., Beckman, D.L., and Kranz, R.G. (1997) A thioreduction pathway tethered to the membrane for periplasmic cytochromes c biogenesis; in vitro and in vivo studies. *J Mol Biol* 271: 679-692.

Nicholson, D.W., and Neupert, W. (1989) Import of cytochrome c into mitochondria: reduction of heme, mediated by NADH and flavin nucleotides, is obligatory for its covalent linkage to apocytochrome c. *Proc Natl Acad Sci U S A* 86: 4340-4344.

Ouyang, N., Gao, Y.G., Hu, H.Y., and Xia, Z.X. (2006) Crystal structures of E. coli CcmG and its mutants reveal key roles of the N-terminal beta-sheet and the fingerprint region. *Proteins* 65: 1021-1031.

Rayapuram, N., Hagenmuller, J., Grienenberger, J.M., Bonnard, G., and Giege, P. (2008) The three mitochondrial encoded CcmF proteins form a complex that interacts with CCMH and c-type apocytochromes in Arabidopsis. *J Biol Chem* 283: 25200-25208.

Ren, Q., and Thony-Meyer, L. (2001) Physical interaction of CcmC with heme and the heme chaperone CcmE during cytochrome c maturation. *J Biol Chem* 276: 32591-32596.

Ren, Q., Ahuja, U., and Thony-Meyer, L. (2002) A bacterial cytochrome c heme lyase. CcmF forms a complex with the heme chaperone CcmE and CcmH but not with apocytochrome c. *J Biol Chem* 277: 7657-7663.

Richard-Fogal, C., and Kranz, R.G. (2010) The CcmC:heme:CcmE complex in heme trafficking and cytochrome c biosynthesis. *J Mol Biol* 401: 350-362.
Richard-Fogal, C.L., Frawley, E.R., Feissner, R.E., and Kranz, R.G. (2007) Heme concentration dependence and metalloporphyrin inhibition of the system I and II cytochrome c assembly pathways. *J Bacteriol* 189: 455-463.
Richard-Fogal, C.L., Frawley, E.R., Bonner, E.R., Zhu, H., San Francisco, B., and Kranz, R.G. (2009) A conserved haem redox and trafficking pathway for cofactor attachment. *Embo J* 28: 2349-2359.
Richard-Fogal, C.L., San Francisco, B., Frawley, E.R., and Kranz, R.G. (2012) Thiol redox requirements and substrate specificities of recombinant cytochrome c assembly systems II and III. *Biochim Biophys Acta* 1817: 911-919.
Robertson, I.B., Stevens, J.M., and Ferguson, S.J. (2008) Dispensable residues in the active site of the cytochrome c biogenesis protein CcmH. *FEBS Lett* 582: 3067-3072.
San Francisco, B., Bretsnyder, E.C., Rodgers, K.R., and Kranz, R.G. (2011) Heme ligand identification and redox properties of the cytochrome c synthetase, CcmF. *Biochemistry* 50: 10974-10985.
Sanders, C., Turkarslan, S., Lee, D.W., Onder, O., Kranz, R.G., and Daldal, F. (2008) The cytochrome c maturation components CcmF, CcmH, and CcmI form a membrane-integral multisubunit heme ligation complex. *J Biol Chem* 283: 29715-29722.
Sanders, C., Turkarslan, S., Lee, D.W., and Daldal, F. (2010) Cytochrome c biogenesis: the Ccm system. *Trends Microbiol* 18: 266-274.
Sawyer, E.B., and Barker, P.D. (2012) Continued surprises in the cytochrome c biogenesis story. *Protein Cell* 3: 405-409.
Schulz, H., Fabianek, R.A., Pellicioli, E.C., Hennecke, H., and Thony-Meyer, L. (1999) Heme transfer to the heme chaperone CcmE during cytochrome c maturation requires the CcmC protein, which may function independently of the ABC-transporter CcmAB. *Proc Natl Acad Sci U S A* 96: 6462-6467.
Setterdahl, A.T., Goldman, B.S., Hirasawa, M., Jacquot, P., Smith, A.J., Kranz, R.G., and Knaff, D.B. (2000) Oxidation-reduction properties of disulfide-containing proteins of the Rhodobacter capsulatus cytochrome c biogenesis system. *Biochemistry* 39: 10172-10176.
Simon, J., and Hederstedt, L. (2011) Composition and function of cytochrome c biogenesis System II. *Febs J* 278: 4179-4188.
Stevens, J.M., Daltrop, O., Higham, C.W., and Ferguson, S.J. (2003) Interaction of heme with variants of the heme chaperone CcmE carrying active site mutations and a cleavable N-terminal His tag. *J Biol Chem* 278: 20500-20506.
Turkarslan, S., Sanders, C., Ekici, S., and Daldal, F. (2008) Compensatory thio-redox interactions between DsbA, CcdA and CcmG unveil the apocytochrome c holdase role of CcmG during cytochrome c maturation. *Mol Microbiol* 70: 652-666.
Uchida, T., Stevens, J.M., Daltrop, O., Harvat, E.M., Hong, L., Ferguson, S.J., and Kitagawa, T. (2004) The interaction of covalently bound heme with the cytochrome c maturation protein CcmE. *J Biol Chem* 279: 51981-51988.
Verissimo, A.F., Yang, H., Wu, X., Sanders, C., and Daldal, F. (2011) CcmI subunit of CcmFHI heme ligation complex functions as an apocytochrome c chaperone during c-type cytochrome maturation. *J Biol Chem* 286: 40452-40463.

Xie, Z., and Merchant, S. (1998) A novel pathway for cytochromes c biogenesis in chloroplasts. *Biochim Biophys Acta* 1365: 309-318.
Zheng, X.M., Hong, J., Li, H.Y., Lin, D.H., and Hu, H.Y. (2012) Biochemical properties and catalytic domain structure of the CcmH protein from Escherichia coli. *Biochim Biophys Acta* 1824: 1394-1400.

Figures

Fig 1. CcmFGH attaches heme to cytochrome c in the absence of CcmABCDE.

(A) Heme staining of BPER cell extracts showing synthesis of 24-kDa holocytochrome c4:His6 as a function of expression of separate Ccm components, as indicated. (B) Heme staining and (C) anti-cytochrome c2 immunoblot of BPER cell extracts showing synthesis of 106-kDa holocytochrome c2:Pho by CcmFGH as a function of induction with IPTG and/or arabinose. One hundred μg total protein was loaded in each lane. MW, molecular weight standards (lanes 1).

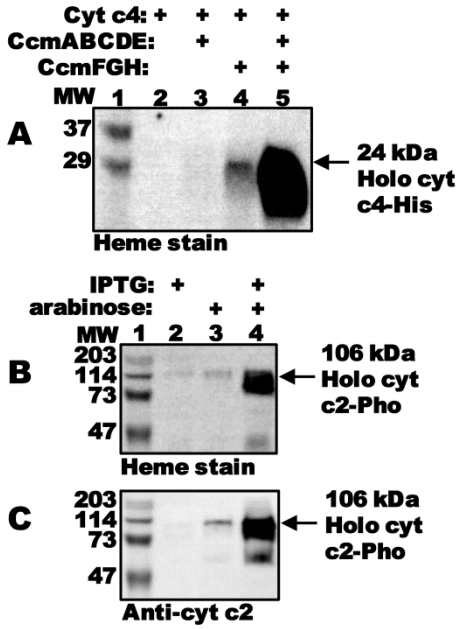
Cyt c4: + + + +
CcmABCDE: + +
CcmFGH: + +
MW 1 2 3 4 5
A
37
29
24 kDa
Holo cyt
c4-His
Heme stain
IPTG: + +
arabinose: + +
MW 1 2 3 4
B
203
114
73
47
106 kDa
Holo cyt
c2-Pho
Heme stain
C
203
114
73
47
106 kDa
Holo cyt
c2-Pho
Anti-cyt c2

Fig 2. Characterization of cytochrome c produced by CcmFGH-ind.

(A) Coomassie blue staining of purified cytochrome c4:His6 showing full length 24-kDa holocytochrome c4 and proteolyzed 12-kDa holocytochrome c4'. (B) Heme staining of purified cytochrome c4 showing 24-kDa and 12-kDa forms. (C) Anti-cytochrome c4 immunoblot showing 24-kDa and 12-kDa holocytochrome c4. For (A)-(C), abbreviations are M, molecular weight standards; S, soluble fraction; FT, flow through; W1, wash 1; W2, wash 2; W3, wash 3; W4, wash 4; E1, elution 1; E2, elution 2; E3, elution 3. (D) UV-Vis absorption spectra of purified, sodium dithionite-reduced holocytochrome c4 produced by the full system I (blue line) or in the absence of CcmABCDE (red line). (Inset) Sodium dithionite-reduced pyridine hemochrome spectrum of purified holocytochrome c4 produced by the full system I (blue line) or in the absence of CcmABCDE (red line) from 500-600 nm. Absorption maxima are indicated.

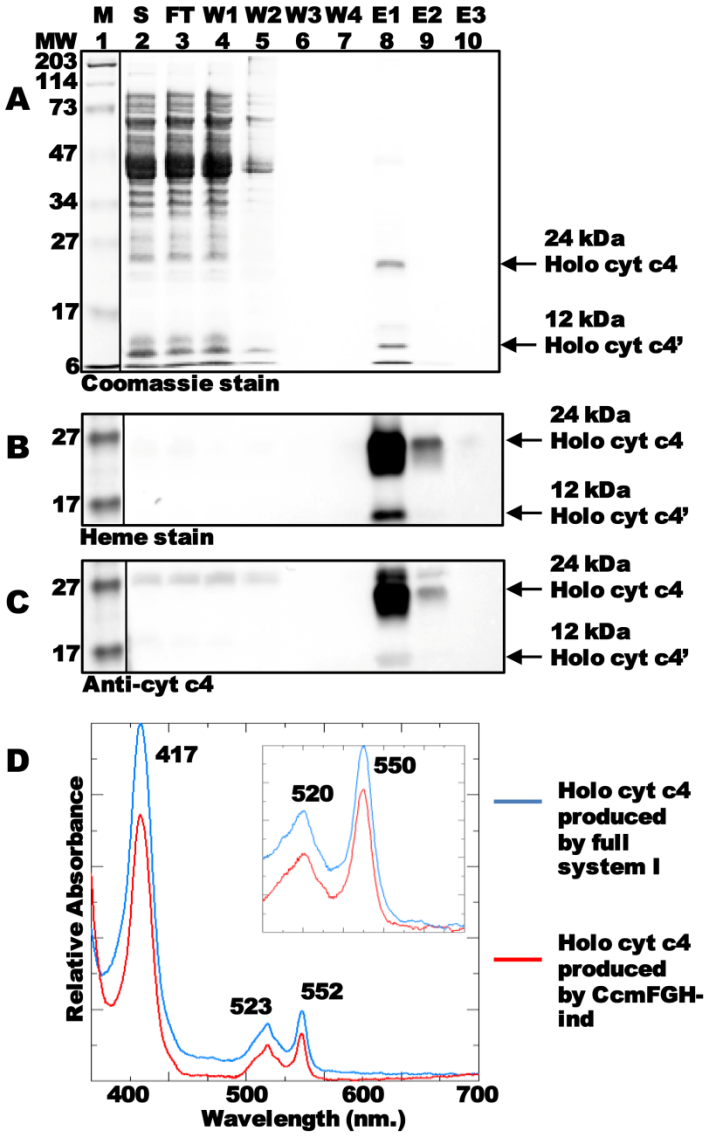
M S FT W1 W2 W3 W4 E1 E2 E3
MW 1 2 3 4 5 6 7 8 9 10
203
114
73
47
34
27
17
6
A
Coomassie stain
24 kDa
Holo cyt c4
12 kDa
Holo cyt c4'
B
27
17
Heme stain
24 kDa
Holo cyt c4
12 kDa
Holo cyt c4'
C
27
17
Anti-cyt c4
24 kDa
Holo cyt c4
12 kDa
Holo cyt c4'
D
417
520
550
523
552
Relative Absorbance
400
500
600
700
Wavelength (nm.)
Holo cyt c4 produced by full system I
Holo cyt c4 produced by CcmFGH-ind

Fig 3. Optimization of holocytochrome c4 produced by CcmFGH-ind.

(A) Heme staining of TALON-purified proteins showing relative levels of holocytochrome c4 synthesized for each indicated condition. "↑ arab," increase in arabinose from 0.2 % to 0.4 %; "ALA," addition of ALA to 50 μg mL^{-1}; "↓ rpm," decrease in shaking during growth from 230 rpm to 120 rpm; "p-c4," single plasmid system with cytochrome c4 engineered into pBAD CcmFGH; "***," each of the four additives/conditions together. (B) Sodium dithionite-reduced pyridine hemochrome spectra of TALON-purified proteins for each condition, from 500-600 nm. Absorption maxima are indicated. (C) Quantification of yields of holocytochrome c4 (based on 550 nm. absorption in reduced pyridine hemochrome) for each condition from three independent experiments. Error bars denote standard deviation. ND, none detected. (D) Anti-CcmF immunoblot of DDM-solubilized membrane fractions showing 54-kDa CcmF. (E) Anti-CcmH immunoblot of DDM-solubilized membrane fractions showing 37-kDa CcmH. (F) Anti-CcmE immunoblot of DDM-solubilized membrane fractions showing 20-kDa CcmE. Labels are as in (A).

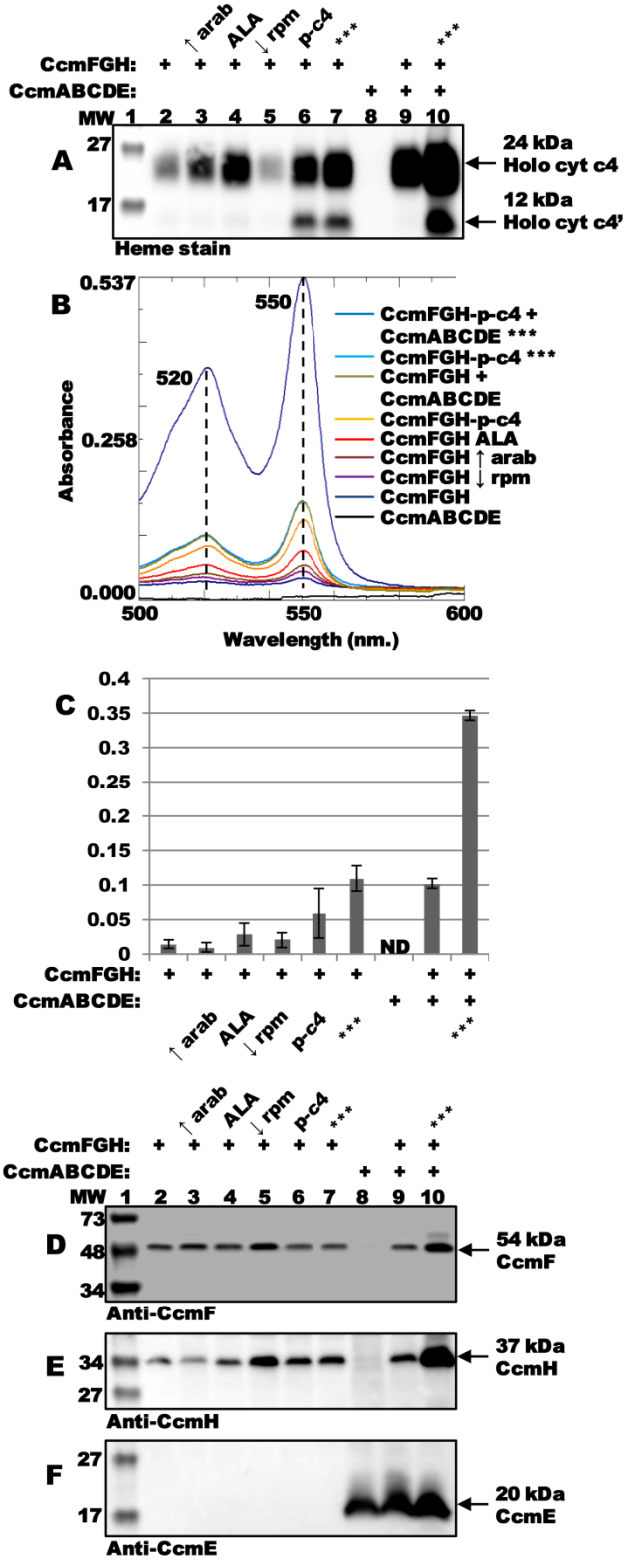
↑arab
ALA
↓rpm
p-c4
***
***
CcmFGH:
CcmABCDE:
MW 1 2 3 4 5 6 7 8 9 10
A
27
17
24 kDa
Holo cyt c4
12 kDa
Holo cyt c4'
Heme stain
B
0.537
0.258
0.000
Absorbance
520
550
500
550
600
Wavelength (nm.)
CcmFGH-p-c4 + CcmABCDE ***
CcmFGH-p-c4 ***
CcmFGH + CcmABCDE
CcmFGH-p-c4
CcmFGH ALA
CcmFGH ↑arab
CcmFGH ↓rpm
CcmFGH
CcmABCDE
C
0.4
0.35
0.3
0.25
0.2
0.15
0.1
0.05
0
ND
CcmFGH:
CcmABCDE:
↑arab
ALA
↓rpm
p-c4
***
***
CcmFGH:
CcmABCDE:
MW 1 2 3 4 5 6 7 8 9 10
D
73
48
34
54 kDa
CcmF
Anti-CcmF
E
34
27
37 kDa
CcmH
Anti-CcmH
F
27
17
20 kDa
CcmE
Anti-CcmE

Fig 4. Topologies of CcmF and CcsBA.

Topology of the system I CcmF protein from *Escherichia coli* (A) and the system II CcsBA fusion protein from *Helicobacter hepaticus* (B). Possible histidine axial ligands to heme are starred, and are designated P-His1, P-His2, TM-His1, and TM-His2. The highly conserved WWD domain and the hydrophobic patches are shaded. Completely conserved amino acids (red) were identified by individual protein alignments using CcmF or the CcsB and CcsA ORFs from selected organisms, as described in (Kranz *et al.*, 2009). Diagram is modified from (Kranz *et al.*, 2009).

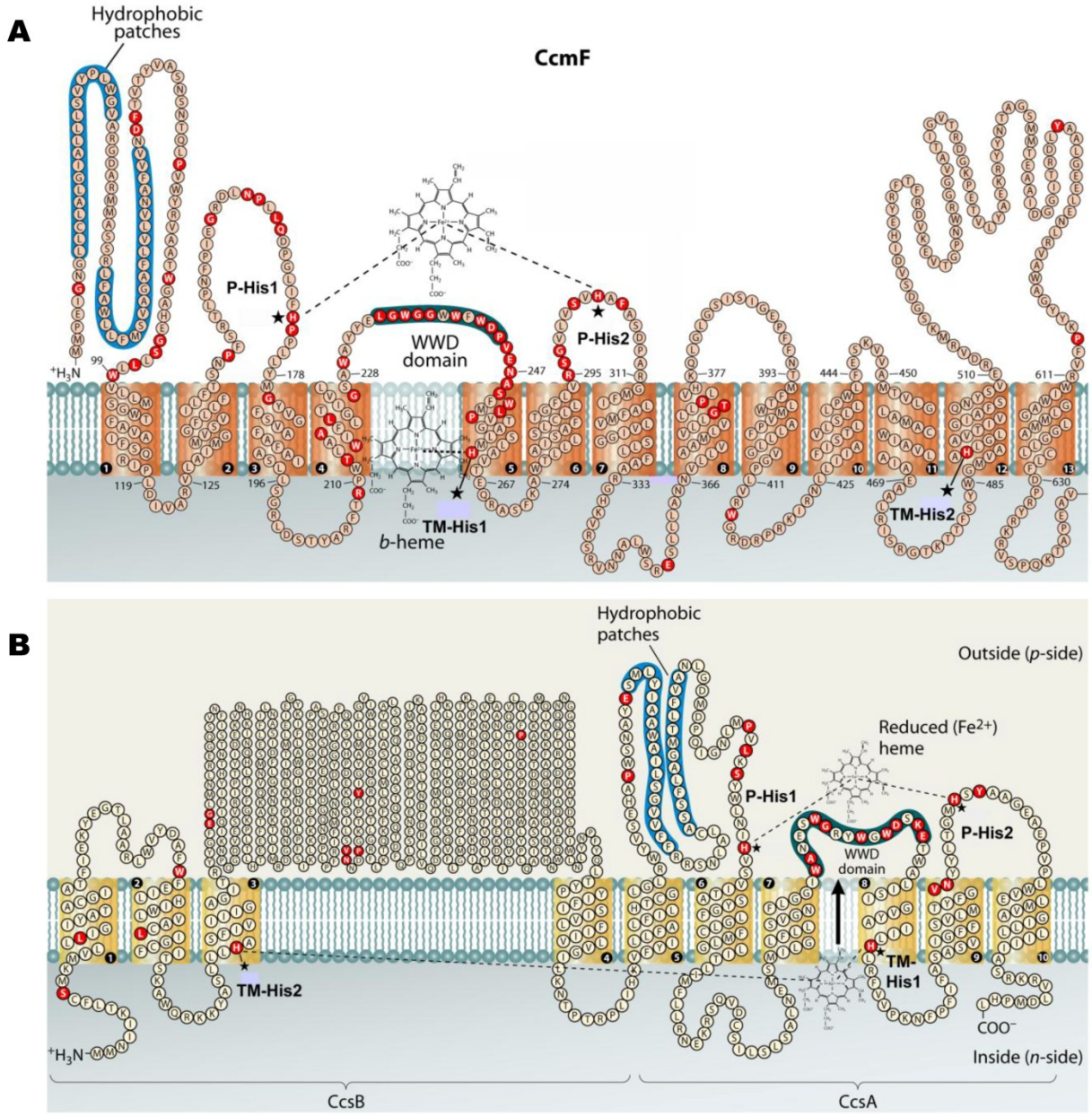
A
Hydrophobic patches
CcmF
P-His1
WWD domain
P-His2
TM-His1
b-heme
TM-His2
B
Hydrophobic patches
Outside (p-side)
Reduced (Fe2+) heme
P-His1
P-His2
WWD domain
TM-His1
TM-His2
Inside (n-side)
CcsB
CcsA

Fig 5. Role of conserved His residues in CcmF in CcmFGH-ind.

(A) Heme staining of purified holocytochrome c4 assembled by WT and site-directed variants of CcmF. (B) Quantification of the results of heme staining (24 kDa holocytochrome c4) from purified fractions from three independent experiments. (C) Heme staining of purified holocytochrome c4 assembled by WT and the indicated site-directed variants at CcmF P-His1 (upper panel) or P-His2 (lower panel). (D) Quantification of the results of heme staining from purified fractions from three independent experiments. For (B) and (D), synthesis of holocytochrome c4 is relative to WT, which has been set at 100 %. Error bars denote standard deviation. ND, none detected.

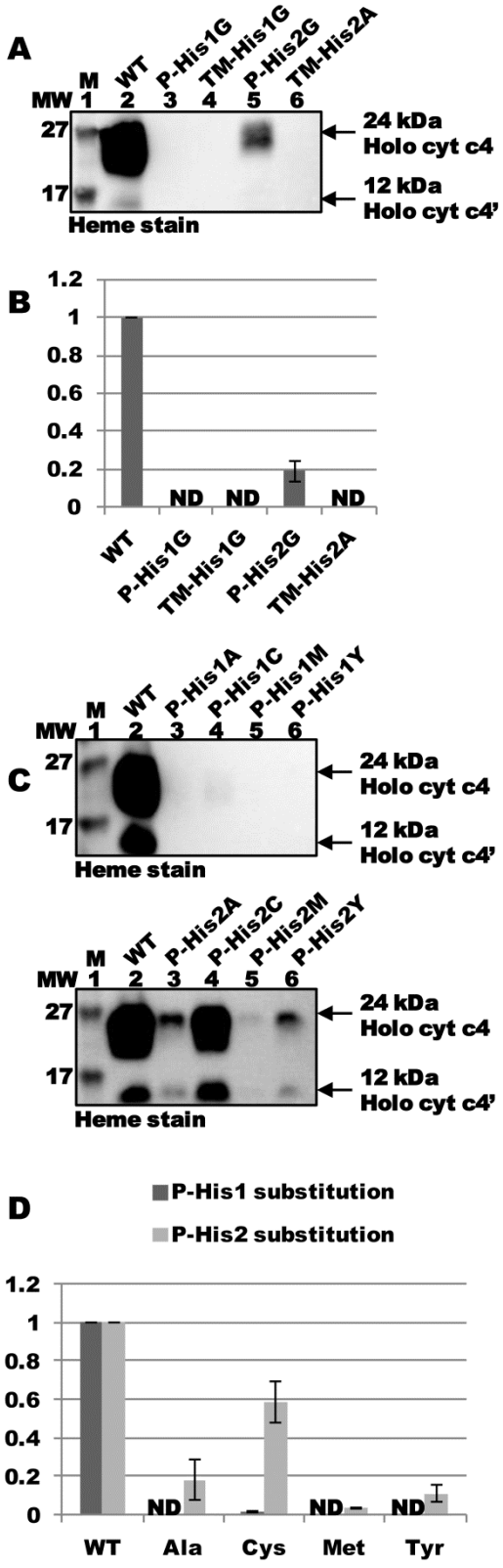
A
M
WT
P-His1G
TM-His1G
P-His2G
TM-His2A
MW 1 2 3 4 5 6
27
17
24 kDa
Holo cyt c4
12 kDa
Holo cyt c4'
Heme stain
B
1.2
1
0.8
0.6
0.4
0.2
0
ND
ND
ND
WT
P-His1G
TM-His1G
P-His2G
TM-His2A
C
M
WT
P-His1A
P-His1C
P-His1M
P-His1Y
MW 1 2 3 4 5 6
27
17
24 kDa
Holo cyt c4
12 kDa
Holo cyt c4'
Heme stain
M
WT
P-His2A
P-His2C
P-His2M
P-His2Y
MW 1 2 3 4 5 6
27
17
24 kDa
Holo cyt c4
12 kDa
Holo cyt c4'
Heme stain
D
P-His1 substitution
P-His2 substitution
1.2
1
0.8
0.6
0.4
0.2
0
ND
ND
ND
WT
Ala
Cys
Met
Tyr

Fig 6. Conserved cysteines in CcmG and CcmH are required for CcmFGH-ind.

(A) Heme staining of purified holocytochrome c4 assembled by WT and the indicated site-directed variants at CcmG and CcmH. "Gmut" is a Cys80Ser/Cys83Ser double mutant, and "Hmut" is a Cys43Ser/Cys46Ser double mutant. (B) Quantification of the results of heme staining (24 kDa holocytochrome c4) from purified fractions from three independent experiments. Synthesis of holocytochrome c4 is relative to WT, which has been set at 100 %. ND, none detected.

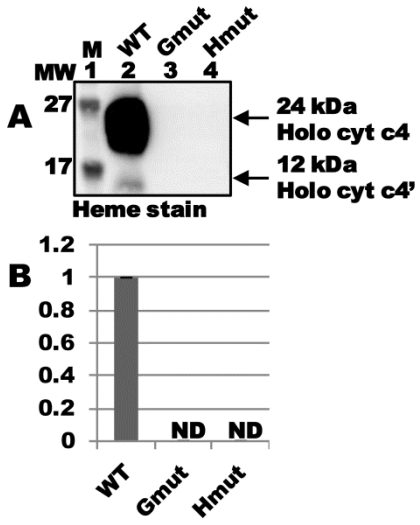
M
WT
Gmut
Hmut
MW
1
2
3
4
A
27
17
24 kDa
Holo cyt c4
12 kDa
Holo cyt c4'
Heme stain
B
1.2
1
0.8
0.6
0.4
0.2
0
ND
ND
WT
Gmut
Hmut

Supplementary Material

Fig S1. Confirmation of Δ*ccm* by genomic PCR.

Ethidium bromide staining of the products from 4 separate PCRs using the indicated genomic DNA templates. Primer sets A, B, and C anneal to different regions of the ccm operon (panel C), and control primer set D anneals to regions flanking *E. coli* menB. For WT *E. coli*, all PCRs yielded products of the expected sizes (panel A, lanes 1-4). No products corresponding to the *ccm* operon were detected for any of the Δ*ccm* strains (panels A and B), with the exception of primer set A for strain Δ*ccm* c4:His6 int + pBAD CcmF:His6GH, as expected since this strain carries the ccmFGH genes on a plasmid. PCRs using control primer set D yielded products of the expected size for each strain. This confirms that our Δ*ccm* strains lack the endogeneous genes for cytochrome c synthesis; therefore, holocytochrome c formation in these strains is completely dependent on plasmid-based expression of the *ccm* genes. Lanes 5 and 10 in (A) and (B) contain MW markers; bp indicates base pairs.

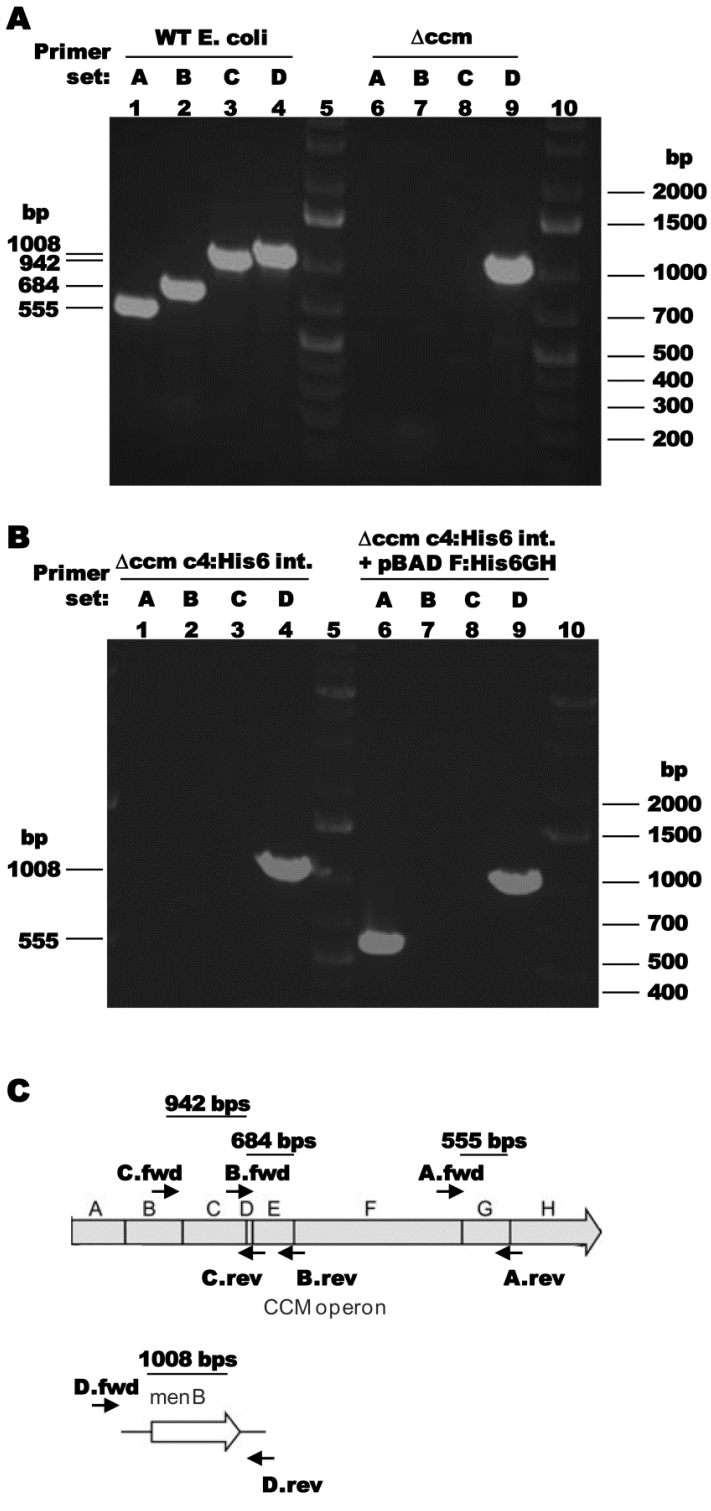
A
Primer set:
WT E. coli
Δccm
A B C D A B C D
1 2 3 4 5 6 7 8 9 10
bp
1008
942
684
555
bp
2000
1500
1000
700
500
400
300
200
B
Primer set:
Δccm c4:His6 int.
Δccm c4:His6 int. + pBAD F:His6GH
A B C D A B C D
1 2 3 4 5 6 7 8 9 10
bp
1008
555
bp
2000
1500
1000
700
500
400
C
942 bps
684 bps
555 bps
C.fwd
B.fwd
A.fwd
A B C D E F G H
C.rev
B.rev
A.rev
CCM operon
1008 bps
D.fwd
menB
D.rev

Fig S2. Mass spectral analysis of holocytochrome c4:His6.

Mass spectral analysis of holocytochrome c4:His6 produced by CcmFGH in the presence (A) or absence (B) of CcmABCDE. After deconvolution of the positive ion mass spectra, two species were identified from each sample with the indicated molecular weights (each was within 2 Daltons of the reported average masses for full length holocytochrome c4:His6 and proteolyzed holocytochrome c4:His6', respectively). (C) Amino acid sequence of the *Bordetella pertussis* cytochrome c4:His6. The signal sequence is underlined and heme attachment sites (Cys-Xxx-Xxx-Cys-His) are in bold. Arrows indicate the periplasmic signal cleavage site and the site of endogeneous proteolysis giving rise to holocytochrome c4:His6'. The presence of identical molecular weight species in preparations of holocytochrome c4:His6 produced by full system I and by CcmFGH-ind confirms proper cleavage of the cytochrome c4 periplasmic secretion sequence, and covalent attachment of heme.

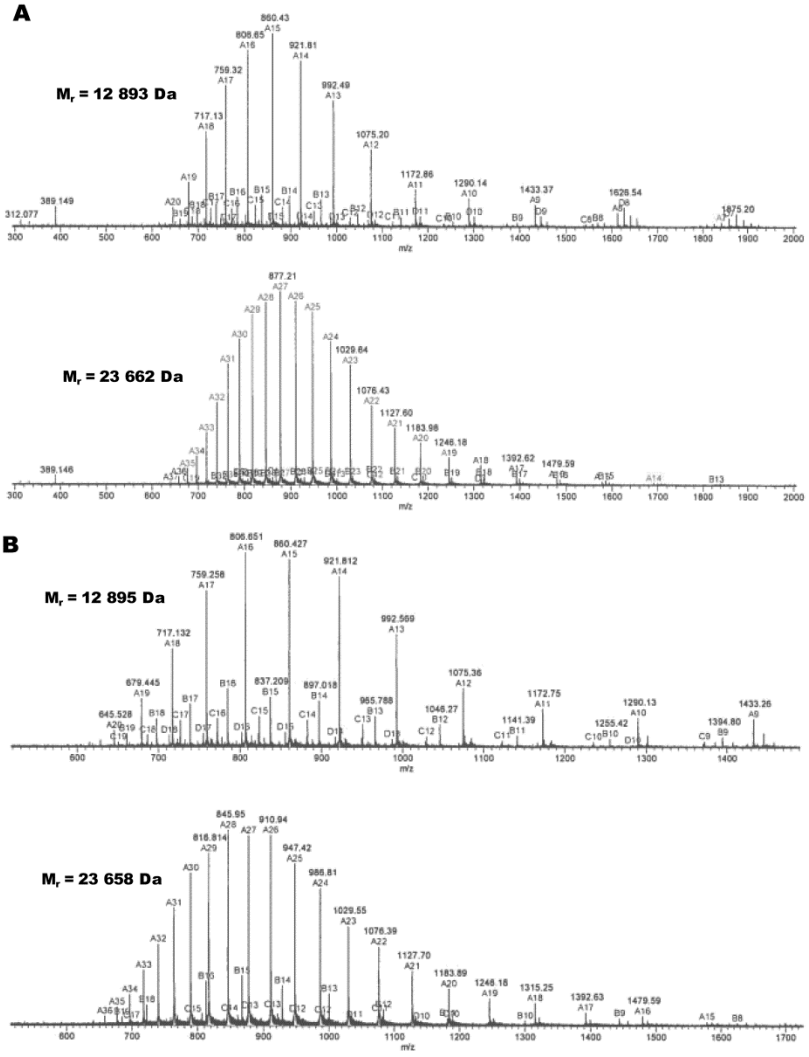

C

Signal cleavage site

MKRVLSRMLVASGLVLGASVHSMSFAADGAAGPAKPDAAK	40
GAQLYDQGDASRGVIA**CASCH**GAAGSSTIPANPNLAAQPH	80
EYLVKQLTEFKVKEGEKLPLRMGPGGNPTPMTAMAQPLTA	120
QDMQNVALYLSQQPLKEPATAGHENLVELGQKIWRGGLAD	160
RNVPA**CAACH**GATGAGIPGQYPRLSGQFSSYIEEQLKLFR	200
SGERGNSVPMHDIADRMSDADIKAVADYAAGLRHHHHHH	239

Table S1. Strains, plasmids, and oligonucleotide primers

Strain	Description	Reference
RK103	MG1655 Δccm	(Feissner *et al.*, 2006)
RK111	MG1655 Δccm *cyt c4*:His6 chromosomal integrate	(San Francisco *et al.*, 2011)

Plasmid	Description	Reference
--	pUCA6 *cyt c*2:Pho	(Beckman *et al.*, 1992)
pRGK332	pBAD *cyt c*4:His6	(Feissner *et al.*, 2006)
pRGK388	pBAD *ccmF*:His6*GH*	(Richard-Fogal *et al.*, 2009)
pRGK402	pGEX *ccmABCDE*	(San Francisco *et al.*, 2011)
pRGK434	pBAD *ccmF*(His173Ala):His6*GH*	(San Francisco *et al*., submitted)
pRGK435	pBAD *ccmF*(His173Gly):His6*GH*	(San Francisco *et al*., submitted)
pRGK436	pBAD *ccmF*(His173Cys):His6*GH*	(San Francisco *et a*l., submitted)
pRGK437	pBAD *ccmF*(His173Met):His6*GH*	(San Francisco *et al*., submitted)
pRGK438	pBAD *ccmF*(His173Tyr):His6*GH*	(San Francisco *et al*., submitted)
pRGK439	pBAD *ccmF*(His303Ala):His6*GH*	(San Francisco *et al*., submitted)
pRGK440	pBAD *ccmF*(His303Gly):His6*GH*	(San Francisco *et al*., submitted)
pRGK441	pBAD *ccmF*(His303Cys):His6*GH*	(San Francisco *et al*., submitted)
pRGK442	pBAD *ccmF*(His303Met):His6*GH*	(San Francisco *et al*., submitted)
pRGK443	pBAD *ccmF*(His303Tyr):His6*GH*	(San Francisco *et al*., submitted)
pRGK444	pBAD ccmF(His261Gly):His6GH	This work
pRGK445	pBAD ccmF(His491Ala):His6GH	This work
pRGK446	pBAD *ccmF*:His6*G*(Cys80Ser/Cys83Ser)*H*	This work
pRGK447	pBAD *ccmF*:His6*GH*(Cys43Ser/Cys46Ser)	This work
pRGK448	pBAD *ccmF*:His6*GH—cyt c*4:His6	This work

Primer	Sequence (5'-3')	Purpose
C4:His_PstI_RBS_Fwd	GATCTGCAGAGGAGGAATATCATATGAAGCGTGTGCTGTCCCGG	pRGK448
C4:His_PstI_Rev	GATCTGCAGTCAGTGGTGGTGGTGGTGGTG	pRGK448
ccmG_C80A/C83A_Fwd	CTGGGCGACCTGGGCTCCGACCGCCCGTGCGGAACAT	pRGK446
ccmG_C80A/C83A_Rev	ATGTTCCGCACGGGCGGTCGGAGCCCAGGTCGCCCAG	pRGK446
ccmH_C43A/C46A_Fwd	CTCACTGAAGAACTGCGCGCCCCGAAAGCCCAGAACAACAGCATTGC	pRGK447
ccmH_C43A/C46A_Rev	GCAATGCTGTTGTTCTGGGCTTTCGGGGCGCGCAGTTCTTCAGTGAG	pRGK447
ccmF_H261G_Fwd	GGACTGCGCTGATGGGCTCACTGGCGGTCA	pRGK444
ccmF_H261G_Rev	TGACCGCCAGTGAGCCCATCAGCGCAGTCC	pRGK444
ccmF_H491A_Fwd	GGGATGGTGGCGGCTGCCCTTGGGCTGGC	pRGK445
ccmF_H491A_Rev	GCCAGCCCAAGGGCAGCCGCCACCATCCC	pRGK445
A.Fwd (delCcmF_right)	GCCGGAGGCCATATGAAGCGCAAAGTATTGTTA	gPCR
A.Rev (delCcmH_left)	GCGCCAATAAAAAGCTTATTGTGCGGCCTCCTT	gPCR
B.Fwd (delCcmC_right)	AAGAGGCCGCATATGACCCCTGCATTTGCTTCC	gPCR
B.Rev (delCcmF_left)	CCGAATTCTGGCATCATATGGCTGGGTCCTTAT	gPCR
C.Fwd (delCcmB_right)	GGTATCGAACATATGAGGAAAACACTGCATCAACT	gPCR
C.Rev (delCcmC_left)	AGTGTTTTCCACATATGTTCGATACCAGACTCG	gPCR
D.Fwd (menBflank_right)	CGCAGGCAAACATACAGCCC	gPCR
D.Rev (menBflank_left)	CGGACATAACGCGCATCGG	gPCR

Supplementary Information References

Beckman, D.L., Trawick, D.R., and Kranz, R.G. (1992) Bacterial cytochromes c biogenesis. *Genes Dev* 6: 268-283.

Feissner, R.E., Richard-Fogal, C.L., Frawley, E.R., Loughman, J.A., Earley, K.W., and Kranz, R.G. (2006) Recombinant cytochromes c biogenesis systems I and II and analysis of haem delivery pathways in Escherichia coli. *Mol Microbiol* 60: 563-577.

Richard-Fogal, C.L., Frawley, E.R., Bonner, E.R., Zhu, H., San Francisco, B., and Kranz, R.G. (2009) A conserved haem redox and trafficking pathway for cofactor attachment. *Embo J* 28: 2349-2359.

San Francisco, B., Bretsnyder, E.C., Rodgers, K.R., and Kranz, R.G. (2011) Heme ligand identification and redox properties of the cytochrome c synthetase, CcmF. *Biochemistry* 50: 10974-10985.

Chapter 5: The human mitochondrial holocytochrome *c* synthase's heme binding, maturation determinants, and complex formation with cytochrome *c*

Brian San Francisco, Eric C. Bretsnyder, Robert G. Kranz[1]

Department of Biology, Washington University in St. Louis, St. Louis, MO 63130, USA

Published in *Proc Natl Acad Sci U S A*. (2013) 110(9):E788-97

Short Title: The human mitochondrial holocytochrome *c* synthase

Classification: Biological Sciences (major); Biochemistry (minor)

[1] Corresponding author

Email: kranz@biology.wustl.edu

Washington University, Department of Biology, Campus Box 1137, One Brookings Drive, St. Louis, MO 63130

Tel: 314-935-4278

Fax: 314-935-4432

Abstract

Proper functioning of the mitochondrion requires the orchestrated assembly of respiratory complexes with their cofactors. Cytochromes *c*, essential electron carriers in mitochondria and critical components of the apoptotic pathway, contain a heme cofactor covalently attached to the protein at a conserved CXXCH motif. While it has been known for over two decades that heme attachment requires the mitochondrial protein holocytochrome *c* synthase (HCCS), the mechanism has remained unknown. We purified the membrane-bound human HCCS with endogenous heme, and in complex with its cognate human apocytochrome *c*. Spectroscopic analyses of HCCS alone and complexes of HCCS with site-directed variants of cytochrome *c* revealed the fundamental steps of heme attachment and maturation. A conserved histidine in HCCS (His154) provided the key ligand to the heme iron. Formation of the HCCS:heme complex served as the platform for interaction with the apocytochrome *c*. Heme was the central molecule mediating contact between HCCS and apocytochrome *c*. A conserved histidine in apocytochrome *c* (His19 of CXXCH) supplied the second axial ligand to heme in the trapped HCCS:heme:cytochrome *c* complex. We also examined the substrate specificity of human HCCS and converted a bacterial cytochrome *c* into a robust substrate for the HCCS. The results allow us to describe the molecular mechanisms underlying the holocytochrome *c* synthase reaction.

Introduction

Renewed interest in mitochondria stems from recent associations of malfunctioning mitochondria with many cancers (1), neurological diseases (2-4), and even reduced life span (5). The basis for these associations lies in the respiratory chains that power aerobic life. Three-dimensional structures for many respiratory complexes and carriers (6-8) have elucidated the detailed mechanisms of electron transport, proton pumping, the reduction of oxygen to water, and ATP formation. Less is known about the biogenesis of these respiratory chain components. The synthesis and insertion of cofactors (e.g., heme and metals) into large, multi-subunit membrane complexes represents a new frontier in the study of mitochondrial function. *C*-type cytochromes, among the best-studied players in mitochondrial electron transport (9, 10), are redox active heme proteins whose biosynthesis is only just emerging. Cytochrome *c* is a soluble electron carrier in the intermembrane space (IMS) of mitochondria that functions in electron transport between the quinol:cytochrome *c* oxidoreductase (complex III, or cytochrome bc_1) and the cytochrome *c* oxidase (complex IV, or cytochrome a/a3). In addition to its role in mitochondrial respiration, cytochrome *c* plays a crucial role in apoptotic signaling (11). A second, membrane-bound *c*-type cytochrome, cytochrome c_1, is an integral part of complex III.

Cytochromes *c* differ from other cytochromes in that the heme is covalently attached to the protein via two thioether linkages between the heme vinyls and two cysteine residues of a conserved CysXxxXxxCysHis (CXXCH) heme binding motif. Two major pathways have been identified for the biogenesis of cytochromes *c* in mitochondria: CCM (cytochrome *c* maturation) (12-15) and CCHL (cytochrome *c* heme lyase), also called HCCS (holocytochrome *c* synthase, which will be used here) (16, 17). The CCM system is composed of eight or nine integral

membrane proteins and functions in the mitochondrial inner membrane of plants and some protozoa, as well as the cytoplasmic membranes of alpha- and gamma-proteobacteria (18). Most mitochondria (e.g., those of fungi, invertebrates, vertebrates, and some protozoa) use HCCS for synthesis of cytochrome *c*. In fungi, there are two related homologs, HCCS and HCC_1S, dedicated to maturation of cytochrome *c* and cytochrome c_1, respectively (19, 20*)*, whereas in animals a single HCCS enzyme is active toward both cytochrome *c* and cytochrome c_1 (17, 21). Additionally, in yeast and other fungi, the FAD-containing protein Cyc2p is required for heme attachment to apocytochrome *c* (22-24).

The human HCCS has been increasingly implicated in disease. For example, chromosomal mutations in the gene encoding HCCS can lead to a condition called microphthalmia with linear skin defects syndrome (MLS; (25, 26)). Additionally, a role for HCCS in apoptosis (separate from that of cytochrome *c*) has been described in injured motor neurons (27). Despite the identification of HCCS as the gene product responsible for heme attachment to cytochrome *c* in *S. cerevisiae* over twenty-five years ago (19), the enzyme has never been purified or characterized and the mechanism of covalent heme attachment is unknown (16, 17). In yeast, HCCS is nuclear-encoded and is imported directly into the mitochondrial IMS from the cytosol via the translocase of the outer membrane (TOM) complex (20, 28, 29). Studies in *S. cerevisiae* have shown that HCCS is membrane-associated in mitochondria and is exposed to the IMS (28-30). The apparent absence of transmembrane helices suggests that membrane association is likely peripheral. Pioneering studies by Neupert and Sherman and colleagues have demonstrated that HCCS also plays an essential role in the import of the apocytochrome *c* from the cytosol to the mitochondrion (30-33). It is unknown

how heme enters the IMS from its site of synthesis in the mitochondrial matrix, although early studies showed that reduced heme (Fe^{2+}) is necessary for covalent attachment to cytochrome *c* (34, 35). Preliminary genetic results suggested that heme binding by HCCS occurred at partially conserved "Cys-Pro" sequences (36), which serve as heme-regulatory motifs in several other proteins. However, neither of the Cys-Pro sequences in *S. cerevisiae* HCCS is required for heme attachment to cytochrome *c* (37), and several HCCS proteins lack Cys-Pro sequences entirely.

Both the mechanism by which HCCS mediates covalent heme attachment to the apocytochrome, and the specificity determinants for recognition of heme and the apocytochrome *c* are poorly understood. Recombinant systems for production of mitochondrial cytochromes *c* in *E. coli*, developed by Mauk and colleagues (38), have facilitated some progress in this regard (e.g., (39-41)) (see *SI Appendix*, Table S1). The N-terminal region of the apocytochrome *c* substrate (including the CXXCH motif) is important for recognition by *S. cerevisiae* HCCS (reviewed in (16)), and a few residues in this region have been identified as important for holocytochrome *c* maturation (42, 43). However, the features of the cytochrome *c* substrate that are recognized by the human HCCS have never been examined. Here, we report successful purification and characterization of the human holocytochrome c synthase from recombinant *E. coli*. The human HCCS is membrane associated and is purified with endogenous heme coordinated by conserved His154. We define the amino acids in the human cytochrome *c* that are required for holocytochrome *c* formation by HCCS, and we successfully convert a non-substrate cytochrome *c*, cytochrome c_2 from the alpha-proteobacterium *Rhodobacter capsulatus*, into a robust substrate for the human HCCS by introducing three sequence alterations. Finally, we report purification of trapped heme-containing complexes between cytochrome *c* and HCCS,

with heme ligands coming from His19 (of the CXXCH motif) in cytochrome *c* and His154 of HCCS. We show that mutation of either Cys in the conserved CXXCH motif of the cytochrome *c* leads to accumulation of trapped cytochrome *c*, with a single covalent attachment to the remaining cysteine, on the HCCS enzyme. Our results suggest mechanisms for heme binding, interaction with apocytochrome *c*, thioether formation, and a requirement for release of mature holocytochrome *c* from HCCS.

Results

Purified human HCCS contains heme.

Despite longstanding interest in HCCS, the enzyme has remained refractile to successful purification and biochemical characterization(e.g., (43-45)). To address this, we engineered the cDNA for the human HCCS in three different vectors (pET Blue-2 with an N-terminal His6 tag, pTXB1 with a C-terminal Intein fusion, and pGEX with an N-terminal GST fusion) for expression and purification in *E. coli*. Early attempts at purifying HCCS from cytoplasmic fractions were largely unsuccessful for each of the above constructs. However, upon fractionation of *E. coli* expressing GST-HCCS, we observed that the membrane fraction appeared to be enriched for a polypeptide of 57 kDa, the predicted molecular weight for the GST-HCCS fusion protein (*SI Appendix*, Fig S1). Thus, we directed our efforts towards purifying human HCCS from membranes, by solubilization in n-dodecyl β-D-maltopyranoside (DDM) (Fig 1A, B, C) or Triton X-100. Purified full-length GST-HCCS (~57 kDa) and three minor proteolytic products each reacted with GST antisera (Fig 1B, lane 9). Note that soluble (cytoplasmic) fractions contained mostly the degraded products and very low levels of full-length GST-HCCS (Fig 1B, lane 2). Densitometry analysis indicated that over 98 % of the purified, Coomassie-stained protein from the membrane fraction was GST-HCCS. Analysis by LC-MS/MS confirmed that the 57 kDa species was the GST-HCCS fusion protein (*SI Appendix*, Fig S2). To test the function of human HCCS, it was co-expressed with an arabinose-inducible gene encoding the human cytochrome *c*. Maturation of the 12 kDa holo-cytochrome *c* (Fig 1D) confirmed that the GST-HCCS fusion protein was active in heme attachment to cytochrome *c*

(see below). Approximately 3-4 mg of human holocytochrome *c* was produced per liter of *E. coli* culture.

Preparations of purified GST-HCCS were tinted red, and heme-staining revealed that full-length GST-HCCS contained heme (Fig 1C, lane 9). Heme proteins exhibit characteristic absorptions in the UV and visible regions of the spectrum, referred to as the α, β, and Soret bands. These spectral features can provide information about the identity of the axial ligands, and the spin and oxidation states of the heme iron (46). Purified human HCCS showed a Soret peak at 423 nm and three broad shoulders at 540 nm, 570 nm, and 660 nm (Fig 1E, black line). Longer wavelength Soret absorptions (like 423 nm) are often characteristic of hexacoordinate, reduced heme (Fe^{2+}) (46). Addition of the reducing agent sodium dithionite to purified GST-HCCS caused no shift in the Soret maximum. However, the Soret band sharpened (due to loss of its lower-wavelength shoulder) and absorbance increased, along with the appearance of small peaks at 559 nm and 530 nm (Fig 1E, red line). These spectral features, in combination with the 556 nm absorption in the reduced pyridine hemochrome spectrum (Fig 1E, inset) (47), are consistent with non-covalent, or *b*-type, heme. Since some heme remains with HCCS upon SDS-PAGE (Fig 1C), we cannot absolutely rule out the possibility that some heme may be covalently bound. However, our spectral results and the detection of variable amounts of free heme in heme stains lead us to favor that heme in HCCS is *b*-type. Addition of the oxidizing agent ammonium persulfate to purified GST-HCCS caused the Soret band to shift 13 nm to 410 nm, a wavelength typical of hexacoordinate, oxidized heme (Fe^{3+}), and diminished the shoulders at 540 nm, 570 nm, and 660 nm (Fig 1E, blue line). These observations suggest a mixture of oxidized heme and hexacoordinate, reduced heme in purified GST-HCCS.

To further interrogate the heme-binding environment in HCCS, exogenous imidazole was added to purified GST-HCCS and UV-Vis absorption spectra were recorded. Imidazole is the side-chain of histidine, and is often used to probe heme-ligand interactions in vitro (e.g., (48, 49)). Upon addition of 100 mM imidazole, the Soret peak shifted from 423 nm to 413 nm (Fig 1F, purple line). Subsequent addition of sodium dithionite to GST-HCCS in the presence of imidazole (Fig 1F, red line) caused a shift in the Soret from 413 nm to 422 nm, and resulted in the appearance of pronounced absorptions at 530 nm and 559 nm. These spectral features are hallmarks of hexacoordinate reduced heme with bis-His axial ligation but are rarely observed in hemes with His-Cys, His-Tyr, or His-Met axial ligation (50-52). These observations are consistent with at least one natural histidine axial ligand in HCCS, and an unknown axial ligand (possibly a small molecule) that can be replaced by exogenous imidazole.

His154 is a heme ligand in HCCS.

There are two histidines (His154 and His211 in human HCCS) conserved in HCCSs from a wide variety of organisms (*SI Appendix*, Fig S3). Given the established role of His residues as axial heme ligands, and our spectroscopic analyses of pure HCCS, we reasoned that one or both of these histidines might coordinate heme in HCCS. We engineered substitutions of each His residue and, to test the function of the resulting HCCS variants, co-expressed each with WT human cytochrome *c* in *E. coli* Δccm (Fig 2A, top panel). HCCS His154 is essential for heme attachment; mutation to Ala, Gly, or Tyr completely abolished synthesis of human holocytochrome *c* (Fig 2A, top panel, lanes 1-3). For His211, substitutions showed only minor effects on heme attachment (Fig 2A, top panel, lanes 5-8).

To further investigate the function of His154, we tested whether the cytochrome *c* assembly defect of the His154 mutants could be restored by addition of exogenous imidazole to *E. coli* culture. *In vivo* chemical complementation by imidazole has been used to correct the heme binding function of histidine mutants for recombinant myoglobin (53), and the cytochrome *c* synthetases CcsBA (54) and CcmF (55). Addition of 10 mM imidazole restored the cytochrome *c* assembly defects of the H154A and H154G HCCS mutants to approximately 40 % of WT levels (Fig 2A, bottom panel, lanes 1 and 2) but HCCS H154Y was not corrected (lane 3). This is consistent with our previous findings on correction of His mutants in CcmF (*55*), which showed that amino acids with bulkier side chains (like tyrosine) do not accommodate imidazole in the heme binding "cavity," and thus are not functionally complemented. For the His211 substitutions in HCCS, imidazole addition had no effect on cytochrome *c* assembly (Fig 2A, bottom panel, lanes 5-8). To directly test whether His154 was required for binding of heme to HCCS, we expressed and purified the non-functional GST-HCCS(H154A) (Fig 2B and C). GST-HCCS(H154A) was purified as a stable polypeptide with yields similar to the WT GST-HCCS, but GST-HCCS(H154A) contained no detectable heme by heme stain (Fig 2D, lane 9) or UV-Vis absorption spectroscopy (Fig 2E, orange line). We conclude that His154 is an axial ligand to the heme iron in HCCS.

Key determinants in human cytochrome *c* for maturation by the human HCCS.

To define the apocytochrome *c* substrate requirements of the human HCCS, we utilized the IPTG-inducible human GST-HCCS and a compatible, arabinose-inducible pBAD plasmid carrying the human cytochrome *c*. Based on previous studies with *S. cerevisiae* HCCS (see *SI Appendix*, Table S1) we focused on several conserved residues in the amino-terminus of the *H.*

sapiens cytochrome *c* (Lys6, Phe11, Cys15, Cys18, and His19; see Fig 3A, bolded residues). Throughout our report we refer to the initiation methionine of human cytochrome *c* as residue 1. Cell extracts of recombinant *E. coli* expressing both human HCCS and cytochrome *c* were assayed for covalent heme attachment (to human cytochrome *c*) by SDS-PAGE followed by heme stain (Fig3B, C) and UV-Vis absorption spectroscopy (Fig 3D). In the absence of HCCS, no holocytochrome *c* was detected by heme stain (Fig 3B, lane 10) or spectrally (Fig 3D, vector control). Co-expression of human HCCS and cytochrome *c* resulted in the production of a 12 kDa holocytochrome *c* (Fig 3B, lane 11) that showed a UV-Vis absorption spectrum consistent with covalent heme attachment, based on the typical α maximum at 550 nm (Fig 3D, WT). Replacement of Lys6 with Ala, Arg, or Asp did not impair maturation of human cytochrome *c* (Figs 3B, C, and D). Substitution of Phe11 with Ala impaired heme attachment to cytochrome *c* by approximately 75 % relative to WT under these conditions (Figs 3B and C). Human cytochrome c_1 contains a Tyr residue instead of the Phe at this position (Fig 3A); to test whether Tyr could substitute for Phe in human cytochrome *c*, we engineered a Tyr substitution at Phe11. Co-expression of the F11Y variant with human HCCS resulted in levels of heme attachment equal to WT cytochrome *c* (Fig 3B and C), and the peak at 550 nm in the UV-Vis absorption spectrum confirmed covalent heme attachment (Fig 3D). We also engineered substitutions at the two Cys residues and the single His residue of the CXXCH motif (Cys15, Cys18, and His19) in human cytochrome *c*. The C15S and C18A substitutions were matured at approximately 8 % and < 3 % of WT levels, respectively (Fig 3B and C). Substitution of Ala for His19 resulted in undetectable levels of cytochrome *c* (Fig 3B and C).

Our results with regard to the importance of Phe11 differ somewhat from two previous studies which showed that an F11A variant of cytochrome *c* was not detectably matured by *S. cerevisiae* HCCS in the *E. coli* cytoplasm (42, 43). This could be due to the broader substrate specificity of the human HCCS relative to the *S. cerevisiae* HCCS. In *S. cerevisiae*, there are two related homologs, HCCS and HCC_1S, that are dedicated to maturation of cytochrome *c* and cytochrome c_1, respectively, whereas in humans (and all animals), a single HCCS matures both the mitochondrial cytochrome *c* and cytochrome c_1.

Requirements for recognition of bacterial cytochromes *c* by the human HCCS.

Previous studies have shown that *S. cerevisiae* HCCS is unable to mature certain bacterial cytochromes *c* (44) despite the structural and functional similarities to the mitochondrial cytochrome *c* (*SI Appendix*, Fig S4). Recently, it was shown that a chimeric cytochrome *c* composed of the N-terminal 18 amino acids of yeast cytochrome *c* followed by the C-terminal region of cytochrome c_{550} from *Paracoccus denitrificans* (including the CXXCH motif from *P. denitrificans*) could be matured by *S. cerevisiae* HCCS (43). Using the *R. capsulatus* cytochrome c_2, where the methionine start codon of the human cytochrome *c* is the engineered initiation codon (Fig 4A), holo-cytochrome c_2 was not detected above background levels upon co-expression with the human HCCS (Fig 4B, lane 1). A notable difference between the N-terminal sequences of *R. capsulatus* cytochrome c_2 and human cytochrome *c* is the amino acid spacing between the conserved Phe (Phe11 in human cytochrome *c*) and the CXXCH motif (refer to boxed region in Fig 4A). To test whether a three-residue spacing is a requirement for recognition by human HCCS, we engineered an Ala insertion between Asn11 and Lys12 (human numbering) in *R. capsulatus* cytochrome c_2 and co-expressed it with the human HCCS (in *E. coli*

Δccm). Analysis of cell extracts by heme stain showed that cyt c_2(Ala-ins) was also not matured (Fig 4B, lane 3).

An additional difference between *R. capsulatus* cyt c_2 and human cytochrome *c* is the local charge in the region preceding the conserved Phe (Fig 4A); specifically, cytochrome c_2 contains two negatively charged Glu residues (Fig 4A, bolded residues). We engineered E8K and E10I substitutions in the WT cyt c_2 and the cyt c_2(Ala-ins) variant. Co-expression of cyt c_2(E8K/E10I/Ala-ins) with the human HCCS led to the production of high levels of a 13 kDa species with covalent heme (Fig 4B, lane 6; Fig 4D). Immunoblotting with cytochrome c_2 antisera confirmed that this covalent heme species was *R. capsulatus* cytochrome c_2 (Fig 4C, lane 7). UV-Vis absorption spectra confirmed covalent heme attachment to cyt c_2(E8K/E10I/Ala-ins) (Fig 4E). Approximately 1-2 mg of holocytochrome c_2(E8K/E10I/Ala-ins) was produced per liter of *E. coli* culture. By contrast, cyt c_2(E8K/E10I), containing its natural two-residue spacing between Phe11 and CXXCH, was not matured (Fig 4B, lane 2; Fig 4D). We also engineered each single Glu substitution into cyt c_2(Ala-ins) to generate cyt c_2(E8K/Ala-ins) and cyt c_2(E10I/Ala-ins), and although both cyt c_2(E8K/Ala-ins) and cyt c_2(E10I/Ala-ins) were matured at higher levels than WT cyt c_2 (Fig 4B, lanes 4 and 5; Fig 4D), neither was as high as the double substitution.

While our manuscript was in preparation, a report was published on the conversion of *R. capsulatus* cytochrome c_2 into a substrate for *S. cerevisiae* HCCS (56), with results that are consistent with our findings utilizing the human HCCS. In their study, a Lys insertion was engineered (instead of an alanine) and Glu10 was replaced with Leu (instead of Ile). Our results here indicate that positively charged and neutral residues at positions 8 and 10, respectively, and

proper spacing between Phe11 and CXXCH, constitute the minimal determinants for maturation by human HCCS. We describe evolutionary implications of these results in Supporting Information (see *SI Appendix*).

HCCS co-purifies with human cytochrome *c*.

To further investigate interactions between HCCS and the substrate cytochrome *c*, we co-expressed several of the human cytochrome *c* variants (F11A, C15S, C18A, H19A) or WT cytochrome *c* with the human HCCS and analyzed the soluble and membrane fractions. We noticed that the detergent-solubilized membrane fractions from cells expressing the C15S or the C18A cytochrome *c* variant (along with HCCS) had higher levels of holocytochrome *c* than the soluble fractions (see *SI Appendix*, Fig S5C and D, lanes 3, "L" fractions). Membrane fractions from cells expressing the WT, F11A or H19A variants of cytochrome *c* contained low levels of holocytochrome *c* (see *SI Appendix*, Fig S5A, B, E, lanes 3, "L" fractions).

To investigate whether the apparent membrane localization of the cytochrome *c* variants was related to the association of HCCS with the *E. coli* membrane, we purified GST-HCCS and analyzed each preparation for the presence of the human cytochrome *c*. In each case, GST-HCCS was purified from detergent-solubilized membranes as a stable polypeptide with minimal degradation (Fig 5A). In addition to the full-length GST-HCCS fusion protein (~57 kDa) we observed in the elution fraction a 12 kDa polypeptide of the molecular weight for cytochrome *c* (*SI Appendix*, Fig S6A). Analysis by LC-MS/MS (*SI Appendix*, Fig S7) and immunoblotting with cytochrome *c* antisera (Fig 5B) confirmed that cytochrome *c* co-purified with GST-HCCS. Table I quantifies the heme and apocytochrome bound in each complex, and summarizes the spectral properties of each complex. Heme staining after SDS-PAGE revealed that the WT

cytochrome *c* and each of the variants contained heme, although at very low levels for the H19A variant (Fig 5C). Covalent heme attachment to the 12 kDa cytochrome *c* was confirmed by retention of the heme through SDS-PAGE after boiling and treatment with 8 M urea (*SI Appendix*, Fig S8). HCCS complexes with C15S and C18A variants contained approximately 8-fold more heme than HCCS alone, and the WT, F11A, and H19A complexes contained approximately 4-fold more heme (Table 1, column C). Total heme in each complex was proportional to the amount of cytochrome *c* polypeptide bound in each complex (Table 1, column B), suggesting that the interaction of HCCS with heme is stabilized by the presence of the cytochrome *c* acceptor. To determine the role of heme in formation of the complex between HCCS and cytochrome *c*, we investigated whether HCCS(H154A), which is defective in heme binding (see Fig 2), co-purified with any of the cytochrome *c* variants. Purified HCCS(H154A) (Fig 5D) contained no detectable cytochrome *c* (Fig 5E) or heme (Fig 5F), just as HCCS(H154A) alone had no heme. The failure of HCCS(H154A) to co-purify with cytochrome *c* indicates that heme binding by HCCS (through His154) is a requirement for interaction with the apocytochrome *c*.

Spectral analyses of the HCCS:heme:cytochrome *c* complexes.

UV-Vis spectra were recorded on each of the purified complexes to gain additional insight into the heme:protein interactions within each complex. In the absence of residue His19 of apocytochrome *c* (i.e., the HCCS-H19A complex), the UV-Vis absorption spectrum is reminiscent of the spectrum of HCCS alone, with a Soret absorption at 425 nm and broad absorptions at 540 nm and 570 nm (Fig 5G, black line). Addition of the reducing agent sodium dithionite to the purified HCCS-H19A complex caused minor changes in the Soret peak and the

α-β region of the spectrum (Fig 5G, red line). To further probe ligand interactions in the HCCS-H19A complex, we added 100mM imidazole to purified HCCS-H19A and recorded spectra (Fig 5H, purple line). The effect of imidazole addition on heme in the HCCS-H19A complex was similar to that observed with HCCS alone, with a blue-shift in the Soret band to 418 nm. Upon addition of sodium dithionite to HCCS-H19A in the presence of imidazole, the Soret band shifted to 425 nm and pronounced α and β absorptions at 559 nm and 530 nm were observed (Fig 5H, red line). These results suggest that in the HCCS:heme:cytochrome *c*(H19A) complex, His154 of HCCS provides one axial ligand and that exogenous imidazole can occupy the second axial coordination site. In contrast, the spectra of each of the other complexes of cytochrome *c* with HCCS (Fig 5I; full spectra are shown in *SI Appendix*, Fig S9) were markedly different from that of HCCS alone, and imidazole caused no change in the spectra of these complexes (*SI Appendix*, Fig S10). We propose that, in the C15S, C18A, F11A, and WT complexes of cytochrome *c* with HCCS, heme is coordinated by His154 of HCCS and His19 of cytochrome *c*.

To analyze the heme environment in each complex (see Table 1, columns G, H, and I), we focused on the sodium dithionite-reduced absorptions in the α-β region of the spectrum (500 nm to 600 nm; see Fig 5I), which are diagnostic for covalent heme attachment and ligand interactions with the heme iron (46). The reduced spectrum of the HCCS-cytochrome *c*(WT) complex exhibited α and β maxima at 555 nm and 523 nm, respectively (Fig 5I, purple line). The complex of HCCS with the F11A variant of cytochrome *c* showed α and β absorptions at 552 and 524 nm (Fig 5I, orange line). The HCCS-C15S complex exhibited a unique and rare split α maximum (57) at 555-560 nm and a split β peak at 526-535 nm (Fig 5I, blue line). We note that a split α absorption has been observed at room temperature for heme in the CcmCDE

complex (58, 59), where, similarly, there is a single covalent attachment to a heme vinyl and bis-His coordination of the heme iron. The HCCS-C18A complex exhibited a strong α absorption at 561 nm and a β peak at 531 nm (Fig 5I, black line). For the C18A variant, since the α maximum was atypical for a *c*-type heme (i.e., 561 nm absorption; Fig 5I, black line) we confirmed covalent attachment of the heme group to the protein by mass spectrometry, where a trypsinized peptide corresponding to the heme binding motif of this variant plus covalent heme was detected (*SI Appendix*, Fig S11).

Thus, for each complex of cytochrome *c* with HCCS, there are signature absorptions in the reduced UV-Vis spectrum that are diagnostic for the specific heme-protein interactions of that complex. We note that the spectra of the complexes of HCCS with WT cytochrome *c* and the C15S variant are markedly different from the spectra that have been reported for released, mature WT holocytochrome *c* (41, 44) and site-directed variants of Cys15 (60, 61), respectively. This supports our contention that the spectra of the complexes are indeed reflective of interactions with the heme by both the HCCS and the cytochrome *c*. We propose that these complexes are isolated, trapped intermediates on the path to full maturation and release of the human cytochrome *c* by the human HCCS.

Discussion

Our results are discussed in the context of four distinct steps in the synthesis of holocytochrome *c* by the human HCCS: heme binding, apocytochrome *c* substrate recognition, thioether formation, and release of holocytochrome *c* (Fig 6A). We also address longstanding questions on the mechanisms of heme binding by HCCS and the roles of individual residues in both HCCS and the apocytochrome *c* substrate. A major conclusion is that heme is the central molecule mediating interaction between HCCS and apocytochrome *c*.

Step 1. Heme binding by HCCS.

The human HCCS is purified from membrane fractions as a full-length GST fusion protein with endogenous heme. Given that the function of HCCS is to covalently attach heme to apocytochrome *c*, heme binding by this enzyme has long been suspected (34, 36, 62) but has never been shown directly. Spectral studies provided insight into the HCCS heme-binding environment, suggesting that one ligand to the heme iron was a histidine and that the second axial coordination site was occupied by an unknown ligand that could be replaced by exogenous imidazole in vitro. Various approaches were used to demonstrate that residue His154 in HCCS was an axial ligand to the heme in HCCS (Fig 2). First, HCCS(H154A) did not purify with heme. Additionally, HCCS(H154A) was not functional in holocytochrome *c* synthesis, but activity was corrected in vivo by addition of exogenous imidazole. Finally, HCCS(H154A) did not form ternary complexes with heme and cytochrome *c* (Fig 5). We therefore conclude that it is the heme-bound form of HCCS to which apocytochrome *c* binds (see step 2).

Step 2. Recognition of apocytochrome *c* by HCCS:heme.

We undertook two approaches to define the substrate determinants in the apocytochrome *c* that the human HCCS requires for formation of a mature holocytochrome *c*. The first was to identify key residues in the N-terminus of the cognate human apocytochrome *c* that were required for holocytochrome formation, and the second was to convert a non-substrate bacterial cytochrome *c* (*R. capsulatus* cytochrome c_2) into a substrate for the human HCCS. For the human apocytochrome *c*, residues Phe11, Cys15, Cys18, and His19 were important (although to differing degrees) for optimal holocytochrome *c* maturation (Fig 3C). Maturation of cytochrome c_2 by HCCS required insertion of an Ala residue between Phe11 and Cys15 and substitution of Glu residues 8 and 10 (Fig 4). Predicted structures of the cytochrome c_2 N-terminus demonstrate that the Ala insertion significantly repositions Phe11 and the two Glu residues (*SI Appendix*, compare Fig S12A to B); therefore, both amino acid spacing and charge (*SI Appendix*, compare Fig S12A to C) are critical for heme attachment by HCCS. Fig 6B shows the predicted structure of the first twenty residues in the human apocytochrome *c*, with each of the critical determinants highlighted.

We gained remarkable insight into HCCS substrate recognition when we discovered that each human cytochrome *c* variant (F11A, C15S, C18A, H19A) co-purified with HCCS (Fig 5 and Table 1). Each of the HCCS:heme:cytochrome *c* complexes comprised a unique heme environment (Fig 5F), suggesting that each variant complex represented a distinct, intermediate in maturation. Thus, these variants are not defective in step 2 (recognition by and binding to HCCS:heme) but are defective in a later step in maturation, as described below. Our results are consistent with prior genetic studies in yeast, where a class of mutant apocytochromes *c* (including variants at Cys15, Cys18, and His19) were found to be competent for mitochondrial

import (in an HCCS-dependent manner), and therefore were still recognized by HCCS, but were not matured into holocytochromes *c* (63).

Fig 6C diagrams the central role of heme in the formation of the complex of HCCS (blue) with the apocytochrome *c* N-terminus (PEP-FOLD generated structure, green). Each complex of HCCS with apocytochrome *c* (including HCCS-H19A) contained more total heme than HCCS alone (Table 1, column C). This indicates that apocytochrome c binding stabilizes heme in the HCCS:heme:cytochrome *c* ternary complex (Fig 6A, step 2). His19 of the apocytochrome CXXCH supplies the 2nd axial ligand to heme iron in the complex with HCCS, and HCCS His154 provides the first (Fig 6C). This is suggested by spectral analyses of the HCCS:heme:cytochrome *c*(H19A) complex compared to those of the complexes with WT and other cytochrome *c* variants. That the HCCS:heme:cytochrome *c*(H19A) complex contained more total heme than HCCS alone further indicates that other residues in apocytochrome *c* (in addition to His19) likely interact with heme. The spectral features and biochemical characterization of these ternary complexes also inform us of the later steps in holocytochrome *c* synthesis.

Step 3. Formation of thioether bonds.

Each of the complexes of cytochrome *c* with HCCS contained at least WT-levels of covalent 12 kDa heme, with the exception of the H19A variant (Table 1, column D). While heme in the complex with HCCS was still stabilized by binding of cytochrome *c*(H19A) (Table 1, column C), thioether formation was very low for this variant. We conclude that His19 of CXXCH in the apocytochrome *c* is essential for efficient thioether formation. We propose that coordination of the heme iron by His19 in the HCCS:heme:cytochrome *c* complex positions the

two cysteines for stereospecific ligation to reduced (Fe^{2+}) heme, preparing it for thioether bond formation. This is consistent with the effect of exogenous imidazole on the heme environment in the HCCS:heme:cytochrome *c*(H19A) complex, as described in results (Fig 5H and I). The essential role of His19 in step 3 is further supported by the complete absence of released holocytochrome *c*(His19) (Table 1, column E; Fig 3B and C).

Holocytochromes C15S and C18A were bound to HCCS at steady-state levels two-fold higher than the WT holocytochrome *c* (Table 1, columns B and D). Since the levels of mature holocytochrome *c* were very low relative to WT (8 % for C15S and < 3 % for C18A), it appears that these variants are trapped in HCCS, unable to undergo release. Thus, covalent bond formation at both cysteines appears to be required for efficient release from HCCS. Interestingly, Wang and colleagues (1996) observed a class of mutant apocytochromes *c* (including variants in the Cys residues of CXXCH) whose expression inhibited the maturation of normal cytochrome *c* when co-expressed in *S. cerevisiae*. They speculated that this class of variant apocytochromes might be forming "dead-end" complexes with HCCS. Here, we show that the Cys variant apocytochromes are indeed bound in non-productive complexes with HCCS, consistent with the "dominant" cytochrome *c* variants observed in the aforementioned study. It is striking that the ratio of released to "trapped" WT cytochrome c is one hundred times higher (than the C18A variant), highlighting the consequences of thioether formation for full release and maturation. Additionally, that both the C15S and C18A single-cysteine complexes contained covalent heme suggests that there may not be a preferred order for thioether formation.

Step 4. Release of holocytochrome *c* from the complex.

In addition to the requirement for formation of two thioether bonds (step 3), optimal production of mature holocytochrome *c* requires a mechanism for release from HCCS (Fig 6A). A number of studies on mitochondrial import of apocytochrome *c* in whole yeast cells (30, 33, 63) and in isolated yeast mitochondria (31, 64) have concluded that apocytochrome residues important for heme attachment may only represent a subset of residues involved in mitochondrial import. Thus, there are likely multiple residues in the apocytochrome (in addition to Phe11, Cys15, Cys18, and His19) that mediate interaction with HCCS:heme. We propose that a dedicated release mechanism (step 4) is essential for the cognate human holocytochrome *c* because of multiple, stable interactions between HCCS:heme and the apocytochrome that are related to HCCS-mediated import of the apocytochrome *c* into the mitochondrion.

Binding of the human HCCS to its cognate cytochrome *c* in the ternary complex is surprisingly stable, as demonstrated by the fact that the HCCS:heme:cytochrome *c* complex can be purified (in the oxidized state) and maintained in vitro. We speculate that, in the cell, the proper milieu (e.g., reducing environment) promotes folding of the WT holocytochrome *c*, which provides the energy to release heme (and the holocytochrome) from the HCCS active site. Although we have not addressed the mechanisms in step 4 directly in our study, a rich history exists on the analysis of holocytochrome *c* folding in vitro, which is useful to consider here. For example, reduced cytochrome *c* (Fe^{2+}) shows a notable difference in folding relative to oxidized cytochrome *c* (Fe^{3+}), exhibiting greater stability towards denaturation (65). Even the binding of small axial ligands like carbon monoxide, which can replace the natural methionine axial ligand, has significant impacts on the folding and unfolding processes (66). Thus, the importance of reduced heme (Fe^{2+}) both for thioether formation and holocytochrome *c* release might be

considered for HCCS-mediated cytochrome *c* maturation. Possible factors involved in this reduction in mitochondria have been described (24). Release of holocytochrome *c* from the ternary complex clearly demands that HCCS axial ligand His154 be discharged from the heme iron (Fig 6C), which may be facilitated by interaction of the heme with other residues in the cytochrome *c* during folding. Although the second axial coordination site in mature holocytochrome *c* is occupied by Met81 (Fig 6D), there is ample evidence that this Met residue can be replaced and still yield mature cytochrome *c* (67). Therefore, other residues in cytochrome *c* may play a role, during folding, in displacing HCCS His154 from the heme. Besides a molecular understanding of the mechanisms underlying HCCS function, our study provides the foundation for future analyses of other key residues in the human HCCS and the cytochrome *c*, and the framework for delineating the steps in which those residues are involved.

Materials and Methods

Bacterial Growth Conditions. *Escherichia coli* strains (*SI Appendix*, Table S2) were grown at 37°C in Luria-Bertani broth (LB; Difco) supplemented with the appropriate antibiotics (Sigma-Aldrich) and other media additives at the following concentrations, unless otherwise noted: carbenicillin, 50 μg ml^{-1}; chloramphenicol, 20 μg ml^{-1}; isopropyl-β-D-thiogalactopyranoside (IPTG, Gold Biotechnology), 0.1 mM; arabinose (Gold Biotechnology), 0.2 % (w/v).

Protein Expression and Purification. For HCCS expression (with or without co-expression of cytochrome *c*), *E. coli* Δ*ccm* strain RK103 (68) or RK112 (69) was used. Starter cultures were initiated from a single colony and grown overnight at 37°C with shaking at 200 rpm in 100 mL of LB with the appropriate antibiotics. 1 L of LB was inoculated to 10 % and was grown with shaking at 120 rpm for 1 hr (OD_{600} < 1.0), at which point the culture was induced with 0.1 mM IPTG for pET Blue-2, pTXBI, or pGEX-based expression for 5 hr. For co-expression of pBAD-based cytochrome *c*, the culture was induced with 0.2 % arabinose (w/v) 3 hr after inoculation (2 hr after induction of HCCS expression) and grown 3 additional hr. Cells were harvested at 5,000 x g for 10 min and frozen at -80°C overnight. Cell pellets were thawed and resuspended in phosphate-buffered saline (100 mM NaCl, 7.5 mM Na_2HPO_4, 2 mM NaH_2PO_4) and treated with phenylmethanylsulfonylfluoride (PMSF, Sigma-Aldrich; 1 mM) and egg white lysozyme (Sigma-Aldrich; 100 μg ml^{-1}) for 30 min while shaking on ice. Cells were disrupted by repeated sonication for 30 sec bursts with a Branson 250 sonicator (50% duty, 60% output) until clearing of the suspension was observed. Crude sonicate was centrifuged at 24,000 x g for 15 min to clear cell debris, and membranes were isolated by centrifugation at 100,000 x g for 45 min. Membrane pellets were solubilized in a modified 1 x glutathione S-transferase (GST) buffer (150

mM NaCl, 50 mM Tris, pH 8; Pierce) with 1 % (w/v) n-dodecyl maltopyranoside (DDM, Anatrace) or Triton X-100 (Sigma-Aldrich) on ice for 1 hour. Detergent-solubilized membranes were centrifuged at 24,000 x g for 15 min to remove unsolubilized material. Solubilized membranes (L; load) were passed over glutathione agarose (Pierce) per the manufacturer's recommendations and washed in 1 x modified GST buffer with 0.02 % (w/v) DDM or Triton X-100. Bound GST-tagged protein was eluted in 1 x modified GST buffer containing 0.02 % (w/v) DDM or Triton X-100 and 20 mM reduced glutathione (E; elution). The purified protein was concentrated and subjected to buffer exchange in an Amicon Ultra Centrifugal Filter 30,000 MWCO (Millipore) after purification (called "EC"; concentrated elution). Total protein concentration was determined using the Bradford Reagent (Sigma-Aldrich) per the manufacturer's instructions and samples were measured with a PowerWave XS2 Microplate Spectrophotometer (BioTek).

Cytochrome Reporter and Imidazole Complementation Assays. Human holocytochrome *c* and *R. capsulatus* holocytochrome c_2 production were assayed in RK103 (68) harboring pGEX:GST-HCCS and one of the following pBAD-based plasmids (human cytochrome *c*: K6A, K6R, K6D, F11A, C15S, C18A, H19A, WT; *R. capsulatus* cytochrome c_2: c_2(WT), c_2(Ala-ins), c_2(E8K/Ala-ins), c_2(E10I/Ala-ins), c_2(E8K/E10I), c_2(E8K/E10I/Ala-ins); see Table S2). Cultures were grown at 37^{o}C with shaking at 200 rpm in 5 mL LB with appropriate antibiotics for 3 hr and induced for an additional 3 hr with 0.8 % arabinose (w/v) and 1 mM IPTG. Cells were harvested by centrifugation at 10,000 x g and the cell pellet was resuspended in 200 µL of BPER (Thermo Scientific) to lyse cells and extract protein. Total protein concentration was determined using the Nanodrop 1000 spectrophotometer (Thermo Scientific) and 100 µg was analyzed by SDS-PAGE

followed by heme stain. Imidazole complementation assays were performed in the same way with the exception that 10 mM imidazole (pH 7) was added to culture prior to inoculation.

Heme stains and other methods. Heme stains and immunoblots were performed as described in (70). BPER fractions were mixed 1:1 (v/v) with loading dye without reducing agents and boiled for 5 min and were separated by 12.5 % SDS-PAGE and transferred to Hybond C nitrocellulose membranes (GE Healthcare). Purified proteins (unboiled) were mixed 1:1 (v/v) with loading dye without reducing agents prior to separation by 12.5 % SDS-PAGE and transfer to nitrocellulose. Antiserum to human cytochrome *c* (Santa Cruz) was used at a dilution of 1:5000. Anti-GST antibody (Sigma-Aldrich) was used at a dilution of 1:10000. Protein A peroxidase (Sigma-Aldrich) was used as the secondary label. The chemiluminescent signal for heme stains and anti-cytochrome *c* immunoblots was developed with the SuperSignal Femto kit (Thermo Scientific), or the Immobilon Western kit (Millipore) for anti-GST immunoblots. Chemiluminescent signal was detected with the LAS-1000 Plus detection system (Fujifilm-GE Healthcare) or the ImageQuant LAS-4000 Mini detection system (Fujifilm-GE Healthcare). Heme concentration in purified preparations was determined by pyridine extraction as described in (47), heme stain as described in (71), or quantification of the indicated UV-Vis spectral absorptions. The relative abundances of purified GST-HCCS and co-purified human cytochrome *c* were quantified by densitometry analysis of the chemiluminescent signal from anti-GST and anti-cytochrome *c* immunoblots, respectively, and normalized to WT levels. Protein purity was assessed by Coomassie Blue staining of SDS-PAGE.

UV/Vis absorption spectroscopy. UV-Visible absorption spectra were recorded with a Shimadzu UV-2101 PC UV-Vis scanning spectrophotometer at room temperature as described in (54). All

spectra were recorded in same buffer in which the proteins were purified: 150 mM NaCl, 50 mM Tris pH 8, 0.02 % (wt/vol) DDM or Triton X-100. Chemical reduction and oxidation of samples was achieved by addition of several grains of sodium ditihionite (sodium hydrosulfite) or ammonium persulfate, respectively. To analyze the effect of imidazole on the electronic spectrum, small quantities of a concentrated imidazole solution (1 M, pH 7) were added to purified protein and spectra were recorded.

Three-dimensional models. Three-dimensional models of the N-terminus of human cytochrome *c* and the cytochrome c_2 variants from *Rhodobacter capsulatus* were generated by PEP-FOLD, an online resource for de novo three-dimensional peptide structure prediction (72, 73) (http://bioserv.rpbs.univ-paris-diderot.fr/PEP-FOLD). Each of the peptides shown represents the lowest energy conformation of the five structures generated by PEP-FOLD. X-ray crystal structures for *E. caballus* cytochrome *c* (pdb HRC1) and *R. capsulatus* cytochrome c_2 (pdb 1c2r) were obtained from the RCSB Protein Data Bank (http://www.rcsb.org/pdb/home/home.do).

Acknowledgements

We thank Huifen Zhu, John D'Allesandro, Cindy Richard-Fogal, Jing Jiang, Shalon Ledbetter, and the Bio437 class (Fall 2011) for technical contributions. We thank Dave Kranz for manuscript comments and Kenton Rodgers for comments on the spectra of purified HCCS. This study was supported by NIH R01 GM47909 to RGK.

References

(1) Seyfried, T. N., and Shelton, L. M. (2010) Cancer as a metabolic disease. *Nutr Metab (Lond) 7*, 7.

(2) Vos, M., Esposito, G., Edirisinghe, J. N., Vilain, S., Haddad, D. M., Slabbaert, J. R., Van Meensel, S., Schaap, O., De Strooper, B., Meganathan, R., Morais, V. A., and Verstreken, P. (2012) Vitamin K2 is a mitochondrial electron carrier that rescues pink1 deficiency. *Science 336*, 1306-10.

(3) Wang, X., Winter, D., Ashrafi, G., Schlehe, J., Wong, Y. L., Selkoe, D., Rice, S., Steen, J., LaVoie, M. J., and Schwarz, T. L. (2011) PINK1 and Parkin target Miro for phosphorylation and degradation to arrest mitochondrial motility. *Cell 147*, 893-906.

(4) Su, B., Wang, X., Zheng, L., Perry, G., Smith, M. A., and Zhu, X. (2010) Abnormal mitochondrial dynamics and neurodegenerative diseases. *Biochim Biophys Acta 1802*, 135-42.

(5) Nunnari, J., and Suomalainen, A. (2012) Mitochondria: in sickness and in health. *Cell 148*, 1145-59.

(6) Lange, C., and Hunte, C. (2002) Crystal structure of the yeast cytochrome bc1 complex with its bound substrate cytochrome c. *Proc Natl Acad Sci U S A 99*, 2800-5.

(7) Sun, F., Huo, X., Zhai, Y., Wang, A., Xu, J., Su, D., Bartlam, M., and Rao, Z. (2005) Crystal structure of mitochondrial respiratory membrane protein complex II. *Cell 121*, 1043-57.

(8) Tsukihara, T., Aoyama, H., Yamashita, E., Tomizaki, T., Yamaguchi, H., Shinzawa-Itoh, K., Nakashima, R., Yaono, R., and Yoshikawa, S. (1996) The whole structure of the 13-subunit oxidized cytochrome c oxidase at 2.8 A. *Science 272*, 1136-44.

(9) Dickerson, R. E., Takano, T., Eisenberg, D., Kallai, O. B., Samson, L., Cooper, A., and Margoliash, E. (1971) Ferricytochrome c. I. General features of the horse and bonito proteins at 2.8 A resolution. *J Biol Chem 246*, 1511-35.

(10) Hampsey, D. M., Das, G., and Sherman, F. (1988) Yeast iso-1-cytochrome c: genetic analysis of structural requirements. *FEBS Lett 231*, 275-83.

(11) Jiang, X., and Wang, X. (2004) Cytochrome C-mediated apoptosis. *Annu Rev Biochem 73*, 87-106.

(12) Kranz, R. G., Richard-Fogal, C., Taylor, J. S., and Frawley, E. R. (2009) Cytochrome c biogenesis: mechanisms for covalent modifications and trafficking of heme and for heme-iron redox control. *Microbiol Mol Biol Rev 73*, 510-28, Table of Contents.

(13) Sanders, C., Turkarslan, S., Lee, D. W., and Daldal, F. (2010) Cytochrome c biogenesis: the Ccm system. *Trends Microbiol 18*, 266-74.

(14) Sawyer, E. B., and Barker, P. D. (2012) Continued surprises in the cytochrome c biogenesis story. *Protein Cell 3*, 405-9.

(15) Stevens, J. M., Mavridou, D. A., Hamer, R., Kritsiligkou, P., Goddard, A. D., and Ferguson, S. J. (2011) Cytochrome c biogenesis System I. *Febs J 278*, 4170-8.

(16) Allen, J. W. (2011) Cytochrome c biogenesis in mitochondria--Systems III and V. *Febs J 278*, 4198-216.

(17) Hamel, P., Corvest, V., Giege, P., and Bonnard, G. (2009) Biochemical requirements for the maturation of mitochondrial c-type cytochromes. *Biochim Biophys Acta 1793*, 125-38.
(18) Beckman, D. L., Trawick, D. R., and Kranz, R. G. (1992) Bacterial cytochromes c biogenesis. *Genes Dev 6*, 268-83.
(19) Dumont, M. E., Ernst, J. F., Hampsey, D. M., and Sherman, F. (1987) Identification and sequence of the gene encoding cytochrome c heme lyase in the yeast Saccharomyces cerevisiae. *Embo J 6*, 235-41.
(20) Zollner, A., Rodel, G., and Haid, A. (1992) Molecular cloning and characterization of the Saccharomyces cerevisiae CYT2 gene encoding cytochrome-c1-heme lyase. *Eur J Biochem 207*, 1093-100.
(21) Bernard, D. G., Gabilly, S. T., Dujardin, G., Merchant, S., and Hamel, P. P. (2003) Overlapping specificities of the mitochondrial cytochrome c and c1 heme lyases. *J Biol Chem 278*, 49732-42.
(22) Dumont, M. E., Schlichter, J. B., Cardillo, T. S., Hayes, M. K., Bethlendy, G., and Sherman, F. (1993) CYC2 encodes a factor involved in mitochondrial import of yeast cytochrome c. *Mol Cell Biol 13*, 6442-51.
(23) Bernard, D. G., Quevillon-Cheruel, S., Merchant, S., Guiard, B., and Hamel, P. P. (2005) Cyc2p, a membrane-bound flavoprotein involved in the maturation of mitochondrial c-type cytochromes. *J Biol Chem 280*, 39852-9.
(24) Corvest, V., Murrey, D. A., Hirasawa, M., Knaff, D. B., Guiard, B., and Hamel, P. P. (2012) The flavoprotein Cyc2p, a mitochondrial cytochrome c assembly factor, is a NAD(P)H-dependent haem reductase. *Mol Microbiol 83*, 968-80.
(25) Prakash, S. K., Cormier, T. A., McCall, A. E., Garcia, J. J., Sierra, R., Haupt, B., Zoghbi, H. Y., and Van Den Veyver, I. B. (2002) Loss of holocytochrome c-type synthetase causes the male lethality of X-linked dominant microphthalmia with linear skin defects (MLS) syndrome. *Hum Mol Genet 11*, 3237-48.
(26) Schwarz, Q. P., and Cox, T. C. (2002) Complementation of a yeast CYC3 deficiency identifies an X-linked mammalian activator of apocytochrome c. *Genomics 79*, 51-7.
(27) Kiryu-Seo, S., Gamo, K., Tachibana, T., Tanaka, K., and Kiyama, H. (2006) Unique anti-apoptotic activity of EAAC1 in injured motor neurons. *Embo J 25*, 3411-21.
(28) Lill, R., Stuart, R. A., Drygas, M. E., Nargang, F. E., and Neupert, W. (1992) Import of cytochrome c heme lyase into mitochondria: a novel pathway into the intermembrane space. *Embo J 11*, 449-56.
(29) Steiner, H., Zollner, A., Haid, A., Neupert, W., and Lill, R. (1995) Biogenesis of mitochondrial heme lyases in yeast. Import and folding in the intermembrane space. *J Biol Chem 270*, 22842-9.
(30) Dumont, M. E., Cardillo, T. S., Hayes, M. K., and Sherman, F. (1991) Role of cytochrome c heme lyase in mitochondrial import and accumulation of cytochrome c in Saccharomyces cerevisiae. *Mol Cell Biol 11*, 5487-96.
(31) Dumont, M. E., Ernst, J. F., and Sherman, F. (1988) Coupling of heme attachment to import of cytochrome c into yeast mitochondria. Studies with heme lyase-deficient mitochondria and altered apocytochromes c. *J Biol Chem 263*, 15928-37.

(32) Nargang, F. E., Drygas, M. E., Kwong, P. L., Nicholson, D. W., and Neupert, W. (1988) A mutant of Neurospora crassa deficient in cytochrome c heme lyase activity cannot import cytochrome c into mitochondria. *J Biol Chem 263*, 9388-94.
(33) Nicholson, D. W., Hergersberg, C., and Neupert, W. (1988) Role of cytochrome c heme lyase in the import of cytochrome c into mitochondria. *J Biol Chem 263*, 19034-42.
(34) Nicholson, D. W., and Neupert, W. (1989) Import of cytochrome c into mitochondria: reduction of heme, mediated by NADH and flavin nucleotides, is obligatory for its covalent linkage to apocytochrome c. *Proc Natl Acad Sci U S A 86*, 4340-4.
(35) Barker, P. D., Ferrer, J. C., Mylrajan, M., Loehr, T. M., Feng, R., Konishi, Y., Funk, W. D., MacGillivray, R. T., and Mauk, A. G. (1993) Transmutation of a heme protein. *Proc Natl Acad Sci U S A 90*, 6542-6.
(36) Steiner, H., Kispal, G., Zollner, A., Haid, A., Neupert, W., and Lill, R. (1996) Heme binding to a conserved Cys-Pro-Val motif is crucial for the catalytic function of mitochondrial heme lyases. *J Biol Chem 271*, 32605-11.
(37) Moore, R. L., Stevens, J. M., and Ferguson, S. J. (2011) Mitochondrial cytochrome c synthase: CP motifs are not necessary for heme attachment to apocytochrome c. *FEBS Lett 585*, 3415-9.
(38) Pollock, W. B., Rosell, F. I., Twitchett, M. B., Dumont, M. E., and Mauk, A. G. (1998) Bacterial expression of a mitochondrial cytochrome c. Trimethylation of lys72 in yeast iso-1-cytochrome c and the alkaline conformational transition. *Biochemistry 37*, 6124-31.
(39) Patel, C. N., Lind, M. C., and Pielak, G. J. (2001) Characterization of horse cytochrome c expressed in Escherichia coli. *Protein Expr Purif 22*, 220-4.
(40) Rumbley, J. N., Hoang, L., and Englander, S. W. (2002) Recombinant equine cytochrome c in Escherichia coli: high-level expression, characterization, and folding and assembly mutants. *Biochemistry 41*, 13894-901.
(41) Jeng, W. Y., Chen, C. Y., Chang, H. C., and Chuang, W. J. (2002) Expression and characterization of recombinant human cytochrome c in E. coli. *J Bioenerg Biomembr 34*, 423-31.
(42) Kleingardner, J. G., and Bren, K. L. (2011) Comparing substrate specificity between cytochrome c maturation and cytochrome c heme lyase systems for cytochrome c biogenesis. *Metallomics 3*, 396-403.
(43) Stevens, J. M., Zhang, Y., Muthuvel, G., Sam, K. A., Allen, J. W., and Ferguson, S. J. (2011) The mitochondrial cytochrome c N-terminal region is critical for maturation by holocytochrome c synthase. *FEBS Lett 585*, 1891-6.
(44) Sanders, C., and Lill, H. (2000) Expression of prokaryotic and eukaryotic cytochromes c in Escherichia coli. *Biochim Biophys Acta 1459*, 131-8.
(45) Sanders, C., Wethkamp, N., and Lill, H. (2001) Transport of cytochrome c derivatives by the bacterial Tat protein translocation system. *Mol Microbiol 41*, 241-6.
(46) Falk, J. (1964) *Porphyrins and Metalloporphyrins: Their General, Physical and Coordination Chemistry, and Laboratory Methods*, Vol. 2, Elsevier Publishing Company, New York.
(47) Berry, E. A., and Trumpower, B. L. (1987) Simultaneous determination of hemes a, b, and c from pyridine hemochrome spectra. *Anal Biochem 161*, 1-15.

(48) Dawson, J. H., Andersson, L. A., and Sono, M. (1982) Spectroscopic investigations of ferric cytochrome P-450-CAM ligand complexes. Identification of the ligand trans to cysteinate in the native enzyme. *J Biol Chem 257*, 3606-17.
(49) Wang, W. H., Lu, J. X., Yao, P., Xie, Y., and Huang, Z. X. (2003) The distinct heme coordination environments and heme-binding stabilities of His39Ser and His39Cys mutants of cytochrome b5. *Protein Eng 16*, 1047-54.
(50) Egeberg, K. D., Springer, B. A., Martinis, S. A., Sligar, S. G., Morikis, D., and Champion, P. M. (1990) Alteration of sperm whale myoglobin heme axial ligation by site-directed mutagenesis. *Biochemistry 29*, 9783-91.
(51) Adachi, S., Nagano, S., Ishimori, K., Watanabe, Y., Morishima, I., Egawa, T., Kitagawa, T., and Makino, R. (1993) Roles of proximal ligand in heme proteins: replacement of proximal histidine of human myoglobin with cysteine and tyrosine by site-directed mutagenesis as models for P-450, chloroperoxidase, and catalase. *Biochemistry 32*, 241-52.
(52) Hildebrand, D. P., Ferrer, J. C., Tang, H. L., Smith, M., and Mauk, A. G. (1995) Trans effects on cysteine ligation in the proximal His93Cys variant of horse heart myoglobin. *Biochemistry 34*, 11598-605.
(53) Barrick, D. (1994) Replacement of the proximal ligand of sperm whale myoglobin with free imidazole in the mutant His-93-->Gly. *Biochemistry 33*, 6546-54.
(54) Frawley, E. R., and Kranz, R. G. (2009) CcsBA is a cytochrome c synthetase that also functions in heme transport. *Proc Natl Acad Sci U S A 106*, 10201-6.
(55) San Francisco, B., Bretsnyder, E. C., Rodgers, K. R., and Kranz, R. G. (2011) Heme ligand identification and redox properties of the cytochrome c synthetase, CcmF. *Biochemistry 50*, 10974-85.
(56) Verissimo, A. F., Sanders, J., Daldal, F., and Sanders, C. (2012) Engineering a prokaryotic apocytochrome c as an efficient substrate for Saccharomyces cerevisiae cytochrome c heme lyase. *Biochem Biophys Res Commun 424*, 130-5.
(57) Reddy, K. S., Angiolillo, P. J., Wright, W. W., Laberge, M., and Vanderkooi, J. M. (1996) Spectral splitting in the alpha (Q0,0) absorption band of ferrous cytochrome c and other heme proteins. *Biochemistry 35*, 12820-30.
(58) Richard-Fogal, C., and Kranz, R. G. (2010) The CcmC:heme:CcmE complex in heme trafficking and cytochrome c biosynthesis. *J Mol Biol 401*, 350-62.
(59) Richard-Fogal, C. L., Frawley, E. R., Bonner, E. R., Zhu, H., San Francisco, B., and Kranz, R. G. (2009) A conserved haem redox and trafficking pathway for cofactor attachment. *Embo J 28*, 2349-59.
(60) Tanaka, Y., Kubota, I., Amachi, T., Yoshizumi, H., and Matsubara, H. (1990) Site-directedly mutated human cytochrome c which retains heme c via only one thioether bond. *J Biochem 108*, 7-8.
(61) Rosell, F. I., and Mauk, A. G. (2002) Spectroscopic properties of a mitochondrial cytochrome C with a single thioether bond to the heme prosthetic group. *Biochemistry 41*, 7811-8.
(62) Tong, J., and Margoliash, E. (1998) Cytochrome c heme lyase activity of yeast mitochondria. *J Biol Chem 273*, 25695-702.
(63) Wang, X., Dumont, M. E., and Sherman, F. (1996) Sequence requirements for mitochondrial import of yeast cytochrome c. *J Biol Chem 271*, 6594-604.

(64) Sprinkle, J. R., Hakvoort, T. B., Koshy, T. I., Miller, D. D., and Margoliash, E. (1990) Amino acid sequence requirements for the association of apocytochrome c with mitochondria. *Proc Natl Acad Sci U S A 87*, 5729-33.
(65) Pascher, T., Chesick, J. P., Winkler, J. R., and Gray, H. B. (1996) Protein folding triggered by electron transfer. *Science 271*, 1558-60.
(66) Jones, C. M., Henry, E. R., Hu, Y., Chan, C. K., Luck, S. D., Bhuyan, A., Roder, H., Hofrichter, J., and Eaton, W. A. (1993) Fast events in protein folding initiated by nanosecond laser photolysis. *Proc Natl Acad Sci U S A 90*, 11860-4.
(67) Lu, Y., Casimiro, D. R., Bren, K. L., Richards, J. H., and Gray, H. B. (1993) Structurally engineered cytochromes with unusual ligand-binding properties: expression of Saccharomyces cerevisiae Met-80-->Ala iso-1-cytochrome c. *Proc Natl Acad Sci U S A 90*, 11456-9.
(68) Feissner, R. E., Richard-Fogal, C. L., Frawley, E. R., Loughman, J. A., Earley, K. W., and Kranz, R. G. (2006) Recombinant cytochromes c biogenesis systems I and II and analysis of haem delivery pathways in Escherichia coli. *Mol Microbiol 60*, 563-77.
(69) Richard-Fogal, C. L., San Francisco, B., Frawley, E. R., and Kranz, R. G. (2012) Thiol redox requirements and substrate specificities of recombinant cytochrome c assembly systems II and III. *Biochim Biophys Acta 1817*, 911-9.
(70) Feissner, R., Xiang, Y., and Kranz, R. G. (2003) Chemiluminescent-based methods to detect subpicomole levels of c-type cytochromes. *Anal Biochem 315*, 90-4.
(71) Richard-Fogal, C. L., Frawley, E. R., Feissner, R. E., and Kranz, R. G. (2007) Heme concentration dependence and metalloporphyrin inhibition of the system I and II cytochrome c assembly pathways. *J Bacteriol 189*, 455-63.
(72) Maupetit, J., Derreumaux, P., and Tuffery, P. (2009) PEP-FOLD: an online resource for de novo peptide structure prediction. *Nucleic Acids Res 37*, W498-503.
(73) Thevenet, P., Shen, Y., Maupetit, J., Guyon, F., Derreumaux, P., and Tuffery, P. (2012) PEP-FOLD: an updated de novo structure prediction server for both linear and disulfide bonded cyclic peptides. *Nucleic Acids Res 40*, W288-93.

Figures

Fig 1. Purified HCCS is a heme protein.

(A) Coomassie blue stain of purified GST-tagged HCCS showing 57 kDa full-length GST-HCCS. **(B)** anti-GST immunoblot of purified GST-tagged HCCS showing 57 kDa full-length GST-HCCS, 44 kDa GST-HCCS**, 32 kDa GST-HCCS*, and 29 kDa GST. **(C)** Heme stain of purified 57 kDa full-length GST-HCCS. For (A), (B), and (C) abbreviations are: CS, crude sonicate; S, soluble fraction; L, load (DDM-solubilized membranes); FT, flow through; W1, wash 1; W2, wash 2; W3, wash3; E, elution; EC, concentrated elution; M, molecular weight standards. **(D)** Heme stain of cytoplasmic extracts (BPER) showing synthesis of the human holocytochrome *c* as a function of HCCS expression and arabinose concentration. 12 kDa holocytochrome *c* is indicated by arrows. 100 μg of total protein was loaded in each lane. For (C) and (D), pre-stained molecular weight standards were overlaid in red onto the heme stains. **(E)** UV-visible absorption spectra of purified GST-HCCS (black line), reduced with sodium dithionite (red line), or oxidized with ammonium persulfate (blue line). Inset, sodium dithionite-reduced pyridine hemochrome spectrum of purified GST-HCCS from 500 nm to 600 nm. **(F)** UV-visible absorption spectra of purified GST-HCCS (black line), in the presence of imidazole (purple line), and in the presence of imidazole reduced with sodium dithionite (red line). For (E) and (F), the region from 500 nm to 700 nm has been multiplied by a factor of three. Absorption maxima are indicated by arrows.

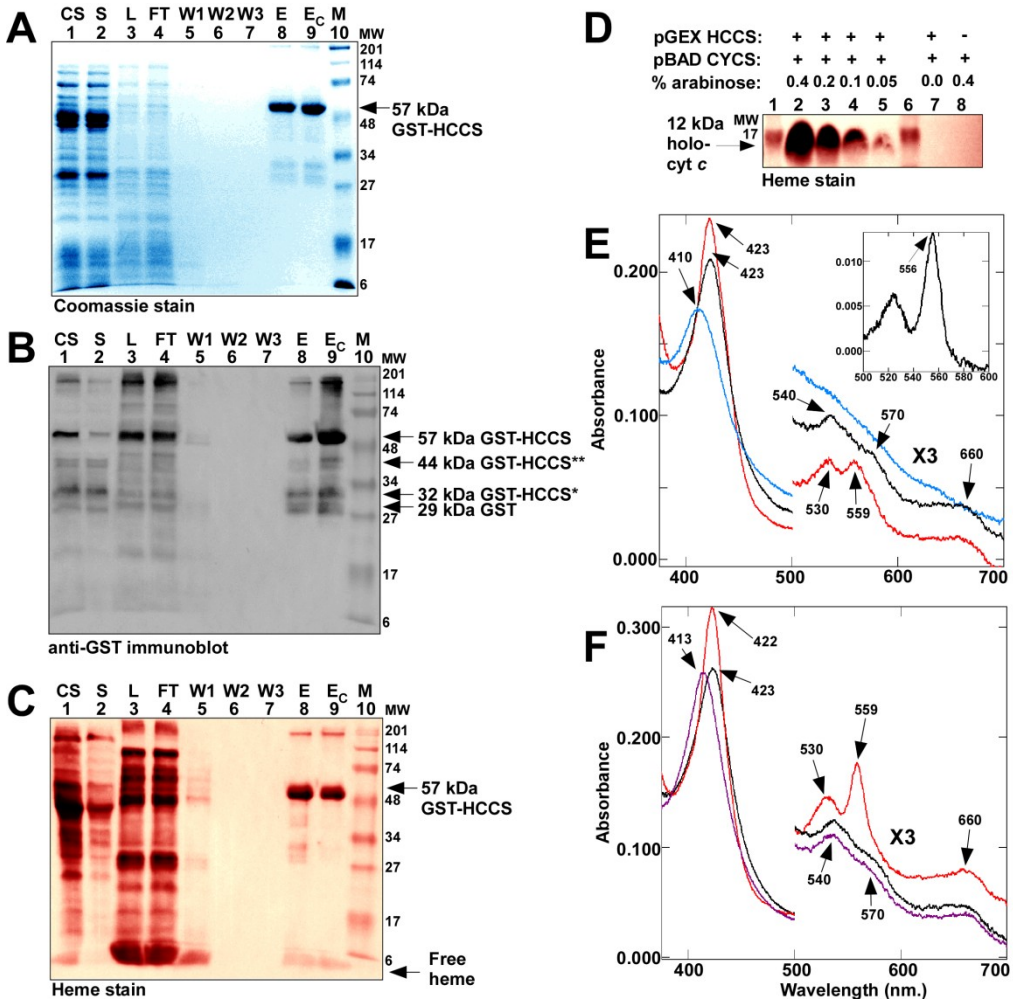
A
CS S L FT W1 W2 W3 E E$_C$ M
1 2 3 4 5 6 7 8 9 10
MW
201
114
74
57 kDa
GST-HCCS
48
34
27
17
6
Coomassie stain
B
CS S L FT W1 W2 W3 E E$_C$ M
1 2 3 4 5 6 7 8 9 10
MW
201
114
74
57 kDa GST-HCCS
48
44 kDa GST-HCCS**
34
32 kDa GST-HCCS*
29 kDa GST
27
17
6
anti-GST immunoblot
C
CS S L FT W1 W2 W3 E E$_C$ M
1 2 3 4 5 6 7 8 9 10
MW
201
114
74
57 kDa
GST-HCCS
48
34
27
17
6
Free
heme
Heme stain
D
pGEX HCCS: + + + + + -
pBAD CYCS: + + + + + +
% arabinose: 0.4 0.2 0.1 0.05 0.0 0.4
1 2 3 4 5 6 7 8
12 kDa
holo-
cyt c
MW
17
Heme stain
E
Absorbance
0.200
0.100
0.000
410
423
423
540
570
X3
660
530
559
400
500
600
700
0.010
0.005
0.000
556
500 520 540 560 580 600
F
Absorbance
0.300
0.200
0.100
0.000
413
422
423
559
530
X3
660
540
570
400
500
600
700
Wavelength (nm.)

Fig 2. HCCS His154 is a heme ligand.

(A) Heme stain of cell extracts (BPER) showing covalent 12 kDa holocytochrome c assembled by WT and site-directed mutants of HCCS in the *E. coli* cytoplasm in the absence (top panel) or presence (bottom panel) of 10 mM imidazole added to culture. His154 was changed to Ala (lane 1), Gly (lane 2), or Tyr (lane 3); His211 was changed to Ala (lane 5), Gly (lane 6), Tyr (lane 7), or Cys (lane 8). Additional labels: WT, wild type; VC, vector control, M, molecular weight standards. **(B)** Coomassie blue stain showing purified 57 kDa full-length GST-tagged HCCS(H154A). **(C)** anti-GST immunoblot showing 57 kDa full-length GST-tagged HCCS(H154A), 44 and 32 kDa degradation products, and 29 kDa GST. **(D)** Heme stain of purified 57 kDa full-length GST-HCCS. For (B), (C), and (D) abbreviations are as follows: CS, crude sonicate; S, soluble fraction; L, load (DDM-solubilized membranes); FT, flow through; W1, wash 1; W2, wash 2; W3, wash3; E, elution; EC, concentrated elution; M, molecular weight standards. For (A) and (D), pre-stained molecular weight standards were overlaid in red onto the heme stains. **(E)** UV-visible absorption spectra of purified GST-HCCS(H154A) (orange line), shown with the spectrum of purified GST-HCCS(WT) (black line).

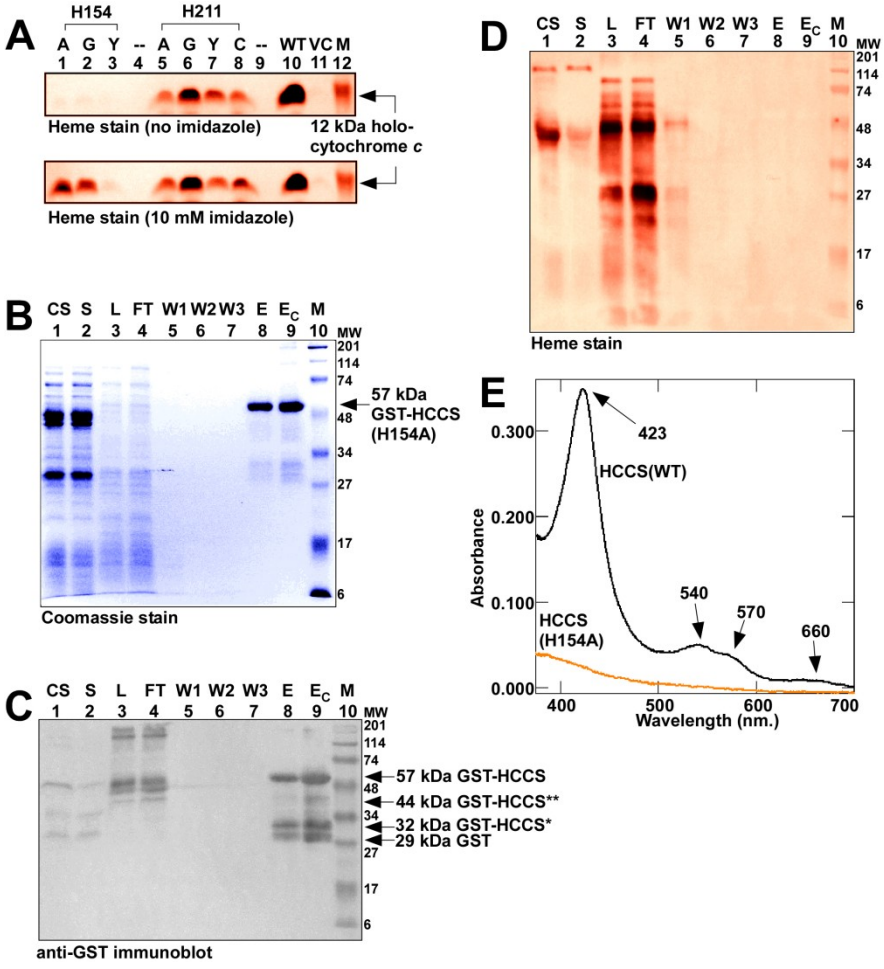
A
H154
H211
A G Y -- A G Y C -- WT VC M
1 2 3 4 5 6 7 8 9 10 11 12
Heme stain (no imidazole)
12 kDa holo-cytochrome c
Heme stain (10 mM imidazole)
B
CS S L FT W1 W2 W3 E EC M
1 2 3 4 5 6 7 8 9 10
MW
201
114
74
48
34
27
17
6
57 kDa GST-HCCS (H154A)
Coomassie stain
C
CS S L FT W1 W2 W3 E EC M
1 2 3 4 5 6 7 8 9 10
MW
201
114
74
48
34
27
17
6
57 kDa GST-HCCS
44 kDa GST-HCCS**
32 kDa GST-HCCS*
29 kDa GST
anti-GST immunoblot
D
CS S L FT W1 W2 W3 E EC M
1 2 3 4 5 6 7 8 9 10
MW
201
114
74
48
34
27
17
6
Heme stain
E
0.300
0.200
0.100
0.000
Absorbance
423
HCCS(WT)
540
570
660
HCCS (H154A)
400
500
600
700
Wavelength (nm.)

Fig 3. Maturation determinants in human cytochrome *c*.

(A) Amino acid sequence alignment of the region encompassing the heme attachment site (CXXCH) for the indicated cytochromes *c* and c_1. The amino acids mutated in this work are bolded and indicated by arrows; numbering begins at the N-terminal Met in *H. sapiens* cytochrome *c*. **(B)** Representative heme stain of BPER extracts showing synthesis of 12 kDa WT holocytochrome *c* and the indicated cytochrome *c* variants by the human HCCS; WT, wild type; VC, vector control, M, molecular weight standards. 100 μg of total protein was loaded in each lane. Pre-stained molecular weight standards were overlaid in red onto the heme stain. **(C)** Quantification of the results of heme staining of BPER extracts from three independent experiments. Percent heme attachment for each variant is relative to synthesis of WT cytochrome *c*, which has been set at 100 %. Error bars denote standard deviation. **(D)** UV-Vis absorption spectra of BPER extracts from cells expressing HCCS along with the indicated cytochrome *c* variant.

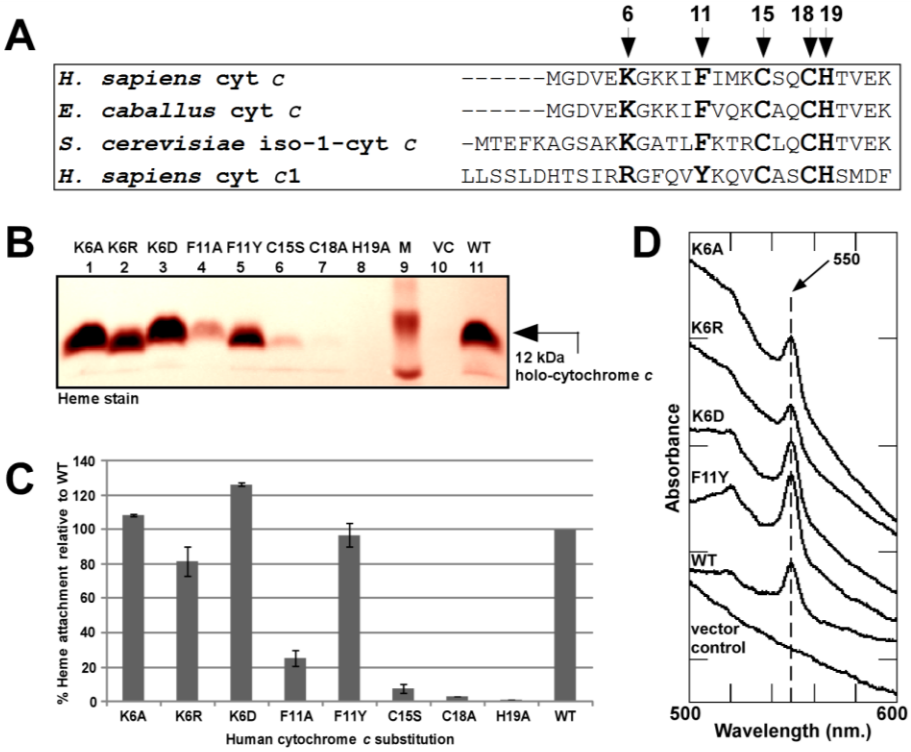
A
6
11
15
18 19
H. sapiens cyt c ------MGDVEKGKKIFIMKCSQCHTVEK
E. caballus cyt c ------MGDVEKGKKIFVQKCAQCHTVEK
S. cerevisiae iso-1-cyt c -MTEFKAGSAKKGATLFKTRCLQCHTVEK
H. sapiens cyt c1 LLSSLDHTSIRRGFQVYKQVCASCHSMDF
B
K6A K6R K6D F11A F11Y C15S C18A H19A M VC WT
1 2 3 4 5 6 7 8 9 10 11
12 kDa
holo-cytochrome c
Heme stain
C
% Heme attachment relative to WT
0 20 40 60 80 100 120 140
K6A K6R K6D F11A F11Y C15S C18A H19A WT
Human cytochrome c substitution
D
K6A
550
K6R
K6D
F11Y
WT
vector control
Absorbance
500
600
Wavelength (nm.)

Fig 4. Sequence requirements for maturation of bacterial cytochrome c_2.

(A) Amino acid sequence alignment of the N-terminal region (including CXXCH) for the indicated cytochromes *c* and cytochrome c_2 variants. The amino acids mutated in this work are bolded and indicated by arrows. The boxed region corresponds to the location of the Ala insertion; numbering refers to the *H. sapiens* cytochrome *c* N-terminal Met. **(B)** Representative heme stain and **(C)** anti-cytochrome c_2 immunoblot of BPER extracts showing synthesis of the indicated 12 kDa cytochrome c_2 variants; M, molecular weight standards. 100 μg of total protein was loaded in each lane. Pre-stained molecular weight standards were overlaid in red onto the heme stain. **(D)** Quantification of the results of heme staining of BPER extracts from three independent experiments. Percent heme attachment for each indicated variant is relative to synthesis of cytochrome c_2(E8K/E10I/Ala-ins), which has been set at 100 %. Error bars denote standard deviation. **(E)** UV-Vis absorption spectra of whole cell extracts expressing HCCS and the indicated cytochrome c_2 variant. Absorption maxima are indicated by arrows.

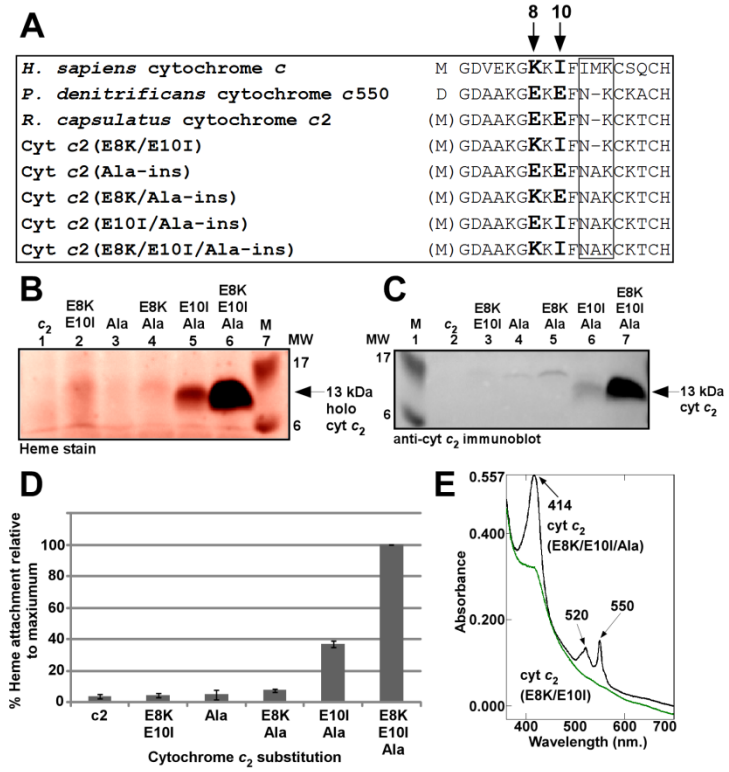
A
8 10
H. sapiens cytochrome c M GDVEKGKKIFIMKCSQCH
P. denitrificans cytochrome c550 D GDAAKGEKEFN-KCKACH
R. capsulatus cytochrome c2 (M) GDAAKGEKEFN-KCKTCH
Cyt c2(E8K/E10I) (M) GDAAKGKKIFN-KCKTCH
Cyt c2(Ala-ins) (M) GDAAKGEKEFNAKCKTCH
Cyt c2(E8K/Ala-ins) (M) GDAAKGKKEFNAKCKTCH
Cyt c2(E10I/Ala-ins) (M) GDAAKGEKIFNAKCKTCH
Cyt c2(E8K/E10I/Ala-ins) (M) GDAAKGKKIFNAKCKTCH
B
c2 E8K E10I Ala E8K Ala E10I Ala E8K E10I Ala M MW
1 2 3 4 5 6 7
17
6
13 kDa holo cyt c2
Heme stain
C
MW M c2 E8K E10I Ala E8K Ala E10I Ala E8K E10I Ala
17 1 2 3 4 5 6 7
6
13 kDa cyt c2
anti-cyt c2 immunoblot
D
% Heme attachment relative to maxiumum
100
80
60
40
20
0
c2 E8K E10I Ala E8K Ala E10I Ala E8K E10I Ala
Cytochrome c2 substitution
E
0.557
0.400
0.200
0.000
Absorbance
414
cyt c2 (E8K/E10I/Ala)
520
550
cyt c2 (E8K/E10I)
400 500 600 700
Wavelength (nm.)

Fig 5. Cytochrome *c* co-purifies with HCCS.

(A) Anti-GST immunoblot showing full-length 57 kDa GST-HCCS, **(B)** anti-cytochrome *c* immunoblot showing 12 kDa cytochrome *c*, and **(C)** heme stain showing 12 kDa holocytochrome *c*, from elution fractions of co-purifications of each cytochrome *c* variant with GST-HCCS(WT). **(D)** Anti-GST immunoblot showing full-length 57 kDa GST-HCCS, **(E)** anti-cytochrome *c* immunoblot, and **(F)** heme stain, from elution fractions of co-purifications of each cytochrome *c* variant with GST-HCCS(H154A). For (A)-(F), 5 μg of purified total protein was loaded in each lane. See Fig S6 for full panels. For (C) and (F), pre-stained molecular weight standards were overlaid in red onto the heme stains. **(G)** UV-visible absorption spectra of GST-HCCS co-purified with cytochrome *c*(H19A) (black line) and reduced with sodium dithionite (red line). **(H)** UV-visible absorption spectra of GST-HCCS co-purified with cytochrome *c*(H19A) (black line), in the presence of imidazole (purple line), and in the presence of imidazole reduced with sodium dithionite (red line). The region from 500 nm to 700 nm has been multiplied by a factor of three. **(I)** The α-β region showing the characteristic sodium dithionite-reduced UV-visible absorption spectrum for each indicated cytochrome *c* variant co-purified with GST-HCCS. Spectra have been offset for clarity. Absorption maxima are indicated by arrows.

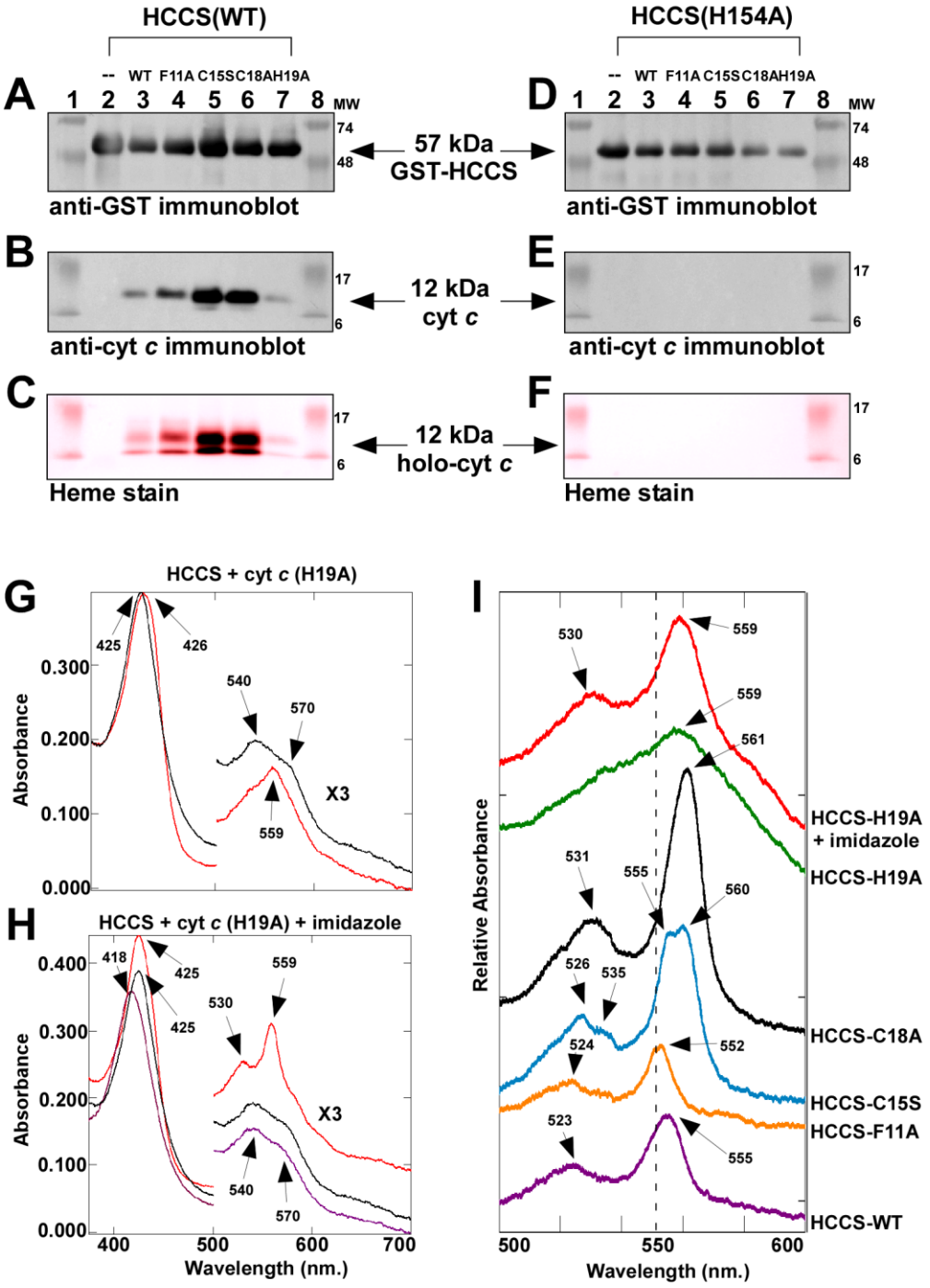
HCCS(WT)
HCCS(H154A)
-- WT F11A C15S C18A H19A
1 2 3 4 5 6 7 8 MW
74
48
57 kDa
GST-HCCS
anti-GST immunoblot
12 kDa
cyt c
anti-cyt c immunoblot
17
6
12 kDa
holo-cyt c
Heme stain
HCCS + cyt c (H19A)
HCCS + cyt c (H19A) + imidazole
Absorbance
Wavelength (nm.)
X3
Relative Absorbance
HCCS-H19A
+ imidazole
HCCS-H19A
HCCS-C18A
HCCS-C15S
HCCS-F11A
HCCS-WT

Fig 6. Steps in the maturation of cytochrome *c* by human HCCS.

(A) Diagram depicting the 4 steps in holocytochrome *c* maturation by HCCS (discussed in text). **(B)** PEP-FOLD generated model of the N-terminal 20 amino acid helix in human cytochrome *c* before interaction with HCCS. Amino acids important for maturation are indicated by arrows. Selected oxygen atoms are shown in red, nitrogens in blue, sulfurs in yellow, the heme macrocyle is in pink, and the Fe atom at the heme center is orange. **(C)** The HCCS:heme:cytochrome *c* complex (modeled with heme, pink) before thioether formation. Heme is coordinated by His19 of apocytochrome *c* (PEP-FOLD ribbon diagram, green, as in B) and His154 of HCCS (overlaid cartoon, blue). Amino acids and heme vinyls important for maturation are indicated by arrows. **(D)** The N-terminal 20 amino acids from the X-ray crystal structure of mature, released *E. caballus* holocytochrome *c* (pdb HRC1). Amino acids important for maturation are indicated by arrows. Heme is coordinated by His19, as in the complex with HCCS, and cytochrome *c* Met81, which replaces HCCS His154 in the folded, released holocytochrome *c*. PyMOL was used for displays in B, C, and D. Amino acid numbering refers to the *H. sapiens* cytochrome *c* N-terminal Met, as shown in Fig 3A (because the initiation Met is processed off, pdb HRC1 refers to Lys8 as Lys7, His19 as His18, Met81 as Met80, etc).

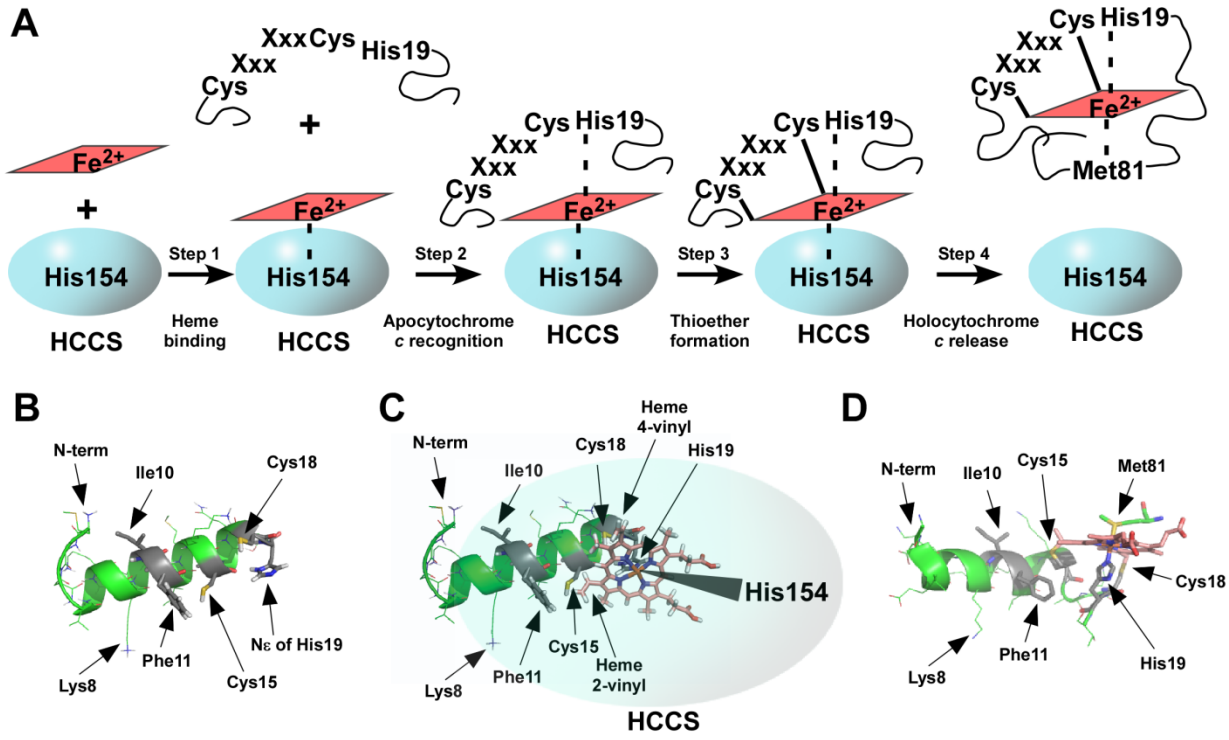
A
Xxx Cys
Xxx
Cys
His19
+
Fe2+
+
His154
HCCS
Step 1
Heme binding
Step 2
Apocytochrome c recognition
Step 3
Thioether formation
Step 4
Holocytochrome c release
Cys His19
Met81
B
N-term
Ile10
Cys18
Nε of His19
Phe11
Cys15
Lys8
C
Heme 4-vinyl
His154
Heme 2-vinyl
D

Table 1. Characterization of the complexes of HCCS with cytochrome *c*

	A	B	C	D	E	F	G	H	I
	GST-HCCS levels[1]	**CYCS bound (in complex)[1]**	**Total heme (in complex)[2]**	**Covalent 12 kDa heme (in complex)[3]**	**Released holo-cyt *c*[3]**	**Reduced α band absorption[4]**	**2nd heme axial ligand[5]**	**1st heme axial ligand[5]**	**Thioether bond formation[5]**
HCCS alone	1.01 ± 0.04	--	0.27 ± 0.09	--	--	559	HCCS His154	Unknown	None
HCCS + cyt *c*(WT)	1	1	1	1	1	555	HCCS His154	cyt *c* His19	Cys15-2-vinyl Cys18-4-vinyl
HCCS + cyt *c*(F11A)	1.03 ± 0.14	0.94 ± 0.14	0.83 ± 0.13	1.02 ± 0.02	0.25 ± 0.05	552	HCCS His154	cyt *c* His19	Cys15-2-vinyl Cys18-4-vinyl
HCCS + cyt *c*(C15S)	1.00 ± 0.11	2.07 ± 0.10	1.84 ± 0.01	2.22 ± 0.24	0.08 ± 0.03	555/560 split	HCCS His154	cyt *c* His19	Cys18-4-vinyl
HCCS + cyt *c*(C18A)	0.98 ± 0.16	1.97 ± 0.07	1.93 ± 0.08	2.24 ± 0.36	0.03 ± 0.01	561	HCCS His154	cyt *c* His19	Cys15-2-vinyl
HCCS + cyt *c*(H19A)	1.00 ± 0.15	0.83 ± 0.02	0.89 ± 0.01	0.25 ± 0.10	Not detected	559	HCCS His154	Unknown	Cys15-2-vinyl Cys18-4-vinyl
Mature cyt c (WT)	--	--	--	--	--	550	Met80	His19	Cys15-2-vinyl Cys18-4-vinyl

Each value is relative to the complex of HCCS with WT cytochrome *c*, which has been set at 1, and is based on at least three separate experiments.

[1] The amount of GST-HCCS and CYCS protein in each complex was calculated by densitometry analysis of the chemiluminescent signal from anti-GST and anti-cytochrome *c* immunoblots, respectively.

[2] Total heme in each complex was calculated from the Soret absorption in the UV-Vis absorption spectrum and adjusted for total protein concentration.

[3] Covalent 12 kDa heme in each complex and released holocytochrome *c* in BPER fractions were calculated by densitometry analysis of the chemiluminescent signal from heme stains.

[4] The reduced α absorption (nm.) for each complex is from the UV-Vis absorption spectrum in the presence of sodium dithionite.

[5] The axial ligands to the heme in each complex and thioether formation between the Cys residues in the cytochrome *c* and the heme vinyls are based on experimental data shown here.

Supporting Information

*for **PNAS***

Classification – Major: Biological Sciences

Classification – Minor: Biochemistry

Supporting Information

The human mitochondrial holocytochrome *c* synthase's heme binding, maturation determinants, and complex formation with cytochrome *c*

Brian San Francisco, Eric C. Bretsnyder, Robert G. Kranz

Department of Biology, Washington University in St. Louis, St. Louis, MO 63130, USA.

Address correspondence to: Robert Kranz, Department of Biology, Washington University in St. Louis, Campus Box 1137, One Brookings Drive, St. Louis, MO 63130, USA. Tel: +1 (314) 935-4278, E-mail: kranz@biology.wustl.edu

Key Words

CCHL, cytochrome *c*, HCCS, heme, mitochondria

Supporting Materials and Methods

Construction of strains and plasmids. All oligonucleotide primer sequences, plasmids, and strains are given in Supplemental Table 2. *E. coli* strains TB1 and HB101 were used as host strains for cloning. To generate N-terminal hexahistidine-tagged HCCS, the human HCCS gene was PCR amplified from a cDNA clone (Origene) as described previously (1), digested, and ligated into the NcoI and HindIII sites in pET Blue-2 (EMD Biosciences) to generate pRGK402. To generate N-terminal GST-tagged HCCS, the human HCCS gene was PCR amplified from pRGK402, digested and ligated into the EcoRI and XhoI sites in pGEX 4T-1 (GE Healthcare) to generate pRGK403. To generate C-terminal Intein-tagged HCCS, the human HCCS gene was PCR amplified from pRGK402, digested, and ligated into the NdeI and SapI sites in pTXB21 (NEB) to generate pRGK404. The human cytochrome *c* gene (CYCS) was PCR amplified from cDNA clone MGC12367 (ATCC), digested, and ligated into the EcoRI and PstI sites in pRGK330 (2) to generate pRGK405. The cytochrome c_2 gene from *Rhodobacter capsulatus* (CYCA) was PCR amplified from pRGK389 (1), with an engineered initiation codon to exclude the native periplasmic signal sequence as depicted in Figure 4, digested, and ligated into the NcoI and XbaI sites of pRGK330 (2) to generate pRGK406. All nucleotide substitutions and insertions were engineered using the QuikChange I Site-Directed Mutagenesis Kit (Agilent Technologies) per the manufacturer's recommendations, and oligonucleotides were synthesized by Sigma-Aldrich. Each of the final constructs was sequenced to verify the mutation(s).

Proteomics analysis. Identification of GST-HCCS and co-purified cytochrome *c* was achieved by ESI-MS by the Donald Danforth Plant Science Center Proteomics and Mass Spectrometry Facility. Briefly, Coomassie-blue stained bands corresponding to 57 kDa GST-HCCS and the co-purified 12 kDa cytochrome *c* for the WT, C15S, and C18A variants were excised, washed

and digested with trypsin overnight. Tryptic peptides were run on a 1hr gradient LC-MS/MS using an LTQ-Orbitrap. The data was searched using Scaffold (for GST-HCCS) or Mascot (for the cytochrome *c* variants) against a custom database including the sequences provided for each of the cytochrome *c* variants and the following variable modifications: deamidation on Asn and Glu, pyroglutamate formation, glutathione and heme on Cys, and Met oxidation. To confirm covalent heme attachment to the C18A variant of cytochrome *c*, the 12 kDa band corresponding to cytochrome *c* was excised, washed, and digested with trypsin overnight as described in (3). Digested samples were subjected to matrix-assisted laser desorption ionization time-of-flight (MALDI-TOF) using an IonSpec ProMALDI FT-MS 7.4 T mass spectrophotometer by the Washington University in St. Louis NCRR Mass Spectrometry Facility.

Supporting Figure Legends

Figure S1. Full-length GST-HCCS localizes largely to the membrane. Anti-GST immunoblot showing cleared sonicate (CS), soluble (S) and DDM-solubilized membrane (M) fractions from *E. coli* cells expressing N-terminal GST-tagged HCCS. Note the increase in full-length 57 kDa GST-HCCS in the DDM-solubilized membrane fraction (M, lane 3) relative to the soluble fraction (S, lane 2).

Figure S2. Identification of purified human HCCS by mass spectrometry. The results of LC-MS/MS on trypsin-digested, full-length 57 kDa GST-HCCS. 23 unique peptides were identified corresponding to human HCCS covering 57 % of the HCCS protein sequence. The sequence of each unique peptide along with the modification and the mass (in Daltons) is given.

Figure S3. Multiple sequence alignment of HCCS and HCC_1S genes from *Homo sapiens*, *Saccharomyces cerevisiae*, *Mus musculus*, *Caenorhabditis elegans, Drosophila melanogaster, Plasmodium falciparum*, *Dictyostelium discoideum*, *Volvox carteri, Chlamydomonas reinhardtii*, and *Neurospora crassa*. Two histidine residues (boxed, arrows), His154 and His211 in the human HCCS, are completely conserved.

Figure S4. The X-ray crystal structures of **(A)** *E. caballus* cytochrome *c* (pbd HRC1) and **(B)** *R. capsulatus* cytochrome c_2 (pdb 1c2r) exhibit similar three-dimensional folding (4). Selected oxygen atoms are shown in red, nitrogens in blue, sulfurs in yellow, the heme macrocyle is in pink, and the Fe atom at the heme center is orange. Note the similar three-dimensional localization of the indicated residues (arrows) with respect to the heme group in the two structures. With the exception of *R. capsulatus* cytochrome c_2 Met95, amino acid designations in (A) and (B) refer to the *H. sapiens* cytochrome *c* N-terminal Met, as in Fig 3 and 4A (even though the initiation Met is cleaved off). PyMOL was used for displays.

Figure S5. Human cytochrome *c* variants co-purify with GST-HCCS. Heme stains showing the co-purification of each cytochrome *c* variant (WT, F11A, C15S, C18A, and H19A) with GST-HCCS. CS, cleared sonicate; S, soluble fraction; L, load (detergent-solubilized membranes); W1-W3, wash 1-wash 3; E, elution; M, molecular weight standards. In all cases, 12 kDa cytochrome *c* co-purified with HCCS (E, lanes 7). 12 kDa holocytochrome *c* is indicated by arrows. Note the abundance of holocytochrome *c* in the detergent-solubilized membrane fractions (L, lanes 3) and in the subsequent purified elution fractions (E, lanes 7) for the C15S and C18A variants relative to that in the soluble fractions (S, lanes 2). Relative levels of holocytochrome *c* bound to HCCS are shown in Fig 5A and quantified in Table 1.

Figure S6. Analysis of GST-HCCS and co-purified human cytochrome *c*. (A) Coomassie stain showing concentrated elution fractions for each of the complexes of HCCS with cytochrome *c*. Full-length 57kDa GST-HCCS and the co-purified 12 kDa cytochrome *c* variants are indicated by arrows. Note the abundance of the C15S and C18A variants relative to the WT, F11A, and H19A variants, quantified in Table 1. (B) Coomassie stain, (C) anti-GST immunoblot, and (D) heme stain showing a representative co-purification of a cytochrome *c* variant (C18A) with GST-HCCS. Note the absence of the 12 kDa cytochrome *c* in the wash fractions of the heme stain

(panel D, lanes 5-7), indicative of a stable interaction between the co-purified cytochrome *c* and HCCS.

Figure S7. Identification of co-purified cytochrome *c* by mass spectrometry. The results of LC-MS/MS identifying WT, C15S, and C18A variants of cytochrome *c* co-purified with GST-HCCS. These data confirmed that the 12 kDa species co-purified with HCCS were variants of human cytochrome *c*. The sequence of each unique peptide along with the modification and the mass (in Daltons) is given.

Figure S8. Heme is stably attached (covalent) to the co-purified cytochrome *c*. Anti-GST immunoblot, anti-cytochrome *c* immunoblot, and heme stain of purified elution fractions for each cytochrome *c* variant co-purified with HCCS(WT) comparing unboiled samples (lanes 2-7) to those boiled and treated with 8 M urea (lanes 9-14). The full-length 57 kDa GST-HCCS and 12 kDa cytochrome *c* (apo- and holo- forms) are indicated by arrows. Boiling and treatment with 8 M urea did not remove the heme from the co-purified cytochrome *c* variants, suggesting that heme binding to cytochrome *c* in the complex with HCCS is covalent.

Figure S9. Spectroscopic analyses of the indicated HCCS:heme:cytochrome *c* complexes. UV-Vis absorption spectra (360 nm-700 nm) for the complexes of HCCS with (A) WT, (B) F11A, (C) C15S, and (D) C18A cytochrome *c* variants. Maxima are indicated by arrows, and the region from 500 nm to 700 nm has been multiplied by a factor of three.

Figure S10. Spectroscopic analyses of the indicated HCCS:heme:cytochrome *c* complexes in the presence of imidazole. UV-Vis absorption spectra (360 nm-700 nm) for the complexes of HCCS with (A) WT, (B) F11A, (C) C15S, and (D) C18A cytochrome *c* variants in the presence of imidazole (100 mM). Imidazole addition did not alter the spectra of any complex of HCCS with cytochrome *c*, with the exception of the H19A variant (Figure 5B). Maxima are indicated by arrows, and the region from 500 nm to 700 nm has been multiplied by a factor of three.

Figure S11. Heme is covalently attached to the HCCS-co-purified cytochrome *c*(C18A) variant. The results of MALDI-TOF mass spectrometry on trypsin-digested 12 kDa C18A cytochrome *c* variant co-purified with HCCS. The peak corresponding to the species with mass of 1617.381 Daltons was within 0.3 Daltons of the calculated neutral monoisotopic mass predicted for a covalent heme-containing peptide of the mutated heme binding motif in the C18A variant of cytochrome *c* (CSQAHTVEK). The presence of this species indicates that heme is bound covalently to the C18A variant of cytochrome *c* (through Cys15) in the complex with HCCS.

Figure S12. Predicted structural outcomes of the *R. capsulatus* cytochrome c_2 variants engineered in this study. Comparison of the PEP-FOLD-generated three-dimensional structures of the N-termini (19-20 residues) of (A) WT *R. capsulatus* cytochrome c_2 (B) cyt c_2(Ala-ins) and (C) cyt c_2(E8K/E10I/Ala-ins). Selected oxygen atoms are shown in red, nitrogens in blue, and sulfurs in yellow. Each structure has been oriented such that residue Cys15 is in the same position. Amino acids important for maturation are indicated by arrows. For clarity, amino acid designations refer to the *H. sapiens* cytochrome c N-terminal Met. Neither WT cyt c_2 nor cyt c_2(Ala-ins) were detectably matured by human HCCS, while cyt c_2(E8K/E10I/Ala-ins) was a

robust substrate for the human HCCS. Note the shift in orientation of E8, E10, and F11 in (B) as a result of the insertion of an Ala residue. Also note that in each case, residue His19 was not part of the predicted helix, suggesting that it may have some flexibility, possibly related to its function as a ligand to the heme in HCCS.

Comment on the evolutionary implications of cytochrome c_2 maturation by human HCCS.

The evolution of the HCCS enzyme occurred after the endosymbiotic event that led to the eukaryotic mitochondrion. This is supported by the fact that the mitochondria of some eukaryotes (e.g., all plants and some protozoa) have retained CCM for the synthesis of *c*-type cytochromes. CCM is utilized by alpha proteobacteria, which are the ancestors of the eukaryotic mitochondrion. CCM is "promiscuous" with regard to substrate specificity, requiring little else than the conserved CXXH heme binding motif for recognition and heme attachment. Most alpha proteobacterial cytochromes *c* (~90 %, or 173 out of 200 analyzed) have a two-residue spacing between conserved Phe and the CXXCH motif. However, for all major groups of alpha proteobacteria, there are some cytochromes *c* with a three-residue spacing, and some that lack the Phe altoghether. Thus, there is not a strictly conserved N-terminal architecture in the alpha proteobacterial cytochromes *c*, which is not unexpected given the flexible substrate requirements of CCM (e.g., Phe is not a requirement for CCM recognition and heme attachment). Indeed, the fact that 90 % of the alpha proteobacteria have retained any conservation of N-terminal architecture (other than CXXCH) is surprising, and may reflect the importance of the conserved Phe, for example, in cytochrome *c* function(s) post-maturation by CCM.

By contrast, all eukaryotic mitochondrial cytochromes *c*, regardless of whether they are matured by CCM or HCCS, contain a conserved N-terminal architecture that consists of a three-residue spacing between conserved Phe (F11) and the CXXCH motif. Although the conservation of this architecture in the CCM-containing mitochondria is surprising, the fact that all HCCS-containing mitochondria possess cytochromes *c* with a three-residue spacing supports the idea that HCCS evolved with this specific architecture, and it is now "locked" into using it for attaching heme to its substrate. Furthermore, the conservation of N-terminal architecture in cytochromes *c* throughout eukarya suggests that the three-residue spacing may have originated in the cytochrome *c* of the mitochondrial progenitor. Consequently, the three-residue spacing is now embedded as part of the specificity determinants for recognition and maturation by HCCS. Animal HCCSs, like the human HCCS studied here, are less discriminatory, recognizing motifs within cytochrome *c* and cytochrome c_1 (e.g., such that Tyr11 can replace Phe11).

It is of note that the organisms from the Euglenozoa phylum, for which no cytochrome *c* assembly system has been discovered, contain cytochromes *c* with this same conserved N-terminal architecture (although lacking the first Cys of the heme binding motif). Allen and colleagues (5) have shown that a Euglenozoa (*T. brucei*) cytochrome *c* is matured by yeast HCCS in *E. coli* at very low levels (less than 1 % WT), even when the cytochrome has been engineered to contain the first Cys of the heme binding motif. *T. brucei* cytochrome *c* has the equivalent of Glu8 (as in *R. capsulatus* cytochrome c_2-see Figure 4), which might explain the low levels of maturation, but this has not been explored.

Figure S1

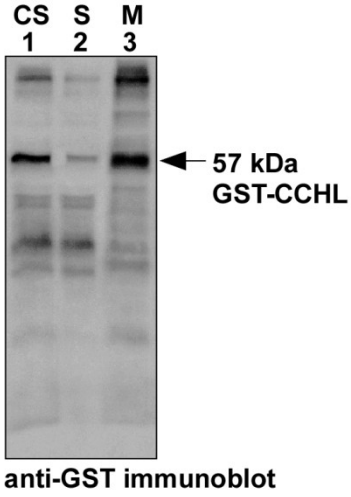

Figure S2

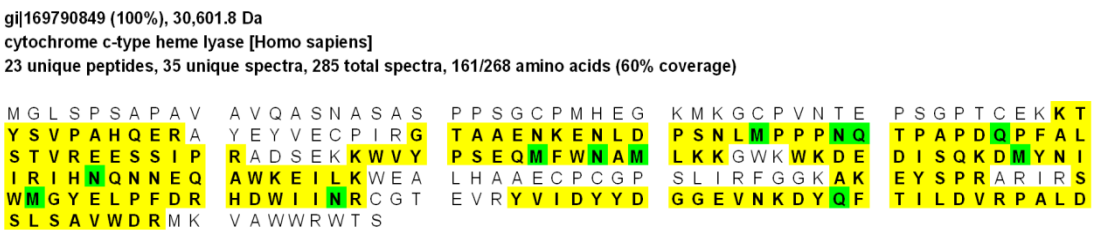

Sequence	Modifications	Observed	Actual Mass	Start	Stop
(K)DEDISQKDMYNIIR(I)		580.6139	1,738.82	139	152
(K)DEDISQKDmYNIIR(I)	Oxidation (+16)	585.9449	1,754.81	139	152
(K)DEDISQKDmYNIIR(I)	Oxidation (+16)	878.4138	1,754.81	139	152
(K)DEDISQKDMYNIIR(I)		870.4168	1,738.82	139	152
(K)ENLDPSNLMPPPNQTPAPDQPFALSTVREESSIPR(A)		1,282.30	3,843.87	77	111
(K)ENLDPSNLmPPPNQTPAPDQPFALSTVREESSIPR(A)	Oxidation (+16)	1,287.63	3,859.87	77	111
(R)GTAAENKENLDPSNLmPPPNQTPAPDQPFALSTVR(E)	Oxidation (+16)	1,245.28	3,732.81	70	104
(R)GTAAENKENLDPSNLmPPPNQTPAPDQPFALSTVR(E)	Oxidation (+16)	934.209	3,732.81	70	104
(R)GTAAENKENLDPSNLMPPPNQTPAPDQPFALSTVR(E)		1,239.94	3,716.81	70	104
(R)GTAAENKENLDPSNLmPPPNQTPAPDQPFALSTVREESSIPR(A)	Oxidation (+16)	1,511.40	4,531.19	70	111
(R)GTAAENKENLDPSNLMPPPNQTPAPDQPFALSTVREESSIPR(A)		1,506.07	4,515.20	70	111
(R)HDWIINR(C)		477.2509	952.4873	215	221
(R)IHNQNNEQAWK(E)		691.333	1,380.65	153	163
(R)IHNQNNEQAWKEILK(W)		622.3253	1,863.95	153	167
(R)IHNQNNEQAWKEILK(W)		932.985	1,863.96	153	167
(K)KTYSVPAHQER(A)		439.2316	1,314.67	49	59
(K)KWVYPSEQmFWNAMLK(K)	Oxidation (+16)	1,037.50	2,072.98	117	132
(K)KWVYPSEQMFWnAMLK(K)	Deamidation (+1)	1,029.99	2,057.97	117	132
(K)KWVYPSEQMFWNAMLKK(G)		729.3695	2,185.09	117	133
(K)KWVYPSEQMFWNAmLKK(G)	Oxidation (+16)	1,101.55	2,201.08	117	133
(R)SWmGYELPFDR(H)	Oxidation (+16)	708.8176	1,415.62	204	214
(R)SWMGYELPFDR(H)		700.8187	1,399.62	204	214
(R)SWmGYELPFDR(H)	Oxidation (+16)	708.8178	1,415.62	204	214
(R)SWmGYELPFDRHDWIInR(C)	Oxidation (+16), Deamidation (+1)	784.7057	2,351.10	204	221
(R)SWmGYELPFDRHDWIINR(C)	Oxidation (+16)	784.3722	2,350.09	204	221
(K)TYSVPAHQER(A)		594.2949	1,186.58	50	59
(K)WKDEDISQK(D)		574.7818	1,147.55	137	145
(K)WKDEDISQKDmYNIIR(I)	Oxidation (+16)	690.6702	2,068.99	137	152
(K)WKDEDISQKDmYNIIR(I)	Oxidation (+16)	518.2537	2,068.99	137	152
(K)WKDEDISQKDMYNIIR(I)		685.3389	2,052.99	137	152
(K)WKDEDISQKDMYNIIR(I)		514.256	2,053.00	137	152
(K)WKDEDISQKDmYNIIR(I)	Oxidation (+16)	1,035.50	2,068.99	137	152
(K)WKDEDISQKDMYNIIR(I)		1,027.50	2,052.99	137	152
(K)WVYPSEQMFWNAMLK(K)		965.4558	1,928.90	118	132
(K)WVYPSEQmFWNAmLK(K)	Oxidation (+16), Oxidation (+16)	981.4504	1,960.89	118	132
(K)WVYPSEQmFWNAmLK(K)	Oxidation (+16), Oxidation (+16)	654.6355	1,960.88	118	132
(K)WVYPSEQmFWnAmLK(K)	Oxidation (+16), Deamidation (+1), Oxidation (+16)	654.9654	1,961.87	118	132
(K)WVYPSEQmFWNAMLK(K)	Oxidation (+16)	973.4531	1,944.89	118	132
(K)WVYPSEQmFWNAmLK(K)	Oxidation (+16), Oxidation (+16)	654.6367	1,960.89	118	132
(K)WVYPSEQmFWNAmLK(K)	Oxidation (+16), Oxidation (+16)	981.4522	1,960.89	118	132
(K)WVYPSEQMFWNAmLK(K)	Oxidation (+16)	973.4536	1,944.89	118	132
(K)WVYPSEQMFWNAMLK(K)		643.9739	1,928.90	118	132
(K)WVYPSEQMFWNAmLK(K)	Oxidation (+16)	649.3039	1,944.89	118	132
(R)YVIDYYDGGEVNK(D)		767.8568	1,533.70	224	236
(R)YVIDYYDGGEVNKDYQFTILDVRPALDSLSAVWDR(M)		1,024.75	4,094.99	224	258
(K)WKDEDISQKDMYNIIR(I)		685.3384	2,052.99	137	152
(R)GTAAENKENLDPSNLmPPPNQTPAPDQPFALSTVR(E)	Oxidation (+16)	934.21	3,732.81	70	104
(R)IHNQNNEQAWK(E)		461.2256	1,380.65	153	163
(K)KTYSVPAHQER(A)		439.2311	1,314.67	49	59
(R)GTAAENKENLDPSNLMPPPNQTPAPDQPFALSTVR(E)		1,239.94	3,716.81	70	104

Figure S3

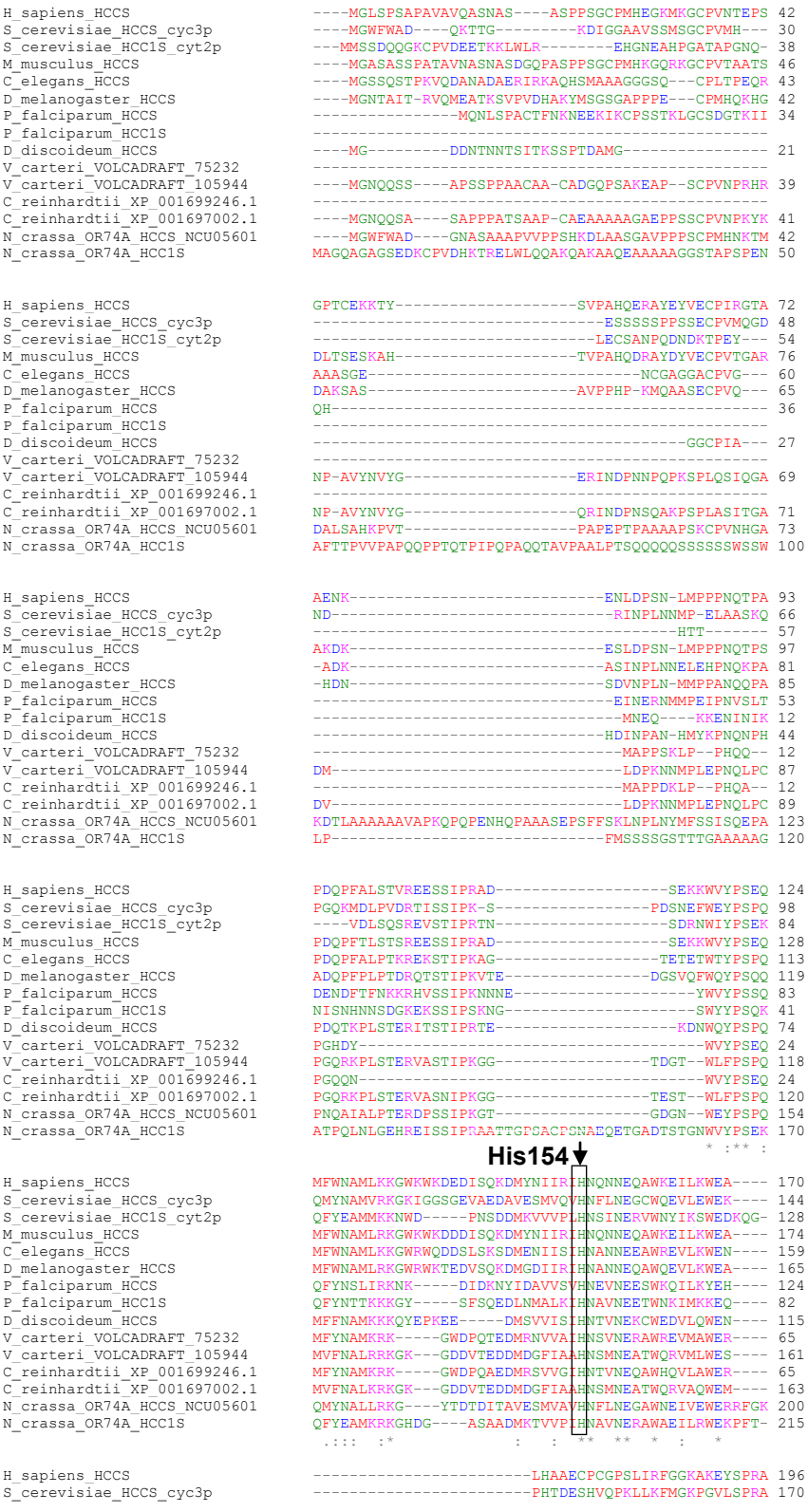

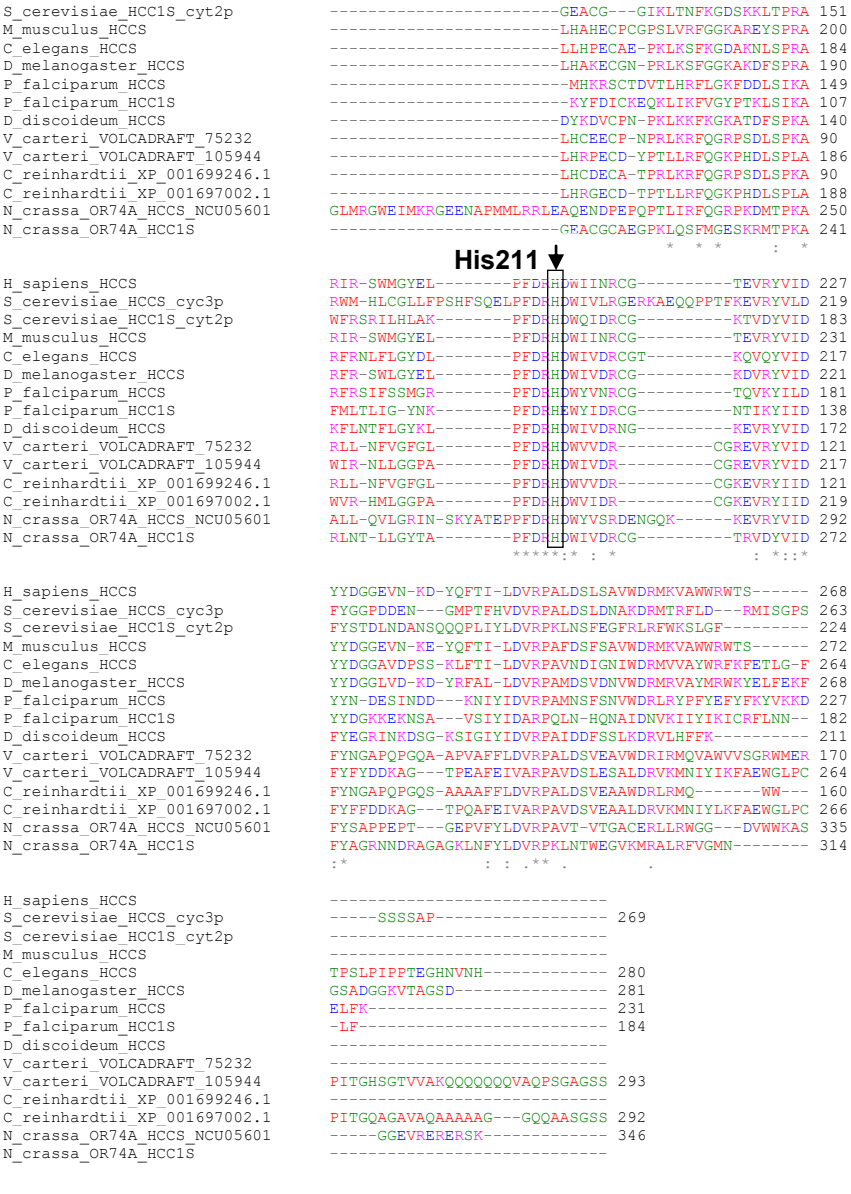
His211

Figure S4

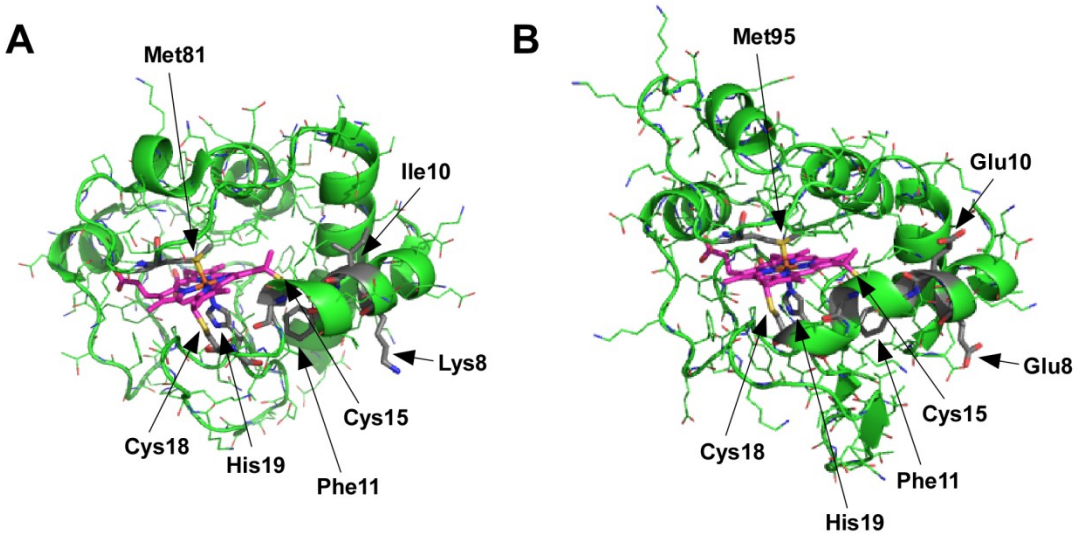
A
Met81
Ile10
Lys8
Cys15
Cys18
His19
Phe11
B
Met95
Glu10
Glu8
Cys15
Cys18
Phe11
His19

Figure S5

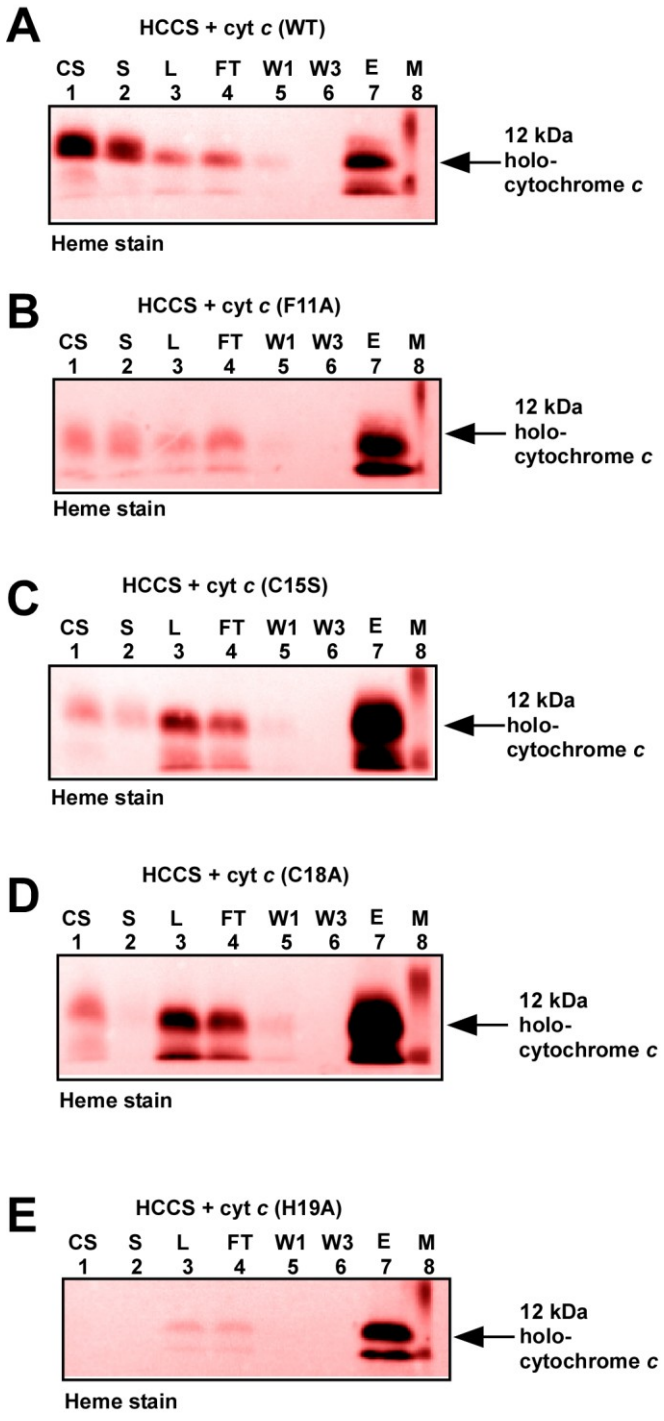
A
HCCS + cyt c (WT)
CS S L FT W1 W3 E M
1 2 3 4 5 6 7 8
12 kDa holo-cytochrome c
Heme stain
B
HCCS + cyt c (F11A)
CS S L FT W1 W3 E M
1 2 3 4 5 6 7 8
12 kDa holo-cytochrome c
Heme stain
C
HCCS + cyt c (C15S)
CS S L FT W1 W3 E M
1 2 3 4 5 6 7 8
12 kDa holo-cytochrome c
Heme stain
D
HCCS + cyt c (C18A)
CS S L FT W1 W3 E M
1 2 3 4 5 6 7 8
12 kDa holo-cytochrome c
Heme stain
E
HCCS + cyt c (H19A)
CS S L FT W1 W3 E M
1 2 3 4 5 6 7 8
12 kDa holo-cytochrome c
Heme stain

Figure S6

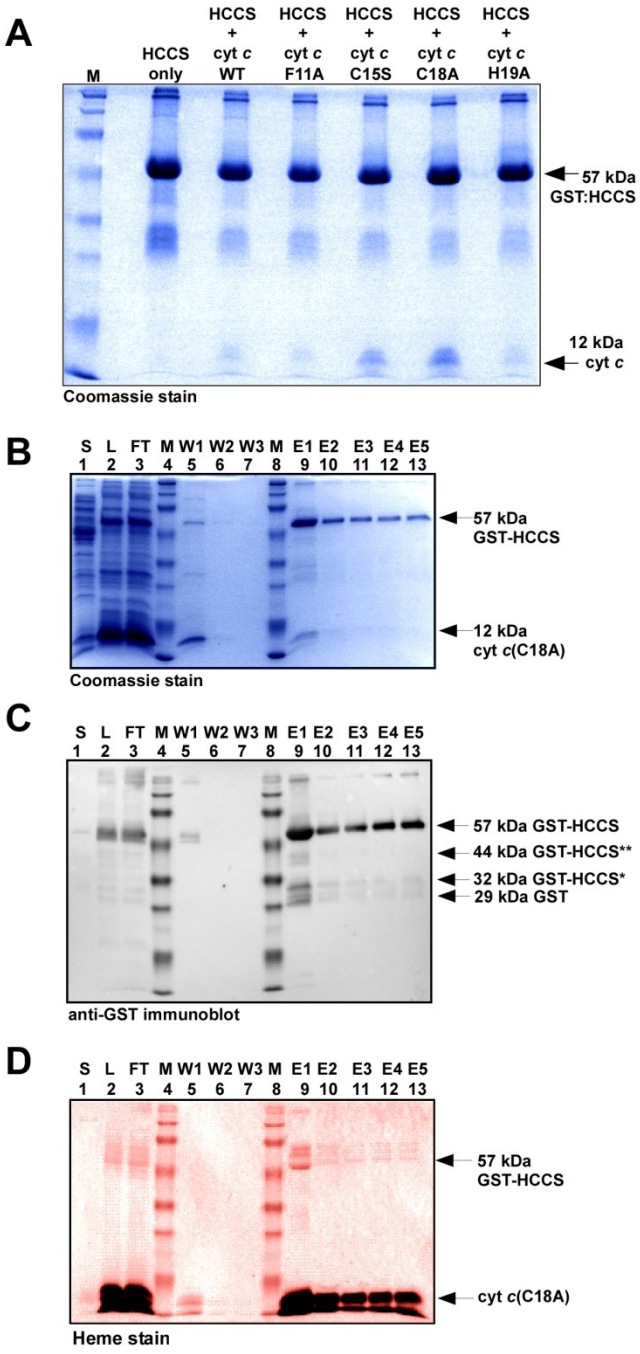
A
M
HCCS only
HCCS + cyt c WT
HCCS + cyt c F11A
HCCS + cyt c C15S
HCCS + cyt c C18A
HCCS + cyt c H19A
57 kDa GST:HCCS
12 kDa cyt c
Coomassie stain
B
S L FT M W1 W2 W3 M E1 E2 E3 E4 E5
1 2 3 4 5 6 7 8 9 10 11 12 13
57 kDa GST-HCCS
12 kDa cyt c(C18A)
Coomassie stain
C
S L FT M W1 W2 W3 M E1 E2 E3 E4 E5
1 2 3 4 5 6 7 8 9 10 11 12 13
57 kDa GST-HCCS
44 kDa GST-HCCS**
32 kDa GST-HCCS*
29 kDa GST
anti-GST immunoblot
D
S L FT M W1 W2 W3 M E1 E2 E3 E4 E5
1 2 3 4 5 6 7 8 9 10 11 12 13
57 kDa GST-HCCS
cyt c(C18A)
Heme stain

Figure S7

Peptide sequence: WT cytochrome c	Seq.	m/z (obs)	Mr (expt)	Mr (calc)
KIFIMK	9-14	390.2439	778.4732	778.4775
KIFIMK	9-14	390.2445	778.4745	778.4775
KIFIMK + ox (M)	9-14	398.2412	794.4678	794.4724
HKTGPNLHGLFGR	27-39	359.1977	1432.7615	1432.7688
HKTGPNLHGLFGR + deam (NQ)	27-39	359.4485	1433.7649	1433.7528
TGPNLHGLFGR	29-39	584.8093	1167.6040	1167.6149
TGPNLHGLFGRK	29-40	432.9085	1295.7036	1295.7099
TGPNLHGLFGRK + deam (NQ)	29-40	433.2413	1296.7020	1296.6939
KTGQAPGYSYTAANK	40-54	778.8813	1555.7480	1555.7630
KTGQAPGYSYTAANKNK	40-56	600.3039	1797.8899	1797.9009
KTGQAPGYSYTAANKNK + deam (NQ)	40-56	600.6311	1798.8716	1798.8849
TGQAPGYSYTAANK	41-54	714.8368	1427.6589	1427.6681
TGQAPGYSYTAANKNK	41-56	557.6061	1669.7966	1669.8060
GIIWGEDTLMEYLENPK + ox (M)	57-73	1012.4795	2022.9444	2022.9608
GIIWGEDTLMEYLENPK + ox (M); deam (NQ)	57-73	1012.9840	2023.9534	2023.9448
KYIPGTK	74-80	403.7397	805.4648	805.4698
MIFVGIK	81-87	404.2414	806.4681	806.4724
MIFVGIK + ox (M)	81-87	412.2377	822.4608	822.4673
MIFVGIKK	81-88	468.2883	934.5620	934.5674
MIFVGIKK + ox (M)	81-88	476.2863	950.5580	950.5623
EERADLIAYLK	90-100	660.8589	1319.7032	1319.7085
EERADLIAYLKK	90-101	483.6068	1447.7985	1447.8034
ADLIAYLK	93-100	453.7657	905.5169	905.5222
ADLIAYLKK	93-101	345.5434	1033.6084	1033.6171

MGDVEKGKKIFIMKCSQCHTVEKGGKHKTGPNLHGLFGRKAANKNKGHWGEDTLMEYLE
NPKKYIPGTKMIFVGIKKKEKATNE 76 % protein sequence coverage

Peptide sequence: C18A cytochrome c	Seq.	m/z (obs)	Mr (expt)	Mr (calc)
KIFIMK	9-14	390.2448	778.4750	778.4775
KIFIMK + ox (M)	9-14	398.2414	794.4683	794.4724
KIFIMKCSQAHTVEK	9-23	441.4909	1761.9345	1761.9270
CSQAHTVEK	15-23	501.7349	1001.4552	1001.4600
HKTGPNLHGLFGR	27-39	359.1978	1432.7622	1432.7688
HKTGPNLHGLFGR + deam (NQ)	27-39	359.4484	1433.7644	1433.7528
TGPNLHGLFGR	29-39	584.8106	1167.6066	1167.6149
TGPNLHGLFGR + deam (NQ)	29-39	585.3031	1168.5917	1168.5989
TGPNLHGLFGRK	29-40	432.9061	1295.6964	1295.7099
TGPNLHGLFGRKTGQAPGYSYTAANK	29-54	677.3450	2705.3510	2705.3674
TGPNLHGLFGRKTGQAPGYSYTAANK + deam (NQ)	29-54	677.5961	2706.3554	2706.3514
KTGQAPGYSYTAANK	40-54	778.8821	1555.7497	1555.7630
KTGQAPGYSYTAANK + deam (NQ)	40-54	519.9261	1556.7563	1556.7471
KTGQAPGYSYTAANKNK	40-56	600.3038	1797.8895	1797.9009
KTGQAPGYSYTAANKNK + deam (NQ)	40-56	600.6306	1798.8700	1798.8849
TGQAPGYSYTAANK	41-54	714.8366	1427.6586	1427.6681
TGQAPGYSYTAANKNK	41-56	557.6059	1669.7958	1669.8060
NKGIIWGEDTLMEYLENPK + ox (M)	55-73	756.0371	2265.0895	2265.0987
NKGIIWGEDTLMEYLENPKK	55-74	793.4031	2377.1873	2377.1987
NKGIIWGEDTLMEYLENPKK + ox (M)	55-74	798.7358	2393.1854	2393.1936
NKGIIWGEDTLMEYLENPKK + ox (M); deam (NQ)	55-74	599.5536	2394.1851	2394.1777
GIIWGEDTLMEYLENPK	57-73	1004.4884	2006.9622	2006.9659
GIIWGEDTLMEYLENPK + ox (M)	57-73	1012.4834	2022.9522	2022.9608
GIIWGEDTLMEYLENPKK	57-74	712.6916	2135.0529	2135.0609
GIIWGEDTLMEYLENPKK + ox (M)	57-74	1076.5340	2151.0534	2151.0558
GIIWGEDTLMEYLENPKK + ox (M); deam (NQ)	57-74	718.3563	2152.0471	2152.0398
GIIWGEDTLMEYLENPKKYIPGTK + ox (M)	57-80	937.8090	2810.4051	2810.4200
KYIPGTK	74-80	403.7396	805.4647	805.4698
MIFVGIK	81-87	404.2420	806.4695	806.4724
MIFVGIK + ox (M)	81-87	412.2395	822.4645	822.4673
MIFVGIKK	81-88	468.2863	934.5581	934.5674
MIFVGIKK + ox (M)	81-88	476.2867	950.5588	950.5623
KEERADLIAYLK	89-100	724.9061	1447.7976	1447.8034
EERADLIAYLK	90-100	660.8576	1319.7006	1319.7085
EERADLIAYLKK	90-101	483.6065	1447.7977	1447.8034
ADLIAYLK	93-100	453.7653	905.5161	905.5222
ADLIAYLKK	93-101	517.8129	1033.6113	1033.6171
ADLIAYLKKATNE	93-105	725.3977	1448.7809	1448.7874

MGDVEKGKKIFIMKCSQAHTVEKGGKHKTGPNLHGLFGRKAANKNKGHWGEDTLMEYLE
NPKKYIPGTKMIFVGIKKKEKATNE 89 % sequence coverage

Peptide sequence: C15S cytochrome c	Seq.	m/z (obs)	Mr (expt)	Mr (calc)
KIFIMK	9-14	390.2450	778.4754	778.4775
KIFIMK + ox (M)	9-14	398.2414	794.4683	794.4724
SSQCHTVEK	15-23	509.7303	1017.4461	1017.4549
HKTGPNLHGLFGR	27-39	359.1981	1432.7633	1432.7688
HKTGPNLHGLFGR + deam (NQ)	27-39	478.9312	1433.7719	1433.7528
HKTGPNLHGLFGRK	27-40	391.2221	1560.8593	1560.8637
TGPNLHGLFGR	29-39	584.8117	1167.6089	1167.6149
TGPNLHGLFGRK	29-40	432.9092	1295.7058	1295.7099
TGPNLHGLFGRK + deam (NQ)	29-40	433.2384	1296.6933	1296.6939
TGPNLHGLFGRKTGQAPGYSYTAANK	29-54	677.3450	2705.3510	2705.3674
KTGQAPGYSYTAANK	40-54	778.8844	1555.7542	1555.7630
KTGQAPGYSYTAANKNK	40-56	600.3039	1797.8898	1797.9009
KTGQAPGYSYTAANKNK + deam (NQ)	40-56	600.6327	1798.8762	1798.8849
TGQAPGYSYTAANK	41-54	714.8344	1427.6543	1427.6681
GIIWGEDTLMEYLENPK + ox (M)	57-73	1012.4833	2022.9520	2022.9608
KYIPGTK	74-80	403.7400	805.4654	805.4698
MIFVGIK + ox (M)	81-87	412.2379	822.4612	822.4673
MIFVGIKK	81-88	468.2899	934.5652	934.5674
MIFVGIKK + ox (M)	81-88	476.2862	950.5579	950.5623
EERADLIAYLK	90-100	660.8595	1319.7044	1319.7085
EERADLIAYLKK	90-101	483.6070	1447.7993	1447.8034
ADLIAYLK	93-100	453.7666	905.5187	905.5222
ADLIAYLKK	93-101	517.8122	1033.6099	1033.6171
ADLIAYLKK	93-101	517.8149	1033.6152	1033.6171
ADLIAYLKKATNE	93-105	483.9343	1448.7811	1448.7874
ADLIAYLKKATNE + deam (NQ)	93-105	484.2661	1449.7766	1449.7715

MGDVEKGKKIFIMKSSQCHTVEKGGKHKTGPNLHGLFGRKAANKNKGHWGEDTLMEYLE
NPKKYIPGTKMIFVGIKKKEKATNE 88 % sequence coverage

Figure S8

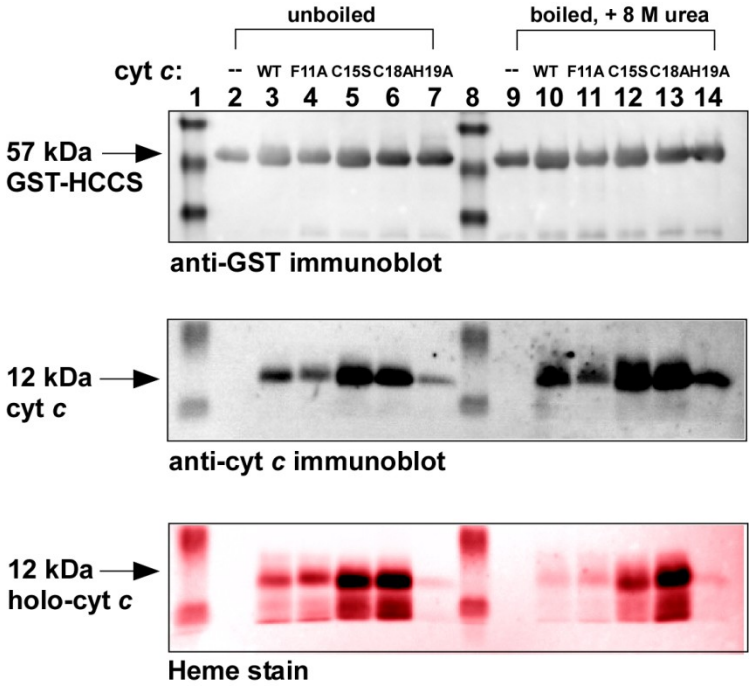
unboiled
boiled, + 8 M urea
cyt c:
-- WT F11A C15SC18AH19A -- WT F11A C15SC18AH19A
1 2 3 4 5 6 7 8 9 10 11 12 13 14
57 kDa
GST-HCCS
anti-GST immunoblot
12 kDa
cyt c
anti-cyt c immunoblot
12 kDa
holo-cyt c
Heme stain

Figure S9

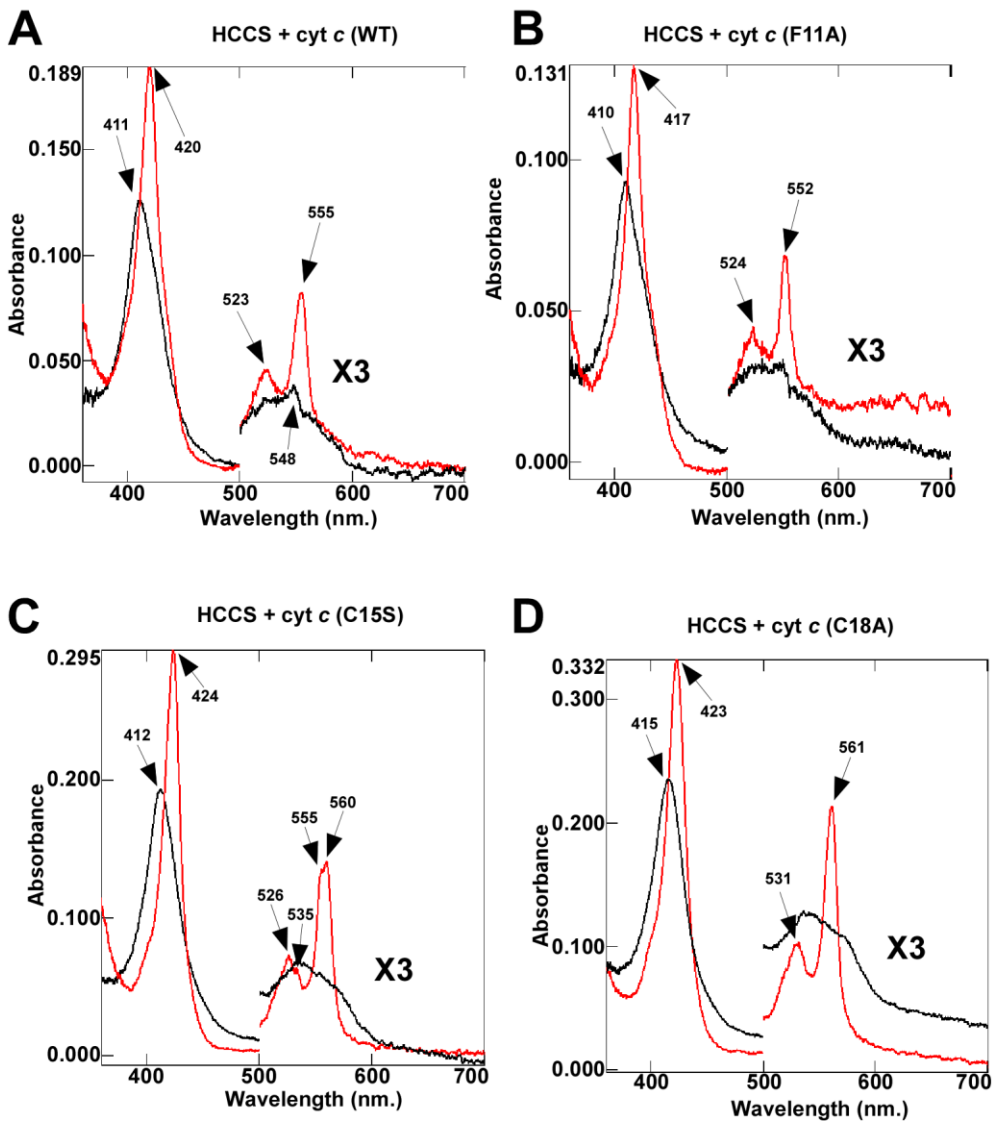
A
HCCS + cyt c (WT)
0.189
0.150
0.100
0.050
0.000
Absorbance
411
420
555
523
548
X3
400
500
600
700
Wavelength (nm.)
B
HCCS + cyt c (F11A)
0.131
0.100
0.050
0.000
Absorbance
410
417
552
524
X3
400
500
600
700
Wavelength (nm.)
C
HCCS + cyt c (C15S)
0.295
0.200
0.100
0.000
Absorbance
412
424
555
560
526
535
X3
400
500
600
700
Wavelength (nm.)
D
HCCS + cyt c (C18A)
0.332
0.300
0.200
0.100
0.000
Absorbance
415
423
561
531
X3
400
500
600
700
Wavelength (nm.)

Figure S10

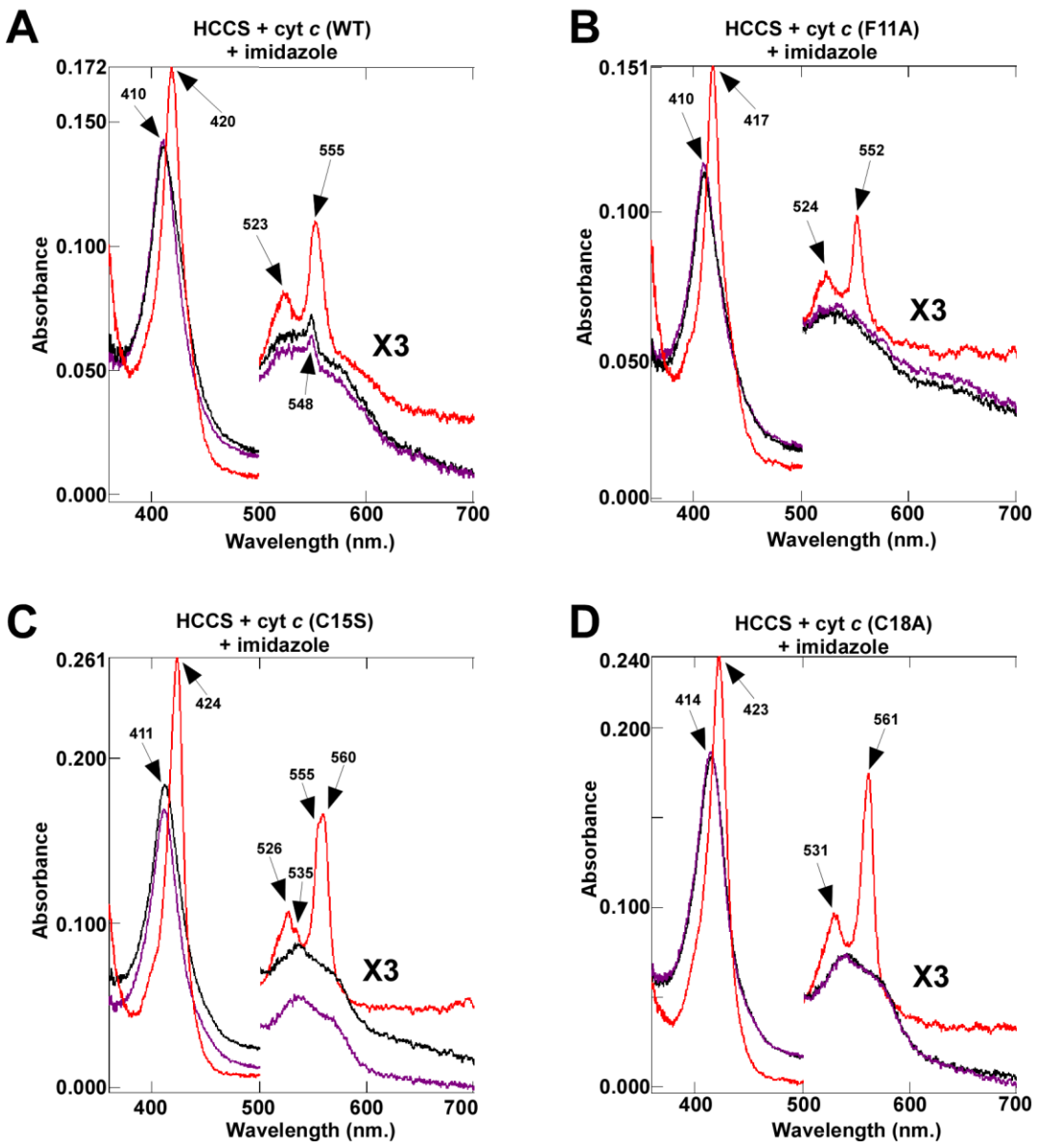
A
HCCS + cyt c (WT)
+ imidazole
0.172
0.150
0.100
0.050
0.000
Absorbance
410
420
555
523
548
X3
400
500
600
700
Wavelength (nm.)
B
HCCS + cyt c (F11A)
+ imidazole
0.151
0.100
0.050
0.000
Absorbance
410
417
552
524
X3
400
500
600
700
Wavelength (nm.)
C
HCCS + cyt c (C15S)
+ imidazole
0.261
0.200
0.100
0.000
Absorbance
411
424
560
555
526
535
X3
400
500
600
700
Wavelength (nm.)
D
HCCS + cyt c (C18A)
+ imidazole
0.240
0.200
0.100
0.000
Absorbance
414
423
561
531
X3
400
500
600
700
Wavelength (nm.)

Figure S11

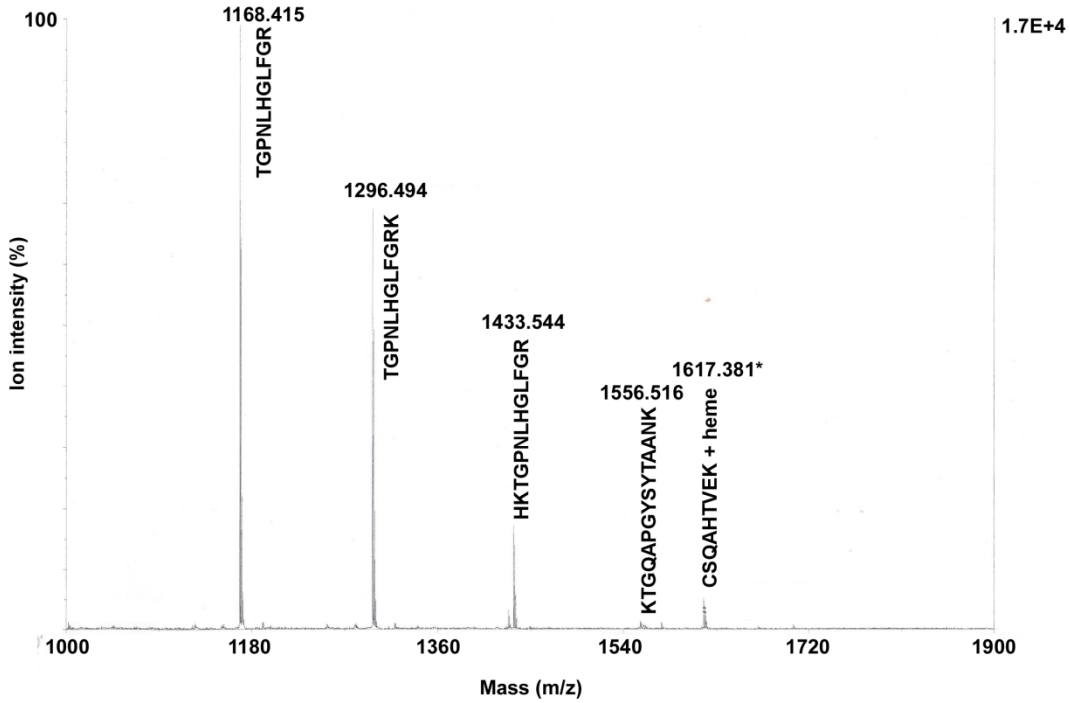

*Neutral monoisotopic mass calculation
CSQAHTVEK (1001.4597 Da) + heme (616.1773 Da) = 1617.637 Da

Figure S12

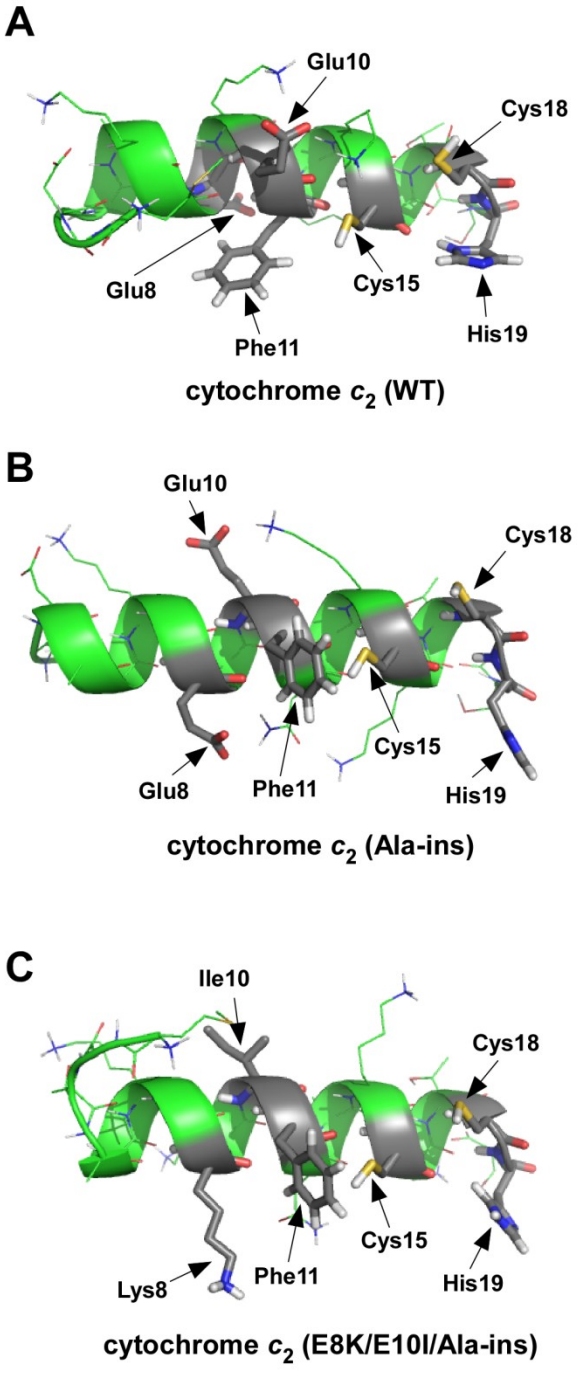
A
Glu10
Cys18
Glu8
Cys15
Phe11
His19
cytochrome c_2 (WT)
B
Glu10
Cys18
Cys15
Glu8
Phe11
His19
cytochrome c_2 (Ala-ins)
C
Ile10
Cys18
Cys15
Lys8
Phe11
His19
cytochrome c_2 (E8K/E10I/Ala-ins)

Table S1. Published studies on maturation of cytochrome *c* by HCCS

Reference	Compartment	HCCS	Cytochrome c	Results
Verissimo et al. (2012) Biochem Biophys Res Comm	*E. coli* cytoplasm	S. *cerevisiae*	• *S. cerevisiae* iso-2-cyt c • *R. capsulatus* cyt c2 • Iso-2-cyt c/cyt c2 chimera • Cyt c2-insK11 • Cyt c2-E9L • Cyt c2-insK11 + E9L • Cyt c2-insK11 + N12T	• *R. capsulatus* cyt c2 not matured • Iso-2-cyt c/cyt c2 chimera (and truncated chimera) fully matured • Cyt c2-insK11 matured at low level • Cyt c2-insK11 + E9L matured at high levels • Cyt c2-E9L not matured • Cyt c2-insK11 + N12T not matured
Stevens et al. (2011) FEBS Lett	*E. coli* cytoplasm	*S. cerevisiae*	• *E. caballus* cyt c • *S. cerevisiae* iso-1-cyt c • *P. denitrificans* cyt c550 • Iso-1-cyt c/cyt c550 chimera	• G6A, F10A in *E. caballus* not matured • F15A (but not G11A) in S. cerevisiae not matured • D2A, E4A, K7A, K5A, K8A matured at WT levels • *P. denitrificans* cyt c550 not matured • Chimera with *S. cerevisiae* N-term up to but not including CXXCH fused to *P. denitrificans* cyt c550 matured at WT levels
Kleingardner and Bren (2011) Metallomics	*E. coli* cytoplasm	*S. cerevisiae*	• *E. caballus* cyt c • *E. caballus* cyt c 1x-ins • *E. caballus* cyt c 3x-ins • *E. caballus* cyt c G13 ins • *E. caballus* F10A	• *E. caballus* cyt c 1x-ins not matured • Cyt c 3x-ins matured at 1/3 levels • Cyt c G13 ins matured at 1/3 levels but spectrally heterogeneous • Cyt c F10A not matured at detectable levels
Fulop et al. (2009) FEBS J	*E. coli* cytoplasm	*S. cerevisiae*	• *T. brucei* cyt c WT (AAQCH) • *T. brucei* cyt c(CAQCH) • *S. cerevisiae* iso-1-cyt c	• Both *T. brucei* cyts c matured at very low levels; 0.25 % the level of *S. cerevisiae* iso-1-cyt c
Rosell and Mauk (2002) Biochem	*E. coli* cytoplasm	*S. cerevisiae*	• *S. cerevisiae* iso-1-cyt c(C14S) • *S. cerevisiae* iso-1-cyt c(C17S)	• Iso-1-cyt c(C14S) matured at 1/10 levels of WT; spectrally distinct from WT • Iso-1-cyt c(C17S) expression 20-fold lower than C14S variant; apparently did not permit enough to conduct analysis
Silkstone et al. (2002) Biophysical Chem	*E. coli* cytoplasm	*S. cerevisiae*	• *S. cerevisiae* iso-1 cyt c(M80D/E/S/A)	• *S. cerevisiae* iso-1 cyt c Met80 variants were matured efficiently
Rumbley et al. (2002) Biochemistry	*E. coli* cytoplasm	*S. cerevisiae*	• *E. caballus* cyt c(E5G) • *E. caballus* cyt c(K9G) • *E. caballus* cyt c(V12G)	• *E. caballus* cyt c E5G, K9G, V12G variants all matured, but with increasing proximity to CXXCH, level of mis-attached heme increased (attributed to interference with formation of N-terminal helix) • Starting *E. caballus* cyt c construct carried H26N, H33N

				mutations
Sanders et al. (2001) Mol Micro	*E. coli* cytoplasm	*S. cerevisiae*	• *S. cerevisiae* iso-2-cyt c/*P. denitrificans* cyt c550 chimera	• Chimera (with N-term and CXXCH from iso-2-cyt c) matured
Sanders and Lill (2000) BBA	*E. coli* cytoplasm	*S. cerevisiae*	• *S. cerevisiae* iso-1-cyt c • *S. cerevisiae* iso-2-cyt c • *P. denitrificans* cyt c • *Synechocystis* sp. PCC 6803 cyt c553	• *S. cerevisiae* iso-1 and iso-2 cyt c matured at high levels • *P. denitrificans* and *Synechocystis* cyt c not matured at detectable levels
Corvest et al. (2010) Genetics	Whole *S. cerevisiae* cells	*S. cerevisiae*	• *S. cerevisiae* cyt c_1(CA[/P/T/H/L/S]CH)	• Cyt c_1(CAPCH) depends on HCCS and Cyc2p for maturation; HCC_1S maturation achieved by overexpression of HCC_1S or substitution of P with H/L/S/T
Bernard et al. (2003) JBC	Whole *S. cerevisiae* cells	Plasmid *S. cerevisiae* HCCS and HCC_1S Plasmid *H. sapiens* HCCS Plasmid *M. musculus* HCCS	• *S. cerevisiae* cyt c • *S. cerevisiae* cyt c_1 WT (CAACH) • *S. cerevisiae* cyt c_1(CAPCH) • *S. cerevisiae* cyt c_1(CADCH)	• *S. cerevisiae* HCC_1S cannot mature cyt c • *S. cerevisiae*, *H. sapiens*, and *M. musculus* HCCS can complement HCC_1S deletion for respiratory growth (i.e., they are active towards both cyt c an cyt c_1) • *S. cerevisiae* HCCS can mature CAPCH and CADCH mutants of cyt c_1
Wang et al. (1996) JBC	Whole *S. cerevisiae* cells	Chromosomal + plasmid *S. cerevisiae*	• *S. cerevisiae* iso-2-cyt c([S/A]XX[S/A]H) • *S. cerevisiae* iso-2-cyt c(F19A) • *S. cerevisiae* iso-2-cyt c(H27A) • *S. cerevisiae* iso-2-cyt c(ΔAla1-Lys14) • *S. cerevisiae* iso-2-cyt c(ΔGly15-Leu18)	• Iso-2-cyt c(S/AXXS/AH) variants not matured, but imported into mitochondria (when HCCS was overexpressed on plasmid) • Iso-2-cyt c(F19A) not matured; 10 % mitochondrial import • Iso-2-cyt c(H27A)not matured; 40 % associated with mitochondria but only 10 % internalized into mitochondria • Iso-2-cyt c(ΔAla1-Lys14) matured at low levels (10 %) • Iso-2-cyt c(ΔGly15-Leu18) not matured; 10 % mitochondrial import
Fumo et al. (1995) Gene	Whole *S. cerevisiae* cells	Chromosomal *S. cerevisiae*	• *S. cerevisiae* iso-1-cyt c(H18A)	• Iso-1-cyt c(H18A) is nonfunctional (did not support growth in medium with liquid lactate, a nonfermentable carbon source) • Iso-1-cyt c(H18A) was not detected spectrally in intact cells • In targeted random mutagenesis experiment, only His was found as a.a. 18 • Iso-1-cyt c(H18R) integrated chromosomally not support growth in lactate medium and holo-cyt c(H18R) was not detected in low temperature difference spectroscopy
Tanaka et al.	Whole *S. cerevisiae*	Chromosomal	• *H. sapiens* cyt	• *H. sapiens* cyt c(C14A)

(1990) J Biochem	cells	*S. cerevisiae*		c(C14A)	efficiently matured and complemented CYC1 deficiency in yeast on lactate medium
Sorrell et al. (1989) JACS	Whole *S. cerevisiae* cells	Chromosomal *S. cerevisiae*	•	*S. cerevisiae* iso-2-cyt c(H18R)	• Iso-2-cyt c(H18R) on a plasmid weakly complemented yeast strain lacking cytochrome c on glycerol or lactate media • Less than 1 mg/10 L culture were purified; spectrally identical to WT iso-2-cyt c • Iso-2-cyt c(H18R) has slower rate of electron transfer than WT
Tong and Margoliash (1998) JBC	Purified *S. cerevisiae* mitochondria "in vitro"	Chromosomal + plasmid *S. cerevisiae*	•	*D. melanogaster* cyt c(C14S) • *D. melanogaster* cyt c(C17S) • *D. melanogaster* cyt c(C14S/C17S)	• *D. melanogaster* cyt c(C14S) matured, but at lower levels than WT • *D. melanogaster* cyt c(C17S) was matured at "trace" amounts • *D. melanogaster* cyt c(C14S/C17S) was undetectable
Veloso et al. (1983) JBC	Purified *S. cerevisiae* mitochondria "in vitro"	Chromosomal *S. cerevisiae*	•	N-terminal 25 residues of *E. caballus* cyt c	• Heme was attached to *E. caballus* cyt c(N-term 25) at 25 % levels of full apocytochrome c • No maturation when Gly replaced Cys in CXXCH

Catalogue of published studies on the effects of cytochrome *c* mutations on maturation by HCCS. Studies are organized according to the biological compartment in which the study was conducted (i.e., *E. coli* cytoplasm, whole *S. cerevisiae* cells, or isolated *S. cerevisiae* mitochondria) and then in reverse chronological order. Full citations for each of the studies above are provided in the references section of the main text.

Table S2. Oligonucleotide primers, plasmids, and strains used in this research.

Oligonucleotide	Sequence (5'-3')	Plasmid Constructed
CYCS_K6A_Fwd	ATGGGTGATGTTGAGGCGGGCAAGAAGATTTTTATTATGAAGTG	pRGK412
CYCS_K6A_Rev	CACTTCATAATAAAAATCTTCTTGCCCGCCTCAACATCACCCAT	pRGK412
CYCS_K6R_Fwd	ATGGGTGATGTTGAGCGCGGCAAGAAGATTTTTATTATGAAGTG	pRGK413
CYCS_K6R_Rev	CACTTCATAATAAAAATCTTCTTGCCGCGCTCAACATCACCCAT	pRGK413
CYCS_K6D_Fwd	ATGGGTGATGTTGAGGACGGCAAGAAGATTTTTATTATGAAGTG	pRGK414
CYCS_K6D_Rev	CACTTCATAATAAAAATCTTCTTGCCGTCCTCAACATCACCCAT	pRGK414
CYCS_F11A_Fwd	GAGAAAGGCAAGAAGATTGCGATTATGAAGTGTTCCCAGTGCC	pRGK415
CYCS_F11A_Rev	GGCACTGGGAACACTTCATAATCGCAATCTTCTTGCCTTTCTC	pRGK415
CYCS_F11Y_Fwd	GTTGAGAAAGGCAAGAAGATTTATATTATGAAGTGTTCCCAGTGC	pRGK416
CYCS_F11Y_Rev	GCACTGGGAACACTTCATAATATAAATCTTCTTGCCTTTCTCAAC	pRGK416
CYCS_C15S_Fwd	GATTTTTATTATGAAGAGCTCCCAGTGCCACACCGTTGAAAAGGG	pRGK417
CYCS_C15S_Rev	CCCTTTTCAACGGTGTGGCACTGGGAGCTCTTCATAATAAAAATC	pRGK417
CYCS_C18A_Fwd	ATGAAGTGTTCCCAGGCGCACCGTTGAAAAGGGAGG	pRGK418
CYCS_C18A_Rev	CCTCCCTTTTCAACGGTGCGCCTGGGAACACTTCAT	pRGK418
CYCS_H19A_Fwd	TATTATGAAGTGTTCCCAGTGCGCGACCGTTGAAAAGGG AGGCAA	pRGK419
CYCS_H19A_Rev	TTGCCTCCCTTTTCAACGGTCGCGCACTGGGAACACTTCATAATA	pRGK419
HCCS_H154A_Fwd	GTATAATATCATTAGAATTGCCAATCAGAATAACGAGCAGGC	pRGK420
HCCS_H154A_Rev	GCCTGCTCGTTATTCTGATTGGCAATTCTAATGATATTATAC	pRGK420
HCCS_H154G_Fwd	CATTAGAATTGGCAATCAGAATAACGAGCAGGCTTGGAAGG	pRGK421
HCCS_H154G_Rev	CCTTCCAAGCCTGCTCGTTATTCTGATTGCCAATTCTAATG	pRGK421
HCCS_H154Y_Fwd	CATTAGAATTTACAATCAGAATAACGAGCAGGC	pRGK422
HCCS_H154Y_Rev	GCCTGCTCGTTATTCTGATTGTAAATTCTAATG	pRGK422
HCCS_H211A_Fwd	GAGTTGCCTTTTGATAGGGCGGATTGGATCATAAACCGTTGC	pRGK423
HCCS_H211A_Rev	GCAACGGTTTATGATCCAATCCGCCCTATCAAAAGGCAACTC	pRGK423
HCCS_H211G_Fwd	GAGTTGCCTTTTGATAGGGGCGATTGGATCATAAACCGTTGC	pRGK424
HCCS_H211G_Rev	GCAACGGTTTATGATCCAATCGCCCCTATCAAAAGGCAACTC	pRGK424
HCCS_H211Y_Fwd	GGTATGAGTTGCCTTTTGATAGGTATGATTGGATCATAAACCG	pRGK425
HCCS_H211Y_Rev	CGGTTTATGATCCAATCATACCTATCAAAAGGCAACTCATACC	pRGK425
HCCS_H211C_Fwd	GAGTTGCCTTTTGATAGGTGCGATTGGATCATAAACCGTTG	pRGK426
HCCS_H211C_Rev	CAACGGTTTATGATCCAATCGCACCTATCAAAAGGCAACTC	pRGK426
pTXB1_HCCS_Nde1_Fwd	GGTGGTCATATGGGTTTGTCTCCATCTGC	pRGK404
pTXB1_HCCS_SapI_Rev	GGTGGTTGCTCTTCCGCATTTCGAGGTCCAACGCCACCAAGCAGC	pRGK404
pBAD_CYTC2_Nco1_Fwd	GACTCCATGGGCGACGCCGCGAAGGGCG	pRGK406
pBAD_CYTC2_XbaI_Rev	CTTCTAGATTATTTCACGACCGAGGCCAG	pRGK406
CYTC2_Ala-ins_Fwd	GGGCGAAAAAGAATTCAACGCCAAGTGCAAGACCTGCCA	pRGK407
CYTC2_Ala-ins_Rev	TGGCAGGTCTTGCACTTGGCGTTGAATTCTTTTTCGCCC	pRGK407
CYTC2_E8K_E10I_Fwd (Ala-ins)	GCGACGCCGCGAAGGGCAAAAAAATATTCAACGCCAAGTGCA	pRGK408
CYTC2_E8K_E10I_Rev (Ala-ins)	TGCACTTGGCGTTGAATATTTTTTTGCCCTTCGCGGCGTCGC	pRGK408
CYTC2_E8K_E10I_Fwd	GGCGACGCCGCGAAGGGCAAAAAAATATTCAACAAGTGCAAGAC	pRGK409
CYT_C2_E8K_E10I_Rev	GTCTTGCACTTGTTGAATATTTTTTTGCCCTTCGCGGCGTCGCC	pRGK409
CYT_C2_E8K_Fwd (Ala-ins)	GACGCCGCGAAGGGCAAAAAAGAATTCAACGC	pRGK410
CYTC2_E8K_Rev (Ala-ins)	GCGTTGAATTCTTTTTTGCCCTTCGCGGCGTC	pRGK410
CYTC2_E10I_Fwd (Ala-ins)	CGCCGCGAAGGGCGAAAAAATATTCAACGCCAAGTGC	pRGK411
CYTC2_E10I_Rev (Ala-ins)	GCACTTGGCGTTGAATATTTTTTCGCCCTTCGCGGCG	pRGK411
pGEX_HCCS_MfeI_Fwd	CTCAATTGATGGGTTTGTCTCCATCTGC	pRGK403
pET-Blue2-Down_Rev	GTTAAATTGCTAACGCAGTCA	pRGK403
pBAD_CYCS_EcoRI_Fwd	GCGGAATTCGCCATGGGTGATGTTGAG	pRGK405
pBAD_CYCS_PstI_Rev	GAGCTGCAGTTACTCATTAGTAGC	pRGK405
pET-Blue-2_HCCS_NcoI_Fwd	CCAGCCATGGGTCATCATCATCATCATCACGGTTTGTCTCCATCTGCTCC	pRGK402
pET-Blue-2_HCCS_HindIII_Rev	CGAAGCTTGTGCATAGTTTTACGAGGTCCAAC	pRGK402

Plasmid	Description	Reference
pRGK330	pBAD24-based plasmid for arabinose inducible expression	Feissner et al. 2006
pRGK389	Template for *R. capsulatus* cytochrome c_2	Richard-Fogal et al. 2012
pRGK402	Expression of N-terminal hexahistidine-tagged HCCS (pET Blue2)	This work

pRGK403	Expression of N-terminal GST-tagged HCCS (pGEX 4T-1)	This work
pRGK404	Expression of C-terminal Intein-tagged HCCS (pTXB1)	This work
pRGK405	Expression of human cytochrome c (pBAD)	This work
pRGK406	Expression of cytoplasmic *R. capsulatus* cytochrome c_2 (pBAD)	This work
pRGK407	pBAD cyt c_2(Ala-ins)	This work
pRGK408	pBAD cyt c_2(E8K/E10I/Ala-ins)	This work
pRGK409	pBAD cyt c_2(E8K/E10I)	This work
pRGK410	pBAD cyt c_2(E8K/Ala-ins)	This work
pRGK411	pBAD cyt c_2(E10I/Ala-ins)	This work
pRGK412	pBAD CYCS(K6A)	This work
pRGK413	pBAD CYCS(K6R)	This work
pRGK414	pBAD CYCS(K6D)	This work
pRGK415	pBAD CYCS(F11A)	This work
pRGK416	pBAD CYCS(F11Y)	This work
pRGK417	pBAD CYCS(C15S)	This work
pRGK418	pBAD CYCS(C18A)	This work
pRGK419	pBAD CYCS(H19A)	This work
pRGK420	pGEX HCCS(H154A)	This work
pRGK421	pGEX HCCS(H154G)	This work
pRGK422	pGEX HCCS(H154Y)	This work
pRGK423	pGEX HCCS(H211A)	This work
pRGK424	pGEX HCCS(H211G)	This work
pRGK425	pGEX HCCS(H211Y)	This work
pRGK426	pGEX HCCS(H211C)	This work

Strain	**Description**	**Reference**
RK103	Δ*ccm E. coli* strain MG1655 deleted for all *ccm* genes	Feissner et al. 2006
RK112	Δ*ccm E. coli* strain BL21 (DE3) deleted for all *ccm* genes	Richard-Fogal et al. 2012

Supporting Information References

(1) Richard-Fogal, C. L., San Francisco, B., Frawley, E. R., and Kranz, R. G. (2012) Thiol redox requirements and substrate specificities of recombinant cytochrome c assembly systems II and III. Biochim Biophys Acta 1817, 911-9.
(2) Feissner, R. E., Richard-Fogal, C. L., Frawley, E. R., Loughman, J. A., Earley, K. W., and Kranz, R. G. (2006) Recombinant cytochromes c biogenesis systems I and II and analysis of haem delivery pathways in Escherichia coli. Mol Microbiol 60, 563-77.
(3) Shevchenko, A., Tomas, H., Havlis, J., Olsen, J. V., and Mann, M. (2006) In-gel digestion for mass spectrometric characterization of proteins and proteomes. Nat Protoc 1, 2856-60.
(4) Sogabe, S., Ezoe, T., Kasai, N., Saeda, M., Uno, A., Miki, M., and Miki, K. (1994) Structural similarity of cytochrome c2 from Rhodopseudomonas viridis to mitochondrial cytochromes c revealed by its crystal structure at 2.7 A resolution. FEBS Lett 345, 5-8.
(5) Fulop, V., Sam, K. A., Ferguson, S. J., Ginger, M. L., and Allen, J. W. (2009) Structure of a trypanosomatid mitochondrial cytochrome c with heme attached via only one thioether bond and implications for the substrate recognition requirements of heme lyase. Febs J 276, 2822-32.

Chapter 6: Summary and Future Investigations

Summary

The studies in this dissertation explore the structure(s) and function(s) of the system I cytochrome c synthetase, CcmF (Fig 1), and the cytochrome c synthase for system III, HCCS. The transmembrane b-heme binding site within CcmF was defined and spectroscopically characterized, the requirements for formation of the CcmF-holoCcmE complex were determined, and CcmFH (along with CcmG) was shown to be a cytochrome c synthetase independent of CcmABCDE. For system III, interactions between HCCS and heme, and HCCS and cytochrome c, were characterized, allowing us to propose mechanisms for heme binding, interaction with apocytochrome *c*, thioether formation, and release of mature holocytochrome *c* from HCCS (Fig 2).

Characterization of the b-heme binding site in CcmF

Purification of CcmF revealed a stoichiometric and stable heme b, present in the absence of the other Ccm components, and heme-binding was shown to depend on a conserved transmembrane histidine (TM-His1) [1]. In Chapter 2 [2], a second conserved transmembrane histidine (TM-His2) is shown to be required for binding the heme b (Fig 1). Exogeneous imidazole is used to correct the cytochrome c assembly defects of mutations at TM-His1 and TM-His2, providing further support for a ligand-type function for these histidines. Resonance Raman spectroscopy is used to confirm the presence of a 6-coordinate, low-spin heme species in CcmF with bis-His coordination. It is shown that replacement of TM-His1 with cysteine (a residue that can substitute as an axial ligand) supports holocytochrome c formation at 70 % WT levels, and purified CcmF TM-His1Cys contains heme b with unique spectral characteristics. The stable heme b is shown to be conserved in CcmF proteins from a diverse set of prokaryotes

(including *Thermophilus thermophilus* and *Desulfovibrio vulgaris*). Finally, the midpoint potential of the CcmF b-heme is determined. These results constitute a thorough characterization of the transmembrane binding site for the CcmF heme b (coordinated by TM-His1 and TM-His2) and suggest a possible mechanism by which heme (from holoCcmE) becomes reduced (to Fe^{2+}), which is required for covalent attachment to the apocytochrome (Fig 1).

Requirements for formation of the CcmF-holoCcmE complex

Despite the wide assumption in the field that formation of a CcmF-holoCcmE complex is an intermediate during cytochrome c biogenesis, experimental evidence in support of this was lacking. In chapter 3, it is shown that CcmF and holoCcmE form a complex in the absence of CcmH. This complex requires conserved CcmF P-His1 and P-His2 (Fig 1). Exogeneous imidazole is used to correct the cytochrome c assembly defects of substitutions at P-His1 and P-His2, suggesting that these WWD-flanking histidines are axial ligands to heme from holoCcmE when it is bound in the CcmF WWD domain. For complex formation to occur, holoCcmE must be released from CcmABCD, and it is shown that the apo-form of CcmE interacts with CcmF at 20-fold lower levels than holoCcmE. These results establish the requirements for formation of the holoCcmE-CcmF complex, an interaction at the heart of heme trafficking in system I cytochrome biogenesis, and suggest a role for CcmH in mediating interaction between CcmF and holoCcmE.

CcmFH (with CcmG) is the system I cytochrome c synthetase

Unlike the synthases for systems II and III (which, when expressed heterologously in *E. coli* Δ*ccm*, are sufficient for holocytochrome c formation [3,4]), the synthetase activity of CcmFH had not been directly demonstrated. In chapter 4, it is shown that CcmFH (and the

periplasmic thioredoxin CcmG) can attach heme covalently to cytochromes c2 and c4 in *E. coli* Δ*ccm*, independent of CcmABCDE. This activity, termed CcmFGH-ind, is sufficient for robust production of holocytochrome c with spectral and biochemical characteristics indistinguishable from those of the holocytochrome c produced by the full system I. It is shown that CcmFGH-ind requires three conserved histidines in CcmF (TM-His1, TM-His2, and P-His2) as well as the conserved cysteine pairs in the thioredoxins CcmG and CcmH. These findings establish that CcmFH (together with CcmG) is the cytochrome c synthetase for system I, and provide unique mechanistic and evolutionary insights into cytochrome c biogenesis, as discussed in chapter 4.

HCCS forms a complex with heme and cytochrome c

Despite the identification of the yeast HCCS over twenty-five years ago [5], progress in understanding the mechanism(s) of HCCS function had been limited by difficulties in purifying the protein [6]. In Chapter 5 [7], the first biochemical work on an HCCS protein (the HCCS from humans) is described. HCCS, expressed in recombinant *E. coli* as an N-terminal fusion to glutathione S-transferase, purifies with a heme b that is coordinated by a conserved histidine (His154, see Fig 2). When co-expressed with its cognate human apocytochrome, HCCS is shown to form a complex with heme and cytochrome c, with axial ligands supplied by conserved His154 of HCCS and His19 (of Cys-Xxx-Xxx-Cys-His) of the cytochrome c. It is shown that the minimal requirements for covalent heme attachment to the apocytochrome are present in the apocytochrome N-terminus (and include, but are not limited to, Cys-Xxx-Xxx-Cys-His), and a non-substrate cytochrome (bacterial cytochrome c2) is converted into a robust substrate for the human HCCS by engineering three sequence alterations. Trapped, intermediate complexes between HCCS and site-directed variants of cytochrome c are characterized. These data allow us

to delineate four steps in the long-sought mechanism of mitochondrial cytochrome c assembly by HCCS, and are diagrammed in Fig 2.

Future studies on system I

The structure of the b-heme binding site in CcmF has been investigated, but the role of the b-heme in cytochrome c biogenesis remains hypothetical. Many of the requirements for formation of the holoCcmE-CcmF complex have been identified, but a direct role for the WWD domain in this interaction has not been described. Only a limited spectral characterization of the holoCcmE-CcmF complex has been undertaken, and knowledge of the role that CcmH plays in mediating complex formation between holoCcmE and CcmF is based only on the inability to trap holoCcmE when CcmH is present. Some of the molecular details of cytochrome c biogenesis by CcmFGH-ind are still unknown; in particular, the origin of the heme that is attached to cytochrome c and the role of the CcmF WWD domain in holoCcmE-independent assembly.

Determining the midpoint potentials of all heme-bound intermediates

Initial attempts at determining the redox potential of the CcmF b-heme by potentiometric methods were severely constrained by the large yields of protein that were required. Critically, the technique described in this thesis (an adaptation of the Massey method [8] that was refined in the laboratory of Emma Raven [9]; see chapter 2) requires yields that we are routinely able to achieve with our membrane proteins. Thus, determining the midpoint potentials for each of the heme carriers in system I (as well as system II, for which yields of holo-protein are similar, and the cytochrome c:heme:HCCS complexes of system III) is a feasible goal.

Heme trafficking during cytochrome c biogenesis (for systems I, II, and III) involves multiple changes in coordination of the heme, and the midpoint potential is very sensitive to changes in axial ligation [10]. Furthermore, it is likely that many of the heme-protein intermediates (e.g., the holoCcmE-CcmF complex, or the complex of HCCS with cytochrome c)

have defined redox requirements that must be satisfied for heme trafficking and/or covalent attachment to proceed. Therefore, establishing the midpoint potentials of the heme-protein complexes would inform our understanding of the mechanistic requirements for the heme reactions in cytochrome c biogenesis.

The role of the CcmF WWD domain

The conserved WWD domain [11] is a hydrophobic, extra-cytoplasmic feature that is the hallmark of the heme-handling protein (HHP) superfamily [12], which includes CcmC, CcmF, and CcsBA. In CcmC, the Kranz lab has shown that the WWD domain is directly involved in binding heme (in holoCcmE): mutation of conserved residues in the WWD domain caused spectral perturbations (and, for some substitutions, heme loss) in the holoCcmCDE complex [13]. Two conserved histidines in CcmC that flank the WWD domain (His60 and His184, here called P-His1 and P-His2, respectively) were shown to be axial ligands to the heme in the WWD domain. For CcmF, although a direct role for the WWD domain in heme binding has yet to be demonstrated, there is strong circumstantial evidence to support its involvement in heme-binding: i) conserved, WWD domain-flanking histidines P-His1 and P-His2 in CcmF (analogous to P-His1 and P-His2 in CcmC) are individually required for cytochrome c assembly by system I, ii) the cytochrome c assembly defects of mutations at P-His1 and P-His2 in CcmF can be corrected by exogeneous imidazole, suggesting that these residues likely have a ligand-type function, and iii) in the absence of either P-His1 or P-His2, holoCcmE forms a complex with CcmF at levels 5-fold lower than WT CcmF, and the double P-His1/P-His2 mutant complexes with holoCcmE at 10-fold lower levels (see chapter 3). Because P-His1 and P-His2 are positioned adjacent to the WWD domain (as they are in CcmC), the above results strongly

suggest a role for the CcmF WWD domain in binding heme from holoCcmE. Nonetheless, direct experimental evidence demonstrating this function is still needed. Most directly (and quickly), the hypothesis that the CcmF WWD domain binds holoCcmE could be tested by engineering substitutions of conserved residues in the WWD domain and assaying for interaction with holoCcmE. Comparing levels of holoCcmE that co-purify with CcmF carrying WWD substitutions with those of WT CcmF (by heme stain and anti-CcmE immunoblot, as described in Chapter 3) would be informative.

The role of the b-heme in system I

The CcmF heme b is required for every activity of CcmF that we have investigated thus far. Holocytochrome c formation in the context of the full system I and by CcmFGH-ind, as well as complex formation with holoCcmE, all require the conserved transmembrane histidines (TM-His1 and TM-His2), for axial coordination of the heme b. However, the precise role(s) of the heme b in each of these functions is largely speculative. For the interaction of CcmF with holoCcmE, we suggest that the transmembrane b-heme establishes a structural feature that is required for holoCcmE to bind in the CcmF WWD domain. This seems likely given that the CcmF protein is significantly destabilized in the absence of the heme b, with the protein being more susceptible to degradation (yields of full-length protein are typically only a quarter of those of WT).

For the CcmFGH-ind pathway, the role of the heme b is particularly intriguing, since the origin of the heme that is ultimately attached to the cytochrome c (in the absence of CcmABCDE) is currently unknown. As discussed in chapter 4, it is possible that, in CcmFGH-ind, the heme b is channeled from the transmembrane binding site to the external WWD domain

for covalent attachment, as in system II cytochrome c synthesis, by CcsBA [14,15]. The evolutionary insights that could be gained from studies comparing cytochrome c assembly by CcmFGH-ind to the full system I under low-iron conditions, for example, are fascinating.

For cytochrome c assembly via the full system I, we have hypothesized that the b-heme may be involved in reducing the heme in holoCcmE, prior to covalent attachment to the apocytochrome [1,2,16]. Recall that reduced heme (Fe^{2+}) is required for thioether formation between the heme vinyls and apocytochrome thiols [17,18]. Additionally, reduction of heme in holoCcmE would favor discharge of the covalent bond to His130 [16]; thus, this role for the heme b provides a mechanism for releasing (apo)CcmE as well as preparing heme for covalent attachment to the apocytochrome. Clarifying the role(s) that the CcmF heme b plays in each of these activities will be challenging, but the information gained would greatly advance our understanding of CcmF function. These studies may require reconstitution, in vitro, using purified holoCcmE, CcmFH and apocytochrome.

The role of CcmH in mediating complex formation between holoCcmE and CcmF

We discovered that in the absence of CcmH, holoCcmE was trapped in complex with CcmF at levels 10-fold higher than when CcmH was present (chapter 3). This suggests that CcmH may play a direct role in mediating complex formation between CcmF and holoCcmE. In cytochrome c biogenesis by system I, it is proposed that holoCcmE delivers heme to the CcmF WWD domain (where heme is coordinated by CcmF P-His1 and P-His2), and CcmH "chaperones" the apocytochrome and orients the thiols (of Cys-Xxx-Xxx-Cys-His) to facilitate covalent attachment to the heme bound in the WWD domain [16,19,20,21,22]. To date, there

has been no evidence of a direct interaction between CcmH and holoCcmE (nor has a direct interaction between CcmF and the apocytochrome been reported).

In chapter 3, we briefly discuss two possible mechanisms by which CcmH may modulate the interaction between CcmF and holoCcmE: i) in the absence of apocytochrome, CcmH may physically occlude the CcmF WWD domain (exerting a "lid-like" function), or ii) CcmH may facilitate rapid binding and release of holoCcmE from the CcmF WWD domain, such that a stable holoCcmE-CcmF complex is difficult to detect when CcmH is present. While distinguishing between the above scenarios may be difficult, defining a domain within CcmH responsible for this apparent activity (modulation of CcmF-holoCcmE complex formation) would be valuable for the field. Candidate domains/residues could be tested directly by engineering stable truncations or site-directed mutations in CcmH, and determining the levels of holoCcmE that co-purify with CcmF (using the same methods described in chapter 3). This line of investigation benefits from past work that has shown the CcmH protein to be quite amenable to engineering approaches, since stable C- and N-terminal truncations, as well as substitutions of conserved residues, have been reported [23,24,25,26,27,28]. Here, as above, in vitro reconstitution studies would be useful; the Kranz lab has expertise purifying holoCcmE [29] and CcmF (alone and in complex with CcmH) [1,2].

Future studies on system III

Our study on the human HCCS [7] (chapter 5) was the first biochemical analysis of an HCCS protein. This seminal study defined the requirements for covalent heme attachment to cytochrome c, characterized complexes between HCCS and cytochrome c, and delineated individual steps for cytochrome c maturation by HCCS. Several intriguing lines of inquiry have arisen from these findings, including defining elements in HCCS and the cytochrome c that mediate complex formation, and further refining our understanding of the process of holocytochrome c release from HCCS.

Requirements for complex formation with cytochrome c versus heme attachment

In chapter 5, we report conversion of a non-substrate cytochrome, the cytochrome c2 from *R. capsulatus*, into a robust substrate for HCCS by introducing three alterations to the N-terminal sequence. This engineered cytochrome, termed here cytochrome c2(+), thus contains the minimal requirements for covalent heme attachment by HCCS. In chapter 5, we also describe purification of HCCS in complex with heme and the human cytochrome c, with heme axial ligands supplied by conserved His154 of HCCS and His19 (of Cys-Xxx-Xxx-Cys-His) of the apocytochrome. The cognate human cytochrome c, therefore, includes elements that mediate complex formation with HCCS in addition to containing the determinants for covalent heme attachment. Intriguingly, cytochrome c2(+) does not detectably co-purify with HCCS (unpublished data), despite being a robust substrate for covalent heme attachment. This indicates that cytochrome c2(+) lacks the elements required for complex formation with HCCS, and, further, that these elements are not required for covalent heme attachment.

We have speculated that the complex formed between the human HCCS and the human cytochrome c in our recombinant *E. coli* may be related to interactions that occur during mitochondrial import of cytochrome c by HCCS (recall that HCCS is required for import of the apocytochrome from the cytosol into the mitochondrial intermembrane space [18,30,31,32,33,34]). Determining the specific amino acids that mediate complex formation, therefore, could inform our understanding of this process. To identify the elements in the human cytochrome c that mediate complex formation with HCCS, a site-directed mutagenesis approach could be taken, initially targeting residues in the human cytochrome c. The elements found to be required for complex formation could subsequently be engineered into the cytochrome c2(+), and we could assay for cytochrome c2(+) in purifications of HCCS. Even low levels of complex would be detectable, owing to our high-titer cytochrome c2 antisera. These studies would establish possible side chain interactions that mediate stable complex formation between cytochrome c and HCCS.

Production of novel cytochromes c by HCCS

Recently, we have discovered that a variant of the human cytochrome c carrying a methionine substitution at conserved His19 (of Cys-Xxx-Xxx-Cys-His) can be matured by HCCS at a low level (unpublished data). To our knowledge, this could turn out to be the first example of a cytochrome c with bis-Met coordination of heme (the 6^{th} axial ligand in cytochrome c is a methionine residue, Met81). Therefore, strategies to improve yields of this novel cytochrome c, thereby facilitating a thorough analysis of its structural and spectroscopic properties, are certainly of a high priority. A method for improving the cytochrome c yields could also open the door for analysis of other novel cytochromes c that may yet be discovered.

Mechanistically, maturation of the His19Met cytochrome c is intriguing because it demonstrates that methionine can serve as a heme axial ligand in the complex with HCCS, promoting covalent attachment and subsequent holocytochrome c release (albeit at a much lower level than the native histidine). As discussed in chapter 5, in the complex of HCCS with the WT human cytochrome c, His19 is required for covalent heme attachment to the cysteines [7]; i.e., holocytochrome c formation cannot proceed in the absence of a suitable axial ligand. Characterization of the complex between HCCS, heme, and the His19Met cytochrome c could further elucidate the requirements for holocytochrome c formation by HCCS.

References

1. Richard-Fogal CL, Frawley ER, Bonner ER, Zhu H, San Francisco B, et al. (2009) A conserved haem redox and trafficking pathway for cofactor attachment. Embo J 28: 2349-2359.
2. San Francisco B, Bretsnyder EC, Rodgers KR, Kranz RG (2011) Heme ligand identification and redox properties of the cytochrome c synthetase, CcmF. Biochemistry 50: 10974-10985.
3. Feissner RE, Richard-Fogal CL, Frawley ER, Loughman JA, Earley KW, et al. (2006) Recombinant cytochromes c biogenesis systems I and II and analysis of haem delivery pathways in Escherichia coli. Mol Microbiol 60: 563-577.
4. Pollock WB, Rosell FI, Twitchett MB, Dumont ME, Mauk AG (1998) Bacterial expression of a mitochondrial cytochrome c. Trimethylation of lys72 in yeast iso-1-cytochrome c and the alkaline conformational transition. Biochemistry 37: 6124-6131.
5. Dumont ME, Ernst JF, Hampsey DM, Sherman F (1987) Identification and sequence of the gene encoding cytochrome c heme lyase in the yeast Saccharomyces cerevisiae. Embo J 6: 235-241.
6. Allen JW (2011) Cytochrome c biogenesis in mitochondria--Systems III and V. Febs J 278: 4198-4216.
7. San Francisco B, Bretsnyder EC, Kranz RG (2012) Human mitochondrial holocytochrome c synthase's heme binding, maturation determinants, and complex formation with cytochrome c. Proc Natl Acad Sci U S A 110: E788-797.
8. Massey V (1991) In: Curti B, Ronchi S, Zanetti G, editors. Flavins and Flavoproteins. New York: Walter de Gruyter and Co. pp. 59-66.
9. Efimov I, Papadopoulou ND, McLean KJ, Badyal SK, Macdonald IK, et al. (2007) The redox properties of ascorbate peroxidase. Biochemistry 46: 8017-8023.
10. Clark WM (1960) Oxidation-Reduction Potentials of Organic Systems. Baltimore, MD: Waverly Press.
11. Beckman DL, Trawick DR, Kranz RG (1992) Bacterial cytochromes c biogenesis. Genes Dev 6: 268-283.
12. Lee JH, Harvat EM, Stevens JM, Ferguson SJ, Saier MH, Jr. (2007) Evolutionary origins of members of a superfamily of integral membrane cytochrome c biogenesis proteins. Biochim Biophys Acta 1768: 2164-2181.
13. Richard-Fogal C, Kranz RG (2010) The CcmC:heme:CcmE complex in heme trafficking and cytochrome c biosynthesis. J Mol Biol 401: 350-362.
14. Frawley ER, Kranz RG (2009) CcsBA is a cytochrome c synthetase that also functions in heme transport. Proc Natl Acad Sci U S A 106: 10201-10206.
15. Merchant SS (2009) His protects heme as it crosses the membrane. Proc Natl Acad Sci U S A 106: 10069-10070.
16. Kranz RG, Richard-Fogal C, Taylor JS, Frawley ER (2009) Cytochrome c biogenesis: mechanisms for covalent modifications and trafficking of heme and for heme-iron redox control. Microbiol Mol Biol Rev 73: 510-528, Table of Contents.
17. Barker PD, Ferrer JC, Mylrajan M, Loehr TM, Feng R, et al. (1993) Transmutation of a heme protein. Proc Natl Acad Sci U S A 90: 6542-6546.

18. Nicholson DW, Neupert W (1989) Import of cytochrome c into mitochondria: reduction of heme, mediated by NADH and flavin nucleotides, is obligatory for its covalent linkage to apocytochrome c. Proc Natl Acad Sci U S A 86: 4340-4344.
19. Hamel P, Corvest V, Giege P, Bonnard G (2009) Biochemical requirements for the maturation of mitochondrial c-type cytochromes. Biochim Biophys Acta 1793: 125-138.
20. Mavridou DA, Ferguson SJ, Stevens JM (2013) Cytochrome c assembly. IUBMB Life 65: 209-216.
21. Sawyer EB, Barker PD (2012) Continued surprises in the cytochrome c biogenesis story. Protein Cell 3: 405-409.
22. Stevens JM, Mavridou DA, Hamer R, Kritsiligkou P, Goddard AD, et al. (2011) Cytochrome c biogenesis System I. Febs J 278: 4170-4178.
23. Ahuja U, Rozhkova A, Glockshuber R, Thony-Meyer L, Einsle O (2008) Helix swapping leads to dimerization of the N-terminal domain of the c-type cytochrome maturation protein CcmH from Escherichia coli. FEBS Lett 582: 2779-2786.
24. Di Matteo A, Gianni S, Schinina ME, Giorgi A, Altieri F, et al. (2007) A strategic protein in cytochrome c maturation: three-dimensional structure of CcmH and binding to apocytochrome c. J Biol Chem 282: 27012-27019.
25. Di Silvio E, Di Matteo A, Malatesta F, Travaglini-Allocatelli C (2013) Recognition and binding of apocytochrome c to P. aeruginosa CcmI, a component of cytochrome c maturation machinery. Biochim Biophys Acta 1834: 1554-1561.
26. Fabianek RA, Hofer T, Thony-Meyer L (1999) Characterization of the Escherichia coli CcmH protein reveals new insights into the redox pathway required for cytochrome c maturation. Arch Microbiol 171: 92-100.
27. Robertson IB, Stevens JM, Ferguson SJ (2008) Dispensable residues in the active site of the cytochrome c biogenesis protein CcmH. FEBS Lett 582: 3067-3072.
28. Verissimo AF, Yang H, Wu X, Sanders C, Daldal F (2011) CcmI subunit of CcmFHI heme ligation complex functions as an apocytochrome c chaperone during c-type cytochrome maturation. J Biol Chem 286: 40452-40463.
29. Feissner RE, Richard-Fogal CL, Frawley ER, Kranz RG (2006) ABC transporter-mediated release of a haem chaperone allows cytochrome c biogenesis. Mol Microbiol 61: 219-231.
30. Dumont ME, Cardillo TS, Hayes MK, Sherman F (1991) Role of cytochrome c heme lyase in mitochondrial import and accumulation of cytochrome c in Saccharomyces cerevisiae. Mol Cell Biol 11: 5487-5496.
31. Dumont ME, Ernst JF, Sherman F (1988) Coupling of heme attachment to import of cytochrome c into yeast mitochondria. Studies with heme lyase-deficient mitochondria and altered apocytochromes c. J Biol Chem 263: 15928-15937.
32. Dumont ME, Schlichter JB, Cardillo TS, Hayes MK, Bethlendy G, et al. (1993) CYC2 encodes a factor involved in mitochondrial import of yeast cytochrome c. Mol Cell Biol 13: 6442-6451.
33. Nargang FE, Drygas ME, Kwong PL, Nicholson DW, Neupert W (1988) A mutant of Neurospora crassa deficient in cytochrome c heme lyase activity cannot import cytochrome c into mitochondria. J Biol Chem 263: 9388-9394.

34. Nicholson DW, Hergersberg C, Neupert W (1988) Role of cytochrome c heme lyase in the import of cytochrome c into mitochondria. J Biol Chem 263: 19034-19042.

Figures

Fig 1. Topology of the CcmF and CcmH integral membrane proteins from *E. coli.*

Possible histidine axial ligands to heme are starred (His173=P-His1; His303=P-His2; His261=TM-His1; His491=TM-His2). The highly conserved WWD domain is shaded as are the hydrophobic patches. Completely conserved amino acids (red) were identified by individual protein alignments using CcmF ORFs from selected organisms, as described in (Kranz, Richard-Fogal et al. 2009). Diagram is from (Kranz, Richard-Fogal et al. 2009).

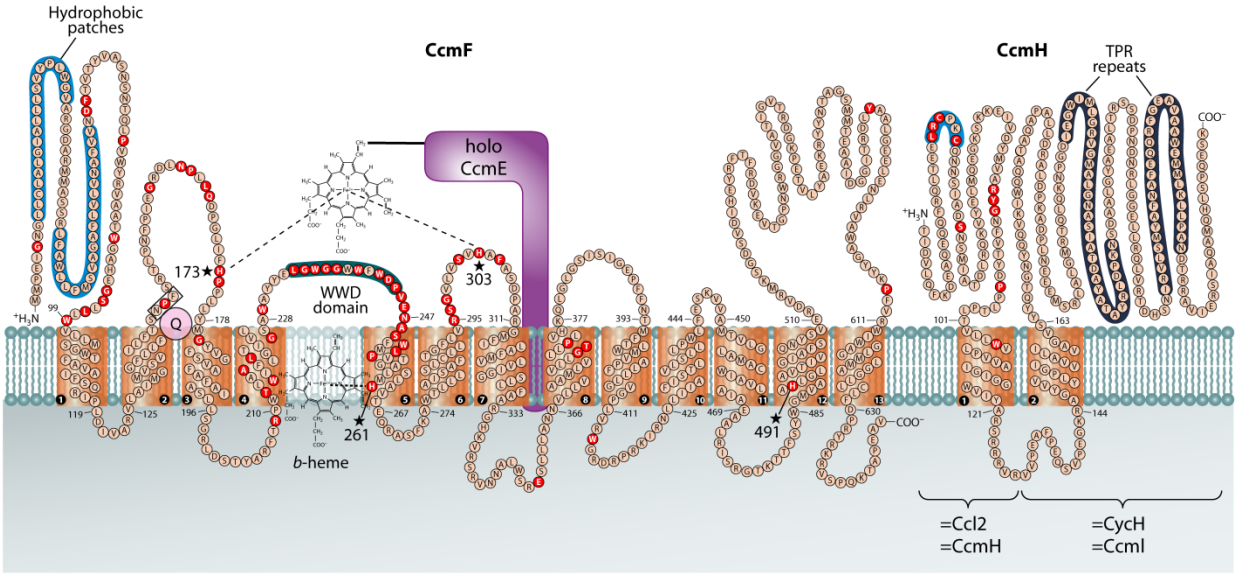
Hydrophobic patches
CcmF
CcmH
TPR repeats
holo CcmE
WWD domain
b-heme
173
303
261
491
Q
=Ccl2
=CcmH
=CycH
=CcmI

Fig 2. Steps in the maturation of cytochrome *c* by human HCCS.

(A) Diagram depicting the 4 steps in holocytochrome *c* maturation by HCCS (discussed in text). **(B)** PEP-FOLD generated model of the N-terminal 20 amino acid helix in human cytochrome *c* before interaction with HCCS. Amino acids important for maturation are indicated by arrows. Selected oxygen atoms are shown in red, nitrogens in blue, sulfurs in yellow, the heme macrocyle is in pink, and the Fe atom at the heme center is orange. **(C)** The HCCS:heme:cytochrome *c* complex (modeled with heme, pink) before thioether formation. Heme is coordinated by His19 of apocytochrome *c* (PEP-FOLD ribbon diagram, green, as in B) and His154 of HCCS (overlaid cartoon, blue). Amino acids and heme vinyls important for maturation are indicated by arrows. **(D)** The N-terminal 20 amino acids from the X-ray crystal structure of mature, released *E. caballus* holocytochrome *c* (pdb HRC1). Amino acids important for maturation are indicated by arrows. Heme is coordinated by His19, as in the complex with HCCS, and cytochrome *c* Met81, which replaces HCCS His154 in the folded, released holocytochrome *c*. PyMOL was used for displays in B, C, and D. Amino acid numbering refers to the *H. sapiens* cytochrome *c* N-terminal Met, as shown in Fig 3A (because the initiation Met is processed off, pdb HRC1 refers to Lys8 as Lys7, His19 as His18, Met81 as Met80, etc).

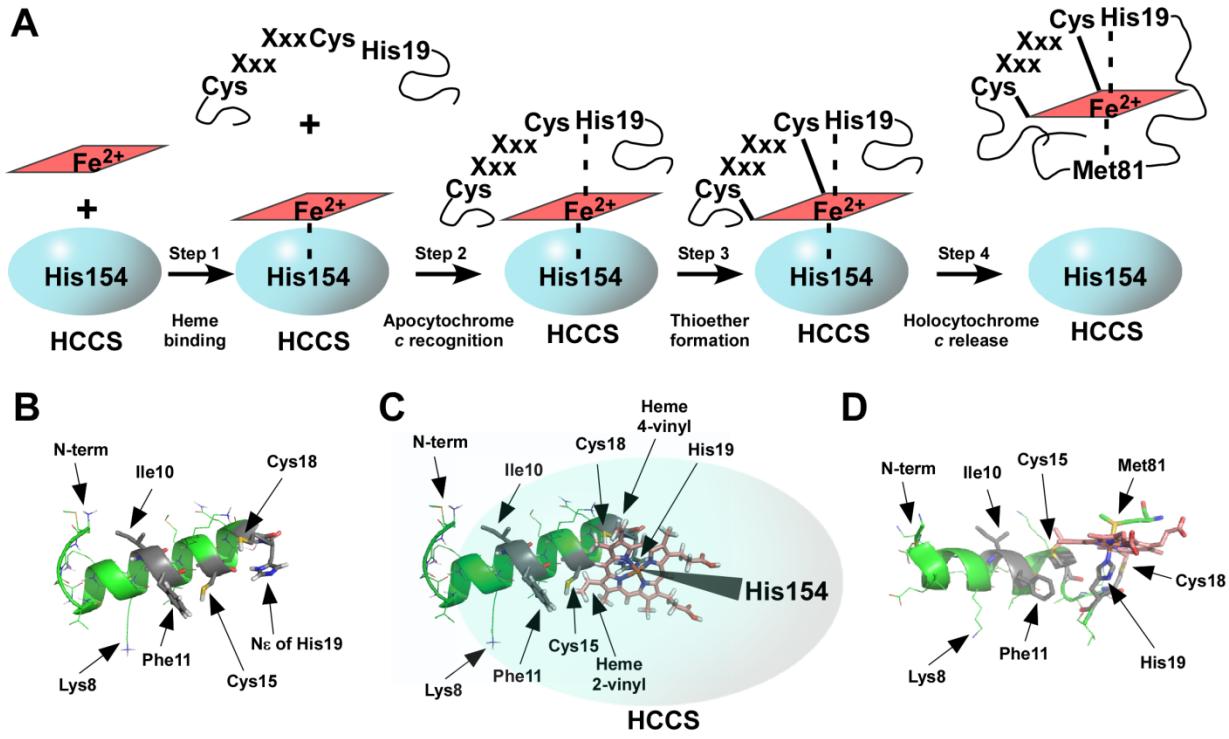
A
Xxx Cys
Xxx
Cys
His19
+
Fe2+
+
His154
HCCS
Step 1
Heme binding
Step 2
Apocytochrome c recognition
Step 3
Thioether formation
Step 4
Holocytochrome c release
Cys His19
Met81
B
N-term
Ile10
Cys18
Nε of His19
Phe11
Lys8
Cys15
C
Heme 4-vinyl
His154
Heme 2-vinyl
D